

CYSTEINE, A FACILITATOR OF HYPOXIA ADAPTATION AND A PROMOTER OF DRUG-RESISTANCE - A NEW ROUTE TO BETTER DIAGNOSE AND TREAT OVARIAN CANCER PATIENTS

ANA SOFIA DE ALMEIDA DA COSTA NUNES

Tese para obtenção do grau de Doutor em Mecanismos de Doença e Medicina Regenerativa

Doutoramento em associação entre:

Universidade NOVA de Lisboa (Faculdade de Ciências Médicas | NOVA Medical School - FCM|NMS/UNL)

Universidade do Algarve (UAlg)

Janeiro, 2019



CYSTEINE, A FACILITATOR OF HYPOXIA ADAPTATION AND A PROMOTER OF DRUG-RESISTANCE - A NEW ROUTE TO BETTER DIAGNOSE AND TREAT OVARIAN CANCER PATIENTS

Ana Sofia de Almeida da Costa Nunes

Orientadores: Jacinta Serpa, Professora Auxiliar da NOVA Medical School - FCM|NMS/UNL

Ana Félix, Professora Associada com agregação da NOVA Medical School - FCM|NMS/UNL

Sofia Pereira, Professora Auxiliar da NOVA Medical School - FCM|NMS/UNL

Tese para obtenção do grau de Doutor em Mecanismos de Doença e Medicina Regenerativa

Doutoramento em associação entre:

Universidade NOVA de Lisboa (Faculdade de Ciências Médicas | NOVA Medical School - FCM|NMS/UNL)

Universidade do Algarve (UAlg)



Janeiro, 2019

The chapters presented in this thesis regarding experimental data correspond to manuscripts already published or in preparation for publishing. I hereby state that I have fully participated in the conception and execution of the experimental work, in the interpretation of the collected data and in the writing of the manuscripts.

The work was approved by the Ethical Committee of NMS|FCM-UNL (24/2018/CEFCM) and by the IPOLFG (UIC-1080 and UIC-1082).

TABLE OF CONTENTS

ABSTRACT	i
RESUMO	iii
FIGURE INDEX	vi
TABLE INDEX	viii
ACKNOWLEDGMENTS	ix
LIST OF PUBLICATIONS	xii
LIST OF ABBREVIATIONS	xiii
CHAPTER 1	1
INTRODUCTION	3
1.1 CANCER AS AN EVOLUTIONARY DISEASE	4
1.1.1 HYPOXIA: A POWERFUL SELECTION PRESSURE ON MALIGNANT PHENOTYPES	5
1.1.2 ESCAPING FROM DRUGS-INDUCED DEATH: THERAPY, A POWERFUL SELECTIVE PRESSURE ON CANCER CELLS EVOLUTION	8
1.2 EPITHELIAL OVARIAN CANCER	12
1.3 CYSTEINE IN CANCER	13
1.3.1 CYSTEINE ROLE IN CANCER AS A PRECURSOR OF THE ANTIOXIDANT GSH	14
1.3.2 CYSTEINE ROLE IN CANCER AS A SOURCE OF H₂S	16
1.4 HYPOTHESIS, AIMS AND THESIS OUTLINE	18
1.5 REFERENCES	19
CHAPTER 2	31
CYSTEINE BOOSTERS THE EVOLUTIONARY ADAPTATION TO HYPOXIA, FAVOURING CARBOPLATIN RESISTANCE IN OVARIAN CANCER	31
ABSTRACT	33
INTRODUCTION	34
MATERIAL AND METHODS	35
RESULTS	39
DISCUSSION	50
REFERENCES	54
SUPPLEMENTS	58
CHAPTER 3	67

CYSTEINE ALLOWS OVARIAN CANCER CELLS TO ADAPT TO HYPOXIA AND TO ESCAPE FROM CARBOPLATIN CYTOTOXICITY	67
ABSTRACT	69
INTRODUCTION.....	70
MATERIAL AND METHODS.....	71
RESULTS	76
DISCUSSION	96
REFERENCES.....	102
SUPPLEMENTS	106
CHAPTER 4	107
CYSTEINE MECHANISTIC ROLE IN OVARIAN CANCER CELLS ADAPTATION TO HYPOXIA.....	107
ABSTRACT	109
INTRODUCTION.....	109
MATERIALS AND METHODS	111
RESULTS	116
DISCUSSION	138
REFERENCES.....	149
SUPPLEMENTS	156
CHAPTER 5	159
GENERAL DISCUSSION	161
5.1 HYPOXIA ADAPTATION FAVOURS A GENERALIST PHENOTYPE IN OVARIAN CANCER CELLS AND DRIVES CARBOPLATIN RESISTANCE.....	161
5.2 CYSTEINE FACILITATES THE ADAPTATION OF OVARIAN CANCER CELLS TO BOTH HYPOXIA AND CARBOPLATIN.....	163
5.3 CYSTEINE MECHANISTIC ROLE IN HYPOXIC OVARIAN CANCER CELLS ...	163
5.4 CYSTEINE AS A SUITABLE BIOMARKER FOR OVARIAN CANCER SCREENING, DIAGNOSIS, PROGNOSIS AND TARGETED-THERAPY	170
5.5 FINAL REMARKS	172
5.6 FUTURE PERSPECTIVES	174
5.7 REFERENCES	176

ABSTRACT

Ovarian cancer is the third most common gynaecologic malignancy and the main cause of death from gynaecologic cancer. Despite in the last 30 years an improvement of the overall survival of ovarian cancer patients has been observed, an increased cure rate was not registered. The high mortality associated with ovarian cancer is mainly due to a late diagnosis and resistance to treatment, barring ovarian cancer cure.

Given the lack of a specific therapy against ovarian cancer, the treatment depends essentially on the use of generalised and comprehensive cytotoxic drugs, most of them belonging to the group of alkylating/oxidative agents, as platinum salts. Chemotherapy imposes high selection pressures in cancer cells, which may affect their evolutionary trajectories, selecting the chemoresistant ones, which will continue the progression and relapse of the disease, contributing to morbidity and mortality.

In recent years, cancer metabolism has acquired a central position in oncobiology, being the metabolic remodelling a requirement for tumour progression, allowing cancer cells to respond to the selective pressures of the microenvironment, such as hypoxia and cytotoxic drugs. These selective pressures promote cell death in non-adapted cells and positively select cells that exhibit growth advantage that will further sustain cancer progression and metastasis. Endogenous metabolism also limits drugs response. A role of cysteine in cancer by contributing for H₂S generation and as a precursor of the antioxidant glutathione (GSH), were already reported. GSH has a crucial role as an antioxidant and also as a detoxifying system allowing the physiological maintenance of metabolic pathways, being intimately associated with chemoresistance. H₂S is involved in several biological processes, acting also as an antioxidant and being associated with cancer progression and chemoresistance.

As a solid tumour grows, such as an ovarian tumour, due to inefficient vascularisation, cancer cells are exposed to regions of hypoxia, known as a boost factor for tumour progression, metastasis and resistance to therapy.

The present thesis aimed to clarify the relevance of cysteine metabolism in ovarian cancer cells adaptability to both hypoxia and platinum salts (carboplatin). These stressful conditions impose strong evolutionary selection pressure on cancer cells.

Our results have provided evidence that cysteine metabolism has a role in ovarian cancer cells fast response and adaptation to hypoxic conditions that, in turn, are capable of driving chemoresistance. Moreover, cysteine showed to present a widespread protective effect against both hypoxia and carboplatin-induced death among ovarian cancer cell lines. Importantly, our findings were also supported in a clinical context, as an overall increase of thiols concentration was found in serum from patients with ovarian neoplasms, regardless malignancy. Strikingly, the free levels of cysteine together with protein-S-cysteinylation levels were able to distinguish patients with malignant tumours from patients with benign tumours and also from healthy individuals, supporting that the levels of cysteine and protein-S-cysteinylation can be putative biomarkers for ovarian cancer early diagnosis. Cysteine was also the prevalent thiol and S-cysteinylation was the most abundant form of S-thiolated proteins in the ascitic fluid from patients with

advanced disease. The ascitic fluid is an important compartment of the ovarian cancer cells microenvironment, supporting a clinical relevance of cysteine also in the progression of the disease.

Given the protective effect of cysteine in hypoxic ovarian cancer cells, we also aimed to address the possible mechanisms by which cysteine would be beneficial under hypoxia. Our results have supported a role of a higher thiols turnover in the adaptation to this environment, especially in ES2 cells. Moreover, results have also supported a role of cysteine in energy production mediated by the xc⁻ system, that requires cysteine metabolism instead of H₂S *per se*. However, the direct role of cysteine in ATP production is still uncertain as this amino acid can have an indirect contribution to ATP synthesis driven by an increased GSH content, allowing the redox equilibrium crucial for the overall cellular metabolism. Strikingly, ¹H-NMR results have suggested that cysteine impacted profoundly ES2 cells metabolism under hypoxia, allowing a metabolic reprogramming, that probably underlies ES2 cells adaptation to hypoxia.

Taken together, this thesis has shed light on new paths for ovarian cancer screening, diagnosis, prognosis and therapy, where cysteine metabolic profile might allow the design of new and useful approaches to fight this disease, thus overcoming its poor prognosis.

KEYWORDS

Ovarian cancer, cysteine, hypoxia, chemoresistance, glutathione (GSH), thiols, H₂S

RESUMO

Apesar de todo o progresso na prevenção e no desenvolvimento de novas abordagens terapêuticas, o cancro é a segunda principal causa de morte a nível mundial. Cancro refere-se a um conjunto de doenças complexas, sendo que existem mais de 200 diferentes tipos de cancro. No entanto, foi proposto que as alterações fisiopatológicas implicadas na transformação maligna são comuns à maioria dos tumores humanos: auto-suficiência em sinais estimuladores de proliferação celular (mitogénese), insensibilidade a sinais que inibem a proliferação, evasão da morte celular programada, capacidade de replicação ilimitada, indução de angiogénese, capacidade de invasão de tecidos e de metastização, reprogramação do metabolismo energético e evasão ao sistema imunitário. Tanto a incidência como a mortalidade por cancro têm vindo a aumentar, não só devido ao envelhecimento e crescimento populacionais mas também devido ao aumento da exposição a factores de risco tais como o tabaco e obesidade.

O cancro do ovário não é exceção a este cenário, sendo o terceiro tipo de cancro ginecológico mais comum e a principal causa de morte de cancro ginecológico. Cancro do ovário define um conjunto de neoplasias distintas, sendo os carcinomas (neoplasia malignas com origem epithelial) o grupo dominante. Apesar de nos últimos 30 anos se ter observado um aumento da sobrevivência de pacientes com esta doença, não se observou um aumento na taxa de cura. O mau prognóstico associado ao cancro do ovário deve-se essencialmente a um diagnóstico tardio e à emergência de resistência à terapia convencional, dificultando o tratamento da doença. O tratamento do cancro do ovário envolve geralmente cirurgia citorrredutora e terapia combinada de sais de platina e de taxanos, ambos agentes oxidativos. Estes fármacos impõem pressões seletivas muito fortes nas células neoplásicas, seleccionando células resistentes responsáveis pela progressão e recidiva da doença. A quimioresistência contribui assim para uma grande morbidade e mortalidade da doença.

Recentemente, o metabolismo do cancro adquiriu uma relevância central em oncobiologia, sendo a remodelação metabólica uma característica necessária para a progressão tumoral, permitindo que as células cancerígenas respondam e se adaptem a inúmeras pressões seletivas diferentes impostas pelo microambiente tumoral, tais como hipóxia, acidez e presença de fármacos citotóxicos. O papel da cisteína em cancro já foi demonstrado devido ao seu envolvimento como precursor de dois compostos essenciais: o glutatião (GSH) e o sulfureto de hidrogénio (H₂S). O GSH é o tiol não proteico mais abundante em células de mamífero, desempenhando diversas funções biológicas tais como uma função antioxidante, e destoxicante, constituindo um mecanismo de quimioresistência em vários tipos de tumores. Por sua vez, o H₂S está também envolvido em vários processos biológicos, tendo também um papel antioxidante e estando também associado a progressão tumoral e quimioresistência.

Durante o crescimento dos tumores sólidos, como os tumores de ovário, as células cancerígenas são sujeitas a gradientes de hipóxia, devido a uma vascularização ineficiente. A hipóxia exerce uma forte pressão seletiva nas células cancerígenas, estando relacionada com a progressão tumoral, metastização e resistência à quimioterapia.

Na presente tese, o nosso objectivo principal foi clarificar a relevância do metabolismo da cisteína na capacidade de adaptação de células de carcinomas do ovário a condições de hipóxia e à presença de sais de platina (carboplatina), duas condições que impõem uma forte pressão seletiva nas células cancerígenas. Para isto, recorreremos essencialmente a duas linhas celulares de cancro de ovário de dois tipos histológicos diferentes: uma linha de carcinoma seroso de alto grau (HG-OSC) – OVCAR3 e uma linha de carcinoma de células claras (OCCC) – ES2. É importante referir que o tipo histológico carcinoma seroso de alto grau (HG-OSC) é o mais frequente, enquanto que o OCCC, apesar de menos frequente, é geralmente resistente à terapia convencional. Adicionalmente, recorreremos a uma linha celular de carcinoma do ovário cujo tipo histológico é desconhecido (A2780 sensíveis/parentais e A2780 resistentes a cisplatina) e a outra linha de HG-OSC (OVCAR8). Recorreremos ainda a amostras de soro de mulheres com tumores de ovário benignos e malignos, assim como a amostras de soro de mulheres saudáveis, a amostras de carcinomas de ovário de diferentes tipos histológicos e a amostras de líquido ascítico de mulheres com cancro de ovário.

No primeiro capítulo de resultados experimentais começámos por investigar qual o efeito da seleção de células ES2 e OVCAR3 em condições de normóxia e em hipóxia na capacidade destas se adaptarem à carboplatina, pretendendo ainda verificar qual o papel da cisteína na resposta a estes dois ambientes hipóxia/carboplatina. Os nossos resultados mostraram que a cisteína facilita a adaptação a condições de hipóxia que, por sua vez, é capaz de induzir quimioresistência.

No segundo capítulo de resultados experimentais pretendemos aprofundar o papel da cisteína na proteção de células de carcinoma do ovário em condições de hipóxia e na presença de carboplatina. Pretendemos ainda verificar se a cisteína apresenta relevância em contexto clínico, averiguando a possibilidade para o seu uso em diagnóstico e como ferramenta de prognóstico da doença. Os nossos resultados indicaram que a cisteína tem um papel protetor amplamente distribuído por diferentes linhas de cancro de ovário, tanto em condições de hipóxia, como na presença de carboplatina. Nas células ES2, os dados sugeriram que as dinâmicas de síntese e degradação de tióis estão subjacentes ao efeito protetor da cisteína em condições de hipóxia. Relativamente ao seu papel em contexto clínico, através da quantificação de tióis em soros de mulheres saudáveis e em mulheres com tumores de ovário benignos e malignos, verificámos que os níveis totais (cisteína livre e proteínas cisteinilada) conjuntamente com os níveis livre totais de cisteína foram capazes de distinguir estes três grupos de mulheres, sugerindo assim que este tiol poderá ser usado como um marcador de diagnóstico precoce da doença. Em amostras de tumores, verificámos uma tendência (não significativa) para níveis de cisteína mais altos no tipo histológico OCCC e também em HG-OSC apenas após quimioterapia, reforçando um papel importante da cisteína no tipo histológico OCCC e na aquisição de quimioresistência. Para além disto, através da análise do conteúdo de tióis em líquidos ascíticos de pacientes com carcinoma de ovário em estadios avançados da doença, verificámos ainda que a cisteína foi o tiol prevalente encontrado nesta importante fracção do microambiente tumoral, suportando um papel relevante deste tiol também na progressão da doença.

No terceiro capítulo referente a dados experimentais, pretendemos clarificar o mecanismo por detrás do papel protetor da cisteína em condições de hipóxia. Assim, para além das dinâmicas de síntese e degradação

de GSH, pretendemos explorar qual o papel do H₂S na adaptação das células de cancro de ovário a condições de hipóxia. Os nossos resultados sugeriram um papel importante da cisteína na produção de ATP, mediado pelo sistema de transporte xc⁻, que requer o metabolismo da cisteína, não sendo o H₂S por si suficiente para aumentar a produção de ATP em condições de hipóxia. No entanto, um papel direto da cisteína na produção de ATP é ainda incerto, uma vez que a contribuição deste tiol no metabolismo energético celular poderá ser devido a uma contribuição indireta, conduzido por um aumento dos níveis de GSH, permitindo assim um equilíbrio redox, crucial para o metabolismo celular. Através de ¹H-RMN (espectroscopia por ressonância magnética nuclear) verificámos que a cisteína teve um impacto profundo no metabolismo das células ES2, permitindo uma remodelação metabólica em condições de hipóxia, o que poderá estar subjacente à adaptação destas células nestas condições.

De um modo geral, este trabalho permitiu aumentar o conhecimento e conduzir a novas abordagens para o diagnóstico, prognóstico e terapia do cancro de ovário através do metabolismo da cisteína. Isto poderá permitir a implementação de novas abordagens de rastreio, diagnóstico e tratamento da doença, permitindo assim superar a quimioresistência e o mau prognósticos associados ao cancro do ovário.

PALAVRAS-CHAVE

Cancro do ovário, cisteína, hipóxia, quimioresistência, glutatião (GSH), tióis, H₂S

FIGURE INDEX

CHAPTER 1

FIGURE 1. CELLULAR ANTIOXIDANT SYSTEMS.	6
--	---

CHAPTER 2

FIGURE 1. CoCl ₂ INDUCES HIF-1A EXPRESSION IN ES2 CELLS AND OVCAR3 CELLS.	39
FIGURE 2. PROLIFERATION RATE OF ES2 AND OVCAR3 CELLS SELECTED UNDER NORMOXIA AND HYPOXIA.	40
FIGURE 3. ADAPTATION TO NORMOXIA IS ACCOMPANIED BY AN EVOLUTIONARY TRADE-OFF, WHICH IS SUPRESSED BY CYSTEINE UNDER HYPOXIA IN ES2 CELLS.	41
FIGURE 4. ES2 AND OVCAR3 CELLS RESISTANCE TO HYPOXIA.	42
FIGURE 5. METABOLIC EVOLUTION DRIVEN BY HYPOXIA PROVIDES STRONGER RESISTANCE TO CARBOPLATIN CYTOTOXICITY.	43
FIGURE 6. METABOLIC EVOLUTION DRIVEN BY HYPOXIA PROVIDES STRONGER RESISTANCE TO CARBOPLATIN.	44
FIGURE 7. ES2 CELLS TEND TO PRESENT A STRONGER RESISTANCE TO CARBOPLATIN THAN OVCAR3 CELLS.	45
FIGURE 8. ES2 AND OVCAR3 CELLS PRESENT DIFFERENT DYNAMICS OF RESPONSE TO CARBOPLATIN.	46
FIGURE 9. ES2 CELLS PRESENT METABOLIC DIVERSITY IN ADVERSE ENVIRONMENTS.	48
FIGURE 10. ROS LEVELS IN ES2 AND OVCAR3 ANCESTRAL CELLS, CELLS SELECTED UNDER NORMOXIA AND UNDER HYPOXIA.	49
FIGURE 11. ES2 AND OVCAR3 PRESENT DIFFERENT ADAPTIVE CAPACITIES IN A DRUG FREE ENVIRONMENT, IMPACTING THE RESPONSE TO CARBOPLATIN.	53

CHAPTER 3

FIGURE 1. CYSTEINE HAS A WIDESPREAD PROTECTIVE EFFECT UNDER HYPOXIA IN OVARIAN CANCER CELLS.	77
FIGURE 2. THE DOSE DEPENDENT AND CELL DENSITY DEPENDENT EFFECTS OF CYSTEINE IN HYPOXIA ADAPTATION IN ES2 AND OVCAR3 CELLS.	79
FIGURE 3. MITOCHONDRIAL MEMBRANE POTENTIAL UNDER NORMOXIA AND HYPOXIA WITH AND WITHOUT CYSTEINE IN ES2 AND OVCAR3 CELLS.	80
FIGURE 4. ES2 CELLS ADAPTATION TO HYPOXIA RELIES ON FREE INTRACELLULAR CYSTEINE AVAILABILITY.	82
FIGURE 5. EFFECT OF CYSTEINE AND HYPOXIA IN ES2 AND OVCAR3 CELLS RESPONSE TO PACLITAXEL ALONE OR IN COMBINATION WITH CARBOPLATIN.	83
FIGURE 6. CYSTEINE AND HYPOXIA HAVE A ROLE ON OVARIAN CANCER CELLS RESPONSE TO CARBOPLATIN.	85
FIGURE 7. CD133 LEVELS ARE INDUCED UPON HYPOXIA AND CARBOPLATIN EXPOSURE IN ES2, OVCAR8 AND A2780.	87
FIGURE 8. TOTAL THIOLS IN PATIENTS WITH OVARIAN TUMOURS.	89

FIGURE 9. FREE TOTAL THIOLS IN PATIENTS WITH OVARIAN TUMOURS.	90
FIGURE 10. THIOL PROTEIN-BOUND FRACTION IN PATIENTS WITH OVARIAN TUMOURS.	91
FIGURE 11. TOTAL THIOLS IN DIFFERENT OVARIAN CARCINOMAS.	93
FIGURE 12. FREE TOTAL THIOLS IN DIFFERENT OVARIAN CARCINOMAS.	93
FIGURE 13. THIOL PROTEIN-BOUND FRACTION IN DIFFERENT OVARIAN CARCINOMAS.	94
FIGURE 14. CYSTEINE IS THE PREVALENT THIOL IN ASCITIC FLUID FROM PATIENTS WITH OVARIAN CANCER.	95
FIGURE 15. ROLE OF CYSTEINE IN CELLS RESPONSE TO CARBOPLATIN AND HYPOXIA ADAPTATION. .	101
SUPPLEMENT FIGURE 1. ES2 AND OVCAR3 SPHEROID EXPOSURE TO CHEMOTHERAPEUTIC TREATMENT: PROTECTIVE EFFECT OF CYSTEINE.	106

CHAPTER 4

FIGURE 1. HYPOXIA INDUCED ATP SYNTHESIS UNDER HYPOXIA.	116
FIGURE 2. XCT LOCALISES IN OVARIAN CANCER CELLS MITOCHONDRIA.	118
FIGURE 3. CYSTEINE IS ABLE TO RESCUE THE IMPAIRED ATP SYNTHESIS TRIGGERED BY XCT INHIBITION UNDER HYPOXIA.	119
FIGURE 4. HYPOXIA INDUCES H ₂ S PRODUCTION IN ES2 CELLS.	120
FIGURE 5. HYPOXIA TENDS TO INDUCE H ₂ S PRODUCTION ALSO IN OVCAR3 CELLS.	122
FIGURE 6. CBS AND CSE INHIBITION DOES NOT IMPAIR ATP SYNTHESIS IN OVARIAN CANCER CELLS.	124
FIGURE 7. CBS AND CSE INHIBITION AFFECT ES2 CELLS SURVIVAL, MAINLY UNDER HYPOXIA.	125
FIGURE 8. CBS AND CSE INHIBITION DOES NOT AFFECT OVCAR3 CELLS SURVIVAL.	126
FIGURE 9. CYSTEINE, BUT NOT NAHS, IS ABLE TO RESCUE ATP SYNTHESIS UNDER HYPOXIA TRIGGERED BY XCT INHIBITION.	127
FIGURE 10. NAHS IMPAIRS ATP SYNTHESIS UNDER HYPOXIA IN OVARIAN CANCER CELLS.	128
FIGURE 11. CYSTEINE IS NOT ABLE TO RESCUE ATP PRODUCTION UPON B-OXIDATION AND GLYCOLYSIS INHIBITION.	129
FIGURE 12. ¹ H-NMR SPECTRA OF ES2 CELLS.	131
FIGURE 13. ¹ H-NMR SPECTRA OF OVCAR3 CELLS.	132
FIGURE 14. CYSTEINE RESCUES ES2 CELLULAR METABOLISM UNDER HYPOXIA.	134
FIGURE 15. COBALT CHLORIDE (CoCl ₂) AFFECTS HISTIDINE LEVELS.	135
FIGURE 16. UNDER HYPOXIA, CYSTEINE IMPACTS SEVERAL METABOLIC PATHWAYS IN ES2 CELLS. .	135
FIGURE 17. EFFECT OF CYSTEINE IN OVCAR3 METABOLITES UNDER NORMOXIA AND HYPOXIA.	136
FIGURE 18. COBALT CHLORIDE (CoCl ₂) AFFECTS HISTIDINE LEVELS.	137
FIGURE 19. EFFECT OF HYPOXIA IN GLUCOSE, LACTATE, PYRUVATE, FUMARATE AND GLUTAMINE LEVELS IN OVARIAN CANCER CELLS.	137
FIGURE 20. CYSTEINE POSSIBLE DIRECT AND INDIRECT ROLES IN ATP SYNTHESIS AND IN CARBON METABOLISM REPROGRAMMING UNDER HYPOXIA IN OVARIAN CANCER CELLS.	148
SUPPLEMENT FIGURE 1. ES2 CELLS EXPRESS HIGHER BASAL mRNA LEVELS OF XCT THAN OVCAR3 CELLS.	156
SUPPLEMENT FIGURE 2. EFFECT OF CBS AND CSE INHIBITION IN ATP SYNTHESIS IN OVARIAN CANCER CELLS.	156

SUPPLEMENT FIGURE 3. MPST PROTEIN LEVELS IN ES2 AND OVCAR3 CELLS.....	157
SUPPLEMENT FIGURE 4. CYTOSOLIC AND MITOCHONDRIAL MPST PROTEIN LEVELS IN ES2 AND OVCAR3 CELLS.....	157

CHAPTER 5

FIGURE 1. PROPOSED MODEL FOR CYSTEINE PROTECTIVE EFFECT UNDER HYPOXIA IN OVARIAN CANCER CELLS.....	165
FIGURE 2. PROPOSED MODEL FOR THE PROTECTIVE EFFECT OF CYSTEINE IN OVARIAN CANCER CELLS UPON HYPOXIA AND CARBOPLATIN EXPOSURE.....	173
FIGURE 3. PROPOSED GROUPS FOR A PILOT CLINICAL STUDY TO VALIDATE CYSTEINE (AND HOMOCYSTEINE) AS BIOMARKERS FOR OVARIAN CANCER SCREENING, EARLY DIAGNOSIS AND PROGRESSION.....	175

TABLE INDEX

CHAPTER 1

SUPPLEMENT TABLE I: OVARIAN CANCER CELL LINES, SELECTION AND CULTURE CONDITIONS.	58
SUPPLEMENT TABLE II: ADAPTATION TO NORMOXIA CONFERS A HIGHLY PROLIFERATIVE ABILITY TO ES2 CELLS.	59
SUPPLEMENT TABLE III. ADAPTATION TO NORMOXIA IS ACCOMPANIED BY AN EVOLUTIONARY TRADE-OFF THAT IS SUPPRESSED BY CYSTEINE UNDER HYPOXIA IN ES2 CELLS.	59
SUPPLEMENT TABLE IV. ES2 AND OVCAR3 CELLS RESISTANCE TO HYPOXIA.	60
SUPPLEMENT TABLE V. HYPOXIA PROVIDES STRONGER RESISTANCE TO CARBOPLATIN.....	61
SUPPLEMENT TABLE VI. METABOLIC EVOLUTION DRIVEN BY HYPOXIA PROVIDES STRONGER RESISTANCE TO CARBOPLATIN.	62
SUPPLEMENT TABLE VII. ES2 CELLS TEND TO PRESENT A STRONGER RESISTANCE TO CARBOPLATIN THAN OVCAR3 CELLS.	63
SUPPLEMENT TABLE VIII. ES2 AND OVCAR3 CELLS DYNAMICS OF RESPONSE TO CARBOPLATIN.	63
SUPPLEMENT TABLE IX. ROS LEVELS IN ES2 AND OVCAR3 ANCESTRAL CELLS, CELLS SELECTED UNDER NORMOXIA AND UNDER HYPOXIA.....	65

ACKNOWLEDGMENTS

I cannot even believe I am writing the acknowledgments. During these four years, in the darkest periods, I used to think about this part of the thesis, to whom I would thank and why. Maybe as a way of self-motivation. If I were able to write the acknowledgments it would have meant that I had not abandoned this journey somewhere in time. And I did not. The feelings are mixed, but relief and nostalgia are the most meaningful ones.

I guess Biology was the natural degree for me to opt for. Because of my extreme love for life, all kinds of it. And because of the philosophical thinking that especially evolutionary biology awakened in me.

Many people were part of this journey, directly or indirectly. I thank everybody who helped me to get here and without whom all of this would not be possible.

I must start by acknowledging the ProRegeM board for admitting me into the program. It was a vote of confidence that I won't forget. It was the beginning of all. I would also like to thank FCT (Fundação para a Ciência e a Tecnologia), FSE (Fundo Social Europeu) and POCH (Programa Operacional Capital Humano) for funding my PhD scholarship (Ref. PD/00117/2012 and PD/BD/105893/2014). I also thank iNOVA4Health for funding (UID/Multi/04462/2013) and IPOLFG for allowing me to develop my PhD project there.

Then, I must thank Dr. Jacinta Serpa, who accepted to be my supervisor. I thank her for all the guidance, help and support, but I especially thank her for letting me move beyond the project's confinements. She gave me scientific freedom, respecting my scientific interests, for which I deeply thank her. I also thank Dr. Ana Félix and Dr. Sofia Pereira, my co-supervisors, for their suggestions and contributions throughout these four years. To Dr. Sofia Pereira for her enthusiasm, motivation and passion for science.

I also thank all our collaborators, without whom this thesis would be impossible, especially to Luís Gonçalves for the introduction to NMR, for all his help with the data analysis and for his suggestions and to Catarina Sequeira for all the help with HPLC.

I would also like to acknowledge my previous supervisors, Francisco Dionísio and Henrique Teotónio, who have helped me to define who I want to be as a scientist. To Francisco, for the confidence and support during my master's and to Henrique for trusting me with the "limits project". It undoubtedly gave me the confidence needed to apply for a PhD programme.

I thank my lab colleagues without whom this thesis would be impossible. To the present and the former ones. To Carolina Nunes and Filipa Coelho, for welcoming me into the lab and for all they taught me. To Sofia Gouveia for bringing peace and friendship to the lab. To Armanda Rodrigues

for the philosophical conversations. To Cindy and Inês for all their energy and joy. It was beautiful to watch the beginning of their friendship and the mutual help between them. To Inês Santos, it was a privilege contributing to your guidance during your master's. I am sorry for my lack of patience sometimes and for my crazy rhythm. Please do not lose all your enthusiasm, joy and kindness! To Cristiano Ramos, thank you for all the help during this last year. Without you this would not be possible. To all of you I thank for the motivational words and support during these years.

I would also like to thank everybody at UIPM-IPO, for all the lunches and laughs. A special thanks to Dona Joaquina, without whom everything would be much more difficult and to Marta Sebastião, for listening and comforting me in especially difficult times.

I also thank my colleagues from ProRegeM for the welcoming environment during the courses. A special thanks to Inês Marques, for all the *getting something off my chest*. Talking to someone who is going through a similar emotional roller coaster during these years is of extreme importance. It shows us that we are not alone and that we are not crazy.

To my family and friends, humans and non-humans, you were a central part of this journey. A special thanks to my parents, for all their support and motivation, and for trying to understand me. To my parents-in-law for all their help. To Nelson for taking care of our cat-daughter when I had to go to Algarve for the courses and for the annual ProRegeM meetings. To Ana, André and Anita for their friendship. I am sorry for all the *no's* to dinners and concerts. I do not know where all my energy went during these last years. To Ana Paula Marques and Sara Santos, who told me to check the e-mail with the ProRegeM application. Without your warning I would have missed that e-mail and I would not have embarked on this journey. To Sara, a profound acknowledgement for showing me that it is ok to ask for help. I truly miss those times at IGC, our pauses to *smoke*, our conversations, your friendship. To Dr. Mafalda for all her help, guidance and support during these last years. She has helped me to re-encounter myself and to redefine my way in accordance with who I am and who I want to be. To my beloved non-human, who I have lost almost ten years ago, who taught me what unconditional love is. I cannot even believe that ten years already went by since I have lost you. I have lost a big part of me then. I have lost the most faithful and beautiful friendship possible between two living beings. You will always be with me as long as I live. And beyond. To my other non-human friends for making it all worthwhile. To a life that accidentally and unexpectedly entered my life and helped me heal. That filled my heart again. To my dog, I know you won't be here much more longer. I am sorry for all those hurried walks, and for the walks that I did not let you command. An entire life with all of you would not have been enough.

Finally, I thank my partner in life, the love of my life, Bruno. You have been central in my life, not only during these four years but also these last 17 years. I thank you for all your support, for all

the cries, despair and hopelessness you put up. For all the times that I simply had no energy to talk or even listen to you, preferring the silence. Thank you for knowing me better than myself, for all your caring, loving, understanding and friendship. Above all, thank you for not letting me drown and for keep rowing. Without you everything would mean nothing.

LIST OF PUBLICATIONS

Papers:

Nunes SC, Ramos C, Lopes-Coelho F, Sequeira CO, Silva F, Gouveia-Fernandes S, Rodrigues A, Guimarães A, Silveira M, Abreu S, Santo VE, Brito C, Félix A, Pereira SA, Serpa, J. Cysteine allows ovarian cancer cells to adapt to hypoxia and to escape from carboplatin cytotoxicity. *Sci. Rep.* 2018;8:9513–29.

Nunes SC, Lopes-Coelho F, Gouveia-Fernandes S, Ramos C, Pereira SA, Serpa J. Cysteine boosts the evolutionary adaptation to CoCl₂ mimicked hypoxia conditions, favouring carboplatin resistance in ovarian cancer. *BMC Evol. Biol.* 2018;18:97–113.

Nunes SC, Serpa J. Glutathione in ovarian cancer: A double-edged sword. *Int. J. Mol. Sci.* 2018;19:1882–96.

Lopes-Coelho F, Gouveia-Fernandes S, **Nunes SC** and Serpa J. Metabolic Dynamics in Breast Cancer: Cooperation between Cancer and Stromal Cells. *J Clin Breast Cancer Res.* 2017;1:1001–7.

Poster presentations:

Sofia C. Nunes, Filipa Coelho, João B. Vicente, Ana Félix, Sofia A. Pereira, Jacinta Serpa. Cysteine metabolism protects ovarian clear cell carcinoma (OCCC) cells in hypoxia. Cancer and Metabolism Conference, Cambridge (Abcam); September 28-30 2015.

Ana Félix, Fernanda Silva, Cristiano Ramos, Filipa Lopes-Coelho, **Sofia C. Nunes**, Jacinta Serpa. LAMININ332 (α 3; β 3; γ 2) genes and protein expression in cervical carcinomas. 25th Biennial Congress of the European Association for Cancer Research, Amsterdam, The Netherlands; 30 June – 3 July 2018.

Oral presentations:

Sofia C. Nunes, Cristiano Ramos, João B. Vicente, Sofia A. Pereira, Jacinta Serpa. Enzymes involved in cysteine metabolism underlie hypoxia adaptation in ovarian cancer. 8th International Conference on Tumor Microenvironment: progression, therapy & Prevention. Lisbon, Portugal: June 10-14 2018.

Sofia C. Nunes, Filipa Lopes-Coelho, Catarina O. Sequeira, Fernanda Silva, Sofia Gouveia-Fernandes, Armada Rodrigues, António Guimarães, Margarida Silveira, Ana Félix, Sofia A. Pereira, Jacinta Serpa, Cysteine allows ovarian cancer cells to adapt to hypoxia and to escape from carboplatin cytotoxicity. XLVIII Annual Reunion of Sociedade Portuguesa de Farmacologia. Lisboa, Portugal: February 5-7 2018.

LIST OF ABBREVIATIONS

- ¹H-NMR – Proton nuclear magnetic resonance
- A – Ancestral cells
- A2780cpR – A2780 resistant to carboplatin and paclitaxel
- AA – Antibiotic-antimycotic
- ANOVA – analysis of variance
- AOAA – O-(Carboxymethyl)hydroxylamine hemihydrochloride
- AP-1 – Activator protein 1
- ARID1A – Adenine thymine-rich interactive domain 1A gene
- ATCC - American Type Culture Collection
- ATP – Adenosine triphosphate
- AzMC – 7-Azido-4- Methylcoumarin
- BRAF – Proto-oncogene serine/threonine-protein kinase variant B
- BRCA1 – Breast cancer 1 gene
- BRCA2 – Breast cancer 2 gene
- BSA – Bovine serum albumin
- BSO – Buthionine Sulfoximine
- c-MYC – Myc proto-oncogene protein
- CAT – Cysteine aminotransferase
- CBS – Cystathionine-β-synthase
- CDK12 – Cyclin Dependent Kinase 12
- CSE – cystathionine-γ-lyase
- CTNNB1 – Catenin Beta 1
- CYP17A – Steroid 17-alpha-hydroxylase/17,20 lyase
- Cys – Cysteine
- CysGly – Cysteinylglycine
- CysGlySSP – S-cysteinylglycinylated proteins
- CysSSP – S-cysteinylated proteins
- Eco-index – Ecological classification system for neoplasms
- EDTA – Ethylenediaminetetraacetic acid
- EMT – Epithelial–mesenchymal transition
- EOC – Epithelial ovarian cancer
- ERBB2 – Erb-B2 Receptor Tyrosine Kinase 2

ERK – Extracellular signal-regulated kinase
Evo-index – Evolutionary classification system for neoplasms
FACS – Fluorescence-activated cell sorting
FBS – Fetal bovine serum
FGFR – Fibroblast growth factor receptor
FITC – Fluorescein isothiocyanate FOXM1 forkhead box M1
GCL – Glutamate cysteine ligase
GCLC – Catalytic subunit of glutamate cysteine ligase
GCLM – Modifier subunit of glutamate cysteine ligase
GluCys – Glutamylcysteine
GluCysSSPS – S-Glutamylcysteinylated proteins
GPX – Glutathione peroxidase
Grx – Glutaredoxin
GRx – Glutathione reductase
GRX2 – Glutaredoxin 2
GSH – Glutathione
GSSG – Oxidised GSH
GSSP – S-glutathionylated proteins
GSTM1 – Glutathione-S-transferase class μ
GSTP1 – Glutathione S-transferase P1
H – Hypoxia
HC – Hypoxia with cysteine supplementation
HCys – Homocysteine
HcySSP – S-homocysteinylated proteins
HG-OSC – High-grade ovarian serous carcinoma
HH – Cells selected in hypoxia and cultured in hypoxia
HHC – Cells selected in hypoxia and cultured in hypoxia with cysteine supplementation
HIF – Hypoxia-inducible transcription factors
HIF-1 α – Hypoxia inducible factor-1 alpha
HIF-2 α – Hypoxia inducible factor-2 alpha
HN – Cells selected in hypoxia and cultured in normoxia
HNC – Cells selected in hypoxia and cultured in normoxia with cysteine supplementation
HNF1 β – Hepatocyte nuclear factor 1 β
HPLC – High-Performance Liquid Chromatography

IMS – Inter mitochondrial space
JNK – Jun N-terminal Kinase
KRAS – Kirsten Rat Sarcoma viral oncogene homolog
LAS17 – Dichlorotriazine-containing compound
LG-OSC – Low-grade ovarian serous carcinoma
MAPK – mitogen-activated protein kinase
MDR1 – Multi-Drug Resistance protein 1
MpST – 3-mercapto-pyruvate sulphurtransferase
mtDNA – Mitochondrial DNA
N – Normoxia
NC – Normoxia with cysteine supplementation
NF1 – Neurofibromin 1 (NF1),
NFkB – Nuclear Factor-kappaB
NH – Cells selected in normoxia and cultured in hypoxia
NHC – Cells selected in normoxia and cultured in hypoxia with cysteine supplementation
NN – Cells selected in normoxia and cultured in normoxia
NNC – Cells selected in normoxia and cultured in normoxia with cysteine supplementation
NOX1 – NADPH oxidase subunit
NP-40 – Nonidet P-40
NRAS – Neuroblastoma RAS viral oncogene homolog
Nrf2 – Nuclear factor-erythroid 2 (NF-E2) p45-related factor (Nrf2)
OCCC – Ovarian clear cell carcinoma
OEC – Ovarian endometrioid carcinoma
OMC – Ovarian mucinous carcinoma
OXPHOS – Mitochondrial oxidative phosphorylation
PAG – DL-propargylglycine
pAKT– Phosphorylated serine/Threonine kinase akt
pATM – Phosphorylated Serine-protein kinase ATM
PBS – Phosphate-buffered saline
pCHK1 – Phosphorylated Serine/threonine-protein kinase Chk1
PCR – Polymerase chain reaction
PERK – Endoplasmic reticulum kinase
PFA – Paraformaldehyde
pGSK3b– Phosphorylated Glycogen synthase kinase-3 beta

PI – Propidium iodide
PI3KCA – Phosphatidylinositol-4,5-Bisphosphate 3-Kinase Catalytic Subunit Alpha
PKC – Protein Kinase C
PLP – Pyridoxal 5'-phosphate
PPP2R1 α – Protein Phosphatase 2 Scaffold Subunit Alpha
PRXs – Peroxiredoxins
PTEN – Phosphatase and Tensin homolog
RAF – Serine/threonine-specific protein kinases
RAS – Rat Sarcoma virus protein
RB1 – RB transcriptional corepressor 1
ROS – Reactive oxygen species
RSSP – Total S-thiolated proteins
SD – Standard deviation
SLC3A1 – Solute carrier family 3, member 1
SLC7A11 – Solute carrier family 7 member 11
SODs – Superoxide dismutases
TCA cycle – Tricarboxylic acid cycle
TP53 – Tumour Protein P53
Trx – Thioredoxin
TrxR – Thioredoxin reductase
Vol – Volume(s)
 $\Delta\psi_m$ – Mitochondrial membrane potential

CHAPTER 1

INTRODUCTION

This chapter is partially based on the following publication:

Nunes SC, Serpa J. Glutathione in ovarian cancer: A double-edged sword. *Int. J. Mol. Sci.* 2018;19:1882–96.

“Begin at the beginning,’ the King said, very gravely, ‘and go on till you come to the end: then stop.’”

Lewis Carrol

INTRODUCTION

Despite all the progresses developed in prevention and new treatment approaches, cancer is the second leading cause of death worldwide [1]. In accordance with the International Agency for Research on Cancer, 14.1 million cancer cases [2] and 8.2 million cancer deaths [3] were estimated worldwide in 2012. For 2020, 17.1 million incidences and 10.05 million cancer deaths [2] are estimated. Metastatic disease accounts for over 90% of all cancer-related deaths, where the treatment with surgery, conventional chemotherapy and radiation is ineffective [4]. The late diagnosis combined with resistance to the conventional anti-cancer drugs used, are the major causes of cancers poor prognosis.

More than 200 different types of cancer exist [5], however, the physiological alterations that entail the malignant transformation were proposed to be common to the majority or even to all types of human tumours [6]. Therefore, in 2000, Hanahan and Weinberg proposed the existence of six core hallmarks of cancer cells: self-sufficiency in growth signals, insensitivity to growth-inhibitory signals, evasion of programmed cell death, limitless replicative potential, sustained angiogenesis, and tissue invasion and metastasis [6]. Eleven years later, the authors revisited those original hallmarks, and included energy metabolism reprogramming and evading immune destruction, as emerging hallmarks of cancer [7]. Underlying those hallmarks, the authors suggested two consequential characteristics of neoplasia that facilitate acquisition of both core and emerging hallmarks: genome instability, and inflammation [7]. The acquisition of these hallmarks is an evolutionary process, involving natural selection among the neoplastic cells, allowing cancer initiation, progression and chemoresistance [8].

The best characterised metabolic phenotype observed in tumour cells is the Warburg effect, proposing that cancer cells present an increased rate of glycolysis even under normal oxygen concentrations due to defective mitochondrial oxidative phosphorylation (OXPHOS) [9]. However, evidence accumulates showing that mitochondrial OXPHOS function is intact in most tumours [10–14]. Moreover, evidence also supports that the bioenergetics of tumour cells is highly complex, where cancer cells have the ability to use several substrates in order to support energy production, including glucose, glutamine, fatty acids, and acetate [14]. Also, in cancer cells, both glycolytic and oxidative metabolisms coexist, enhancing metabolic plasticity and improving tumorigenesis and metastasis [13,15], hence highlighting the metabolic complexity of cancer cells that allows coping with changing microenvironments. Recent studies have disclosed the Warburg effect as a way of cancer cells to sustain cell

proliferation rather than producing energy [16–18], once the glycolytic intermediates are deviated to serve as building blocks needed for replicating DNA and cellular machinery prior to mitosis [18]. Other hypothesis that explain the advantage of the Warburg effect on cancer cells is that it supports an ideal tumour microenvironment, sustaining cancer cells proliferation (e.g. acid-mediated invasion hypothesis) and that altered glucose metabolism alters cancer cell signalling, promoting tumorigenesis via reactive oxygen species (ROS) and the modulation of chromatin state (reviewed in [19]).

In the next sections, the concept of cancer as an evolutionary disease, and the metabolic strategies developed by cancer cells in order to survive to several tumour environmental stresses, in particular hypoxia and anti-cancer drugs, will be thoroughly presented.

1.1 CANCER AS AN EVOLUTIONARY DISEASE

In 1976 Nowell's described cancer as an evolutionary disease, proposing that the majority of neoplasms present a unicellular origin, and that the tumour progression results from acquired genetic variability within the original clone, allowing the sequential selection of more aggressive subclones [20]. In 1975, Cairns had also argued cancer as an evolutionary process, driven by mutation and natural selection [21]. Thus, cancer cells evolve under the same rules as Darwin's finches on the Galapagos, in which several genetically heterogeneous individual cells that are present within a tumour, fight for growth and survival in continuously changing environments [22]. Therefore, cancer is an evolutionary and an ecological process, being cancer cells subject to competition for space and resources, predation by the immune system and cooperation to disperse and colonise new organs [23,24]. Strengthening the relevance of evolution and ecology on cancer, recently, Maley and colleagues have developed an evolutionary and ecological classification system for neoplasms in order to improve the clinical management of cancer. Hence, the authors proposed the classification of neoplasms based on the Evo-index, including the intratumoural heterogeneity and its changes over time, and the Eco-index, including the hazards to neoplastic cell survival and the resources available to these cells [25].

Hypoxia and acidosis are common features of the tumour microenvironment, being highly selective and inducing genetic instability, hence promoting somatic evolution [26]. Cytotoxic anti-cancer drugs also drive evolution of cancer cells, by imposing strong evolutionary selection pressures on the surviving cells [26]. In the next sections we will focus

on the strategies that cancer cells evolve in order to cope both with hypoxia and with anti-cancer drugs, allowing disease progression and resistance to treatment.

1.1.1 HYPOXIA: A POWERFUL SELECTION PRESSURE ON MALIGNANT PHENOTYPES

Several microenvironmental conditions such as hypoxia, ROS and acidosis, that are common features of the tumour microenvironment, impose highly selective pressures in cancer cells, inducing also genetic instability [26].

As a solid tumour grows, cancer cells are exposed to regions of hypoxia, strictly linked to oxidative stress [27,28] and known to be responsible for tumour progression and resistance to therapy [29,30]. Evidence suggest that 50 to 60% of locally advanced solid tumours contain regions of hypoxia and/or anoxia caused by an oxygen delivery and consumption imbalance [4,29]. This is mainly due to abnormal vasculature together with the high proliferation rates of cancer cells [4]. In here, we will focus on how cancer cells evolve adaptive mechanisms to cope with oxidative stress, an imbalanced ratio between ROS production and the cellular antioxidant capacity [31], addressing the role of antioxidant defence systems and the role of hypoxia-inducible transcription factors (HIF) in mediating hypoxia adaptation.

The evolution of aerobic respiration is closely linked with the evolution of anti-oxidant defence systems [32]. Aerobic organisms present several antioxidant defensive systems, including enzymatic and non-enzymatic antioxidants that react and inactivate ROS [33]. Moreover, in order to maintain oxygen homeostasis, metazoan organisms present the hypoxic signalling pathway that allows oxygen delivery and cellular adaptation to oxygen deprivation [30].

The primary antioxidant enzymes include superoxide dismutases (SODs) (catalysing the dismutation of superoxide anion radical into hydrogen peroxide (H_2O_2)); catalase and glutathione peroxidase (GPX) (which convert H_2O_2 into water and oxygen) and glutathione reductase (GRx) that removes H_2O_2 by oxidation of reduced glutathione (GSH) into oxidised glutathione (GSSG). GRx then regenerates GSH from GSSG, with NADPH as a reducing agent. GPx also reduces lipid or nonlipid hydroperoxides concomitant with GSH oxidation [33,34]. Peroxiredoxins (PRXs) and thioredoxin (Trx) are other important antioxidant enzymatic systems. The thioredoxin reductase (Trx) system is formed by thioredoxin

reductase (TrxR), Trx and NADPH. TrxR is a selenoprotein involved not only in the regulation of the cellular redox status but also in redox control of transcription factors, oxidative stress defence, and cell growth [31]. Peroxiredoxins (PRXs) are considered one of the most important cell redox state-regulating enzymes, reducing alkyl hydroperoxides and H_2O_2 to the corresponding alcohol or water [31]. The figure 1 illustrates the cellular antioxidant systems.

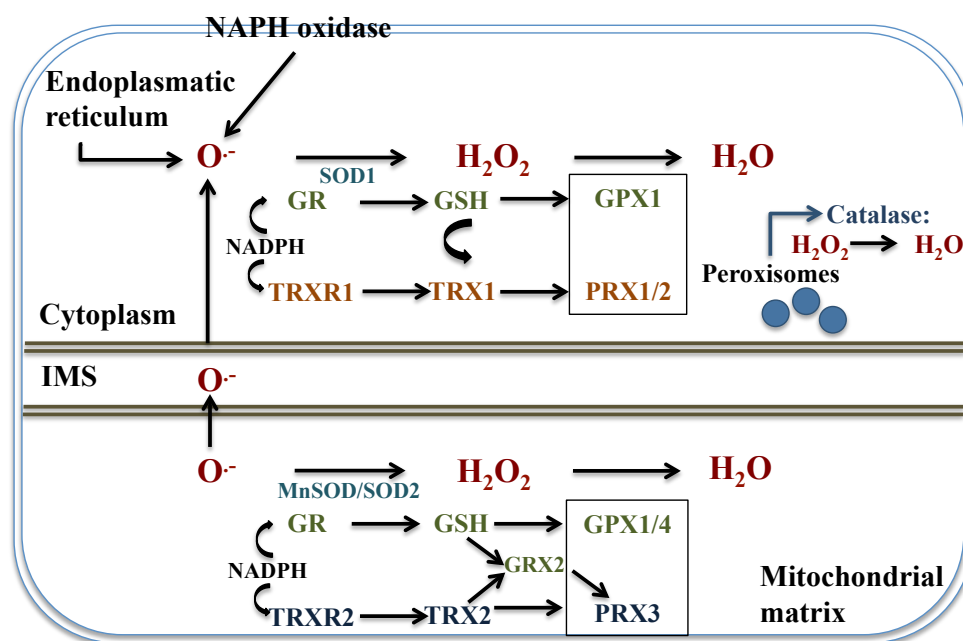


Figure 1. Cellular antioxidant systems.

The major sources of ROS are the mitochondria, NAPH oxidase, and the endoplasmic reticulum [35]. Anion superoxide ($O^{\cdot -}$) is the principal form of ROS which is rapidly converted into hydrogen peroxide (H_2O_2) by superoxide dismutase (SOD) [35]. In the cytosol, this reaction is catalysed by SOD1, whereas in the mitochondria, this reaction is catalysed MnSOD and SOD2 [36]. H_2O_2 can be then catalysed by GSH peroxidase (GPX), peroxiredoxins (PRXs) (dependent or thioredoxin-dependent peroxide reductases) and catalase. GPX reduce hydroperoxides using GSH as a substrate and generating GSSG, which can be then reduced by GSH reductase (GR) [35]. The thioredoxin system includes thioredoxin (TRX), PRX and thioredoxin reductase (TRXR) and is essential for counteracting oxidative stress by removing hydrogen peroxide (H_2O_2) [37].

This system donates electron to thioredoxin-dependent peroxidases (Prx1 and 2 in the cytosol and 3 in the mitochondria). In the mitochondria PRX3 can also be reduced by glutaredoxin 2 (GRX2).

Peroxiredoxins (PRXs) reduce alkyl hydroperoxides and H_2O_2 to their corresponding alcohol or H_2O [35]. There is a crosstalk between GSH and thioredoxin systems, where the GSH system can also reduce TRX1 in the cytoplasm [38].

Both Trx and glutaredoxin (Grx) reduce protein disulphides and Grx also catalyses protein deglutathionylation [39]. Adapted from Nogueira and Hay [36], Marengo and colleagues [35], Castaldo *et al.* [40] and Lu *et al.* [38]. IMS - inter mitochondrial space.

The nonenzymatic antioxidants include metabolic and nutrient antioxidants. The metabolic ones belong to endogenous antioxidants, result from body's metabolism and the most relevant are lipid acid, L-arginine, coenzyme Q10, melatonin, uric acid, bilirubin,

metal-chelating proteins, transferrin and GSH [33]. Importantly, GSH is a thiol present in almost all animal cells [41], that can function as a reducing agent, an antioxidant, a free-radical scavenger and is also involved in the metabolism of xenobiotics and other cell molecules [42]. The nutrient antioxidants belong to exogenous antioxidants being provided through diet, including vitamin E, vitamin C, carotenoids, trace metals (selenium, manganese, zinc), flavonoids, omega-3 and omega-6 fatty acids [33].

The transcription factor nuclear factor-erythroid 2 (NF-E2) p45-related factor 2 (Nrf2) is a pivotal player in cellular redox homeostasis regulation, strongly influencing intrinsic resistance to oxidative stress and controlling adaptive responses to several stressful environmental conditions [43]. Nrf2 is not only involved in the regulation of the GSH-based antioxidant system, but also regulates the expression of cytosolic thioredoxin (TRX1), TrxR1 and sulphiredoxin1 [43].

In order to counteract oxidative stress, cancer cells present enhanced antioxidant defence systems [44,45] that actively upregulate and contribute to tumour progression [44–47]. For instance, increased levels of both GSH and glutamate cysteine ligase (GCL) were reported in several human cancer tissues (reviewed in [48]). TrxR expression was also found to be upregulated in several human cancers, including breast, thyroid, liver, prostate carcinomas and melanoma (reviewed in [31]). In human colorectal carcinomas, both increased TrxR activity and expression were found (reviewed in [31]). Moreover, the increased expression of PRXs was also found in several cancer cell types and experimental evidence have shown that the silencing of several PRXs sensitises cancer cells to ROS-induced apoptosis [49]. Strikingly, Roh *et al.* reported that the inhibition of both GSH and TRX systems presented a synergistic effect on head and neck cancer cells death, but the effect was suboptimal due to the activation of Nrf2-antioxidant response element pathway in resistant cells [45]. However, with the simultaneously blocking of GSH, Trx and the Nrf2-ARE pathways, the authors were able to eliminate the resistant head and neck cancers [45]. These results strongly support a key role of the antioxidant defence systems in cancer biology, thus suggesting that targeting multiple antioxidant pathways simultaneously could be a successful strategy to fight several types of cancer.

Importantly, hypoxia is known to activate HIF signalling within tumours. Besides the enhanced antioxidant defence systems, intratumoural hypoxia activates HIF-1 and HIF-2, with HIF-1 α overexpression being strongly associated with increased metastasis and mortality in several cancer types [50,51]. HIF-1 α targets includes genes involved in angiogenesis, glucose metabolism, cell proliferation/viability, invasion and migration, thus,

the upregulation of HIF-1 α activates several hallmarks of cancer [51]. Benita and colleagues have shown that the cellular response to hypoxia differs between cell types and reported over 6000 differentially expressed genes under hypoxia [52], thus showing the complexity of the cellular hypoxia response via HIF-1. Moreover, Malec and colleagues have reported a role of NADPH oxidase subunit NOX1 in the activation of Nrf2 by protein stabilization, which subsequently induced TRX1 expression, resulting in enhanced HIF-1 α signalling under intermittent hypoxia conditions in adenocarcinoma A549 cells [53]. The authors have provided, therefore, a link between Nrf2 and HIF-1 α pathways in cancer cells [53].

Finally, hypoxia can also drive and maintain genetic instability and a mutator phenotype [54], increasing the levels of genetic variation among cells, thus accelerating the rate of somatic evolution in carcinogenesis [8]. In fact, increased mutagenesis was observed in cells exposed to *in vitro* and *in vivo* hypoxic conditions, confirming the hypothesis that the hypoxic environment drives a mutator phenotype [54–56]. Importantly, the deregulation of HIF-1 α was reported to promote the malignant phenotype and genomic instability through interplay with oncoproteins like c-MYC [57]. Koshiji and colleagues also reported a role of HIF-1 α in hypoxia-induced genetic instability through the inhibition of MutS α expression, a DNA mismatch repair gene [58].

With this section, we intended to clearer the key role of hypoxia in driving and maintaining malignant and aggressive phenotypes. In the next section we will focus on how cancer cells escape from drugs-induced death, a feature that is also intimately related with hypoxia.

1.1.2 ESCAPING FROM DRUGS-INDUCED DEATH: THERAPY, A POWERFUL SELECTIVE PRESSURE ON CANCER CELLS EVOLUTION

Besides hypoxia, cytotoxic cancer therapies also impose intense evolutionary selection pressures on cancer cells [26] that evolve mechanisms enabling drug-induced death avoidance. Drug resistance can be intrinsic (exists prior to treatment) or acquired during treatment [59] and two general causes of drug resistance exist: host factors and specific genetic or epigenetic alterations in the cancer cells [60]. Importantly, tumours present a high molecular heterogeneity [61], allowing therapy-induced selection of a resistant subpopulation of cells, thus leading to drug resistance emergence [59].

Several mechanisms were already associated with drug resistance, including the

increased drug efflux and decreased drug influx, drug inactivation, alterations in drug target, increased DNA damage repair, deregulation of apoptosis, autophagy, activation of prosurvival signalling, oncogenic bypass and pathway redundancy and epithelial–mesenchymal transition [59]. The tumour microenvironment has been implicated not only in tumour growth, invasion, and metastasis but also in acquired drug resistance, mediated by myeloid cells, cancer-associated fibroblasts, mesenchymal stem cells and the interaction with the extracellular matrix [62]. Moreover, hypoxia is a common tumour microenvironmental condition that is intimately related to chemoresistance driven by the cellular responses described previously and also by other factors such as decreased drug activity in the absence of O₂; decreased drug effect in hypoxic cells with low proliferation rates or with altered pH gradients; induction of gene amplification; and a generally insufficient drug delivery to cells that are far from functional vasculature [54].

Because this thesis is focused on ovarian cancer, which is conventionally treated with surgery combined with carboplatin-paclitaxel chemotherapy [63], we will focus on the resistance mechanisms described to these drugs.

It is well known that platinum-based therapy involves ROS-mediated apoptosis [64–66]. Cisplatin and carboplatin are highly reactive molecules that bind to RNA, DNA and proteins, leading to the formation of adducts [63,66]. The nuclear DNA adducts are thought to be mainly responsible for cisplatin cytotoxicity, inducing cell death as a result of DNA damage and inhibition of replication and transcription [63,66]. Marullo *et al.* reported a role of cisplatin also in ROS production driven by protein synthesis impairment [66]. Strikingly, cisplatin and carboplatin resistance can be achieved by several different mechanisms such as decreased drug uptake, increased efflux, intracellular inactivation, mismatch repair deficiency, increased DNA repair, defective apoptosis, anti-apoptotic factors effects of several signalling pathways or extracellular matrix factors, showing the high complexity involved in platinum-drug resistance [67,68]. Importantly, GSH is known to mediate resistance both to cisplatin and carboplatin through several mechanisms, such as drug uptake reduction and increased intracellular drug detoxification/ inactivation, increased DNA repair and inhibition of apoptosis drug-induced oxidative stress [67,69–71]. Moreover, Champa and colleagues have selected multiple carboplatin resistant clones derived from a single cell that, while presenting no significant genetic alterations, each resistant clone activated different resistance mechanisms, leading to transcriptional heterogeneity [72]. These results strengthen again the complexity involved in the platinum acquired resistance.

Paclitaxel cytotoxicity is associated with its binding to intracellular β -tubulin, which

leads to microtubule stabilization, G2-M arrest and apoptosis [63,73]. However, Alexandre *et al.* reported that paclitaxel exposure also induces ROS production, as H₂O₂ accumulation showed to be an early and crucial step in paclitaxel cytotoxicity [65]. Concerning paclitaxel resistance, also several different mechanism have been reported including over-expression of transmembrane efflux transporters, tubulin mutations or alterations in the microtubules stability and decreased function of apoptotic proteins [74]. Interestingly, Datta and colleagues reported increased activity of antioxidant systems during paclitaxel resistance development. The authors have shown a gradual increase in GSH content and in the activities of catalase and glutathione peroxidase (GPX) along with paclitaxel resistance development in A549 human lung adenocarcinoma cells [75], thus linking GSH also with paclitaxel resistance.

Recently, Vaidyanathan and colleagues, using the ovarian cancer cell line A2780 have developed several drug-resistant cell lines, and reported that A2780 resistant to both carboplatin and paclitaxel (A2780cpR) cells presented a distinct phenotype, that differed from both A2780 carboplatin resistant and A2780 paclitaxel resistant cells. Importantly, they have identified significant increases in the expression of targetable phosphoproteins important in cell signalling, such as pATM, pAKT, pCHK1 and pGSK3b in A2780cpR cells. The authors also compared the expression of 377 miRNAs in their cell line panel, and have identified several differentially expressed miRNAs, common to all resistant cells and exclusive to each drug-resistant phenotypes [76].

It is crucial to emphasize that conventional cancer therapies, which administer cytotoxic drugs at maximum tolerated doses until progression, strongly select for resistant phenotypes and, by eliminating all the competitors, allow a rapid proliferation of the resistant populations even in the absence of drugs - an evolutionary phenomenon designated “competitive release” [77–79]. However, as more and more evidence accumulates highlighting cancer as an evolutionary disease, in 2011, Atkipis *et al.* analysed 6228 publications concerning therapeutic resistance and/or cancer relapse and reported that in abstracts, evolution terms were present in only about 1% since the 1980s [80]. Moreover, Darwinian dynamics are still rarely integrated into anti-cancer protocols in clinical contexts [79].

In 2009, Gatenby and colleagues have explored the conceptual model of adaptive therapy that defends that, since the tumour populations that are exposed to treatment are dynamic, the treatment should be also dynamic with continuous adjustment of drugs, dose, and timing [81], thus employing a therapeutic strategy that evolves along with cancer cells. The authors have developed mathematical models that predicted that an optimal treatment strategy adjust therapy in order to maintain a stable population of chemosensitive cells that are more fitted in

the absence of therapy, being able to inhibit the growth of resistant populations due to fitness costs of resistance [81]. The same authors confirmed the benefits of the adaptive therapy in *in vivo* experiments with OVCAR3 xenografts treated with carboplatin, showing that this strategy was able to maintain a stable tumour population for a prolonged period of time, allowing a long-term survival [81]. Enriquez-Navas and colleagues reported similar findings in different preclinical models of breast cancer [78]. Gallaher *et al.* went furthered and identified two different adaptive strategies that are able to control heterogeneous tumours, a dose modulation strategy that controls the majority of tumours with fewer drug, and a more vacation-oriented strategy that is able to control more invasive tumours [82]. Interestingly, by using single-cell DNA sequencing, Xue and colleagues found that parallel evolution lead to the selection and spread of different *BRAF*-amplified subclones, allowing the tumours to adapt to ERK inhibitor treatment while maintaining intratumoral heterogeneity [83]. They proposed the fitness threshold model to explain their findings, being the fitness threshold the barrier that subclonal populations have to overcome in order to recover fitness during drug treatment. The model predicted that sequential treatment was not effective, prediction that was supported by their results showing that treatment with a RAF inhibitor followed by an ERK inhibitor induced a gradual increase in *BRAF* copy number, allowing a fitness advantage in the presence of the drugs [83]. Moreover, the same authors reported that an intermittent three-drug treatment combination was able to inhibit tumour growth in *BRAF*^{V600E} patient-derived tumour xenografts models for lung cancer and melanoma, hence being able to increase the fitness threshold and counteracting the spread of subclones with *BRAF*-amplification [83].

Recently, Zhang and colleagues have integrated evolutionary dynamics into a pilot clinical trial of patients with metastatic castrate-resistant prostate cancer in order to avoid the evolution of resistance to abiraterone (that inhibits CYP17A, an enzyme responsible for testosterone auto-production). The authors reported that the adaptive therapy treatment increased time to progression and reduced the cumulative drug dose to less than a half compared to the standard strategy [79].

As Gallaher and colleagues argued, the future of precision medicine should not be (only) in the development of new drugs. Instead, evolutionary principles should be applied (also) in the pre-existing ones [82].

1.2 EPITHELIAL OVARIAN CANCER

This thesis is focused on ovarian cancer, in particular epithelial ovarian cancer (EOC, ovarian carcinoma), hence, in this section, we will emphasise on the diverse histopathology and molecular/genetic features of this disease.

Ovarian cancer includes a group of distinct diseases that present a common anatomical location [84], corresponding to the major cause of death from gynaecological cancer and the third most common gynaecological malignancy worldwide [85]. The risk factors for this disease currently include genetic, physiological, socioeconomic and environmental aspects [86]. Despite the overall survival of ovarian cancer patients has been improved in the last 30 years, the cure rate did not [87]. This is mainly due to late diagnosis and resistance to therapy [88,89], barring ovarian cancer cure.

EOC includes most ovarian malignancies [88,90] that can be classified based on histopathology and molecular/genetic features, being the ovarian carcinomas mainly classified as serous low grade (LG-OSC, <5%) and high-grade (HG-OSC, 70%), endometrioid (OEC, 10%), clear cell (OCCC, 10%) and mucinous (OMC, 3%) [91,92]. Recently, the histological types seromucinous carcinomas and Brenner tumours were also included [93]. Each of the main histological subtypes were already associated to a specific genetic and transcriptional signature: LG-OSC generally comprising proto-oncogene serine/threonine-protein kinase variant B (*BRAF*), Kirsten RAS oncogene (*KRAS*), neuroblastoma RAS viral oncogene homolog (*NRAS*), Erb-B2 receptor tyrosine kinase 2 (*ERBB2*) mutations; HG-OSC comprising mutations in Tumour Protein P53 (*TP53*), *BRCA1/2*, Neurofibromin 1 (*NF1*), RB transcriptional corepressor 1 (*RBI*), Cyclin Dependent Kinase 12 (*CDK12*), homologous recombination repair of DNA damage defective in approximately 50% of HG-OSC and alterations in signalling pathways such as PI3K/Ras/Notch/FoxM1. The OEC subtype involve mutations in AT-Rich Interaction Domain 1A (*ARID1A*), Phosphatidylinositol-4,5-Bisphosphate 3-Kinase Catalytic Subunit Alpha (*PI3KCA*), Phosphatase and Tensin homolog (*PTEN*), Protein Phosphatase 2 Scaffold Subunit Alpha (*PPP2R1α*), and mismatch repair deficiency. The OCCC subtype comprises *de novo* expression of HNF1β [94,95] and *ARID1A*, *PI3KCA*, *PTEN*, Catenin Beta 1 (*CTNNB1*) and *PPP2R1α* mutations. The OMC subtype comprises tumours with mutations in *KRAS* and high frequency of *ERBB2* amplification with overexpression of mucin coding genes [96,97].

HG-OSC is the most prevalent histological type [89] with diagnosis at an advanced stage in approximately 70% of patients [84]. In contrast, OCCC, is a rather uncommon histological type of ovarian cancer that is frequently diagnosed at an initial stage [98]. However, OCCC tumours present markedly different clinical behaviours compared to other EOC subtypes presenting, generally, poor prognosis given intrinsic chemoresistance to conventional platinum or taxane-based therapy [98] which, together with surgery, constitute the standard care for ovarian cancer [63].

Despite initial response to treatment, 85% of advanced ovarian cancer patients suffer from disease recurrence [99], being of extremely importance to deepen our knowledge on this group of diseases in order to gain insight in novel possible strategies to fight them.

1.3 CYSTEINE IN CANCER

L-cysteine is a semi-essential amino acid [100,101] present extracellularly mainly in its oxidised form cystine, and intracellularly mainly in the form of cysteine due to the highly intracellular reducing conditions [102]. This amino acid plays an essential role in cellular homeostasis, as cysteine is a precursor of protein synthesis, GSH, taurine, hydrogen sulphide (H_2S) [103,104], pyruvate and coenzyme A [103]. L-cysteine sources are the absorption from diet, the transsulphuration pathway from L-methionine degradation, endogenous proteins and GSH degradation [100]. Several systems were already associated with L-cysteine and L-cystine transport, such as A, ASC, L, Xc-, Bo,+ , and X-AG systems [101].

The intracellular free cysteine pool is tightly regulated in the mammalian liver [103]. L-cysteine synthesis occurs through condensation of serine and methionine-derived homocysteine to form L-cystathionine, being this reaction catalysed by cystathionine- β -synthase (CBS). Subsequently, L-cystathionine is converted into cysteine, α -ketobutyrate and ammonia by cystathionine- γ -lyase (CSE) [100].

In the next sections we will focus on the role of cysteine in cancer, mediated by both GSH and H_2S generation. Interestingly, Visscher *et al.* reported that many oncogenic mutations consist in an insertion of a novel cysteine in the protein sequence [105]. They also reported that acquired cysteines account for at least 12% of all activating mutations found in *KRAS* in cancer, and 88% of mutations in fibroblast growth factor receptor (*FGFR*). They suggested that when acquired cysteines are found that often, they should play a role in tumorigenesis [105] probably by contributing for tumour suppressor genes inactivation and

oncogenes activation.

1.3.1 CYSTEINE ROLE IN CANCER AS A PRECURSOR OF THE ANTIOXIDANT GSH

Rey-Pailhade's described Philothion in 1888, as a molecule that reacted spontaneously with sulphur, producing hydrogen sulphide [106,107]. Years later, Hopkins' concluded that Philothion and GSH were identical and in 1935, its' structure was established as a tripeptide, composed by glutamic acid, cysteine, and glycine [106,108]. Since then, a countless number of papers have been published regarding GSH role in health and disease.

GSH is mainly found in Gram-negative bacteria and eukaryotes, being rare in Gram-positive bacteria. In Archaea or in amitochondrial eukaryotes, GSH is not generally found, leading Copley and Dhillon to suggest that bacteria transferred the genes for GSH biosynthesis to eukaryotes via the progenitor of mitochondria [109]. However, the evolutionary history of GSH biosynthesis genes showed to be more complex, as data suggested that these genes evolved separately and their spread possibly involved events of horizontal gene transfer, including a transfer from an alpha-proteobacterium to a plant and also convergent evolution [109], as bacterial and eukaryotic proteins share a common structural fold, but with very divergent sequences.

The built blocks of GSH are glutamic acid, cysteine and glycine, which biosynthesis involves two ATP-requiring enzymes: glutamate cysteine ligase (GCL) and GSH synthetase. The first enzyme catalyses the formation of a dipeptide bond between the γ -carboxylate of glutamic acid and the amino group of cysteine and the latter catalyses the subsequent formation of a peptide bond between the cysteinyl carboxylate of γ -Glu-Cys and the amino group of glycine. Besides substrate availability, GCL is the rate-limiting enzyme in GSH synthesis, which presents two different subunits: the catalytic subunit (GCLC), containing the active site responsible for the bond formation between the amino group of cysteine and the γ -carboxyl group of glutamic acid, and the modifier subunit (GCLM) that interacts with GCLC, increasing the catalytic efficiency of GCLC [110].

It is well known that GSH not only plays a main role in intracellular redox balance [108] but it is also pivotal in cellular processes such as cell differentiation, proliferation, and apoptosis [42,111,112]. Moreover, GSH was associated to resistance to ionizing radiation and drug-induced cytotoxicity [41,42,112–114].

As already mentioned, GSH is known to mediate resistance both to cisplatin and carboplatin through several mechanisms [67,69–71]. Specifically in ovarian cancer, although with some controversy [115,116], several reports already associated high GSH levels or glutathione S-transferase P1 (GSTP1) activity with cisplatin or carboplatin resistance [117–124]. More recently, Sawers *et al.* [125] have shown that the stable deletion of GSTP1 significantly and selectively increased sensitivity both to cisplatin and carboplatin in A2780 ovarian cancer cells [125]. Crawford and Weerapana, reported a dichlorotriazine-containing compound (LAS17) that selectively and irreversibly inhibited GSTP1 activity, thus providing a promising cancer therapeutic target [126]. In addition, Chen *et al.* have shown that the overexpression of the microRNA miR-133b increased ovarian cancer cell sensitivity to both cisplatin and paclitaxel by decreasing GSTP1 and Multi-Drug Resistance protein 1 (MDR1) expression [127]. Okuno *et al.* [128] reported that the transport system x_c^- (xCT), involved in cystine and glutamate transport, was associated with intracellular GSH level and with cisplatin resistance in human ovarian cancer cell lines. Wang and colleagues explored the role of ovarian cancer cells microenvironment and showed that fibroblasts decreased the nuclear accumulation of platinum in cancer cells, through GSH and cysteine release. On the other hand, they demonstrated that CD8⁺T cells counteracted this resistance by changing GSH and cysteine metabolism in fibroblasts [129]. Moreover, Moheel and colleagues reported an active methylene quinuclidinone compound derived from the prodrug APR-246 (PRIMA-1^{MET}), that not only binds to cysteine residues in mutant p53, restoring its wild-type conformation, but also binds to cysteine from GSH, leading to decreased intracellular free GSH concentrations [130]. This compound was able to restore the sensitivity to both cisplatin and doxorubicin of p53-mutant drug-resistant ovarian cancer cells [130].

Importantly, our team [131] found differences among ovarian cancer histotypes in what concerns to carboplatin resistance and GSH levels. We have found that OCCC cells were more resistant to carboplatin than HG-OSC cells, and that the inhibition of GSH production by L-Buthionine Sulfoximine (BSO) sensitised these cells to carboplatin, both *in vitro* and *in vivo* [131]. Those results highlight that ovarian cancer is a complex disease in which, each histotype presents unique features in what concerns to thiols metabolism and response to chemotherapeutic agents that should be taken into account in the clinical context.

Paradoxically, concerning the role of GSH in paclitaxel resistance, Liebmann *et al.* have shown that the depletion of cellular GSH by BSO resulted in increased resistance to taxol in MCF-7 and A549 cells [132]. However, Medeiros *et al.* reported that patients with ovarian cancer, who are carriers of glutathione-S-transferase class μ (*GSTM1*)-null genotype or

carriers of non-*GSTM1-wt/ GSTT1-wt* genotypes- when treated with both paclitaxel and cisplatin, presented higher mean survival time [133], suggesting a role for GSH also in paclitaxel resistance. As already mentioned, Datta and colleagues have shown a gradual increase in GSH content and in the activities of catalase and glutathione peroxidase (GPX) along with paclitaxel resistance development in A549 human lung adenocarcinoma cells [75], linking GSH with paclitaxel resistance once again.

Therefore, evidence suggests a critical role of GSH in mediating resistance especially to platinum-based drugs. Moreover, cysteine is the thiol component of GSH and the reversible thiolation of proteins was already associated with the regulation of several metabolic processes such as enzyme activity, transport activity, signal transduction and gene expression [112]. Several proteins - such as Rat Sarcoma virus (Ras) protein, Jun N-terminal Kinase (JNK)- 2, Activator Protein 1 (AP-1), Nuclear Factor-kappaB (NFkB), Protein Kinase C (PKC), caspases, thioredoxin and p53 [112,134], which are known to have important roles in ovarian cancer [135–146], are regulated by thiol oxidation [134]. Interestingly the oxidation of cysteine residues of p53 induces the protein inactivation, which accounts for carcinogenesis [134].

1.3.2 CYSTEINE ROLE IN CANCER AS A SOURCE OF H₂S

In 2002, Wang proposed H₂S as another gasotransmitter, along with nitric oxide and carbon monoxide [147]. H₂S is involved in several biological processes such as autophagy, cellular metabolism, stem cells fate regulation, inflammation, cell cycle and cell death, being crucial both in health and disease [148]. This signalling molecule interacts and modifies target proteins through reaction with metal cores and through cysteine persulfidation, leading to protein structure and function changes [149].

In mammalian cells, H₂S is generated mainly via enzymatic pathways and from the metabolism of L-cysteine by the catalysis of three key enzymes: cystathionine β-synthase (CBS), cystathionine γ-lyase (CSE) and by 3-mercapto-pyruvate sulphurtransferase (MpST) accompanied by cysteine aminotransferase (CAT) [150], enzymes that were already reported to be altered in several types of cancer (reviewed in [151]). Importantly, H₂S exhibits both pro-cancer (through bioenergetics and angiogenesis stimulation, inhibiting apoptosis and promoting cell cycle progression) and anti-cancer (by inducing uncontrolled cellular acidification, suppressing cell survival and inducing cell cycle arrest) activities (reviewed in

[151]).

H₂S is the only inorganic compound presenting a bioenergetic role in mammalian cells mitochondria [152]. At low concentrations (nM), H₂S is known to stimulate mitochondrial bioenergetics through different mechanisms: through donation of electron equivalents to the quinol pool via sulphide:quinone oxidoreductase; by the glycolytic enzyme glyceraldehyde 3-phosphate dehydrogenase activation, and by persulfidation of ATP synthase (reviewed in [149]). Módis and colleagues, using isolated mitochondria from rat liver and murine hepatoma cells observed that an endogenous intramitochondrial H₂S-producing pathway, governed by MpST complemented and balanced the bioenergetic role of Krebs cycle-derived electron donors [153]. In addition, Li and Yang reported a role of CSE/H₂S system in enhancing mtDNA replication and cellular bioenergetics both in smooth muscle cells and mouse aorta tissues [154]. In human cancers, there is also evidence that H₂S inside mitochondria is able to sustain mitochondrial ATP production [155,156]. Specifically in the context of ovarian cancer, Bhattacharyya *et al.* found a role of CBS in promoting ovarian tumour growth, cisplatin resistance and cellular bioenergetics [155]. More recently, Chakraborty and colleagues reported a new role of CBS in the regulation of mitochondria morphogenesis, promoting tumour progression in ovarian cancer [157].

In particular under hypoxia conditions, H₂S was reported to induce ATP synthesis, mediated by CSE translocation to the mitochondria in vascular smooth muscle cells [158] and to decrease ROS levels, mediated by CBS accumulation in human hepatoma Hep3B cells [159]. In the kidney, especially in the medulla, experimental evidence supports a role of H₂S as an O₂ sensor, as a higher content of H₂S was found in renal medulla (that presents a lower O₂ availability) compared with the renal cortex [160]. If H₂S is a direct source of energy in renal medulla is still unclear [160]. A role of H₂S as an O₂ sensor was also already suggested in cardiovascular system, respiratory system and gastrointestinal tract [160].

H₂S was also found to be associated with malignancy and resistance to treatment in different types of cancer. Gai *et al.* observed a correlation between the increased protein levels and catalytic activities of CBS, CSE, and MpST and the increase of malignant degrees in human bladder tissues and human urothelial cell carcinoma of bladder cell lines [161]. Pan *et al.* explored the role of endogenous H₂S in hepatocellular carcinoma cells radiotherapy response. They observed that radiation treatment promoted the invasion capability of cells through epithelial-mesenchymal transition mediated by endogenous H₂S/CSE signalling via the p38MAPK pathway [162]. Sen and colleagues found a role for CBS in human breast cancer cells in the protection against oxidative stress induced by activated macrophages

[163]. Moreover, data have been supporting a role of H₂S as a pro-proliferative factor in human cancer cells by accelerating cell cycle progression [148].

However, as already mentioned, H₂S can be also disadvantageous for cancer cells. While, in general, endogenous or low exogenous H₂S levels are advantageous for cancer cells, the exposure to high levels is disadvantageous [151,164], exhibiting a bell-shaped curve effect [164]. Lee and colleagues reported that a slow-releasing H₂S donor, GYY4137, lead to cell death in a concentration-dependent manner in several human cancer cell lines, while it did not impair the survival of normal human lung fibroblasts [165]. Moreover, Panza and colleagues reported that CSE-derived H₂S leads to cell cycle arrest and induce apoptosis in human melanoma cells to a larger extent compared to CBS and MpST overexpression [166]. The same authors confirmed the role of CSE-derived H₂S in inhibiting melanoma tumour growth also in an *in vivo* mice model, since the protective effect of L-cysteine was lost when a selective CSE inhibitor was co-administrated to mice [166]. Interestingly, Takano *et al.* reported that decreased CBS expression in glioma induced HIF2 α protein levels and HIF2 target gene expression, promoting glioma tumour formation [167].

Together, evidence supports that cysteine is a pivotal player not only in ovarian cancer progression and resistance to treatment but also in several types of cancer, as it provides a dual role of cellular protection: GSH-mediated and H₂S-mediated chemoresistance, redox balance maintenance, and allows the regulation of several metabolic processes central to cancer cells, thus supporting their survival and adaptation to changing microenvironments.

1.4 HYPOTHESIS, AIMS AND THESIS OUTLINE

Ovarian cancer is the third most common gynaecological malignancy worldwide [85] and the major cause of death from gynaecological cancer, mainly due to late diagnosis and resistance to therapy [85,88,89].

Cysteine role in cancer cells survival was already associated with its role as a precursor of the antioxidant glutathione (GSH) [48,131,168] and due to hydrogen sulphide (H₂S) generation [113,114,119,120,122,121,125], leading us to hypothesise that cysteine metabolism plays an essential role in cancer cells selection and tumour progression on one hand, as a thiol, contributing for the dynamics of thiol synthesis and degradation that are determinant to cancer chemoresistance and adaptation to hypoxia; and on the other hand, as a

sulphur source mediated by H₂S generation able to sustain ATP production under hypoxic conditions.

Hence, our main focus is to clarify the relevance of cysteine metabolism in ovarian cancer cells selection and tumour progression. Thus, the major aims of this thesis are:

- 1) to explore the effect of ovarian cancer cells selection under normoxia and hypoxia conditions on cells response to carboplatin, and the effect of cysteine supplementation in this response (Chapter 2);
- 2) to address if cysteine has a widespread protective effect in ovarian cancer cells against hypoxia and carboplatin-induced death (Chapter 3);
- 3) to explore if cysteine has a clinical role in ovarian cancer patients (Chapter 3);
- 4) to disentangle the mechanism by which cysteine protects ovarian cancer cells from hypoxia-induced death (Chapter 4).

This thesis includes 5 chapters. In the 1st chapter there is a presentation of a general theoretical framework concerning the issues approached in this thesis. The following chapters include the results obtained in this PhD project (Chapter 2-4). Each chapter contains an abstract, a short introduction, methods, results and discussion. In the final chapter (Chapter 5), a global discussion on the relevance of the major findings of this thesis in ovarian cancer research is presented as well as future perspectives to follow some new research lines paved by this project.

1.5 REFERENCES

1. Fitzmaurice C, Dicker D, Pain A, Hamavid H, Moradi-Lakeh M, MacIntyre MF, *et al.* The Global Burden of Cancer 2013. *JAMA Oncol.* 2015;1:505–27.
2. Ferlay J, Soerjomataram I, Ervik M, Dikshit R, Eser S, Mathers C, Rebelo M, Parkin DM, Forman D, Bray F. GLOBOCAN 2012 v1.0, Cancer Incidence and Mortality Worldwide: IARC CancerBase No. 11. Lyon, Fr. Int. Agency Res. Cancer. 2013 [cited 2018 Aug 24]. Available from: <http://globocan.iarc.fr>
3. Ferlay J, Soerjomataram I, Ervik M, Dikshit R, Eser S, Mathers C, Rebelo M, Parkin DM, Forman D, Bray F. GLOBOCAN 2012 v1.0, Cancer Incidence and Mortality Worldwide: IARC CancerBase No. 11. Lyon, Fr. Int. Agency Res. Cancer. 2013 [cited 2018 Aug 30]. Available from: <http://globocan.iarc.fr>
4. Rankin EB, Giaccia AJ. Hypoxic control of metastasis. *Science.* 2016;352:175–80.

5. <https://www.cancerresearchuk.org/>
6. Hanahan D, Weinberg RA. The hallmarks of cancer. *Cell*. 2000;100:57–70.
7. Hanahan D, Weinberg RA. Hallmarks of cancer: The next generation. *Cell*. 2011;144:646–74.
8. Crespi B, Summers K. Evolutionary biology of cancer. *Trends Ecol. Evol.* 2005;20:545–52.
9. Warburg O. On the Origin of Cancer Cells On the Origin of Cance. *Source Sci. New Ser.* 1956;123:309–14.
10. Rodríguez-Enríquez S, Torres-Márquez ME, Moreno-Sánchez R. Substrate oxidation and ATP supply in AS-30D hepatoma cells. *Arch. Biochem. Biophys.* 2000;375:21–30.
11. Rodríguez-Enríquez S, Vital-González PA, Flores-Rodríguez FL, Marín-Hernández A, Ruiz-Azuara L, Moreno-Sánchez R. Control of cellular proliferation by modulation of oxidative phosphorylation in human and rodent fast-growing tumor cells. *Toxicol. Appl. Pharmacol.* 2006;215:208–17.
12. Guppy M, Leedman P, Zu X, Russell V. Contribution by different fuels and metabolic pathways to the total ATP turnover of proliferating MCF-7 breast cancer cells. *Biochem. J.* 2002;364:309–15.
13. Viale A, Corti D, Draetta GF. Tumors and mitochondrial respiration: a neglected connection. *Cancer Res.* 2015;75:3685–6.
14. Alam MM, Lal S, FitzGerald KE, Zhang L. A holistic view of cancer bioenergetics: mitochondrial function and respiration play fundamental roles in the development and progression of diverse tumors. *Clin. Transl. Med.* 2016;5:3–16.
15. Yu L, Lu M, Jia D, Ma J, Ben-Jacob E, Levine H, *et al.* Modeling the Genetic Regulation of Cancer Metabolism: Interplay Between Glycolysis and Oxidative Phosphorylation. *Cancer Res.* 2017;77:1564–74.
16. Liu T, Yin H. PDK1 promotes tumor cell proliferation and migration by enhancing the Warburg effect in non-small cell lung cancer. *Oncol. Rep.* 2017;37:193–200.
17. Liang C, Qin Y, Zhang B, Ji S, Shi S, Xu W, *et al.* ARF6, induced by mutant Kras, promotes proliferation and Warburg effect in pancreatic cancer. *Cancer Lett.* 2017;388:303–11.
18. Lopes-Coelho F, Nunes C, Gouveia-Fernandes S, Rosas R, Silva F, Gameiro P, *et al.* Monocarboxylate transporter 1 (MCT1), a tool to stratify acute myeloid leukemia (AML) patients and a vehicle to kill cancer cells. *Oncotarget.* 2017;8:82803–23.
19. Liberti M V., Locasale JW. The Warburg Effect: How Does it Benefit Cancer Cells? *Trends Biochem Sci.* 2016;41:211–8.
20. Nowell PC. The clonal evolution of tumor cell populations. *Science.* 1976;194:23–8.
21. Cairns J. Mutation selection and the natural history of cancer. *Nature.* 1975;255:197–200.
22. Polyak K. Breast cancer stem cells: A case of mistaken identity? *Stem Cell Rev.* 2007;3:107–9.
23. Merlo LMF, Pepper JW, Reid BJ, Maley CC. Cancer as an evolutionary and ecological process. *Nat. Rev. Cancer.* 2006;6:924–35.
24. Axelrod R, Axelrod DE, Pienta KJ. Evolution of cooperation among tumor cells. *Proc. Natl.*

Acad. Sci. U. S. A. 2006;103:13474–9.

25. Maley CC, Aktipis A, Graham TA, Sottoriva A, Boddy AM, Janiszewska M, *et al.* Classifying the evolutionary and ecological features of neoplasms. *Nat. Rev. Cancer.* 2017;17:605–19.

26. Gillies RJ, Verduzco D, Gatenby RA. Evolutionary dynamics of carcinogenesis and why targeted therapy does not work. *Nat. Rev. Cancer.* 2012;12:487–93.

27. Fruehauf JP, Meyskens FL. Reactive oxygen species: A breath of life or death? *Clin. Cancer Res.* 2007;13:789–94.

28. Saed GM, Diamond MP, Fletcher NM. Updates of the role of oxidative stress in the pathogenesis of ovarian cancer. *Gynecol. Oncol.* 2017;145:595–602.

29. Vaupel P, Mayer A. Hypoxia in cancer: Significance and impact on clinical outcome. *Cancer Metastasis Rev.* 2007;26:225–39.

30. Semenza GL. Hypoxia-inducible factors: Mediators of cancer progression and targets for cancer therapy. *Trends Pharmacol. Sci.* 2012;33:207–14.

31. Landriscina M, Maddalena F, Laudiero G, Esposito F. Adaptation to oxidative stress, chemoresistance, and cell survival. *Antioxid. Redox Signal.* 2009;11:2701–16.

32. Halliwell B. Antioxidant defence mechanisms: from the beginning to the end (of the beginning). *Free Radic Res.* 1999;31:261–72.

33. Gupta RK, Patel AK, Shah N, Chaudhary AK, Jha UK, Yadav UC, *et al.* Oxidative stress and antioxidants in disease and cancer: a review. *Asian Pac. J. Cancer Prev.* 2014;15:4405–9.

34. Halliwell B. Biochemistry of oxidative stress. *Biochem. Soc. Trans.* 2007;35:1147–50.

35. Marengo B, Nitti M, Furfaro AL, Colla R, Ciucis C De, Marinari UM, *et al.* Redox homeostasis and cellular antioxidant systems: Crucial players in cancer growth and therapy. *Oxid. Med. Cell. Longev.* 2016;22:1–16

36. Nogueira V, Hay N. Molecular pathways: Reactive oxygen species homeostasis in cancer cells and implications for cancer therapy. *Clin. Cancer Res.* 2013;19:4309–14.

37. Pannala VR, Dash RK. Mechanistic characterization of the thioredoxin system in the removal of hydrogen peroxide. *Free Radic. Biol. Med.* 2015;78:42–55.

38. Lu J, Holmgren A. The thioredoxin antioxidant system. *Free Radic. Biol. Med.* 2014;66:75–87.

39. Aoyama K, Nakaki T. Glutathione in cellular Redox homeostasis: Association with the excitatory amino acid carrier 1 (EAAC1). *Molecules.* 2015;20:8742–58.

40. Castaldo SA, Freitas JR, Conchinha NV, Madureira PA. The Tumorigenic Roles of the Cellular REDOX Regulatory Systems. *Oxid. Med. Cell. Longev.* 2016;3:1–17.

41. Meister A. Glutathione deficiency produced by inhibition of its synthesis, and its reversal; Applications in research and therapy. *Pharmacol. Ther.* 1991;51:155–94.

42. Estrela JM, Ortega A, Obrador E. Glutathione in cancer biology and therapy. *Crit. Rev. Clin. Lab. Sci.* 2006;43:143–81.

43. Hayes JD, Dinkova-Kostova AT. The Nrf2 regulatory network provides an interface between

- redox and intermediary metabolism. *Trends Biochem. Sci.* 2014;39:199–218.
44. Diehn M, Cho RW, Lobo NA, Kalisky T, Jo M, Kulp AN, *et al.* Association of Reactive Oxygen Species Levels and Radioresistance in Cancer Stem Cells. *Nature.* 2009;458:780–3.
 45. Roh J-L, Jang H, Kim EH, Shin D. Targeting of the Glutathione, Thioredoxin, and Nrf2 Antioxidant Systems in Head and Neck Cancer. *Antioxid. Redox Signal.* 2017;27:106–14.
 46. Schafer ZT, Grassian AR, Song L, Jiang Z, Gerhart-Hines Z, Irie HY, *et al.* Antioxidant and oncogene rescue of metabolic defects caused by loss of matrix attachment. *Nature.* 2009;461:109–13.
 47. Denicola GM, Karreth FA, Humpton TJ, Gopinathan A, Wei C, Frese K, *et al.* Oncogene-induced Nrf2 transcription promotes ROS detoxification and tumorigenesis. *Nature.* 2011;475:106–10.
 48. Balendiran GK, Dabur R, Fraser D. The role of glutathione in cancer. *cell Biochem. Funct.* 2004;22:343–52.
 49. Neumann CA, Fang Q. Are peroxiredoxins tumor suppressors? *Curr. Opin. Pharmacol.* 2007;7:375–80.
 50. Zhou J, Schmid T, Schnitzer S, Brüne B. Tumor hypoxia and cancer progression. *Cancer Lett.* 2006;237:10–21.
 51. Balamurugan K. HIF-1 at the crossroads of hypoxia, inflammation, and cancer. *Int J Cancer.* 2016;138:1058–66.
 52. Benita Y, Kikuchi H, Smith AD, Zhang MQ, Chung DC, Xavier RJ. An integrative genomics approach identifies Hypoxia Inducible Factor-1 (HIF-1)-target genes that form the core response to hypoxia. *Nucleic Acids Res.* 2009;37:4587–602.
 53. Malec V, Gottschald OR, Li S, Rose F, Seeger W, Hänze J. HIF-1 α signaling is augmented during intermittent hypoxia by induction of the Nrf2 pathway in NOX1-expressing adenocarcinoma A549 cells. *Free Radic. Biol. Med.* 2010;48:1626–35.
 54. Bristow RG, Hill RP. Hypoxia and metabolism: hypoxia, DNA repair and genetic instability. *Nat. Rev. Cancer.* 2008;8:180–92.
 55. Reynolds TV, Rockwell S, Gazer PM. Genetic Instability Induced by the Tumor Microenvironment. *Cancer Res.* 1996;56:5754–7.
 56. Li C, Little JB, Hu K. Persistent Genetic Instability in Cancer Cells Induced by Non-DNA-damaging Stress Exposures *Advances in Brief Persistent Genetic Instability in Cancer Cells Induced by Non-DNA-damaging.* *Cancer Res.* 2001;61:428–32.
 57. Luoto KR, Kumareswaran R, Bristow RG. Tumor hypoxia as a driving force in genetic instability. *Genome Integr.* 2013;4:5–19.
 58. Koshiji M, To KKW, Hammer S, Kumamoto K, Harris AL, Modrich P, *et al.* HIF-1 α induces genetic instability by transcriptionally downregulating MutSa expression. *Mol. Cell.* 2005;17:793–803.
 59. Holohan C, Van Schaeybroeck S, Longley DB, Johnston PG. Cancer drug resistance: An evolving paradigm. *Nat. Rev. Cancer.* 2013;13:714–26.
 60. Gottesman MM. Mechanisms of cancer drug resistance. *Annu. Rev. Med.* 2002;53:615–27.

61. Swanton C. Intratumour Heterogeneity : Evolution through Space and Time An Evolutionary Perspective on Cancer Heterogeneity. *Cancer Res.* 2013;72:4875–82.
62. Son B, Lee S, Youn H, Kim E, Kim W, Youn B. The role of tumor microenvironment in therapeutic resistance. *Oncotarget.* 2017;8:3933–45.
63. Agarwal R, Kaye SB. Ovarian cancer: strategies for overcoming resistance to chemotherapy. *Nat. Rev. Cancer.* 2003;3:502–16.
64. Dasari S and Tchounwou PB. Cisplatin in cancer therapy : molecular mechanisms of action. *Eur J Pharmacol.* 2015;5:364–78.
65. Alexandre J, Batteux F, Nicco C, Chéreau C, Laurent A, Guillemin L, *et al.* Accumulation of hydrogen peroxide is an early and crucial step for paclitaxel-induced cancer cell death both in vitro and in vivo. *Int. J. Cancer.* 2006;119:41–8.
66. Marullo R, Werner E, Degtyareva N, Moore B, Altavilla G, Ramalingam SS, *et al.* Cisplatin induces a mitochondrial-ros response that contributes to cytotoxicity depending on mitochondrial redox status and bioenergetic functions. *PLoS One.* 2013;8: e81162.1–15.
67. Stewart DJ. Mechanisms of resistance to cisplatin and carboplatin. *Crit Rev Oncol Hematol.* 2007;63:12–31.
68. Galluzzi L, Senovilla L, Vitale I, Michels J, Martins I, Kepp O, *et al.* Molecular mechanisms of cisplatin resistance. *Oncogene.* 2012;31:1869–83.
69. Siddik ZH. Cisplatin : mode of cytotoxic action and molecular basis of resistance. *Oncogene.* 2003;7265–79.
70. Kelland LR. Preclinical perspectives on platinum resistance. *Drugs.* 2000;59 Suppl 4:1–8; discussion 37–8.
71. Johnson SW, Ozols RF, Hamilton TC. Mechanisms of drug resistance in ovarian cancer. *Cancer.* 1993;71:644–9.
72. Champa D, Sun S, Tsai C-Y, Howell SB, Harismendy O. Evolution and characterization of carboplatin resistance at single cell resolution. *bioRxiv.* 2017;1–34.
73. Dumontet C, Sikic BI. Mechanisms of action of and resistance to antitubulin agents: microtubule dynamics, drug transport, and cell death. *J Clin Oncol.* 1999;17:1061–70.
74. Barbuti AM, Chen ZS. Paclitaxel through the ages of anticancer therapy: Exploring its role in chemoresistance and radiation therapy. *Cancers (Basel).* 2015;7:2360–71.
75. Datta S, Choudhury D, Das A, Das Mukherjee D, Das N, Roy SS, *et al.* Paclitaxel resistance development is associated with biphasic changes in reactive oxygen species, mitochondrial membrane potential and autophagy with elevated energy production capacity in lung cancer cells: A chronological study. *Tumor Biol.* 2017;39:1-14.
76. Vaidyanathan A, Sawers L, Chakravarty P, Bray SE, McMullen KW, Ferguson MJ, *et al.* Identification of novel targetable resistance mechanisms and candidate clinical response biomarkers in drug-resistant ovarian cancer, following single-agent and combination chemotherapy. *Addressing Crit. Quest. Ovarian Cancer Res. Treat.* Pittsburgh, PA. Philadelphia: AACR; Clin Cancer Res; 2017.
77. Enriquez-navas PM, Wojtkowiak JW, Gatenby RA. Application of Evolutionary Principles to

Cancer Therapy Cancer Therapy. *Cancer Res.* 2015;75:4675–80.

78. Enriquez-Navas PM, Kam Y, Das T, Hassan S, Silva A, Foroutan P, *et al.* Exploiting evolutionary principles to prolong tumor control in preclinical models of breast cancer. *Sci. Transl. Med.* 2016;8:1–9.

79. Zhang J, Cunningham JJ, Brown JS, Gatenby RA. Integrating evolutionary dynamics into treatment of metastatic castrate-resistant prostate cancer. *Nat. Commun.* 2017;8:1–9.

80. Aktipis CA, Kwan VSY, Johnson KA, Neuberg SL, Maley CC. Overlooking Evolution: A Systematic Analysis of Cancer Relapse and Therapeutic Resistance Research. *PLoS One.* 2011;6:e26100.1–9.

81. Gatenby RA, Silva AS, Gillies RJ, Frieden BR. Adaptive therapy. *Cancer Res.* 2009;69:4894–903.

82. Gallaher JA, Enriquez-Navas PM, Luddy KA, Gatenby RA, Anderson ARA. Spatial Heterogeneity and Evolutionary Dynamics Modulate Time to Recurrence in Continuous and Adaptive Cancer Therapies. *bioRxiv.* 2017;1-21.

83. Xue Y, Martelotto L, Baslan T, Vides A, Solomon M, Mai TT, *et al.* An approach to suppress the evolution of resistance in BRAF V600E-mutant cancer. *Nat. Med.* 2017;23:929–37.

84. Vaughan S, Coward JI, Jr RCB, Berchuck A, Berek JS, Brenton JD, *et al.* Rethinking ovarian cancer: recommendations for improving outcomes. *Nat. Rev.* 2011;11:719–25.

85. Bray F, Ferlay J, Soerjomataram I, Siegel RL, Torre LA, Jemal A. Global Cancer Statistics 2018: GLOBOCAN Estimates of Incidence and Mortality Worldwide for 36 Cancers in 185 Countries. *CA Cancer J Clin.* 2018;68:394–424.

86. Jessmon P, Boulanger T, Zhou W, Patwardhan P. Epidemiology and treatment patterns of epithelial ovarian cancer. *Expert Rev. Anticancer Ther.* 2017;17:427–37.

87. Wright JD, Chen L, Tergas AI, Patankar S, Burke WM, Hou JY, *et al.* Trends in Relative Survival for Ovarian Cancer From 1975 to 2011. *Obs. Gynecol.* 2015. 2015;125:1345–52.

88. Bast Jr RC, Hennessy B, Mills GB. The biology of ovarian cancer: New opportunities for translation. *Nat. Rev. Cancer.* 2009;9:415–28.

89. Bowtell DD. The genesis and evolution of high-grade serous ovarian cancer. *Nat Rev Cancer.* 2010;10:803–8.

90. Desai A, Xu J, Aysola K, Qin Y, Okoli C, Hariprasad R, *et al.* Epithelial ovarian cancer: An overview. *World J Transl Med.* 2014;3:10–29.

91. Prat J. Ovarian carcinomas: Five distinct diseases with different origins, genetic alterations, and clinicopathological features. *Virchows Arch.* 2012;460:237–49.

92. Reid BM, Permuth JB, Sellers TA. Epidemiology of ovarian cancer: a review. *Cancer Biol. Med.* 2017;14:9–32.

93. Meinhold-Heerlein I, Fotopoulou C, Harter P, Kurzeder C, Mustea A, Wimberger P, *et al.* The new WHO classification of ovarian, fallopian tube, and primary peritoneal cancer and its clinical implications. *Arch. Gynecol. Obstet.* Springer Berlin Heidelberg; 2016;293:695–700.

94. Shen H, Fridley BL, Song H, Lawrenson K, Cunningham JM, Ramus SJ, *et al.* Epigenetic analysis leads to identification of HNF1B as a subtype-specific susceptibility gene for ovarian cancer. *Nat. Commun.* 2013;4:1628–46.
95. Mabuchi S, Kawase C, Altomare DA, Morishige K, Sawada K, Hayashi M, *et al.* mTOR is a promising therapeutic target both in cisplatin-sensitive and cisplatin-resistant clear cell carcinoma of the ovary. *Clin. Cancer Res.* 2009;15:5404–13.
96. Jayson GC, Kohn EC, Kitchener HC, Ledermann JA. Ovarian cancer. *Lancet.* 2014;384:1376–88.
97. Banerjee S, Kaye SB. New strategies in the treatment of ovarian cancer: Current clinical perspectives and future potential. *Clin. Cancer Res.* 2013;19:961–8.
98. Itamochi H, Kigawa J, Terakawa N. Mechanisms of chemoresistance and poor prognosis in ovarian clear cell carcinoma. *Cancer Sci.* 2008;99:653–8.
99. Ip CKM, Li S, Tang MH, Sy SKH, Ren Y. Stemness and chemoresistance in epithelial ovarian carcinoma cells under shear stress. *Sci. Rep.* 2016;6:26788–98.
100. Stipanuk MH. SULFUR AMINO ACID METABOLISM: Pathways for Production and Removal of Homocysteine and Cysteine. *Annu. Rev. Nutr.* 2004;24:539–77.
101. Yin J, Ren W, Yang G, Duan J, Huang X, Fang R, *et al.* L-Cysteine metabolism and its nutritional implications. *Mol. Nutr. Food Res.* 2015;1–31.
102. Conrad M, Sato H. The oxidative stress-inducible cystine/glutamate antiporter, system xc⁻: cystine supplier and beyond. *Amino Acids.* 2012;42:231–46.
103. Stipanuk MH, Dominy JE, Lee J, Coloso RM. Mammalian Cysteine Metabolism: New Insights into Regulation of Cysteine Metabolism. *Am. Soc. Nutr.* 2006;136:S1652–9.
104. Yin S, Huai J, Chen X, Yang Y, Zhang X, Gan Y, *et al.* Intracellular delivery and antitumor effects of a redox-responsive polymeric paclitaxel conjugate based on hyaluronic acid. *Acta Biomater.* 2015;26:274–85.
105. Visscher M, Arkin MR, Dansen TB. Covalent targeting of acquired cysteines in cancer. *Curr. Opin. Chem. Biol.* 2016;30:61–7.
106. Meister A. On the discovery of glutathione. *Trends Biochem. Sci.* 1988;13:185–8.
107. de Rey-Pailhade J. Sur un corps d'origine organique hydrogénant le soufre à froid. *CR Acad Sci.* 1888;106:1683–4.
108. Meister A. Glutathione metabolism and its selective modification. *J. Biol. Chem.* 1988;263:17205–8.
109. Copley SD, Dhillon JK. Lateral gene transfer and parallel evolution in the history of glutathione biosynthesis genes. *Genome Biol.* 2002;3:0025.1–16
110. Franklin CC, Backos DS, Mohar I, White CC, Forman HJ, Kavanagh TJ. Structure, function, and post-translational regulation of the catalytic and modifier subunits of glutamate cysteine ligase. *Mol. Aspects Med.* 2009;30:86–98.
111. Sies H. Glutathione and its role in cellular functions. *Free Radic. Biol. Med.* 1999;27:916–21.

112. Traverso N, Ricciarelli R, Nitti M, Marengo B, Furfaro AL, Pronzato MA, *et al.* Role of Glutathione in Cancer Progression and Chemoresistance. *Oxid. Med. Cell. Longev.* 2013;2013:1–10.
113. Calvert P, Yao KS, Hamilton TC, O'Dwyer PJ. Clinical studies of reversal of drug resistance based on glutathione. *Chem. Biol. Interact.* 1998;111-112:213–24.
114. Arrick BA, Nathan CF. Glutathione Metabolism as a Determinant of Therapeutic Efficacy: A Review. *Cancer Res.* 1984;44:4224–32.
115. Ghazal-Aswad S, Hogarth L, Hall AG, George M, Sinha DP, Lind M, *et al.* The relationship between tumour glutathione concentration, glutathione S-transferase isoenzyme expression and response to single agent carboplatin in epithelial ovarian cancer patients. *Br J Cancer.* 1996;468–73.
116. Wrigley EC, McGown A T, Buckley H, Hall A, Crowther D. Glutathione-S-transferase activity and isoenzyme levels measured by two methods in ovarian cancer, and their value as markers of disease outcome. *Br. J. Cancer.* 1996;73:763–9.
117. Godwin AK, Meistert A, Dwyer PJO, Huangt CS, Hamilton TC, Andersont ME. High resistance to cisplatin in human ovarian cancer cell lines is associated with marked increase of glutathione synthesis. *Proc Natl Acad Sci U S A.* 1992;89:3070–4.
118. Green JA, Robertson LJ, Clark AH. Glutathione S-transferase expression in benign and malignant ovarian tumours. *Br. J. Cancer.* 1993;68:235–9.
119. Lewandowicz GM, Britt P, Elgie AW, Williamson CJ, Coley HM, Hall AG, *et al.* Cellular Glutathione Content , in Vitro Chemoresponse , and the Effect of BSO Modulation in Samples Derived from Patients with Advanced Ovarian Cancer. *Gynecol Oncol.* 2002;304:298–304.
120. Mayr D, Pannekamp U, Baretton GB, Flens MJ, Sch R, Gropp M, *et al.* Immunohistochemical Analysis of Drug Resistance- associated Proteins in Ovarian Carcinomas. *Pathol Res Pr.* 2000;196:469–75.
121. Satoh T, Nishida M, Tsunoda H, Kubo T. Expression of glutathione S-transferase pi (GST-pi) in human malignant ovarian tumors. *Eur J Obs. Gynecol Reprod Biol.* 2001;96:202–8.
122. Surowiak P, Materna V, Kaplenko I, Spaczyński M, Dietel M, Lage H., *et al.* Augmented expression of metallothionein and glutathione S-transferase pi as unfavourable prognostic factors in cisplatin-treated ovarian cancer patients. *Virchows Arch.* 2005;447:626–33.
123. Rabik CA, Dolan ME. Molecular mechanisms of resistance and toxicity associated with platinating agents q. *Cancer Treat Rev.* 2007;07281:9–23.
124. Cheng X, Kigawa J, Minagawa Y, Kanamori Y, Itamochi H, Okada M, *et al.* Glutathione S-transferase-pi expression and glutathione concentration in ovarian carcinoma before and after chemotherapy. *Cancer.* 1997;79:521–7.
125. Sawers L, Ferguson MJ, Ihrig BR, Young HC, Chakravarty P, Wolf CR, *et al.* Glutathione S-transferase P1 (GSTP1) directly influences platinum drug chemosensitivity in ovarian tumour cell lines. *Br. J. Cancer.* 2014;111:1150–8.
126. Crawford LA, Weerapana E. A Tyrosine-Reactive Irreversible Inhibitor for Glutathione S-Transferase Pi (GSTP1). *Mol Biosyst.* 2016;12:1768–71.
127. Chen S, Jiao JW, Sun KX, Zong ZH, Zhao Y. MicroRNA-133b targets glutathione S-transferase π expression to increase ovarian cancer cell sensitivity to chemotherapy drugs. *Drug Des. Devel.*

Ther. 2015;9:5225–35.

128. Okuno S, Sato H, Tamba M, Wang H, Sohda S, Hamada H, *et al.* Role of cystine transport in intracellular glutathione level and cisplatin resistance in human ovarian cancer cell lines. *Br J Cancer.* 2003;88:951–6.

129. Wang W, Kryczek I, Dostál L, Lin H, Tan L, Zhao L, *et al.* Effector T Cells Abrogate Stroma-Mediated Chemoresistance in Ovarian Cancer. *Cell.* 2016;165:1092–105.

130. Mohell N, Alfredsson J, Fransson A, Uustalu M, Byström S, Gullbo J, *et al.* APR-246 overcomes resistance to cisplatin and doxorubicin in ovarian cancer cells. *Cell Death Dis.* 2015;6:1–11.

131. Lopes-Coelho F, Gouveia-Fernandes S, Gonçalves LG, Nunes C, Faustino I, Silva F, *et al.* HNF1B drives glutathione (GSH) synthesis underlying intrinsic carboplatin resistance of ovarian clear cell carcinoma (OCCC). *Tumor Biol.* 2016;37:4813–29.

132. Liebmann JE, Hahn SM, Cook JA, Lipschultz C, Mitchell JB, Kaufman DC. Glutathione Depletion by L-Buthionine Sulfoximine Antagonizes Taxol Cytotoxicity Glutathione Depletion by L-Buthionine Sulfoximine Antagonizes Taxol Cytotoxicity. *Cancer Res.* 1993;2066–70.

133. Medeiros R, Pereira D, Afonso N, Palmeira C, Faleiro C, Afonso-Lopes C, *et al.* Platinum/paclitaxel-based chemotherapy in advanced ovarian carcinoma: Glutathione S-transferase genetic polymorphisms as predictive biomarkers of disease outcome. *Int. J. Clin. Oncol.* 2003;8:156–61.

134. Mieczal JJ, Gallogly MM, Qanungo S, Sabens EA, Shelton MD. Molecular Mechanisms and Clinical Implications of Reversible Protein S -Glutathionylation. *Antioxid. Redox Signal.* 2008;10:1941–88.

135. Emmanuel C, Chiew YE, George J, Etemadmoghadam D, Anglesio MS, Sharma R, *et al.* Genomic classification of serous ovarian cancer with adjacent borderline differentiates Ras pathway and TP53-mutant tumors and identifies NRAS as an oncogenic driver. *Clin. Cancer Res.* 2014;20:6618–30.

136. van Jaarsveld MTM, van Kuijk PF, Boersma AWM, Helleman J, van IJcken WF, Mathijssen RHJ, *et al.* miR-634 restores drug sensitivity in resistant ovarian cancer cells by targeting the Ras-MAPK pathway. *Mol. Cancer.* 2015;14:1–13.

137. Mackenzie R, Kommoss S, Winterhoff BJ, Kipp BR, Garcia JJ, Voss J, *et al.* Targeted deep sequencing of mucinous ovarian tumors reveals multiple overlapping RAS-pathway activating mutations in borderline and cancerous neoplasms. *BMC Cancer.* 2015;15:1–10.

138. Zheng GF, Cai Z, Meng XK, Zhang Y, Zhu W, Pang XY, *et al.* Unfolded protein response mediated JNK/AP-1 signal transduction, a target for ovarian cancer treatment. *Int. J. Clin. Exp. Pathol.* 2015;8:6505–11.

139. Chen R, Ngan H, Chan D. The AMPK/TAK1/NF- κ B signaling axis is indispensable for modulating ovarian cancer cell metabolism and peritoneal metastases. 21st Res. Postgrad. Symp. Li Ka Shing Fac. Med. Univ. Hong Kong, Hong Kong, 1-2 December 2016.

140. Carduner L, Picot CR, Leroy-Dudal J, Blay L, Kellouche S, Carreiras F. Cell cycle arrest or survival signaling through α v integrins, activation of PKC and ERK1/2 lead to anoikis resistance of ovarian cancer spheroids. *Exp. Cell Res.* 2014;320:329–42.

141. Al-Alem LF, McCord LA, Southard RC, Kilgore MW, Curry TE. Activation of the PKC

Pathway Stimulates Ovarian Cancer Cell Proliferation, Migration, and Expression of MMP7 and MMP101. *Biol. Reprod.* 2013;89:1–7.

142. Hajiahmadi S, Panjehpour M, Aghaei M, Shabani M. Activation of A2b adenosine receptor regulates ovarian cancer cell growth : involvement of Bax / Bcl-2 and caspase-3. *Biochem Cell Biol.* 2015;9:1–9.

143. Su Y, Gao L, Teng L, Wang Y, Cui J, Peng S, *et al.* Id1 enhances human ovarian cancer endothelial progenitor cell angiogenesis via PI3K/Akt and NF-kappaB/MMP-2 signaling pathways. *J. Transl. Med.* 2013;11:132–9.

144. Echevarría-Vargas IM, Valiyeva F, Vivas-Mejía PE. Upregulation of miR-21 in cisplatin resistant ovarian cancer via JNK-1/c-Jun pathway. *PLoS One.* 2014;9: e97094.1–11.

145. Yang-Hartwich Y, Soteras MG, Lin ZP, Holmberg J, Sumi N, Craveiro V, *et al.* P53 Protein Aggregation Promotes Platinum Resistance in Ovarian Cancer. *Oncogene.* 2015;34:3605–16.

146. Wu R, Baker SJ, Hu TC, Norman KM, Fearon ER, Cho KR. Type I to type II ovarian carcinoma progression: Mutant Trp53 or Pik3ca confers a more aggressive tumor phenotype in a mouse model of ovarian cancer. *Am. J. Pathol.* 2013;182:1391–9.

147. Wang R. Two's company, three's a crowd: can H₂S be the third endogenous gaseous transmitter? *FASEB J.* 2002;16:1792–8.

148. Sen N. Functional and Molecular Insights of Hydrogen Sulfide Signaling and Protein Sulfhydration. *J. Mol. Biol.* 2017;429:543–61.

149. Giuffrè A, Vicente JB. Hydrogen Sulfide Biochemistry and Interplay with Other Gaseous. *Oxid. Med. Cell. Longev.* 2018;11:1-31.

150. Wang R. Physiological Implications of Hydrogen Sulfide: A Whiff Exploration That Blossomed. *Physiol. Rev.* 2012;92:791–896.

151. Cao X, Ding L, Xie Z, Yang Y, Whiteman M, Moore PK, *et al.* A Review of Hydrogen Sulfide Synthesis, Metabolism, and Measurement: Is Modulation of Hydrogen Sulfide a Novel Therapeutic for Cancer? *Antioxid. Redox Signal.* 2018;1-107.

152. Goubern M, Andriamihaja M, Nubel T, Blachier F, Bouillaud F. Sulfide, the first inorganic substrate for human cells. *FASEB J.* 2007;21:1699–706.

153. Módis K, Coletta C, Erdélyi K, Papapetropoulos A, Szabo C. Intramitochondrial hydrogen sulfide production by 3-mercaptopyruvate sulfurtransferase maintains mitochondrial electron flow and supports cellular bioenergetics. *FASEB J.* 2013;27:601–11.

154. Li S, Yang G. Hydrogen Sulfide Maintains Mitochondrial DNA Replication *via* Demethylation of *TFAM*. *Antioxid. Redox Signal.* 2015;23:630–42.

155. Bhattacharyya S, Saha S, Giri K, Lanza IR, Nair KS, Jennings NB, *et al.* Cystathionine Beta-Synthase (CBS) Contributes to Advanced Ovarian Cancer Progression and Drug Resistance. *PLoS One.* 2013;8:e79167.1-12.

156. Szabo C, Coletta C, Chao C, Módis K, Szczesny B, Papapetropoulos A. Tumor-derived hydrogen sulfide, produced by cystathionine-β-synthase, stimulates bioenergetics, cell proliferation, and angiogenesis in colon cancer. *PNAS Pharmacol.* 2013;110:12474–9.

157. Chakraborty PK, Murphy B, Mustafi SB, Dey A, Xiong X, Rao G, *et al.* Cystathionine β -synthase regulates mitochondrial morphogenesis in ovarian cancer. *FASEB J.* 2018;32:4145-4157.
158. Fu M, Zhang W, Wu L, Yang G, Li H, Wang R. Hydrogen sulfide (H₂S) metabolism in mitochondria and its regulatory role in energy production. *Proc. Natl. Acad. Sci.* 2012;109:2943–8.
159. Teng H, Wu B, Zhao K, Yang G, Wu L, Wang R. Oxygen-sensitive mitochondrial accumulation of cystathionine β -synthase mediated by Lon protease. *Proc. Natl. Acad. Sci.* 2013;110:12679–84.
160. Cao X, Bian JS. The role of hydrogen sulfide in renal system. *Front. Pharmacol.* 2016;7:1–12.
161. Gai JW, Qin W, Liu M, Wang HF, Zhang M, Li M, *et al.* Expression profile of hydrogen sulfide and its synthases correlates with tumor stage and grade in urothelial cell carcinoma of bladder. *Urol. Oncol. Semin. Orig. Investig.* 2016;34:166.e15–e20.
162. Pan Y, Zhou C, Yuan D, Zhang J, Shao C. Radiation Exposure Promotes Hepatocarcinoma Cell Invasion through Epithelial Mesenchymal Transition Mediated by H₂S/CSE Pathway. *Radiat. Res.* 2015;185:96–105.
163. Sen S, Kawahara B, Gupta D, Tsai R, Khachatryan M, Farias-eisner R, *et al.* Role of cystathionine β -synthase in human breast Cancer. *Free Radic. Biol. Med.* 2015;86:228–38.
164. Hellmich MR, Coletta C, Chao C, Szabo C. The Therapeutic Potential of Cystathionine β -Synthetase/Hydrogen Sulfide Inhibition in Cancer. *Antioxid. Redox Signal.* 2015;22:424–48.
165. Lee ZW, Zhou J, Chen CS, Zhao Y, Tan CH, Li L, *et al.* The slow-releasing Hydrogen Sulfide donor, GYY4137, exhibits novel anti-cancer effects in vitro and in vivo. *PLoS One.* 2011;6:e21077.1–7.
166. Panza E, De Cicco P, Armogida C, Scognamiglio G, Gigantino V, Botti G, *et al.* Role of the cystathionine γ lyase/hydrogen sulfide pathway in human melanoma progression. *Pigment Cell Melanoma Res.* 2015;28:61–72.
167. Takano N, Sarfraz Y, Gilkes DM, Chaturvedi P, Xiang L, Suematsu M, *et al.* Decreased Expression of Cystathionine β -Synthase Promotes Glioma Tumorigenesis. *Mol. Cancer Res.* 2014;12:1398–406.
168. Schnelldorfer T, Gansauge S, Gansauge F, Schlosser S, Beger HG, Nussler AK. Glutathione depletion causes cell growth inhibition and enhanced apoptosis in pancreatic cancer cells. *Cancer.* 2000;89:1440–7.
169. Szczesny B, Marcatti M, Zatarain JR, Druzhyzna N, Wiktorowicz JE, Nagy P, *et al.* Inhibition of hydrogen sulfide biosynthesis sensitizes lung adenocarcinoma to chemotherapeutic drugs by inhibiting mitochondrial DNA repair and suppressing cellular bioenergetics. *Sci. Rep.* 2016;6:36125-35.

CHAPTER 2

CYSTEINE BOOSTERS THE EVOLUTIONARY ADAPTATION TO HYPOXIA, FAVOURING CARBOPLATIN RESISTANCE IN OVARIAN CANCER

This chapter is based on the following publication:

Nunes SC, Lopes-Coelho F, Gouveia-Fernandes S, Ramos C, Pereira SA, Serpa J. Cysteine boosts the evolutionary adaptation to CoCl_2 mimicked hypoxia conditions, favouring carboplatin resistance in ovarian cancer. *BMC Evol. Biol.* 2018;18:97–113.

“As humans spread around the world, so did their domesticated animals. Ten thousand years ago, not more than a few million sheep, cattle, goats, boars and chickens lived in restricted Afro-Asian niches. Today the world contains about a billion sheep, a billion pigs, more than a billion cattle, and more than 25 billion chickens. And they are all over the globe. The domesticated chicken is the most widespread fowl ever.

Following Homo sapiens, domesticated cattle, pigs and sheep are the second, third and fourth most widespread large mammals in the world. From a narrow evolutionary perspective, which measures success by the number of DNA copies, the Agricultural Revolution was a wonderful boon for chickens, cattle, pigs and sheep.

Unfortunately, the evolutionary perspective is an incomplete measure of success. It judges everything by the criteria of survival and reproduction, with no regard for individual suffering and happiness. Domesticated chickens and cattle may well be an evolutionary success story, but they are also among the most miserable creatures that ever lived. The domestication of animals was founded on a series of brutal practices that only became crueller with the passing of the centuries.” - Yuval Noah Harari

ABSTRACT

Ovarian cancer is the third most common gynaecologic malignancy and the most common cause of death from gynaecologic cancer, especially due to diagnosis at an advanced stage together with resistance to therapy. As a solid tumour grows, such as an ovarian tumour, cancer cells are exposed to regions of hypoxia, known to be partially responsible for tumour progression, metastasis and resistance to therapies. This suggests that hypoxia entails a selective pressure in which the adapted cells not only have a fitness increase under the selective environment, but also in non-selective adverse environments. In here, we used two different ovarian cancer cell lines – OVCAR3, a serous carcinoma cell line and ES2, a clear cell carcinoma cell line– in order to address the effect of selection under normoxia and hypoxia on the evolutionary outcome of cancer cells.

Our results showed that the adaptation to normoxia and hypoxia leads cells to display opposite strategies. Whereas cells adapted to hypoxia tend to proliferate less but present increased survival in adverse environments, cells adapted to normoxia proliferate rapidly but at the cost of increased mortality in adverse environments. Moreover, results also support that cysteine allows a quicker response and adaptation to hypoxic conditions that, in turn, are capable of driving chemoresistance.

KEYWORDS

Cancer, chemoresistance, cysteine, hypoxia, evolution, ovarian, tumour, selection.

INTRODUCTION

Ovarian cancer is the third most common gynaecologic malignancy worldwide [1] and the major cause of death from gynaecologic disease especially due to late diagnosis and resistance to therapy [1–3]. Epithelial ovarian cancer (EOC) includes most malignant ovarian neoplasms [4], being the high-grade ovarian serous carcinoma (HG-OSC) the most prevalent histological type [3] with diagnosis at an advanced stage in approximately 70% of patients [5]. In contrast, ovarian clear cell carcinoma (OCCC) is a rather uncommon histological type of ovarian cancer in West countries that is frequently diagnosed at an initial stage [6]. However, OCCC tumours present noticeably different clinical behaviours compared to other ovarian carcinomas presenting, generally, poor prognosis given chemoresistance to conventional platinum-drugs and taxane-based chemotherapy [6]. The standard treatment for advanced ovarian cancer is a combination of surgery and paclitaxel–carboplatin chemotherapy [7], however, despite initial response, there is a recurrence of the disease in over 85% of advanced ovarian cancer patients [8]. Usually, HG-OSC shows an initial response to platinum based therapy with further progression to resistance [9] while OCCC is intrinsically resistant to platinum salts [6,10,11].

Serpa and Dias have suggested that the metabolic remodelling is determinant for tumour progression. They have proposed a model in which the selective pressure of the microenvironment involving metabolic pathways switching induces cell death in non-adapted cells and positively selects those cells with growth advantage, increased invasiveness and altered adhesiveness, allowing local and angio (vascular) invasion, and leading to cancer progression and distant metastasis [12]. Soon after this report, Hanahan and Weinberg had also included reprogramming of energy metabolism as an emerging hallmark of cancer [13].

As a solid tumour grows, cancer cells are exposed to intermittent episodes of hypoxia. The effects of these episodes on cancer biology have been related to the aberrant blood circulation observed in solid tumours. This results in recurrent intra-tumoral episodic hypoxia and assaults metabolically less privileged cell niches. Studies showed that hypoxia is partially responsible for tumour progression, metastasis and resistance to therapies [14–17]. This evidence supports that hypoxia entails a selective pressure in which the adapted cells present a fitness increase not only under the selective environment, but also in non-selective environments. Interestingly, Cutter *et al.* [18] have recently reported that ovarian cancer cell lines subjected to hypoxia presented a more invasive, migratory and transformed epithelial–mesenchymal transition (EMT) phenotype. Hence, ovarian cancer is a valuable model to

address the effects of hypoxia selection on the evolutionary outcome of several traits of ovarian cancer cells.

The contribution of cysteine on cancer cells survival has been explored mainly due to hydrogen sulphide (H₂S) generation [19–24] and as a precursor of the antioxidant glutathione (GSH) [25–27]. It was already showed that increased levels of cytoplasmic thiol-containing species, especially GSH or metallothioneins are associated with resistance to platinum-based chemotherapy [25,28,29]. Our group also showed that different ovarian cancer histological types presented different metabolic outcomes concerning thiols and chemoresistance [25]. Under normoxic conditions, the OCCC cells were more resistant to carboplatin than HG-OSC cells and the inhibition of GSH production by buthionine sulphoximine (BSO) sensitized OCCC cells to carboplatin, both *in vitro* and *in vivo* [25]. These results suggest that the ability to metabolise thiols by cancer cells is directly linked to poorer disease outcome.

In here, we used two different ovarian cancer cell lines with different histological types, OCCC and HG-OSC, in order to address the effect of cancer cells selection under normoxia and hypoxia mimicked by cobalt chloride (CoCl₂), on the evolutionary outcome of cancer cells. Cobalt is known as a hypoxia mimicking agent both *in vivo* [30] and in cell culture [31–33], altering several systemic mechanisms related to hypoxia [31–33], namely the stabilization of hypoxia inducible factor 1 alpha (HIF-1 α), thus preventing its degradation [34]. Chemically, CoCl₂ reacts with oxygen avoiding its dissolution and oxygenation of aqueous solutions [35], thus impairing the availability of oxygen in culture media.

Herein, we hypothesised that selection under hypoxia and normoxia leads cells to display different evolutionary outcomes, predicting that hypoxia selected cells would be more resistant to carboplatin than normoxia selected cells. Moreover, we hypothesised that selection under hypoxia is linked to a higher efficacy of cysteine metabolism, resulting in a poorer evolutionary outcome.

MATERIAL AND METHODS

Cell culture

Cell lines from OCCC (ES2; CRL-1978) and HG-OSC (OVCAR-3; HTB-161) were obtained from American Type Culture Collection (ATCC). Cells were maintained at 37°C in a humidified 5% CO₂ atmosphere. Cells were cultured in DMEM (41965-039, Gibco, Life

Technologies) containing 4.5 g/L of D-glucose and 0.58g/L of L-glutamine supplemented with 1% fetal bovine serum (FBS S 0615, Merck), 1% antibiotic-antimycotic (AA) (P06-07300, PAN Biotech).

Prior to any experiment, cells were synchronized under starvation (culture medium without FBS) for 8 h at 37°C and 5% CO₂.

After 24 h of experimental conditions, the medium was changed and fresh conditions were added, with the exception of proliferation curve and cell cycle analysis in which the medium was not changed.

Immunofluorescence analysis

Cells (4×10^4 cells/well) were seeded in 8-well Tek chamber slides (Thermo scientific 177402) coated with Poly-L-Lysine (Biochrom AG L 7240) and cultured either in control condition or exposed to 0.1 mM CoCl₂. Cells were collected after 8 hours of conditions and then cells were fixed with 2% paraformaldehyde for 15 min at 4 °C and permeabilized with PBS-BSA 0.1% with 0.1% Triton X-100 for 30 min. Cells were incubated with primary antibody (anti-HIF-1 α ; anti-mouse antibody from BD Biosciences 610959) overnight at 4°C (diluted in PBA-BSA 0.1%, 1:100). Secondary antibody was the anti-mouse Alexa Fluor® 488 (1:1000 in PBA-BSA 0.1%. Antibody from Jackson ImmunoResearch Laboratories 115-545-003), 2 h at room temperature. The slides were mounted in VECTASHIELD media with DAPI (4'-6-diamidino-2-phenylindole) (Vector Labs) and examined by standard fluorescence microscopy using a Zeiss Imajer.Z1 AX10 microscope. Images were acquired and processed with CytoVision software.

Cell lines selection

ES2 and OVCAR3 cells (1×10^6 cells) were cultured in 25 cm² tissue culture flasks and selected under normoxia and under hypoxia mimicked with 0.1 mM CoCl₂. After reaching confluency ($\approx 2 \times 10^6$ cells) cells were trypsinised and cultured in 75 cm² tissue culture flasks, under selective conditions (hypoxia mimicked with 100 μ M CoCl₂). Every 48 h, cells undergone passaging if confluency reached $\sim 80\%$ ($\sim 7.5 \times 10^6$) or culture media was only changed if this confluency was not achieved. As the proliferation and survival rates were different between cell lines, the assays were performed with different days of selection for

ES2 cells and for OVCAR3 cells. Within each cell line, selection in normoxia and hypoxia was performed simultaneously. Ancestral cell line was cultured in baseline conditions.

Table I presents the selection and culture conditions for ES2 and OVCAR3 cell lines.

Proliferation curve assay

Cells selected under normoxia and hypoxia (5×10^4 cells/well), were seeded in 24-well plates and cultured either in normoxia or exposed to 0.1 mM CoCl_2 . Cells were collected after 16 h, 32 h and 48 h of conditions. Cells were trypsinized and resuspended in 200 μL of PBS 1x. A total of 15 μL were collected and 5 μL of trypan blue were added. Cells were immediately counted. The remnant cells were used to cell cycle analysis. This assay was performed with 63 days of selection for ES2 cells and 35 days of selection for OVCAR3 cells.

Cell cycle analysis

Cells were harvested by centrifugation at 153 g for 5 min and cells were fixed with 70% ethanol at 4°C. Cells were then centrifuged at 153 g for 5 min, followed by the supernatant discharge. Cells were incubated with 100 μL of propidium iodide (PI) solution (50 $\mu\text{g}/\text{ml}$ PI, 0.1 mg/ml RNase A, 0.05% Triton X-100) for 40 min at 37°C. After the incubation period, cells were washed with PBS 1x, centrifuged at 239 g for 10 min at 4°C and the supernatant was discarded. Cell pellets were suspended in 200 μL of PBS-BSA 0.1%. The acquisition was performed in a FACScalibur (Becton Dickinson). Data were analysed with FlowJo software (www.flowjo.com).

Cell death analysis

Cells selected under normoxia and hypoxia (2×10^5 cells/well) were seeded in 12-well plates and cultured under normoxia and exposed to 0.402 mM L-cysteine and/or 0.1 mM CoCl_2 . In addition, cells were exposed to the previous conditions combined with carboplatin 25 $\mu\text{g}/\text{mL}$. Cells were collected after 48 h of tested conditions. For the analysis of the response dynamics to carboplatin, the cells were collected after 16 h, 24 h and 48 h of conditions. The ancestral (not selected) cell lines were also tested. Half of the cells were used to cell death analysis and the other half was used for reactive oxygen species (ROS)

quantification. This assay was performed with 43 days of selection for ES2 cells and 84 days of selection for OVCAR3 cells.

Cells were harvested by centrifugation at 153 g for 3 min, cells were incubated with 1 μ L FITC-annexin V (640906, BioLegend) in 100 μ L annexin V binding buffer 1x (10 mM HEPES (pH 7.4), 140 mM sodium chloride (NaCl), 2.5 mM calcium chloride (CaCl₂)) and incubated at room temperature and in the dark for 15 min. After incubation, samples were rinsed with 0.1% (w/v) BSA (A9647, Sigma) in PBS 1x and centrifuged at 153 g for 3 min. Cells were suspended in 200 μ L of annexin V binding buffer 1x and 5 μ L Propidium iodide (PI; 50 μ g/mL). Acquisition was performed with a FACScalibur (Becton Dickinson). Data were analysed with FlowJo software (www.flowjo.com).

Reactive oxygen species (ROS) quantification

Cells selected under normoxia and hypoxia (2×10^5 cells/well) were seeded in 12-well plates and cultured in control condition and exposed to 0.402 mM L-cysteine and/or 0.1 mM CoCl₂ and/or carboplatin 25 μ g/mL. Cells were collected after 48 h of tested conditions. The ancestral cell lines were also tested. This assay was performed with 43 days of selection for ES2 cells and 84 days of selection for OVCAR3 cells.

Cells were incubated for 15 min 37°C with 2', 7'-Dichlorofluorescein diacetate (D6883, Sigma) in a final concentration of 10 μ M. The acquisition was performed with FACScalibur (Becton Dickinson). Data were analysed with FlowJo software (www.flowjo.com).

Statistical analysis

Data are presented as the mean \pm SD and all the graphics were done using the PRISM software package (PRISM 6.0 for Mac OS X; GraphPad software, USA, 2013). Assays were performed with 3 replicates per treatment. For comparisons of two groups, two-tailed independent-samples T-test was used. For comparison of more than two groups, One-way analysis of variance (ANOVA) with Tukey's multiple-comparisons post hoc test was used. To assess the existence of a linear relationship between two variables, two-tailed Pearson correlation was used. Statistical significance was established as $p < 0.05$. All statistical analyses were performed using the IBM Corp. Released 2013. IBM SPSS Statistics for Macintosh, Version 22.0. Armonk, NY: IBM Corp. software.

RESULTS

Adaptation to normoxia confers a highly proliferative ability to ES2 cells

We started by confirming CoCl_2 capacity of inducing HIF-1 α expression in ovarian cancer cells. By immunofluorescence analysis, it was possible to verify that HIF-1 α expression was increased upon CoCl_2 exposure in both cell lines (figure 1).

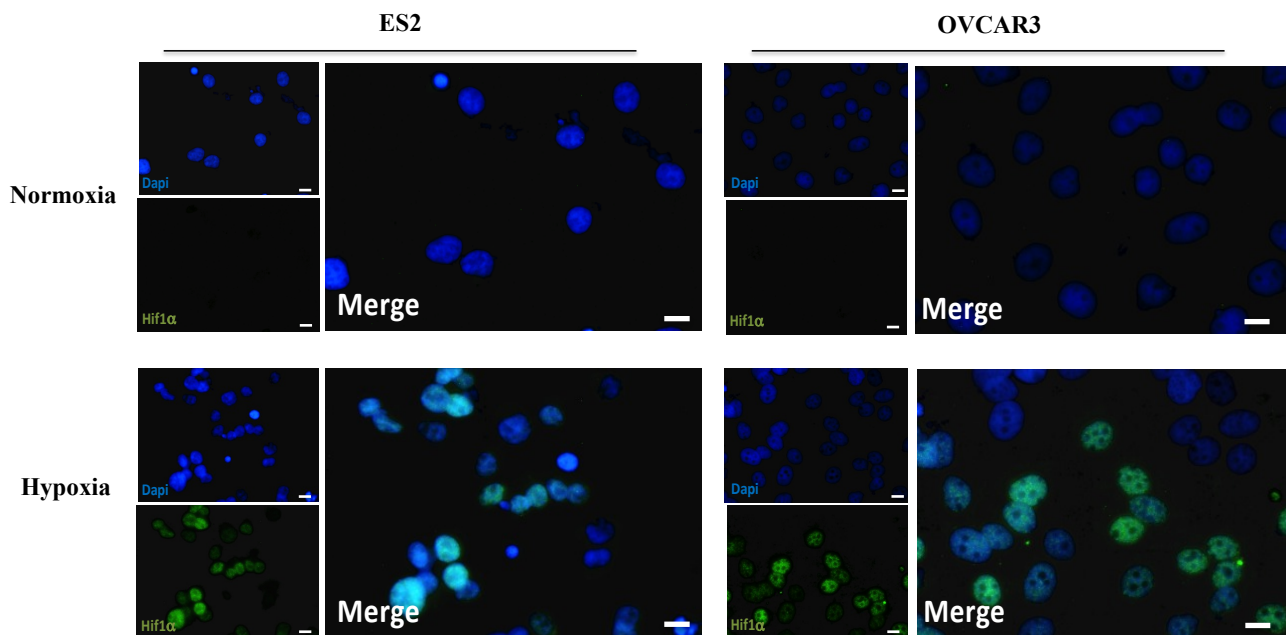


Figure 1. CoCl_2 induces HIF-1 α expression in ES2 cells and OVCAR3 cells.

Immunofluorescence analysis of Hif-1 α expression (green) under normoxia and hypoxia for ES2 and OVCAR3 cells. Nuclei were stained with DAPI (blue). White bars scale mean 20 μm .

We then addressed the effects of selection under normoxia (N) and hypoxia (H) in ES2 and OVCAR3 cells proliferation. The codes of each cell line and culture condition are presented in supplement table I.

The proliferation curves showed that ES2-N cells proliferated more than ES2-H, both under normoxia and hypoxia (supplement table II and figure 2 A). In addition, ES2-NN tended to proliferate more than ES2-NH, which was supported by cell cycle analysis that showed that ES2-NN presented a lower percentage of cells in G0/G1 compared to ES2-NH (figure 2 B).

Regarding OVCAR3 cells, OVCAR3-NN proliferated more than OVCAR3-HH (figure 2 C). In addition, the cell cycle analysis showed that OVCAR3-HH presented a higher percentage of cells in G0/G1 than both OVCAR3-NN and OVCAR3-NH (figure 2 D).

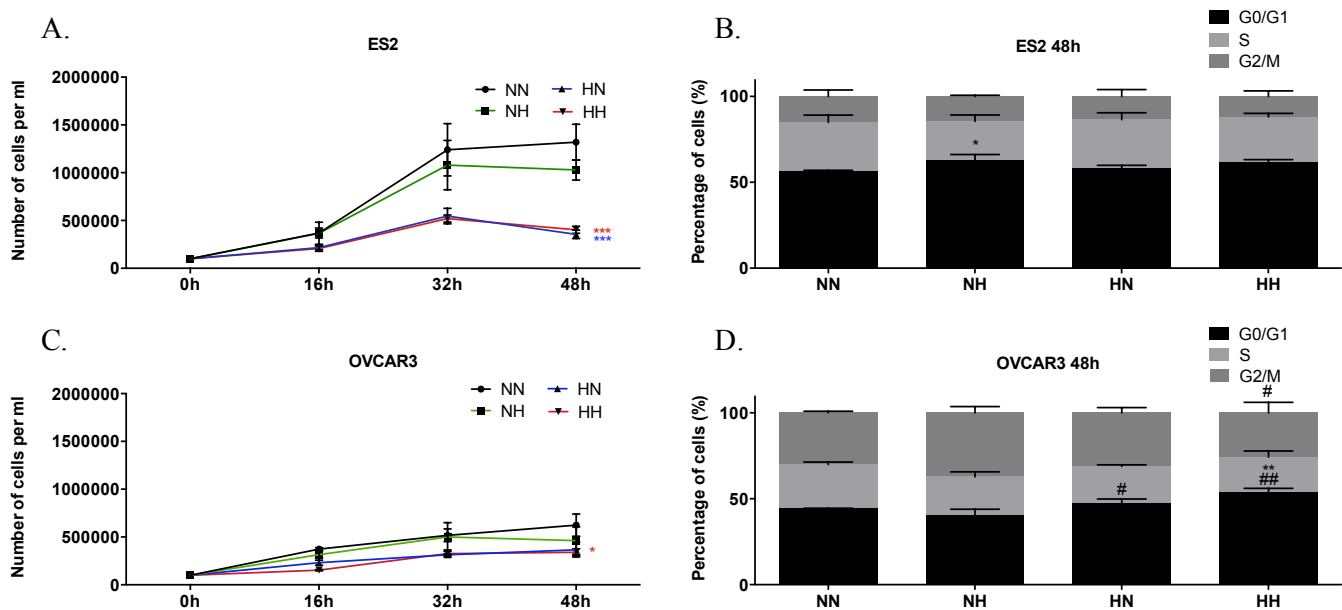


Figure 2. Proliferation rate of ES2 and OVCAR3 cells selected under normoxia and hypoxia.

A. Proliferation curve for ES2 cells, B. Cell cycle analysis for ES2 cells for 48 h of assay, C. Proliferation curve for OVCAR3 cells, and D. Cell cycle analysis for OVCAR3 cells for 48 h of assay. NN – cells selected under normoxia and cultured under normoxia; NH – cells selected under normoxia and cultured under hypoxia; HN – cells selected under hypoxia and cultured under normoxia; HH – cells selected under hypoxia and cultured under hypoxia. Asterisks (*) represent statistical significance in comparison with cells selected under normoxia and cultured under normoxia (NN). Cardinals (#) represent statistical significance in comparison with cells selected under normoxia and cultured under hypoxia (NH). $p < 0.05$, $**p < 0.01$, $***p < 0.001$ (One-way ANOVA with post hoc Tukey tests).

Adaptation to normoxia is accompanied by an evolutionary trade-off that is suppressed by cysteine under hypoxia in ES2 cells

Next, we assessed the effects of normoxia and hypoxia selection in ES2 and OVCAR3 cells death, exploring also the effect of cysteine supplementation in ovarian cancer cells response to hypoxia. The codes of each cell line and culture condition are presented in table I (supplement table 1).

Cell death analysis showed that hypoxia was disadvantageous for both ES2-A and ES2-N. Importantly, ES2-N cells were more sensitive to hypoxia than ES2-A thus indicating an evolutionary trade-off in the adaptation to normoxia. However, under hypoxia, cysteine was able to significantly decrease cell death both in ES2-AH and ES2-NH, indicating that cysteine was able to suppress this trade-off in the adaptation to N (figure 3 A, B and supplement table III A, B). Under normoxia, cysteine did not present a significant effect in ES2-A, ES2-N and ES2-H cells death. For ES2-H, no differences were found among

conditions, thus suggesting that ES2-H performed equally in all environments (figure 3 A, B and supplement table III A, B).

Regarding OVCAR3 cells, OVCAR3-N also showed to be more sensitive to hypoxia than OVCAR3-A, thus showing again an evolutionary trade-off in the adaptation to normoxia (figure 3 C, D and supplement table III C, D). Interestingly, only OVCAR3-A showed a benefit from cysteine under hypoxia, suggesting that selection under normoxia (OVCAR3-N) led to a decreased dependence on cysteine metabolism or to the loss of cellular efficacy in taking advantage from cysteine. Under normoxia, OVCAR3-A, OVCAR3-N and OVCAR3-H showed no differences in the absence and presence of cysteine.

Results also showed that OVCAR3-H was worse adapted to normoxia than both OVCAR3-A and OVCAR3-N. However, under H they performed better than OVCAR3-N (figure 3 C, D and supplement table III C, D), thus indicating that this cell line also present an evolutionary trade-off in the adaptation to hypoxia. However, like ES2-H, OVCAR3-H also performed equally in all environments (figure 3 C, D).

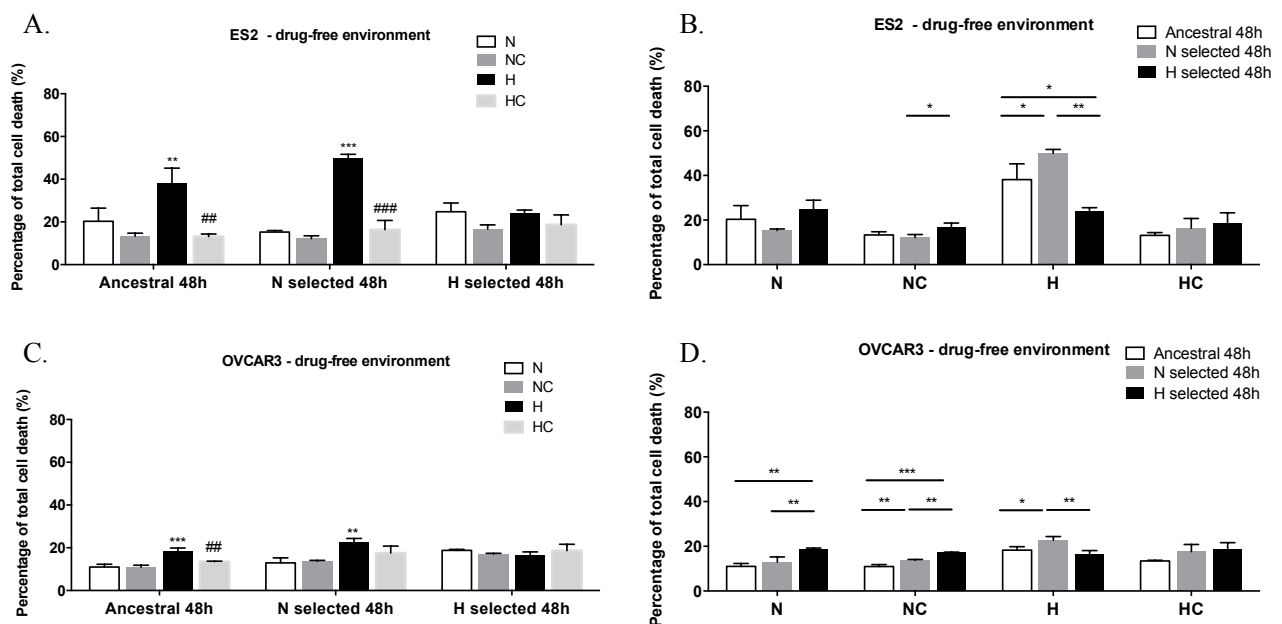


Figure 3. Adaptation to normoxia is accompanied by an evolutionary trade-off, which is suppressed by cysteine under hypoxia in ES2 cells.

Cell death levels in a drug-free environment for A. and B. ES2 cells and C. and D. OVCAR3 cells. N selected – cells selected under normoxia; H selected – cells selected under hypoxia; N – Normoxia; NC – Normoxia supplemented with cysteine; H – Hypoxia; HC – Hypoxia supplemented with cysteine. Results are shown as mean \pm SD. In A. and C. asterisks (*) represents statistical significance compared to cells cultured under normoxia within each cell line. The cardinals (#) represent statistical significance of cells cultured under hypoxia with cysteine compared to cells cultured under hypoxia without cysteine within each cell line. In B. and D. the asterisks (*) represent statistical significance among cell lines within each treatment. * $p < 0.05$, ** $p < 0.01$, *** $p < 0.001$ or # $p < 0.05$, ## $p < 0.01$, ### $p < 0.001$ (One-way ANOVA with post hoc Tukey tests).

We must highlight that there was no difference in the response to hypoxia between OVCAR3 and the respective condition of ES2 cells. Nevertheless, OVCAR3 cells presented lower cell death levels in this treatment compared to the respective ES2 cells (figure 4 A and B and supplementary table IV).

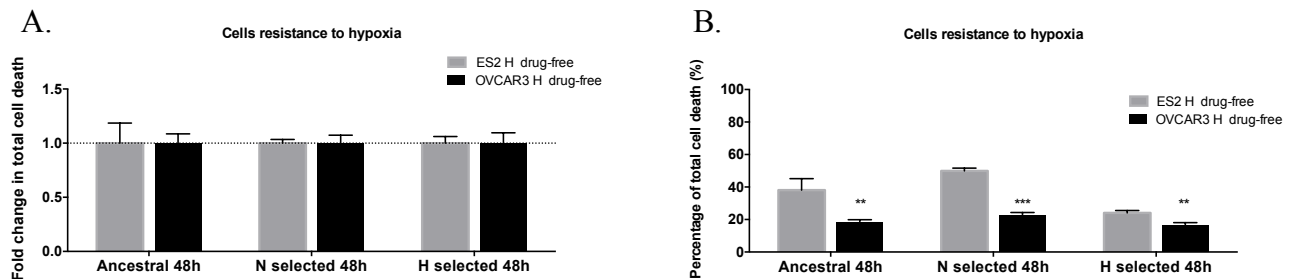


Figure 4. ES2 and OVCAR3 cells resistance to hypoxia.

Comparison of ES2 and OVCAR3 cells resistance to hypoxia for 48 hours of assay for A. ES2 and OVCAR3 cells in which values were normalised to the respective control, and B. ES2 and OVCAR3 cells with non-normalised to control values.

N selected – cells selected under normoxia; H selected – cells selected under hypoxia. Results are shown as mean \pm SD. Asterisks (*) represent statistical significance between ES2 and OVCAR3 cells. *p<0.05, **p<0.01, ***p<0.001 (Independent samples T tests).

Metabolic evolution driven by hypoxia provides stronger resistance to carboplatin

In here, we assessed the effects of selection under normoxia and hypoxia on cells capacity to survive upon carboplatin exposure. The codes of each cell line and culture condition are presented in supplement table I.

Upon carboplatin exposure, cell death levels increased for ES2-A cells in all treatments when compared to a drug-free environment. ES2-N cells showed a similar trend to ES2-A, in all conditions, with the exception of ES2-NH, in which there was a tendency for higher cell death levels upon carboplatin exposure, though not statistically significant (figure 5 A and supplement table V A). Nonetheless, cysteine was advantageous under H in the presence of carboplatin for both ES2-A and ES2-N (figure 6 and supplementary table VI A). Interestingly, for ES2-H cells, upon carboplatin exposure, only ES2-HH showed a slight increase in cell death levels (figure 5A and table V A), indicating that ES2-H cells present a higher survival capacity upon carboplatin exposure than ES2-A and ES2-N cells (figure 5 B and table V C). Interestingly, under H, no differences were observed among ES2-A, ES2-N and ES-H in carboplatin response, suggesting that 48 h of H exposure were sufficient to drive carboplatin response in ES2 cells, independent of the regime of selection.

Strikingly, when compared to the other selection regimes, cysteine was advantageous both under normoxia and hypoxia for the ES2 cells adapted to hypoxia (ES2-H) (figure 5 A, B and supplement table V A, C). On the contrary, ES2 cells selected under normoxia (ES2-N) presented an increased ratio of cell death when cultured in hypoxia with cysteine (ES2-NHC) *versus* without cysteine (ES2-NH), upon carboplatin exposure (figure 5). Together, results suggest that cysteine facilitates the adaptation to hypoxia, which, in turn, drives carboplatin resistance. On the contrary, long-term selection under normoxia drives the selection of cells that have less capacity of benefiting from cysteine protection under hypoxia and upon drug exposure.

Regarding OVCAR3 cells, cell death analysis showed increased cell death levels upon carboplatin exposure in OVCAR3-A, OVCAR3-N and OVCAR3-H cells, when compared to a drug-free environment and in all treatments (figure 5 C, and supplement table IV D). Nonetheless, cysteine was advantageous under H in the presence of carboplatin for all selection regimes of OVCAR3 cells (figure 6 and supplement table VI B). Interestingly, OVCAR3-HN cells presented stronger survival ability upon carboplatin than OVCAR3-AN and OVCAR3-NN (figure 5 D and supplement table V F). Taken together, results suggest that H-selection can also be advantageous for OVCAR3 cells upon carboplatin exposure, however at a lesser extent than ES2 cells.

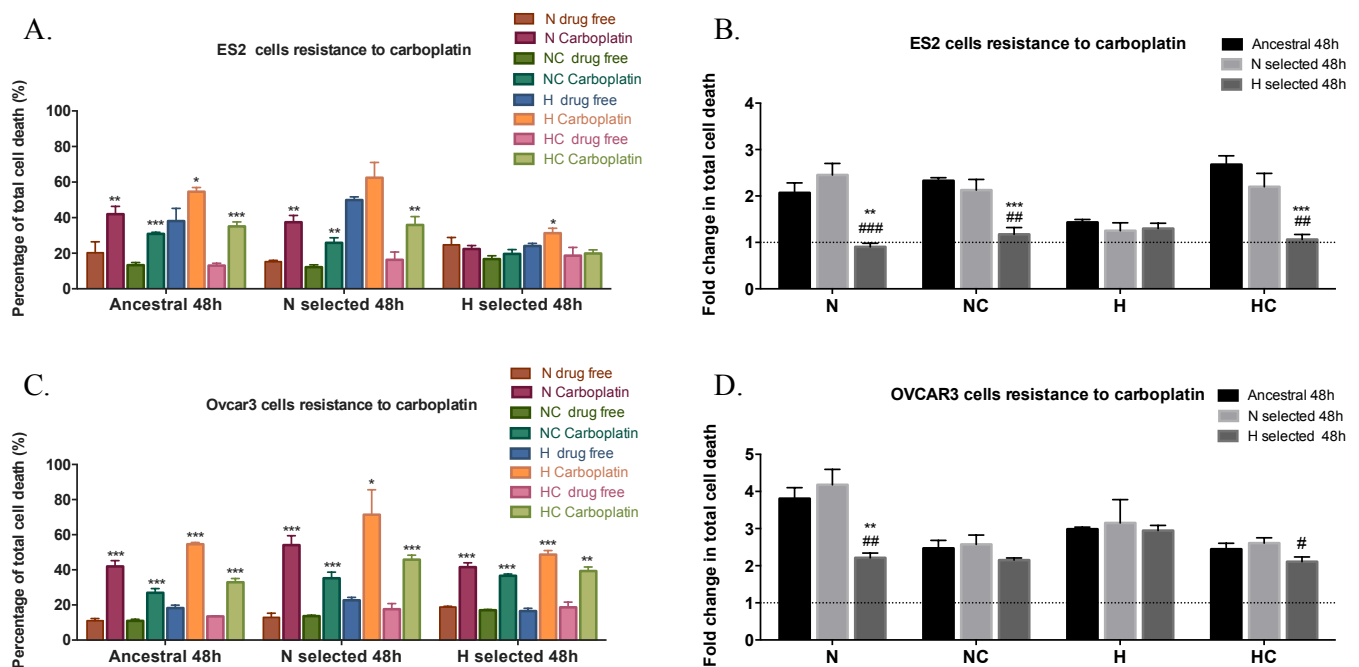


Figure 5. Metabolic evolution driven by hypoxia provides stronger resistance to carboplatin cytotoxicity.

Cells response to Carboplatin exposure for 48 hours of assay for A. ES2 cells with non-normalised to control values, B. ES2 cells in which values were normalised to the respective control, C. OVCAR3 cells

with non-normalised to control values and D. OVCAR3 cells in which values were normalised to the respective control. N selected – cells selected under normoxia; H selected – cells selected under hypoxia; N – Normoxia; NC – Normoxia supplemented with cysteine; H – Hypoxia; HC – Hypoxia supplemented with cysteine. In A. and C. asterisks (*) represent statistical significance compared to the respective control (cells cultured in the same experimental condition but in a free-drug environment) within each cell line. In B. and D. Asterisks (*) represent statistical significance compared to ancestral cells. Cardinals (#) represent statistical significance compared to N-selected cells. Data were normalised to the respective control. Results are shown as mean \pm SD. * p <0.05, ** p <0.01, *** p <0.001 or # p <0.05, ## p <0.01, ### p <0.001 (A. and C. Independent samples T test and B. and D. One-way ANOVA with post hoc Tukey tests).

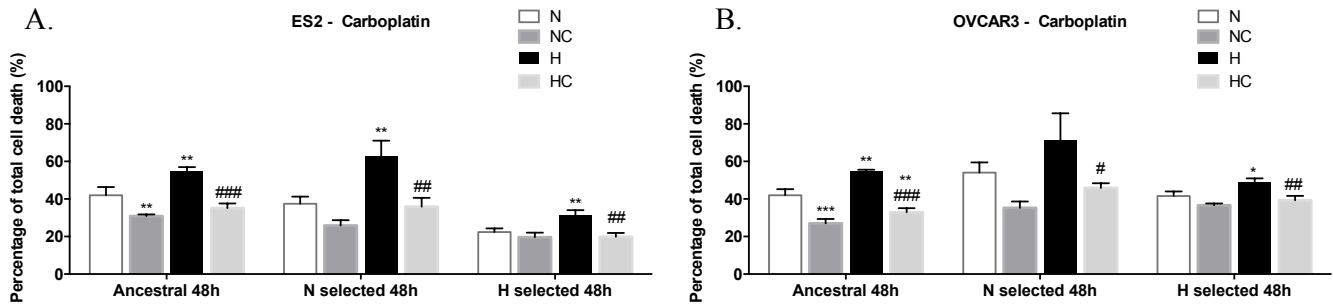


Figure 6. Metabolic evolution driven by hypoxia provides stronger resistance to carboplatin.

Cell death levels (non-normalised values) in the presence of carboplatin for 48 hours of assay for A. ES2 cells and B. OVCAR3 cells. N selected – cells selected under normoxia; H selected – cells selected under hypoxia; N – Normoxia; NC – Normoxia supplemented with cysteine; H – Hypoxia; HC – Hypoxia supplemented with cysteine. Results are shown as mean \pm SD. Asterisks (*) represent statistical significance compared to cells cultured under normoxia within each cell line. Cardinals (#) represent statistical significance compared to cells cultured under hypoxia within each cell line. * p <0.05, ** p <0.01, *** p <0.001 or # p <0.05, ## p <0.01, ### p <0.001 (One-way ANOVA with post hoc Tukey tests).

Carboplatin resistance driven by hypoxia is stronger in ES2 cells

We next compared ancestral and selected ES2 and OVCAR3 cells response dynamics to carboplatin exposure. Results showed that ES2-A cells presented a stronger resistance to carboplatin both under N and H than OVCAR3-A cells for 48 h of assay (figure 7 A and supplement table VII A). Similar results were observed for N selected cell lines, where ES2-NN and ES2-NH presented a stronger carboplatin resistance compared both to OVCAR3-NN and OVCAR3-NH cells (figure 7 B and supplement table VII B). Interestingly, ES2-H cells presented a stronger resistance to carboplatin in all treatments when compared to OVCAR3-H cells (figure 7 C and table VII C).

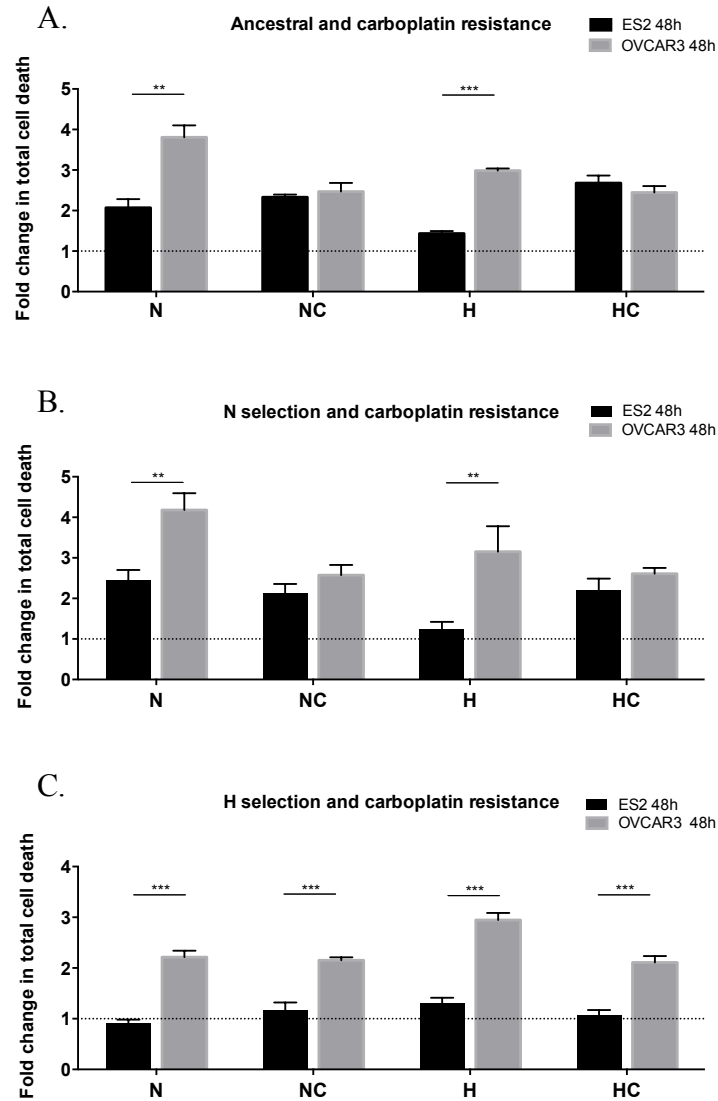


Figure 7. ES2 cells tend to present a stronger resistance to carboplatin than OVCAR3 cells.

Comparison of ES2 and OVCAR3 cells response to carboplatin for 48 h of experimental conditions for A. ancestral ES2 and OVCAR3 cells. B. ES2 and OVCAR3 cells selected under normoxia and C. ES2 and OVCAR3 cells selected under hypoxia. N – Normoxia; NC – Normoxia supplemented with cysteine; H – Hypoxia; HC – Hypoxia supplemented with cysteine. Data were normalised to the respective control. Results are shown as mean \pm SD. * $p < 0.05$, ** $p < 0.01$, *** $p < 0.001$ (Independent samples T test).

In ancestral cells, the dynamics of carboplatin response were similar between ES2 and OVCAR3 cells, in which carboplatin induced cell death in a time-dependent manner (figure 8 A and table VIII A). However, regarding the effect of normoxia selection on carboplatin response, ES2-NH cells showed a stable response to carboplatin over time, whereas OVCAR3-NH cells also presented increased cell death levels with increasing time of carboplatin exposure (figure 8 B and table VIII B). In all conditions, ES2-H cells showed a stable carboplatin response, with the exception of ES2-HH, in which carboplatin induced a slight increase in cell death levels with increasing time of exposure. In OVCAR3-H cells,

carboplatin induced cell death in a time-dependent manner in all treatments (figure 8 C and table VIII C).

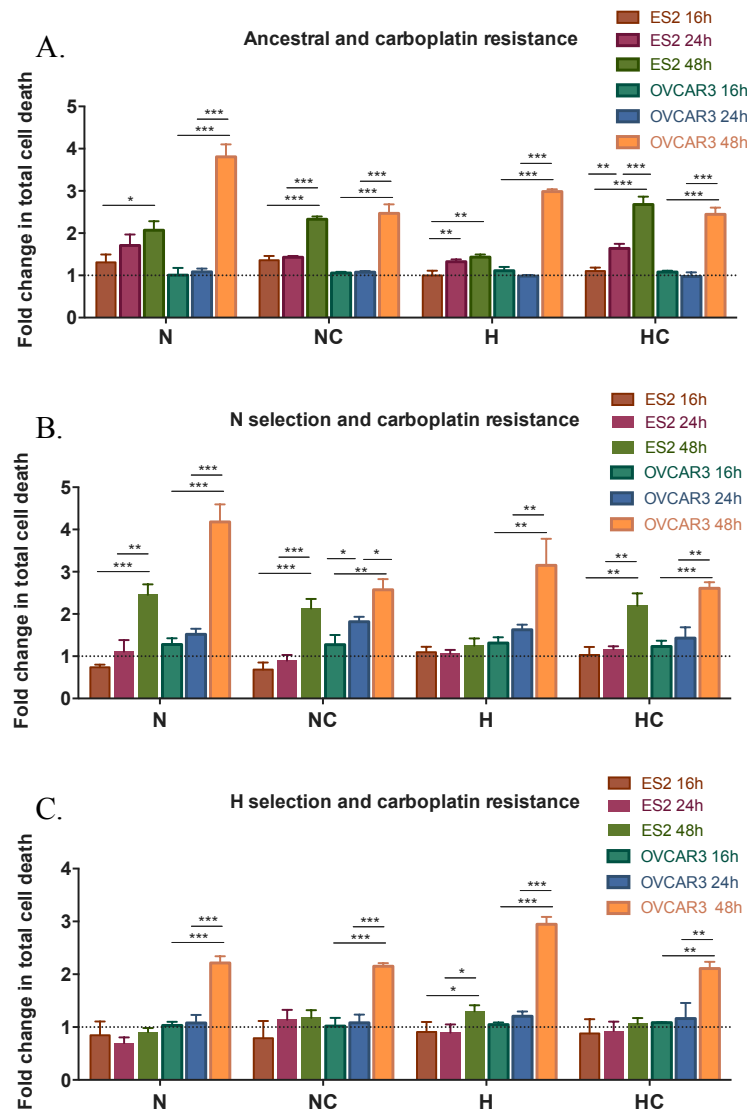


Figure 8. ES2 and OVCAR3 cells present different dynamics of response to carboplatin.

Cells response to Carboplatin over time for A. ancestral ES2 cells and OVCAR3 cells, B. ES2 and OVCAR3 cells selected under normoxia, C. ES2 and OVCAR3 cells selected under hypoxia. N – Normoxia; NC – Normoxia supplemented with cysteine; H – Hypoxia; HC – Hypoxia supplemented with cysteine. Data were normalised to the respective control. Results are shown as mean \pm SD. * $p < 0.05$, ** $p < 0.01$, *** $p < 0.001$ (One-way ANOVA with post hoc Tukey tests).

Taken together, results suggest that hypoxia drives carboplatin resistance in ES2 cells and, at a lower extent, in OVCAR3 cells, thus pointing a more aggressive phenotype in ES2-H than in OVCAR3-H cells. Since ES2-A and ES2-N cells were able to take advantage from cysteine under hypoxia (ES2-AH and ES2-NH), we propose that cysteine allows a quicker response and adaptation to hypoxic conditions that, in turn, drive carboplatin resistance.

ES2 cells present metabolic diversity in adverse environments, favouring resistance to carboplatin

The codes of each cell line and culture condition are presented in supplement table I.

In a drug-free environment, the analysis of ROS levels allowed the observation of two distinct populations in ES2-NH (figure 9 A), indicating the existence of a glycolytic and an oxidative phosphorylative population of cells. Interestingly, hypoxia was especially disadvantageous for the later cells, presenting the higher cell death levels in this condition (figure 3 A). This suggests that metabolic diversity among ES2-N cells could be a strategy to cope with new adverse environments.

In ES2-HH, we only observed one population, thus revealing a higher metabolic adaptive capacity to hypoxia (figure 9 B). Interestingly, in OVCAR3-NH we were not able to distinguish two different populations of cells as in ES2-NH (figure 9 C). Also, we observed a trend to higher ROS levels in both ES2-N and ES2-H than in OVCAR3-N and OVCAR3-H, especially in conditions with cysteine supplementation (Figure 10 A to D and supplementary table IX A to D). This might indicate that cysteine allows higher metabolic activity in ES2 cells, even under hypoxia. Moreover, the detection of ROS, using 2', 7'-Dichlorofluorescein diacetate, never showed a correlation between higher ROS levels and higher cell death levels in any cell line. On the contrary, ROS showed a negative correlation with cell death.

Upon carboplatin exposure, different populations were also observed for ES2-N cells under hypoxia (figure 9 E), thus showing again that this cell line present different cell populations with different metabolic states in an adverse environment. In addition, ES2-HH with cysteine showed a notable increase in ROS levels upon carboplatin exposure (figure 9 F and 10 E and F and supplement table IX E and F). Upon carboplatin exposure, OVCAR3-A, OVCAR3-N and OVCAR3-H cells did not show different populations in any treatment (figure 9 G and H). Interestingly, OVCAR3-H selected cells showed no differences in ROS dynamics, thus suggesting that cells do not present metabolic diversity (figure 9 H).

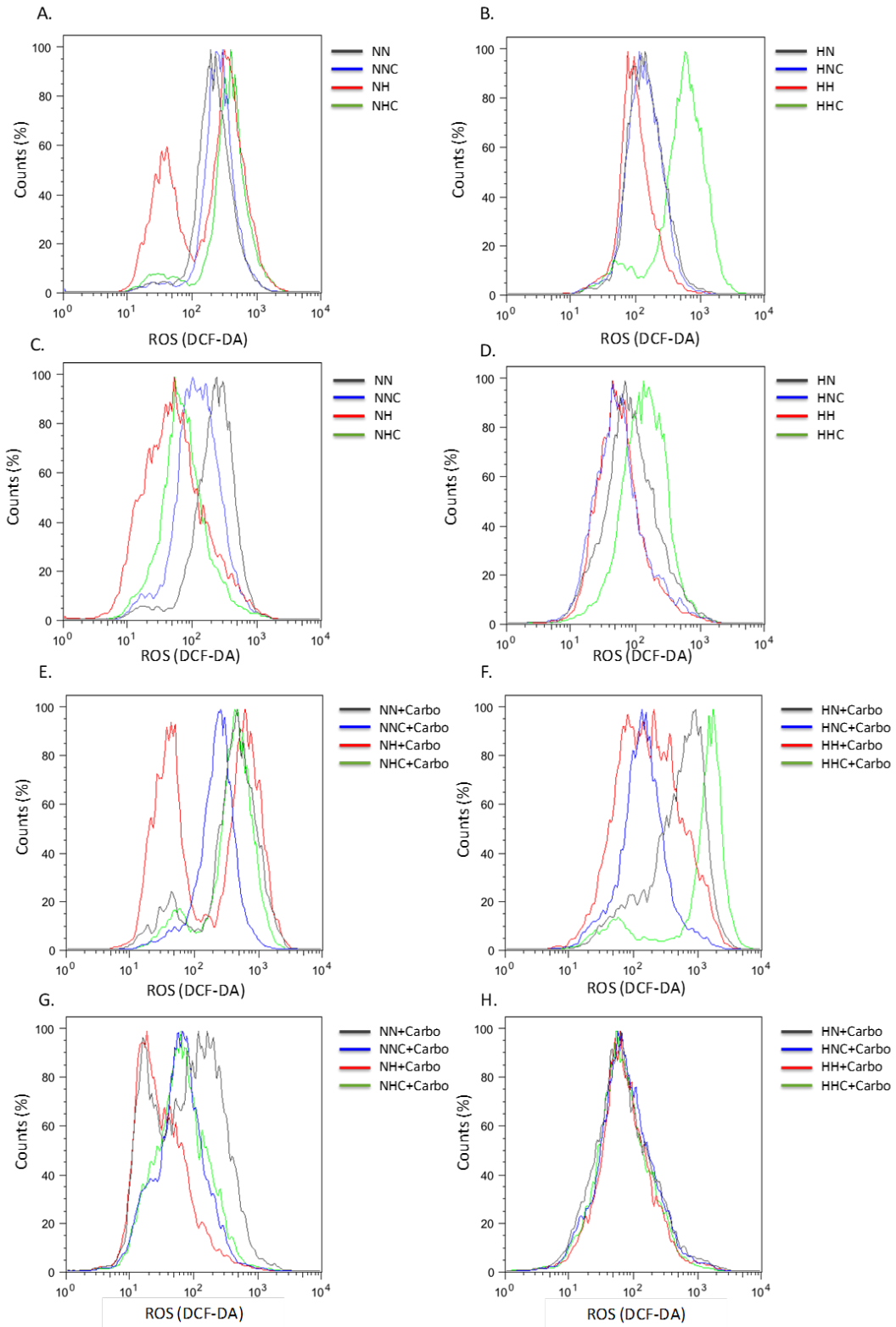


Figure 9. ES2 cells present metabolic diversity in adverse environments.

ROS histogram for A. ES2-N cells, B. ES2-H cells, C. OVCAR3-N cells, D. OVCAR3-H cells in a free drug environment for 48 h of experimental conditions, and ROS histogram for E. ES2-N cells, F. ES2-H cells, G. OVCAR3-N cells and H. OVCAR3-H in the presence of carboplatin. NN – cells selected under normoxia and cultured under normoxia (grey line); NNC – cells selected under normoxia and cultured under normoxia supplemented with cysteine (blue line); NH – cells selected under normoxia and cultured under hypoxia (red line); NHC – cells selected under normoxia and cultured under hypoxia

supplemented with cysteine (green line); HN – cells selected under hypoxia and cultured under normoxia (grey line); HNC – cells selected under hypoxia and cultured under normoxia supplemented with cysteine (blue line); HH – cells selected under hypoxia and cultured under hypoxia (red line); HHC – cells selected under hypoxia and cultured under hypoxia supplemented with cysteine (green line).

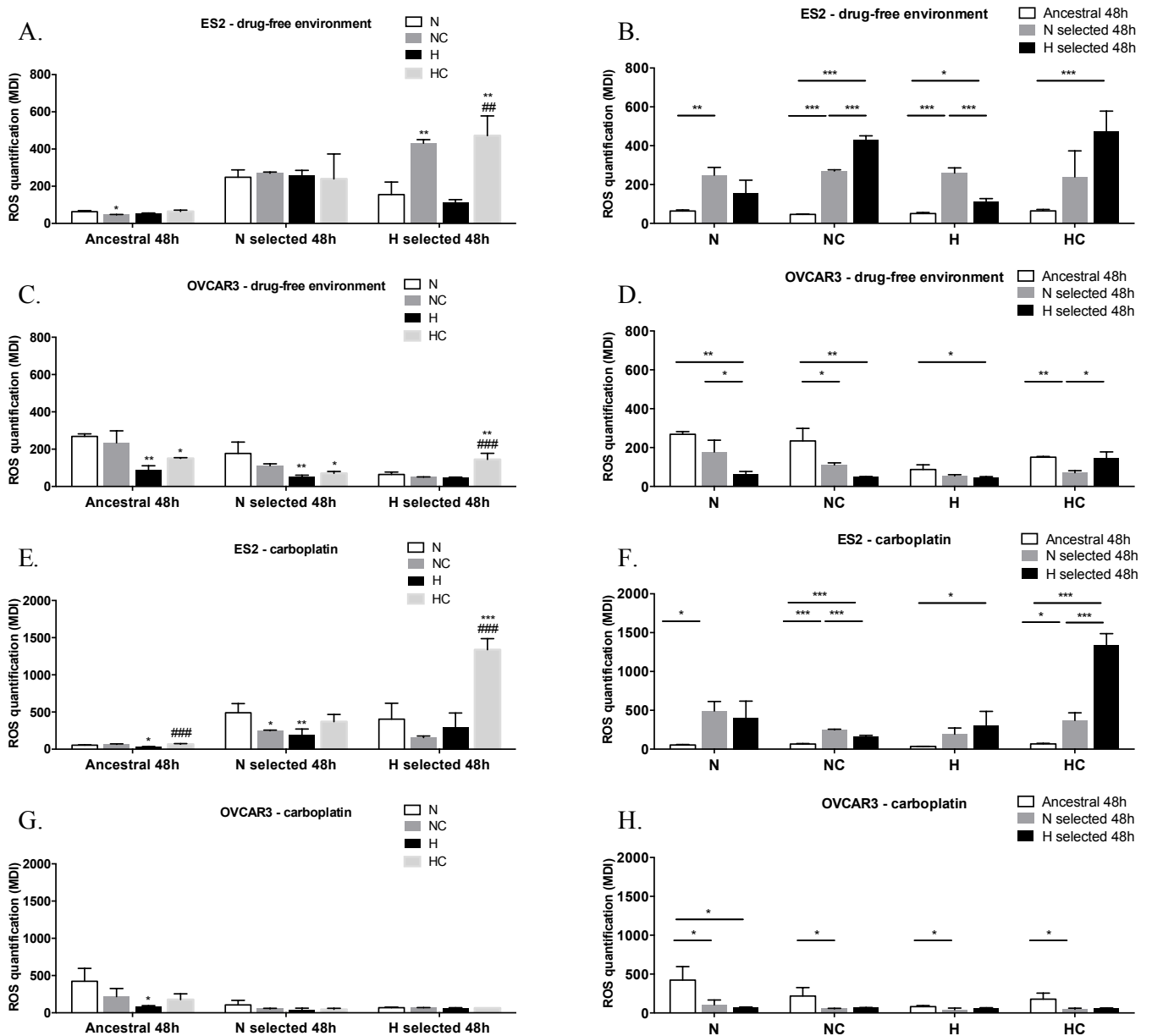


Figure 10. ROS levels in ES2 and OVCAR3 ancestral cells, cells selected under normoxia and under hypoxia.

ROS levels in a drug-free environment for 48 h of assay for A. and B. ES2 cells and C. and D. OVCAR3 cells and ROS levels in the presence of Carboplatin for 48 h of assay for E. and F. ES2 cells and G. and H. OVCAR3. N selected – cells selected under normoxia; H selected – cells selected under hypoxia; N – Normoxia; NC – Normoxia supplemented with cysteine; H – Hypoxia; HC – Hypoxia supplemented with cysteine. Results are shown as mean \pm SD. Asterisks (*) represent statistical significance compared to cells cultured under normoxia within each cell line. Cardinals (#) represent statistical significance compared to cells cultured under hypoxia within each cell line. * p <0.05, ** p <0.01, *** p <0.001 or # p <0.05, ## p <0.01, ### p <0.001 (One-way ANOVA with post hoc Tukey tests).

Taken together, results support that ES2 cells present higher metabolic diversity under adverse environments when compared to OVCAR3 cells. This diversity possibly explains the increased response capacity of ES2 cells to the more stressful environments (hypoxia and carboplatin), whereas, in general, OVCAR3 cells failed to respond to it.

DISCUSSION

Although the outcome prognosis of OCCC and other histological subtypes has been a matter of controversy, it was shown that patients with OCCC present a significantly worse prognosis than patients with ovarian serous carcinomas when matched for age, stage, and level of primary surgical cytoreduction [36,37]. Moreover, while OCCC shows primary resistance to conventional platinum-based chemotherapy [10,11], in HG-OSC both initial sensitiveness with the development of progressive resistance [9,38] and primary resistance exists [38]. Interestingly, Beaufort and colleagues have explored the associations between the cellular and molecular features of 39 ovarian cancer cell lines and their clinical features [39]. They reported an association of the spindle-like tumours with metastasis, advanced stage, suboptimal debulking and poor prognosis [39]. Importantly, ES2 cells were included in this group whereas OVCAR3 cells were not [39]. In here, we used these two different cancer cell lines derived from these two histological types of ovarian cancer and addressed the effect of cells selection under normoxia and CoCl_2 mimicked hypoxia on the evolutionary outcome of cancer cells, exploring also the role of cysteine in this adaptive process.

The adaptation to a specific environment is widely associated to deterioration in other non-selective environments, being accompanied by an evolutionary trade-off [40–43]. Our results supported an evolutionary trade-off in ovarian cancer cells adaptation to normoxic conditions in which, cells adapted under normoxia duplicated rapidly but at the cost of increased mortality in adverse environments. Notably, in ES2 cells, cysteine was able to suppress this trade-off under hypoxia (ES2-NH versus ES2-NHC). It was already reported that intracellular cysteine directly induces the HIF prolyl-hydroxylases, leading to HIF-1 α degradation [44,45], thus indicating that cysteine is able to convert a hypoxic cellular metabolism into a normoxic one. In addition, our data showed that ES2 ancestral cells present both higher intracellular cysteine and GSH degradation levels under hypoxia supplemented with cysteine compared to hypoxia without cysteine supplementation (chapter 3). Those observations could explain the protective effect of cysteine under hypoxia in both ancestral

and normoxia selected ES2 cells, thus allowing counteracting the disadvantage under hypoxia. Moreover, those results also support that ES2 cells selected under normoxia (ES2-N) still present metabolic diversity concerning cysteine metabolism under hypoxic conditions (ES2-NH). Interestingly, OVCAR3-N cells showed less plasticity.

ES2-H presented increased survival in non-selective environments compared to cells selected under normoxia (ES2-N), suggesting a generalist, more adaptive and more aggressive phenotype. Remarkably, results showed that the increased survival was accompanied by lower proliferation rates. Life history theory proposes that cancer cells may be subjected to trade-offs between maximizing cell survival and cell growth, and that both strategies can be successful depending on the environmental conditions [46]. We observed that ES2-H proliferated more slowly than ES2-N, but, nevertheless, presented increased survival in the presence of carboplatin, a cytotoxic agent used in ovarian cancer treatment, thus showing that life-history trade-offs may have clinical implications for cancer patients. These results are in accordance with the observations that hypoxia promote tumour progression and resistance to therapy (reviewed in [47]), having a complex role in the hallmarks of human cancers [13,48,49]. Importantly, hypoxia is known to induce mitochondrial ROS levels [50,51]. ROS levels are widely associated with tumour initiation, progression and chemoresistance [51–53]. Our results showed increased ROS levels in ES2-H cells under hypoxia and cysteine supplementation upon carboplatin exposure. Interestingly, in the same conditions, ES2 cells showed a higher ability to survive upon carboplatin exposure. Nevertheless, it remains unclear if the increased ROS levels are responsible for carboplatin resistance or, on the contrary, if the higher cells adaptability to this environment leads cells to increased metabolic activity, thus increasing ROS levels.

Notably, OVCAR3-A and OVCAR3-N cells showed to be less sensitive to hypoxia than ES2-A and ES2-N cells, suggesting that these cells would be more prone to chemoresistance than ES2 cells. However, OVCAR3 cells presented a poorer response capacity to carboplatin, thus indicating that resistance to hypoxia alone cannot explain the more aggressive phenotypes. OVCAR3 cells also presented decreased cellular diversity concerning ROS levels in adverse environments. Our results highlight the role of hypoxia-induced chemoresistance in combination with metabolic diversity in cancer cells coping with adverse conditions. Whereas ES2 cells showed metabolic diversity, indicative of metabolism reprogramming in adverse conditions, OVCAR3 cells seemed to be ineffective in this process, thus preventing an increased survival upon carboplatin cytotoxicity. These results also reinforce that the metabolic adaptive capacity of cancer cells to cope with new adverse

environments is more important to cancer progression than the size of the cancer cell population, as OVCAR3 cells showed to be less sensitive to hypoxia, nonetheless presenting poor response to carboplatin exposure. In the natural course of cancer disease it is a low number of cells that are capable of resisting to adverse and toxic environments during treatment, that are further responsible for recurrent disease.

We must highlight that ES2 and OVCAR3 cells were selected during different times, due to a lower proliferation rate of OVCAR3 cells under hypoxia compared to ES2, which could explain, in part, the lower diversity observed in OVCAR3 selected cells, as these cells were selected during more time than ES2 cells. However, in what concerns carboplatin resistance, we would expect an association between higher selection time and higher levels of resistance. However, in a general way, OVCAR3 selected cells showed to be less resistant than ES2 selected cells. Moreover, our main propose was to compare the effect of selection under normoxia and hypoxia and cysteine supplementation in the dynamics of adaptation to carboplatin within each cell line (ES2/OVCAR3) and the time of selection was the same in these situations. Also, the ancestral OVCAR3 (OVCAR3-A) cells showed similar dynamics of response to carboplatin as selected cells, corroborating the results. The proliferation curves/cell cycle analysis and cell death analysis /ROS quantification were also performed with different selection times within each cell line but we did not aim to compare proliferation with cell death. The only speculation done was regarding ES2 cells selected under hypoxia and increased survival accompanied by lower proliferation rates. However, since proliferation curves were performed with increased selection time, it would be expected that the same selection time as cell death analysis, would lead to a more pronounced effect on decreased cell proliferation, given less time for adaptation.

Our second hypothesis that selection under hypoxia in ES2 (ES2-H) cells would favour a stronger ability of cells to benefit from cysteine under hypoxia showed to be false in a drug-free environment. Strikingly, in the presence of carboplatin, cysteine was especially advantageous to ES2-H, thus suggesting that they evolved mechanisms to a better usage of this amino acid in new adverse environments. In this study, we only focused on the role of cysteine supplementation in response to hypoxia and further response to carboplatin cytotoxicity. We did not address other amino acids since we were interested in cysteine as a sulphur source in hypoxia and carboplatin resistance. However, in another study we showed that glutamine also played a role in GSH synthesis, as glutamine is a source of glutamate and glycine [25], supporting again a role of thiols in chemoresistance.

Taken together, results have shown that the adaptation to normoxia and hypoxia leads ovarian cancer cells to display opposite strategies. Whereas cells adapted to hypoxia tended to proliferate less but show increased survival in adverse environments, cells adapted to normoxia present the opposite strategy, proliferating rapidly but at the cost of increased mortality in adverse environments. Albeit the limited number of cell lines, those different evolutionary courses should be taken into account in the clinical context, as therapy protocols could be more effective dependent on the evolutionary strategy of cancer cells. Moreover, results highlighted that the ability of ovarian cancer cells to use cysteine has an impact in cancer cells adaptation to hypoxic environment and, ultimately, to platinum-based chemotherapeutic agents, allowing the selection of resistant phenotypes that are more aggressive, being able to carry out cancer progression and recurrence (figure 11).

Finally, our study supports that experimental evolution in cancer is a valuable tool to predict metabolic adaptation underlying drugs resistance, which can further contribute to the improvement of anti-cancer treatment strategies.

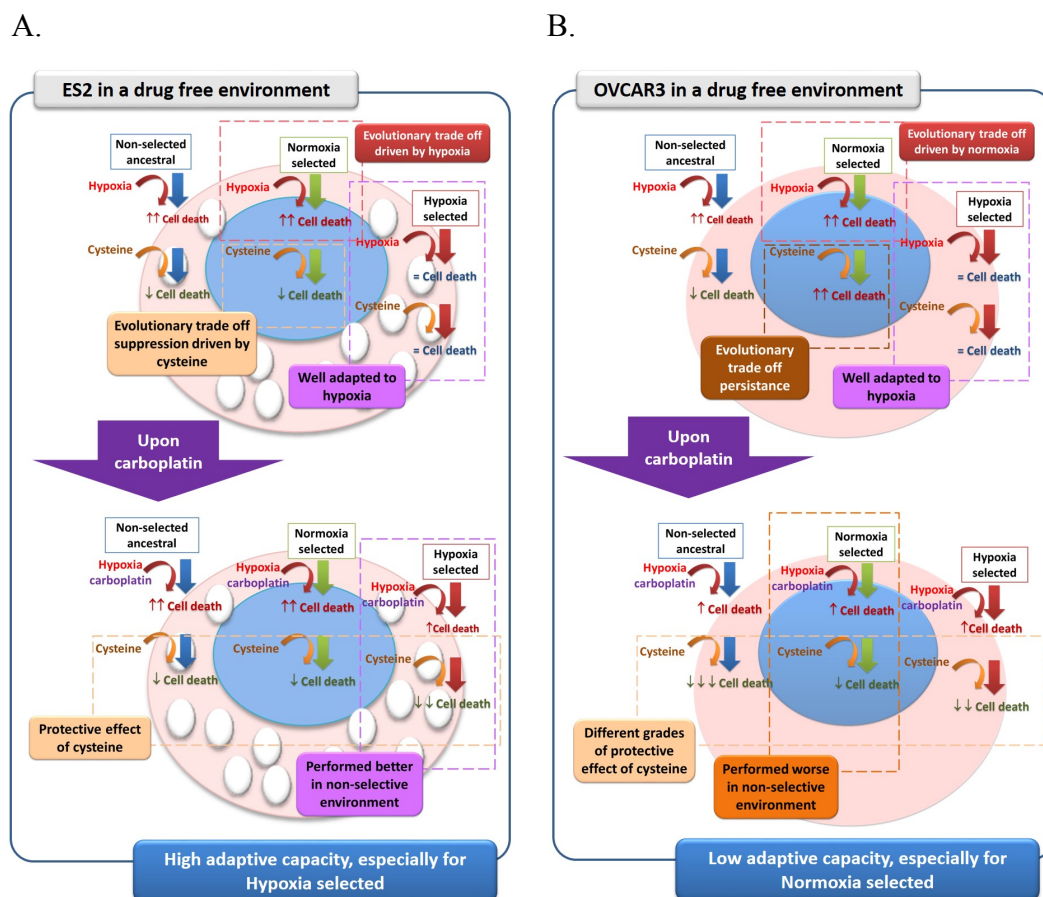


Figure 11. ES2 and OVCAR3 present different adaptive capacities in a drug free environment, impacting the response to carboplatin.

A. Non-selected ancestral and Normoxia selected ES2 cell lines showed disadvantageous under hypoxia that cysteine was able to revert, protecting cells from hypoxia-induced death. Importantly, Normoxia

selected ES2 cell lines present an evolutionary trade-off when exposed to hypoxia, reverted by cysteine. Hypoxia selected cells behave equally in all environments. Upon carboplatin exposure, cysteine protected all ES2 cells variants, decreasing carboplatin cytotoxicity under hypoxia. Thus, ES2 cells exhibited a high adaptive capacity to hypoxia and cysteine, which reflects in a higher fitness upon carboplatin exposure, being hypoxia selected the best fitted. B. Non-selected ancestral and Normoxia selected OVCAR3 cell lines also showed disadvantageous under hypoxia. Normoxia selected OVCAR3 cell lines also showed an evolutionary trade-off when exposed to hypoxia, but cysteine only reverted this disadvantage under hypoxia in Non-selected ancestral cells. Upon carboplatin exposure, cysteine protects all OVCAR3 cells, decreasing carboplatin cytotoxicity under hypoxia. OVCAR3 cells variants benefit from different grades of cysteine protection: Non-selected ancestral > hypoxia selected > Normoxia selected. Overall, OVCAR3 cells exhibited a lower adaptive capacity to hypoxia and cysteine, which reflects in a loss of fitness upon carboplatin exposure. Overall, ES2 cells present a higher metabolic plasticity than OVCAR3 cells. This fact might underlie the intrinsic resistance to carboplatin exhibited by OCCC histology in the clinical context. White ellipses in ES2 cells represent vacuoles characteristic of clear cell carcinoma.

REFERENCES

1. Bray F, Ferlay J, Soerjomataram I, Siegel RL, Torre LA, Jemal A. Global Cancer Statistics 2018: GLOBOCAN Estimates of Incidence and Mortality Worldwide for 36 Cancers in 185 Countries. *CA Cancer J Clin.* 2018;68:394–424.
2. Bast Jr RC, Hennessy B, Mills GB. The biology of ovarian cancer: New opportunities for translation. *Nat. Rev. Cancer.* 2009;9:415–28.
3. Bowtell DD. The genesis and evolution of high-grade serous ovarian cancer. *Nat Rev Cancer.* 2010;10:803–8.
4. Chan JK, Cheung MK, Husain A, Teng NN, West D, Whittemore AS, *et al.* Patterns and progress in ovarian cancer over 14 years. *Obstet. Gynecol.* 2006;108:521–8.
5. Vaughan S, Coward JI, Jr RCB, Berchuck A, Berek JS, Brenton JD, *et al.* Rethinking ovarian cancer: recommendations for improving outcomes Sebastian. *Nat. Rev.* 2011;11:719–25.
6. Itamochi H, Kigawa J, Terakawa N. Mechanisms of chemoresistance and poor prognosis in ovarian clear cell carcinoma. 2008;99:653–8.
7. Agarwal R, Kaye SB. Ovarian cancer: strategies for overcoming resistance to chemotherapy. *Nat. Rev. Cancer.* 2003;3:502–16.
8. Ip CKM, Li S, Tang MH, Sy SKH, Ren Y. Stemness and chemoresistance in epithelial ovarian carcinoma cells under shear stress. *Sci. Rep.* 2016;6:26788–98.
9. Cooke SL, Brenton JD, Way R. Evolution of platinum resistance in high-grade serous ovarian cancer. *Lancet Oncol.* 2011;12:1169–74.
10. Sugiyama T, Kamura T, Kigawa J, Terakawa N, Kikuchi Y, Kita T, *et al.* Clinical characteristics of clear cell carcinoma of the ovary. *Cancer.* 2000;88:2584–9.
11. Goff BA, de la Cuesta RS, Muntz HG, D. F, Ek M, Rice LW, *et al.* Clear cell carcinoma of the ovary: a distinct histologic type with poor prognosis and resistance to platinum-based chemotherapy in stage III disease. *Gynecol. Oncol.* 1996;417:412–7.

12. Serpa J, Dias S. Metabolic cues from the microenvironment act as a major selective factor for cancer progression and metastases formation. *Cell Cycle*. 2011;10:180–1.
13. Hanahan D, Weinberg RA. Hallmarks of cancer: The next generation. *Cell*. 2011;144:646–74
14. Almendros I, Gozal D. Intermittent hypoxia and cancer: Undesirable bed partners? *Respir. Physiol. Neurobiol*. 2017;256:79-86.
15. Mikalsen SG, Jeppesen Edin N, Sandvik JA, Pettersen EO. Separation of two sub-groups with different DNA content after treatment of T-47D breast cancer cells with low dose-rate irradiation and intermittent hypoxia. *Acta radiol*. 2017;59:26-33.
16. Campillo N, Torres M, Vilaseca A, Nonaka PN, Gozal D, Roca-Ferrer J, *et al*. Role of Cyclooxygenase-2 on Intermittent Hypoxia-Induced Lung Tumor Malignancy in a Mouse Model of Sleep Apnea. *Sci. Rep*. 2017;7:44693.1–11.
17. Gutsche K, Randi EB, Blank V, Fink D, Wenger RH, Leo C, *et al*. Intermittent hypoxia confers pro-metastatic gene expression selectively through NF- κ B in inflammatory breast cancer cells. *Free Radic. Biol. Med*. 2016;101:129–42.
18. Cutter NL, Walther T, Gallagher L, Lucito R, Wrzeszczynski K. Hypoxia signaling pathway plays a role in ovarian cancer chemoresistance. *Proc. Am. Assoc. Cancer Res. Annu. Meet*. 2017; April 1-5, 2017; Washington, DC. Abstract 4525.
19. Bhattacharyya S, Saha S, Giri K, Lanza IR, Nair KS, Jennings NB, *et al*. Cystathionine Beta-Synthase (CBS) Contributes to Advanced Ovarian Cancer Progression and Drug Resistance. *PLoS One*. 2013;8:e79167.1-12.
20. Szabo C, Coletta C, Chao C, Módis K, Szczesny B, Papapetropoulos A. Tumor-derived hydrogen sulfide, produced by cystathionine- β -synthase, stimulates bioenergetics, cell proliferation, and angiogenesis in colon cancer. *PNAS Pharmacol*. 2013;110:12474–9.
21. Sen S, Kawahara B, Gupta D, Tsai R, Khachatryan M, Farias-eisner R, *et al*. Role of cystathionine β -synthase in human breast Cancer. *Free Radic. Biol. Med*. 2015;86:228–38.
22. Panza E, De Cicco P, Armogida C, Scognamiglio G, Gigantino V, Botti G, *et al*. Role of the cystathionine γ lyase/hydrogen sulfide pathway in human melanoma progression. *Pigment Cell Melanoma Res*. 2015;28:61–72.
23. Gai JW, Qin W, Liu M, Wang HF, Zhang M, Li M, *et al*. Expression profile of hydrogen sulfide and its synthases correlates with tumor stage and grade in urothelial cell carcinoma of bladder. *Urol. Oncol. Semin. Orig. Investig*. 2016;34:166.e15-20.
24. Pan Y, Zhou C, Yuan D, Zhang J, Shao C. Radiation Exposure Promotes Hepatocarcinoma Cell Invasion through Epithelial Mesenchymal Transition Mediated by H₂S/CSE Pathway. *Radiat. Res*. 2015;185:96–105.
25. Lopes-Coelho F, Gouveia-Fernandes S, Gonçalves LG, Nunes C, Faustino I, Silva F, *et al*. HNF1B drives glutathione (GSH) synthesis underlying intrinsic carboplatin resistance of ovarian clear cell carcinoma (OCCC). *Tumor Biology*; 2016;37:4813–29.
26. Schnelldorfer T, Gansauge S, Gansauge F, Schlosser S, Beger HG, Nussler AK. Glutathione depletion causes cell growth inhibition and enhanced apoptosis in pancreatic cancer cells. *Cancer*. 2000;89:1440–7.

27. Balendiran GK, Dabur R, Fraser D. The role of glutathione in cancer. *cell Biochem. Funct.* 2004;22:343–52.
28. Kigawa J, Minagawa Y, Cheng X, Terakawa N. γ -Glutamyl cysteine synthetase up-regulates Multidrug resistance-associated protein in Patients with chemorresistant epithelial ovarian cancer. *Clin. Cancer Res.* 1998;4:1737–41.
29. Kelland L. The resurgence of platinum-based cancer chemotherapy. *Nat. Rev. Cancer.* 2007;7:573–84.
30. Epstein AC, Gleadle JM, McNeill LA, Hewitson KS, O'Rourke J, Mole DR, *et al.* *C. elegans* EGL-9 and mammalian homologs define a family of dioxygenases that regulate HIF by prolyl hydroxylation. *Cell.* 2001;107:43–54.
31. Wu D, Yotnda P. Induction and Testing of Hypoxia in Cell Culture. *J. Vis. Exp.* 2011;54:1–4.
32. Goldberg MA, Dunning SP, BH. Regulation of the erythropoietin gene: evidence that the oxygen sensor is a heme protein. *Science.* 1988;242:1412–5.
33. Al Okail MS. Cobalt chloride, a chemical inducer of hypoxia-inducible factor-1 α in U251 human glioblastoma cell line. *J. Saudi Chem. Soc. Japanese Association for Dental Science;* 2010;14:197–201.
34. Yuan Y, Hilliard G, Ferguson T, Millhorn DE. Cobalt inhibits the interaction between hypoxia-inducible factor- α and von Hippel-Lindau protein by direct binding to hypoxia-inducible factor- α . *J. Biol. Chem.* 2003;278:15911–6.
35. Ghaly, AE, Kok R. The effect of sodium sulfite and cobalt chloride on the oxygen transfer coefficient. *Applied biochemistry and biotechnology.* 1988;19:259-270.
36. Tammela J, Geisler J, Eskew PJ, Geisler H. Clear cell carcinoma of the ovary: poor prognosis compared to serous carcinoma. *Eur. J. Gynaecol. Oncol.* 1998;19:438–40.
37. Lee Y, Kim T, Kim M, Kim H, Song T, Kyu M, *et al.* Gynecologic Oncology Prognosis of ovarian clear cell carcinoma compared to other histological subtypes: A meta-analysis. *Gynecol. Oncol.* 2011;122:541–7.
38. Slaughter K, Holman LL, Thomas EL, Gunderson CC, Lauer JK, Ding K, *et al.* Primary and acquired platinum-resistance among women with high grade serous ovarian cancer. *Gynecol. Oncol.* 2016;142:225–30.
39. Beaufort CM, Helmijr JCA, Piskorz AM, Hoogstraat M, Ruigrok-Ritstier K, Besselink N, *et al.* Ovarian cancer cell line panel (OCCP): Clinical importance of in vitro morphological subtypes. *PLoS One.* 2014;9:e103988.1-16.
40. Futuyma DJ, Moreno G. The evolution of ecological specialization. *Annu. Rev. Ecol. Evol. Syst.* 1988;19:207–33.
41. Novak M, Pfeiffer T, Lenski RE, Sauer U, Bonhoeffer S. Experimental tests for an evolutionary trade-off between growth rate and yield in *E. coli*. *Am. Nat.* 2006;168:242–51.
42. Bennett AF, Lenski RE. An experimental test of evolutionary trade-offs during temperature adaptation. *Proc. Natl. Acad. Sci. U. S. A.* 2007;104 Suppl 1:8649–54.
43. Stearns S. Trade-offs in life-history evolution. *Funct. Ecol.* 1989;3:259–68.

44. Lu H, Dalgard CL, Mohyeldin A, McFate T, Tait AS, & Verma A. Reversible inactivation of HIF-1 prolyl hydroxylases allows cell metabolism to control basal HIF-1. *Journal of Biological Chemistry*. 2005;280:41928-39.
45. Briggs KJ, Koivunen P, Cao S, Backus KM, Olenchock BA, Patel, H., *et al.* Paracrine induction of HIF by glutamate in breast cancer: EglN1 senses cysteine. *Cell*. 2016; 166:126-39.
46. Aktipis CA, Boddy AM, Gatenby RA, Brown JS, Maley CC. Life history trade-offs in cancer evolution. *Nat. Rev. Cancer*. 2013;13:883–92.
47. Vaupel P, Mayer A. Hypoxia in cancer: Significance and impact on clinical outcome. *Cancer Metastasis Rev*. 2007;26:225–39.
48. Ruan K, Song G, Ouyang G. Role of hypoxia in the hallmarks of human cancer. *J. Cell. Biochem*. 2009;107:1053–62.
49. Hanahan D, Weinberg RA. The hallmarks of cancer. *Cell*. 2000;100:57–70.
50. Sabharwal SS, & Schumacker PT. Mitochondrial ROS in cancer: initiators, amplifiers or an Achilles' heel?. *Nature Reviews Cancer*. 2014;14:709-21.
51. Waypa GB, Marks JD, Guzy R, Mungai PT, Schriewer J, Dokic D, & Schumacker PT. Hypoxia triggers subcellular compartmental redox signaling in vascular smooth muscle cells. *Circulation research*. 2010;106:526-535.
52. Schumacker PT. Reactive oxygen species in cancer: a dance with the devil. *Cancer cell*. 2015;27:156-7.
53. Gupta SC, Hevia D, Patchva S, Park B, Koh W, Aggarwal BB Upsides and downsides of reactive oxygen species for cancer: the roles of reactive oxygen species in tumorigenesis, prevention, and therapy. *Antioxidants & redox signaling*. 2012;16:1295-322.

SUPPLEMENTS

Supplement table I: Ovarian cancer cell lines, selection and culture conditions.

Cell line- histological type	Cell line code	Selection condition	Culture condition	
Ovarian clear cell carcinoma (OCCC; ES2)	ES2-AN	Non selected ancestral cell line	Normoxia	
	ES2-ANC	Non selected ancestral cell line	Normoxia + cysteine	
	ES2-AH	Non selected ancestral cell line	Hypoxia	
	ES2-AHC	Non selected ancestral cell line	Hypoxia + cysteine	
	ES2-NN	Selected under Normoxia	Normoxia	
	ES2-NNC	Selected under Normoxia	Normoxia + cysteine	
	ES2-NH	Selected under Normoxia	Hypoxia	
	ES2-NHC	Selected under Normoxia	Hypoxia + cysteine	
	ES2-HN	Selected under Hypoxia	Normoxia	
	ES2-HNC	Selected under Hypoxia	Normoxia + cysteine	
	ES2-HH	Selected under Hypoxia	Hypoxia	
	ES2-HHC	Selected under Hypoxia	Hypoxia + cysteine	
	Serous carcinoma (HG-OSC; OVCAR3)	OVCAR3-AN	Non selected ancestral cell line	Normoxia
		OVCAR3-ANC	Non selected ancestral cell line	Normoxia + cysteine
OVCAR3-AH		Non selected ancestral cell line	Hypoxia	
OVCAR3-AHC		Non selected ancestral cell line	Hypoxia + cysteine	
OVCAR3-NN		Selected under Normoxia	Normoxia	
OVCAR3-NNC		Selected under Normoxia	Normoxia + cysteine	
OVCAR3-NH		Selected under Normoxia	Hypoxia	
OVCAR3-NHC		Selected under Normoxia	Hypoxia + cysteine	
OVCAR3-HN		Selected under Hypoxia	Normoxia	
OVCAR3-HNC		Selected under Hypoxia	Normoxia + cysteine	
OVCAR3-HH	Selected under Hypoxia	Hypoxia		
OVCAR3-HHC	Selected under Hypoxia	Hypoxia + cysteine		

Supplement table II: Adaptation to normoxia confers a highly proliferative ability to ES2 cells.

A.

Treatments – proliferation curve (48 h)	Tukey test sig.
ES2-NN vs ES2-HN	0.000
ES2-NN vs ES2-HH	0.000
ES2-NH vs ES2-HN	0.000
ES2-NH vs ES2-HH	0.001

B.

Treatments – cell cycle analysis	Tukey test sig.
G0/G1 ES2-NN vs ES2-NH	0.02

C.

Treatments – proliferation curve (48 h)	Tukey test sig.
OVCAR3-NN vs OVCAR3-HH	0.036

D.

Treatments – cell cycle analysis	Tukey test sig.
G0/G1 OVCAR3-NN vs OVCAR3-HH	0.006
G0/G1 OVCAR3-NH vs OVCAR3-HN	0.033
G0/G1 OVCAR3-NH vs OVCAR3-HH	0.001
G2/M OVCAR3-NH vs OVCAR3-HH	0.027

Supplement table III. Adaptation to normoxia is accompanied by an evolutionary trade-off that is suppressed by cysteine under hypoxia in ES2 cells.

A.

Treatments – cell death analysis (48 h)	Tukey test sig.
ES2-AN vs ES2-AH	0.008
ES2-ANC vs ES2-AH	0.001
ES2-AHC vs ES2-AH	0.001
ES2-NN vs ES2-NH	0.000
ES2-NNC vs ES2-NH	0.000
ES2-NHC vs ES2-NH	0.000

B.

Treatments – cell death analysis (48 h)	Tukey test sig.
ES2-NNC vs ES2-HNC	0.030
ES2-NH vs ES2-AH	0.034
ES2-NH vs ES2-HH	0.001
ES2-HH vs ES2-AH	0.016

C.

Treatments – cell death analysis (48 h)	Tukey test sig.
OVCAR3-AN vs OVCAR3-AH	0.000
OVCAR3-ANC vs OVCAR3-AH	0.000
OVCAR3-AHC vs OVCAR3-AH	0.003
OVCAR3-NH vs OVCAR3-NN	0.003
OVCAR3-NH vs OVCAR3-NNC	0.004

D.

Treatments – cell death analysis (48 h)	Tukey test sig.
OVCAR3-AN vs OVCAR3-HN	0.002
OVCAR3-NN vs OVCAR3-HN	0.009
OVCAR3-ANC vs OVCAR3-NNC	0.004
OVCAR3-ANC vs OVCAR3-HNC	0.000
OVCAR3-NNC vs OVCAR3-HNC	0.001
OVCAR3-AH vs OVCAR3-NH	0.036
OVCAR3-HH vs OVCAR3-NH	0.008

Supplement table IV. ES2 and OVCAR3 cells resistance to hypoxia.

Treatments – cell death analysis (48 h)	Independent samples T test sig.
ES2-AH vs OVCAR3-AH	0.009
ES2-NH vs OVCAR3-NH	0.009
ES2-HH vs OVCAR3-HH	0.004

Supplement table V. Hypoxia provides stronger resistance to carboplatin.

A.

Treatments – cell death analysis (48 h)	Tukey test sig.
ES2-AN Ctr vs Carboplatin	0.008
ES2-ANC Ctr vs Carboplatin	0.000
ES2-AH Ctr vs Carboplatin	0.019
ES2-AHC Ctr vs Carboplatin	0.0000
ES2-NN Ctr vs Carboplatin	0.008
ES2-NNC Ctr vs Carboplatin	0.002
ES2-NH Ctr vs Carboplatin	0.069
ES2-NHC Ctr vs Carboplatin	0.006
ES2-HN Ctr vs Carboplatin	0.412
ES2-HNC Ctr vs Carboplatin	0.175
ES2-HH Ctr vs Carboplatin	0.016
ES2-HHC Ctr vs Carboplatin	0.706

B.

Treatments – cell death analysis (48 h)	Tukey test sig.
ES2-HN vs ES2-AN	0.001
ES2-HN vs ES2-NN	0.000
ES2-HNC vs ES2-ANC	0.000
ES2-HNC vs ES2-NNC	0.001
ES2-HHC vs ES2-AHC	0.000
ES2-HHC vs ES2-NHC	0.001

C.

Treatments – cell death analysis (48 h)	Tukey test sig.
OVCAR3-AN Ctr vs Carboplatin	0.000
OVCAR3-ANC Ctr vs Carboplatin	0.000
OVCAR3-AH Ctr vs Carboplatin	0.000
OVCAR3-AHC Ctr vs Carboplatin	0.000
OVCAR3-NN Ctr vs Carboplatin	0.000
OVCAR3-NNC Ctr vs Carboplatin	0.000
OVCAR3-NH Ctr vs Carboplatin	0.026
OVCAR3-NHC Ctr vs Carboplatin	0.000
OVCAR3-HN Ctr vs Carboplatin	0.000
OVCAR3-HNC Ctr vs Carboplatin	0.000
OVCAR3-HH Ctr vs Carboplatin	0.000
OVCAR3-HHC Ctr vs Carboplatin	0.001

D.

Treatments – cell death analysis (48 h)	Tukey test sig.
OVCAR3-HN vs OVCAR3-AN	0.002
OVCAR3-HN vs OVCAR3-NN	0.001
OVCAR3-HHC vs OVCAR3-NHC	0.013

Supplement table VI. Metabolic evolution driven by hypoxia provides stronger resistance to carboplatin.

A.

Treatments – cell death analysis (48 h)	Tukey test sig.
ES2-AN vs ES2-ANC	0.006
ES2-AN vs ES2-AH	0.003
ES2-ANC vs ES2-AH	0.000
ES2-AH vs ES2-AHC	0.000
ES2-NN vs ES2-NH	0.002
ES2-NNC vs ES2-NH	0.000
ES2-NHC vs ES2-NH	0.001
ES2-HN vs ES2-HH	0.006
ES2-HNC vs ES2-HH	0.001
ES2-HHC vs ES2-HH	0.001

B.

Treatments – cell death analysis (48 h)	Tukey test sig.
OVCAR3-AN vs OVCAR3-ANC	0.000
OVCAR3-AN vs OVCAR3-AH	0.001
OVCAR3-AN vs OVCAR3-AHC	0.006
OVCAR3-AH vs OVCAR3-AHC	0.000
OVCAR3-ANC vs OVCAR3-AH	0.000
OVCAR3-NNC vs OVCAR3-NH	0.002
OVCAR3-NHC vs OVCAR3-NH	0.018
OVCAR3-HN vs OVCAR3-HH	0.013
OVCAR3-HNC vs OVCAR3-HH	0.000
OVCAR3-HHC vs OVCAR3-HH	0.003

Supplement table VII. ES2 cells tend to present a stronger resistance to carboplatin than OVCAR3 cells.

A.

Treatments – cell death analysis (48 h)	T test sig.
ES2-AN vs OVCAR3-AN	0.001
ES2-ANC vs OVCAR3-ANC	0.347
ES2-AH vs E OVCAR3-AH	0.000
ES2-AHC vs OVCAR3-AHC	0.179

B.

Treatments – cell death analysis (48 h)	T test sig.
ES2-NN vs OVCAR3-NN	0.003
ES2-NNC vs OVCAR3-NNC	0.085
ES2-NH vs E OVCAR3-NH	0.007
ES2-NHC vs OVCAR3-NHC	0.092

C.

Treatments – cell death analysis (48 h)	T test sig.
ES2-HN vs OVCAR3-HN	0.000
ES2-HNC vs OVCAR3-HNC	0.000
ES2-HH vs E OVCAR3-HH	0.000
ES2-HHC vs OVCAR3-HHC	0.000

Supplement Table VIII. ES2 and OVCAR3 cells dynamics of response to carboplatin.

A.

Treatments – cell death analysis – 16 h vs 24 h vs 48 h	Tukey test sig.
ES2-AN 16 h vs 48 h	0.014
ES2-ANC 16 h vs 48 h	0.000
ES2-ANC 24 h vs 48 h	0.000
ES2-AH 16 h vs 24 h	0.006
ES2-AH 24 h vs 48 h	0.001
ES2-AHC 16 h vs 24 h	0.007
ES2-AHC 16 h vs 48 h	0.000
ES2-AHC 24 h vs 48 h	0.000
OVCAR3-AN 16 h vs 48 h	0.000
OVCAR3-AN 24 h vs 48 h	0.000

OVCAR3-ANC 16 h vs 48 h	0.000
OVCAR3-ANC 24 h vs 48 h	0.000
OVCAR3-AH 16 h vs 48 h	0.000
OVCAR3-AH 24 h vs 48 h	0.000
OVCAR3-AHC 16 h vs 48 h	0.000
OVCAR3-AHC 24 h vs 48 h	0.000

B.

Treatments – cell death analysis – 16 h vs 24 h vs 48 h	Tukey test sig.
ES2-NN 16 h vs 48 h	0.000
ES2-NN 24 h vs 48 h	0.001
ES2-NNC 16 h vs 48 h	0.000
ES2-NNC 24 h vs 48 h	0.000
ES2-NHC 16 h vs 48 h	0.001
ES2-NHC 24 h vs 48 h	0.002
OVCAR3-NN 16 h vs 48 h	0.000
OVCAR3-NN 24 h vs 48 h	0.000
OVCAR3-NNC 16 h vs 24 h	0.041
OVCAR3-NNC 16 h vs 48 h	0.001
OVCAR3-NNC 24 h vs 48 h	0.01
OVCAR3-NH 16 h vs 48 h	0.002
OVCAR3-NH 24 h vs 48 h	0.006
OVCAR3-NHC 16 h vs 48 h	0.000
OVCAR3-NHC 24 h vs 48 h	0.001

C.

Treatments – cell death analysis – 16 h vs 24 h vs 48 h	Tukey test sig.
ES2-HH 16 h vs 48 h	0.048
ES2-HH 24 h vs 48 h	0.043
OVCAR3-HN 16 h vs 48 h	0.000
OVCAR3-HN 24 h vs 48 h	0.000
OVCAR3-HNC 16 h vs 48 h	0.000
OVCAR3-HNC 24 h vs 48 h	0.000
OVCAR3-HH 16 h vs 48 h	0.000
OVCAR3-HH 24 h vs 48 h	0.000
OVCAR3-HHC 16 h vs 48 h	0.001
OVCAR3-HHC 24 h vs 48 h	0.002

Supplement table IX. ROS levels in ES2 and OVCAR3 ancestral cells, cells selected under normoxia and under hypoxia.

A.

Treatments – ROS quantification (48 h)	Tukey test sig.
ES2-AN vs ES2-ANC	0.021
ES2-AHC vs ES2-ANC	0.016
ES2-HN vs ES2-HNC	0.003
ES2-HN vs ES2-HHC	0.001
ES2-HH vs ES2-HNC	0.001
ES2-HH vs ES2-HHC	0.001

B.

Treatments – ROS quantification (48 h)	Tukey test sig.
ES2-AN vs ES2-NN	0.006
ES2-ANC vs ES2-NNC	0.000
ES2-ANC vs ES2-HNC	0.000
ES2-HNC vs ES2-NNC	0.000
ES2-AH vs ES2-NH	0.000
ES2-AH vs ES2-HH	0.013
ES2-HH vs ES2-NH	0.000
ES2-AHC vs ES2-HHC	0.006

C.

Treatments – ROS quantification (48 h)	Tukey test sig.
OVCAR3-AN vs OVCAR3-AH	0.001
OVCAR3-ANC vs OVCAR3-AH	0.004
OVCAR3-AN vs OVCAR3-AHC	0.015
OVCAR3-NN vs OVCAR3-NH	0.006
OVCAR3-NN vs OVCAR3-NHC	0.013
OVCAR3-HN vs OVCAR3-HHC	0.003
OVCAR3-HNC vs OVCAR3-HHC	0.001
OVCAR3-HH vs OVCAR3-HHC	0.001

D.

Treatments – ROS quantification (48 h)	Tukey test sig.
OVCAR3-AN vs OVCAR3-HN	0.001
OVCAR3-NN vs OVCAR3-HN	0.021
OVCAR3-ANC vs OVCAR3-NNC	0.017

OVCAR3-ANC vs OVCAR3-HNC	0.002
OVCAR3-AH vs OVCAR3-HH	0.035
OVCAR3-AHC vs OVCAR3-NHC	0.007
OVCAR3-HHC vs OVCAR3-NHC	0.01

E.

Treatments – ROS quantification (48 h)	Tukey test sig.
ES2-AN vs ES2-AH	0.015
ES2-ANC vs ES2-AH	0.001
ES2-AHC vs ES2-AH	0.000
ES2-NN vs ES2-NNC	0.026
ES2-NN vs ES2-NH	0.008
ES2-HN vs ES2-HHC	0.000
ES2-HH vs ES2-HHC	0.000
ES2-HNC vs ES2-HHC	0.000

F.

Treatments – ROS quantification (48 h)	Tukey test sig.
ES2-AN vs ES2-NN	0.022
ES2-ANC vs ES2-NNC	0.000
ES2-ANC vs ES2-HNC	0.000
ES2-NNC vs ES2-HNC	0.000
ES2-AH vs ES2-HH	0.026
ES2-AHC vs ES2-NHC	0.019
ES2-AHC vs ES2-HHC	0.000
ES2-NHC vs ES2-HHC	0.000

G.

Treatments – ROS quantification (48 h)	Tukey test sig.
OVCAR3-AN vs OVCAR3-AH	0.022

H.

Treatments – ROS quantification (48 h)	Tukey test sig.
OVCAR3-AN vs OVCAR3-NN	0.025
OVCAR3-AN vs OVCAR3-HN	0.016
OVCAR3-ANC vs OVCAR3-NNC	0.044
OVCAR3-AH vs OVCAR3-NH	0.043
OVCAR3-AHC vs OVCAR3-NHC	0.03

CHAPTER 3

CYSTEINE ALLOWS OVARIAN CANCER CELLS TO ADAPT TO HYPOXIA AND TO ESCAPE FROM CARBOPLATIN CYTOTOXICITY

This chapter is based on the following publication:

Nunes, S.C.; Ramos, C.; Lopes-Coelho, F.; Sequeira, C.O.; Silva, F.; Gouveia-Fernandes, S.; Rodrigues, A.; Guimarães, A.; Silveira, M.; Abreu, S.; *et al.* Cysteine allows ovarian cancer cells to adapt to hypoxia and to escape from carboplatin cytotoxicity. *Sci Rep.* 2018;8:9513–29.

“And who by fire, who by water,
Who in the sunshine, who in the night time,
Who by high ordeal, who by common trial,
Who in your merry merry month of may,
Who by very slow decay,
And who shall I say is calling?
And who in her lonely slip, who by barbiturate,
Who in these realms of love, who by something blunt,
And who by avalanche, who by powder,
Who for his greed, who for his hunger,
And who shall I say is calling?
And who by brave assent, who by accident,
Who in solitude, who in this mirror,
Who by his lady's command, who by his own hand,
Who in mortal chains, who in power,
And who shall I say is calling?”
Leonard Cohen

ABSTRACT

In the last 30 years, an improvement of the overall survival of ovarian cancer patients has been observed. However, an increased cure rate was not, and ovarian cancer is still the third most common gynaecologic malignancy and the main cause of death from gynaecologic cancer. The high mortality associated with ovarian cancer is mainly due to late diagnosis and resistance to treatment, barring ovarian cancer cure. Several studies have reported a role of cysteine in cancer by contributing for hydrogen sulphide (H₂S) generation and as a precursor of the antioxidant glutathione (GSH). In the chapter two, our results supported a role of cysteine in a fast response and adaptation to hypoxic conditions that, in turn, were capable of driving chemoresistance.

In here, we aimed to deepen the role of cysteine in hypoxia and anti-cancer drugs response, by addressing if cysteine has a widespread protective effect in ovarian cancer cells. We also explored cysteine role in a clinical context of ovarian cancer patients. Hence, we used several ovarian cancer cell lines: ES2, OVCAR3, OVCAR8, A2780 and A2780cisR (a cisplatin resistant variant). In addition, we also quantified cysteine in peripheral blood serum from patients with ovarian tumours (benign and malignant) and healthy individuals, in samples from ovarian tumours with different histologies and in ascitic fluid derived from patients with advanced ovarian cancer, an important component of disseminated ovarian cancer cells microenvironment.

Results have shown that cysteine presents a widespread protective effect against hypoxia and carboplatin-induced death among ovarian cancer cell lines. Interestingly, while cysteine was able to protect A2780 cisR cell line from carboplatin-induced death, it was not able to protect A2780 parental cells, supporting that cysteine is crucial for chemoresistance. Importantly, our data regarding peripheral blood serum and ascitic fluid from patients also pointed to a role of cysteine in a clinical context of ovarian cancer. Hence, data have shown that GSH degradation and subsequent cysteine recycling pathway were associated with ovarian cancer. Moreover, the levels of S-cysteinylated proteins together with the free levels of cysteine in serum were capable of distinguishing serum from patients with malignant tumours from patients with benign tumours and healthy individuals. Cysteine was also the prevalent thiol found in ascitic fluid from patients with advanced disease.

Herein, this chapter strongly reinforces that cysteine contributes for a worse disease prognosis, allowing a faster adaptation to hypoxia and protecting ovarian cancer cells from carboplatin-induced death. Moreover, data also support a clinical relevance of cysteine,

where serum cysteine levels could be an effective tool for screening, early diagnosis, outcome prediction and follow up of disease progression.

KEYWORDS

Cancer, chemoresistance, cysteine, hypoxia, metabolism, ovarian, tumour, ascitic fluid, protein-S-cysteinylation, thiols.

INTRODUCTION

Ovarian cancer includes different diseases [1] and constitute the main cause of death from gynaecologic cancer, being the third most common gynaecologic malignancy worldwide [2]. The diagnosis at an advanced stage together with resistance to conventional therapy, are the main causes of ovarian cancer poor prognosis [3]. Epithelial ovarian cancer (EOC) is classified based on histopathology and molecular genetic features, being the high-grade serous (HG-OSC) the most prevalent histotype [3,4,5,6]. The OCC is a rather uncommon histotype that is highly chemoresistant [7]. Surgery and a combined paclitaxel-carboplatin chemotherapy is the standard care for ovarian cancer [8]. However, despite an initial response, the disease recurs in over 85% of cases with advanced ovarian cancer [9]. The development of ascites is a common characteristic of these carcinomas [10], containing growth factors secreted by both cancer and stromal cells [10] that are mitogenic to cancer cells, contributing for an ideal microenvironment for tumour growth [11,12].

Metabolism reprogramming, already considered as an emerging hallmark of cancer [13], provides enough sources of energy and biomass to support cancer cell survival and proliferation [14].

Expanding evidence exists on the dependence of these processes on cysteine and its metabolism, as cysteine not only contributes to hydrogen sulphide (H₂S) generation [15–20], as it is the rate-limiting precursor for glutathione (GSH) synthesis [21–23]. It is known that tumours are subjected to intermittent hypoxia [24,25] and that hypoxia-inducible factors (HIFs) mediate adaptive pathophysiological responses underlying resistance to radiation therapy and chemotherapy [26]. In the context of ovarian cancer, Cutter *et al.*, have recently reported that cancer cell lines subject to hypoxia exhibit a more aggressive phenotype [27]. Additionally, higher levels of cytoplasmic thiol-containing species, including GSH or

metallothioneins have been associated with resistance to platinum-based chemotherapy [23,28]. These species are rich in cysteine and result in decreased drug availability and increased intracellular drug detoxification/inactivation, since platinum binds readily to sulphhydryl groups [29].

In the previous chapter, our results supported a role of cysteine in ovarian cancer cells fast response and adaptation to hypoxic conditions that, in turn, were capable to drive chemoresistance. In here, we aimed to deepen the role of cysteine in hypoxia and anti-cancer drugs response, by addressing if cysteine has a widespread protective effect in ovarian cancer cells. Hence, we used several ovarian cancer cell lines, including high grade serous carcinoma (OVCAR3 and OVCAR8, HG-OSC), sensitive and resistant to Cisplatin A2780, unspecified histotype ovarian carcinoma cells (A2780 parental and A2780 cisR) and clear cell carcinoma cells (OCCC- ES2). In addition, we also explored the role of cysteine and other thiols in a clinical context of ovarian cancer, by analysing their levels in peripheral blood serum from patients with benign and malignant tumours, from healthy individuals, in samples from ovarian carcinomas and in ascitic fluid from ovarian cancer patients.

MATERIAL AND METHODS

Cell culture

Cell lines ES2 (CRL-1978), OVCAR-3 (HTB-161) and OVCAR-8 (CVCL-1629) were obtained from American Type Culture Collection (ATCC). Cell line A2780 sensitive (93112519) and A2780 cisplatin resistant (93112517) were obtained from Sigma Aldrich. Cells were maintained at 37°C in a humidified 5% CO₂ atmosphere. ES2, OVCAR3 and OVCAR8 cell lines were cultured in DMEM (41965-039, Gibco, Life Technologies) supplemented with 1% FBS (S 0615, Merck), 1% antibiotic-antimycotic (AA) (P06-07300, PAN Biotech). A2780 parental and A2780 cisR cells were cultured in RPMI 1640 (BE12-167F, Lonza) supplemented with 0.58 g/L of L-glutamine, 1% FBS (S 0615, Merck) and 1% antibiotic-antimycotic (AA) (P06-07300, PAN Biotech).

Cells were exposed to 0.402 mM L-Cysteine (102839, Merck) and/or exposed to hypoxia-induced conditions with 0.1 mM cobalt chloride (CoCl₂) (C8661, Sigma-Aldrich). Cobalt is a hypoxia mimicking agent used in *in vivo* [30] and *in vitro* [31–33] studies. Chemically, CoCl₂ reacts with oxygen impairing its dissolution and oxygenation of aqueous

solutions [34] and is a way of impairing the availability of oxygen in culture media.

Prior to any experiment, cells were synchronized under starvation (culture medium without FBS) for 8 h at 37°C and 5% CO₂.

Peripheral blood serum, tumour samples and ascitic fluid

After collection, the blood was allowed to clot at room temperature, during 15–30 min. The clot was removed by centrifuging at 956 g for 5 min at 4°C. Serum is the resulting supernatant, which were preserved at -80°C.

The tumours samples were frozen with isopentane and preserved at -80°C.

After collection of the ascitic fluid, it was centrifuged at 153 g for 2 min at room temperature, to remove the cells, avoiding cell lysis. The supernatant was preserved at -80°C.

The serum and ascitic fluid samples were collected from different individuals, with the exception of four serum and ascitic fluid samples, in which the patients were the same. The levels of thiols were determined in these biological samples, as described below.

Cell death analysis

Cells (5×10^5 cells/well) were seeded in 6-well plates and cultured in control condition and exposed to 0.402 mM L-cysteine and/or hypoxia induced with 0.1 mM (CoCl₂). Cells were collected at 16 h and 24 h after stimulation.

To test whether the protective effect of cysteine in ES2 and OVCAR3 cells is dose-dependent, cells (5×10^5 cells/well) were seeded in 6-well plates and cultured in control condition and exposed to 0.1 mM, 0.2 mM, 0.4 mM, 0.8 mM and 1.0 mM L-cysteine and/or hypoxia induced with 0.1 mM CoCl₂. Cells were collected at 16 h after stimulation.

To test whether the protective effect of cysteine under hypoxia was dependent on initial cell density, 5×10^3 , 2.5×10^4 , 5×10^4 and 1×10^5 cells/cm² were seeded in 24-well plates and cultured in control condition and exposed to 0.402 mM L-cysteine and/or hypoxia induced with 0.1 mM CoCl₂. Cells were collected at 16 h after stimulation.

Cells were harvested and centrifuged at 153 g for 3 min, followed by incubation with 1 μL FITC-annexin V (640906, BioLegend) in 100 μL annexin V binding buffer 1× (10 mM HEPES (pH 7.4), 0.14 M sodium chloride (NaCl), 2.5 mM calcium chloride (CaCl₂) and incubated at room temperature in the dark for 15min. After incubation, samples were rinsed

with 0.1% (w/v) BSA (A9647, Sigma) in PBS 1× and centrifuged at 153 g for 3 min. Cells were suspended in 200 μL of annexin V binding buffer 1× and 5 μL propidium iodide (PI) (50 μg/mL). Acquisition was performed with a FACScalibur (Becton Dickinson). Data were analysed with FlowJo software.

Mitochondrial membrane potential (MMP)

The MMP was measured in ES2 and OVCAR3 cell lines using JC-1 (M34152, Molecular Probes, Life Technologies) [35], a specific mitochondrial probe, which becomes red when it enters polarized mitochondria and it is green in cytoplasm when mitochondrial potential is lost avoiding its entrance.

Cells (5×10^5 cells/well) were seeded in 6-well plates and cultured in control condition and exposed to 0.402 mM L-cysteine and/or 0.1 mM CoCl₂ and were collected at 16 h after stimulation. Live cells were then washed with phosphate-buffered saline (PBS) 1x, incubated for 30 min with 5 μM JC-1 (37°C, 5% CO₂), washed with PBS 1x, trypsinized, and recovered in a final volume of 300 μL of PBS 1x. A positive depolarized control was used, in which cells were previously incubated with 50 μM CCCP for 5 min (37°C, 5% CO₂) and then incubated with JC-1. Acquisition was performed in a FACScalibur (Becton Dickinson). Data were analysed with FlowJo software.

Cells response to paclitaxel and carboplatin

Cells (1×10^5 cells/well) were seeded in 24-well plates and cultured in control condition and exposed to 0.402 mM L-cysteine and/or 0.1 mM CoCl₂. Cells were also exposed to the previous conditions combined with carboplatin 25 μg/mL, paclitaxel (10 μg/mL) or the combination of both. Cells were collected after one cycle of stimulation (16 h per cycle) and two cycles of stimulation (which was preceded by a period without drugs of proximately 32 h between cycles). Cell death analysis was performed.

CD133 quantification

Cells (2×10^5 cells/well) were seeded in 12-well plates (ES2, OVCAR3 and OVCAR8) or 24-well plates (1×10^5 cells/well) (A2780 and A2780 cisR) and cultured in control condition and exposed to 0.402 mM L-cysteine and/or 0.1 mM CoCl₂. Cells were also exposed to the

previous conditions combined with carboplatin 25 µg/mL. Cells were collected after one cycle of stimulation (16 h per cycle) and two cycles of stimulation (which was preceded by a period without drugs of approximately 32 h between cycles). Cells were collected with PBS 1x-EDTA 2 mM, centrifuged at 153 g for 3 min, re-suspended and incubated with 1 µL of anti-CD133 (AC133-PE human, Miltenyi Biotec) and 99 µL PBS-BSA 0.1% for 20 min in the dark 4°C. Acquisition was performed in a FACScalibur (Becton Dickinson). Data were analysed with FlowJo software.

Thiols quantification

Because thiols can impact protein function by the formation of intra- and inter-molecular disulfide bond(s) with proteins [36], or may exist as free thiols, we measured both total and free thiol levels.

Thiols quantification was performed by high-performance liquid chromatography (HPLC). Cells (4×10^6) were cultured in 75 cm² tissue culture flasks in control conditions and exposed either to 0.402 mM L-cysteine and/or 0.1 mM CoCl₂ for 16 h. The supernatants and the lysates were stored at -80°C. The assessment of the levels of cysteine (Cys), homocysteine (HCys), glutamylcysteine (GluCys), glutathione (GSH) and cysteinylglycine (CysGly) was performed according to Grilo and co-authors [37] and adapted to cell culture. The detector was set at excitation and emission wavelengths of 385 and 515 nm, respectively. The mobile phase consisted of 100 mM acetate buffer (pH 4.5) and methanol [98:2 (v/v)]. The analytes were separated in an isocratic elution mode for 20 min, at a flow rate of 0.6 mL/min. The thiolomic profile was also quantified in peripheral blood serum from healthy individuals and patients with malignant and benign ovarian tumours and in ascitic fluid from patients with ovarian cancer, according to Grilo *et al.* [37].

Serum samples from 12 healthy donors, 25 from patients with benign ovarian tumours and 30 from patients with malignant ovarian tumours were analysed.

Primary ovarian tumours were also analysed in a total of 12 samples, including high grade serous ovarian carcinomas before (n=3) and after chemotherapy (n=3), clear cell carcinomas (n=3) and endometrioid carcinomas (n=3).

Finally we also collected ascitic fluid samples and 41 samples were analysed, with patients diagnosed with ovarian cancer: serous, (n=32), mucinous (n=3), endometrioid (n=1) and without further histotype characterization (n=5).

Statistical analysis

Data are presented as the mean \pm SD and all the graphics were done using the PRISM software package (PRISM 6.0 for Mac OS X; GraphPad software, USA, 2013). Assays were performed with, at least, 3 replicates per experimental condition. For comparisons of two groups, two-tailed independent-samples T-test was used. For comparison of more than two groups, One-way analysis of variance (ANOVA) with Tukey's multiple-comparisons post hoc test was used. To assess the existence of a linear relationship between two variables, two-tailed Pearson correlation was used. To assess differences in cysteine and GSH levels in peripheral blood, in samples from ovarian tumours and in ascitic fluid, 2-sided independent samples Kruskal-Wallis 1-way ANOVA with pairwise comparisons was performed, where the adjusted significance was considered. Statistical significance was established as $p < 0.05$. All statistical analyses were performed using the IBM Corp. Released 2013. IBM SPSS Statistics for Macintosh, Version 22.0. Armonk, NY: IBM Corp. software.

Study approval

All the experiments were developed according to relevant guidelines and regulations.

The human samples were collected under informed consent of patients and blood donors from Instituto Português de Oncologia de Lisboa, Francisco Gentil, EPE. The study protocol was approved by the Ethical Committee IPOLFG (references: UIC/1080 and UIC/1082).

RESULTS

Cysteine has a widespread protective effect under hypoxia in ovarian cancer cells

We started by addressing if the protective effect of cysteine against hypoxia-induced death is widespread in several ovarian cancer cell lines.

Results have shown that cysteine protected ES2 cells from death under hypoxia after 16 h ($p=0.026$) (figure 1A), but the effect was not maintained after 24 h (figure 1 A). Regarding OVCAR3 cells, no differences were found in total cell death levels in both time-points (figure 1 B).

The effect of normoxia with cysteine and hypoxia without cysteine in total cell death was similar between cell lines. However, there was no similarity for the effect of hypoxia plus cysteine on cell death in ES2 and OVCAR3 cells ($p=0.049$). As observed, ES2 cells presented lower death levels compared to its control than OVCAR3 cells (figures 1 A and B). With 24 h of incubation under normoxia, cysteine induced higher levels of cell death in OVCAR3 cells compared to ES2 cells ($p=0.001$). However under hypoxia, there were no significant differences among cell lines.

Next, we addressed the long-term effect of cysteine in ovarian cancer cells, also clarifying if the absence of protection by cysteine under hypoxia with 24 h of assay in ES2 was due to cysteine consumption or CoCl_2 exhaustion. The exposure of ES2 cells to two experimental cycles revealed a significant decrease in total cell death levels in all conditions from the first to the second cycle ($p=0.000$ for N, NC and HC), with the exception of hypoxia without cysteine (figure 1 C). No major alterations were registered from the first to the second cycle in total cell death for OVCAR3 cell line with the exception of total cell death under hypoxia without cysteine, in which cell death levels increased from the first to the second cycle ($p<0.001$; figure 1 D).

We also investigated the effect of cysteine in the adaptation to hypoxia in other ovarian cancer cell lines. In OVCAR8 cell line, total cell death levels increased from the first to the second cycle under hypoxia, especially without cysteine, with no differences under normoxia conditions (under H $p<0.001$, under HC $p=0.020$) (figure 1 E). Nonetheless, in the second cycle, cysteine revealed to be also advantageous for this cell line (H vs HC $p<0.001$).

We also addressed if cysteine impacts differently the adaptive potential to hypoxia in sensitive and cisplatin resistant A2780 cells. Under hypoxia, both A2780 and A2780 cisR cell lines presented increased cell death levels in the second cycle of culture without cysteine and

A2780 cisR with cysteine (A2780 cells $p < 0.001$; A2780 cisR cells $p < 0.001$ under H and HC). Nevertheless, cysteine revealed to be advantageous under hypoxia in the second cycle for both cell lines (H vs HC for A2780 parental cells $p < 0.001$, for A2780 cisR cells $p < 0.001$) (figure 1 F and G).

These results support that different ovarian cancer cells present different abilities to metabolise cysteine. Moreover, results have shown a widespread protective effect of cysteine upon hypoxic stress in ovarian cancer cells from different histological types.

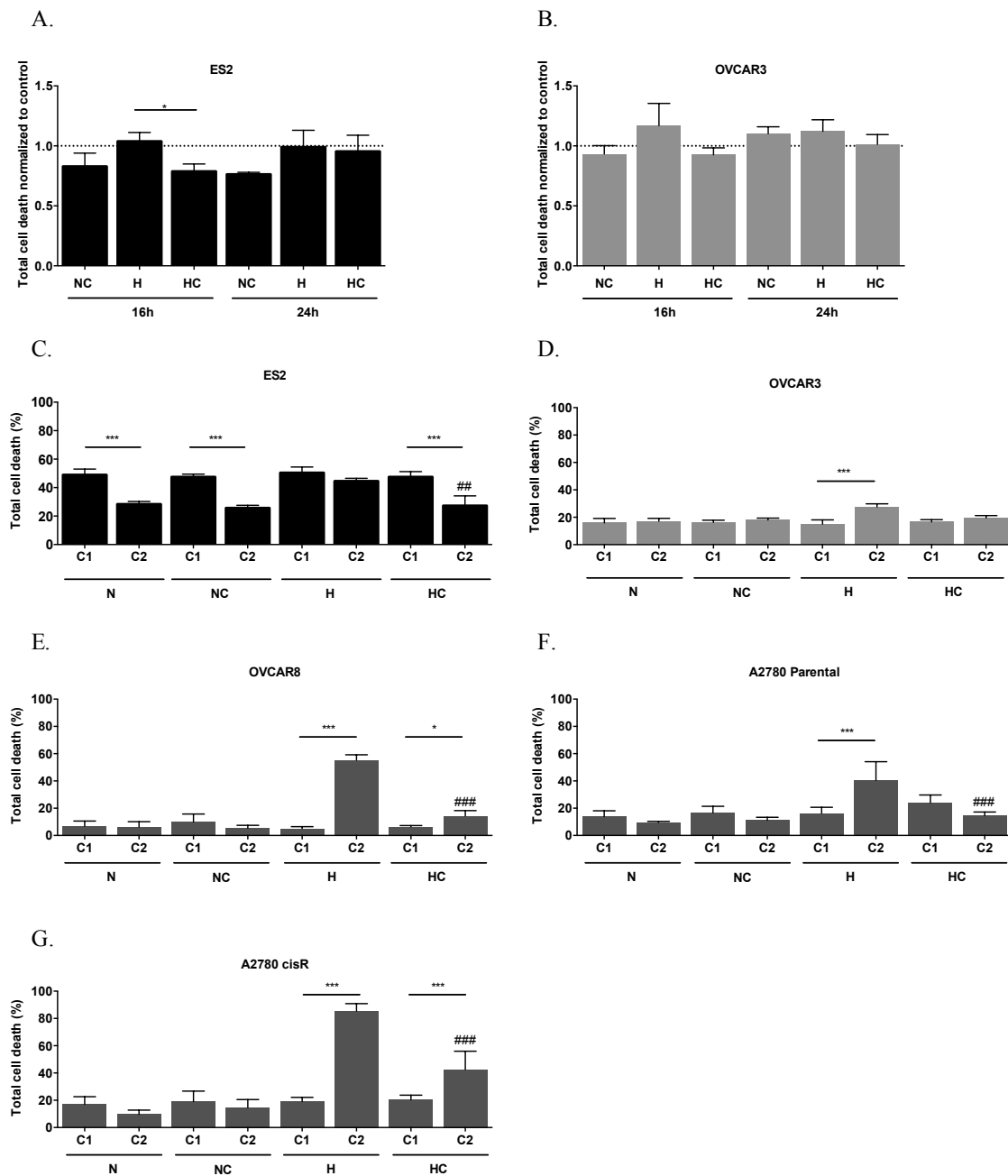


Figure 1. Cysteine has a widespread protective effect under hypoxia in ovarian cancer cells.

Total cell death normalised to control for 16 and 24 h of assay for A. ES2 cells and B. OVCAR3 cells and total cell death in the first cycle (C1) and in the second cycle (C2) of treatments in C. ES2, D.

OVCAR3, E. OVCAR8, F. A2780 parental cells and G. A2780 cisR cells. N - Normoxia; NC - Normoxia supplemented with cysteine; H - Hypoxia; HC - Hypoxia supplemented with cysteine. Results are shown as mean \pm SD. Cardinals (#) represent statistical significance among hypoxia with and without cysteine supplementation within the same cycle of treatments. * p <0.05, ** p <0.01, *** p <0.001 (One-way ANOVA with post hoc Tukey tests).

The protective effect of cysteine under hypoxia in ES2 is dose-dependent and cell density-dependent

Because so far results have pointed to a strong protective effect of cysteine under hypoxia for ES2 cells, we further asked if this protection was cysteine dose-dependent or cell density-dependent.

To test if the protection provided by cysteine under hypoxia was dose-dependent, we performed an assay under normoxia and hypoxia without cysteine and with increasing cysteine concentrations and compared the cell death levels with OVCAR3 cells.

Results have shown that while there were no dose-dependence effects in ES2 under normoxia (figure 2 A), cell death decreased under hypoxia with increasing cysteine concentrations (Pearson $r=-0.777$, $p<0.001$) (figure 2 B).

Regarding OVCAR3 cells, there was no correlation between cell death and cysteine concentration neither under normoxia nor under hypoxia (figure 2 C and D).

To test if this protective effect of cysteine under hypoxia in ES2 cells was dependent on cell density, several initial cell densities were tested. In a general way, results showed a decreased cell death trend with increased cell density ($p<0.001$ for all conditions) (figure 2 E). Moreover, results suggested that the protective effect of cysteine under hypoxia was dependent on cell density, as demonstrated by the decreased cell death ratio HC/H with the increase of cell density (Pearson $r=-0.628$, $p=0.003$) (figure 2F) whereas cell density did not impact on the cell death ratio NC/N (figure 2 F).

Regarding OVCAR3 cells, the results also showed lower levels of cell death with higher cell densities in all conditions ($p=0.004$), with the exception of the control (figure 2 G). However, there was no impact of cell density neither on the NC/N nor on the HC/H ratios (figure 2 H).

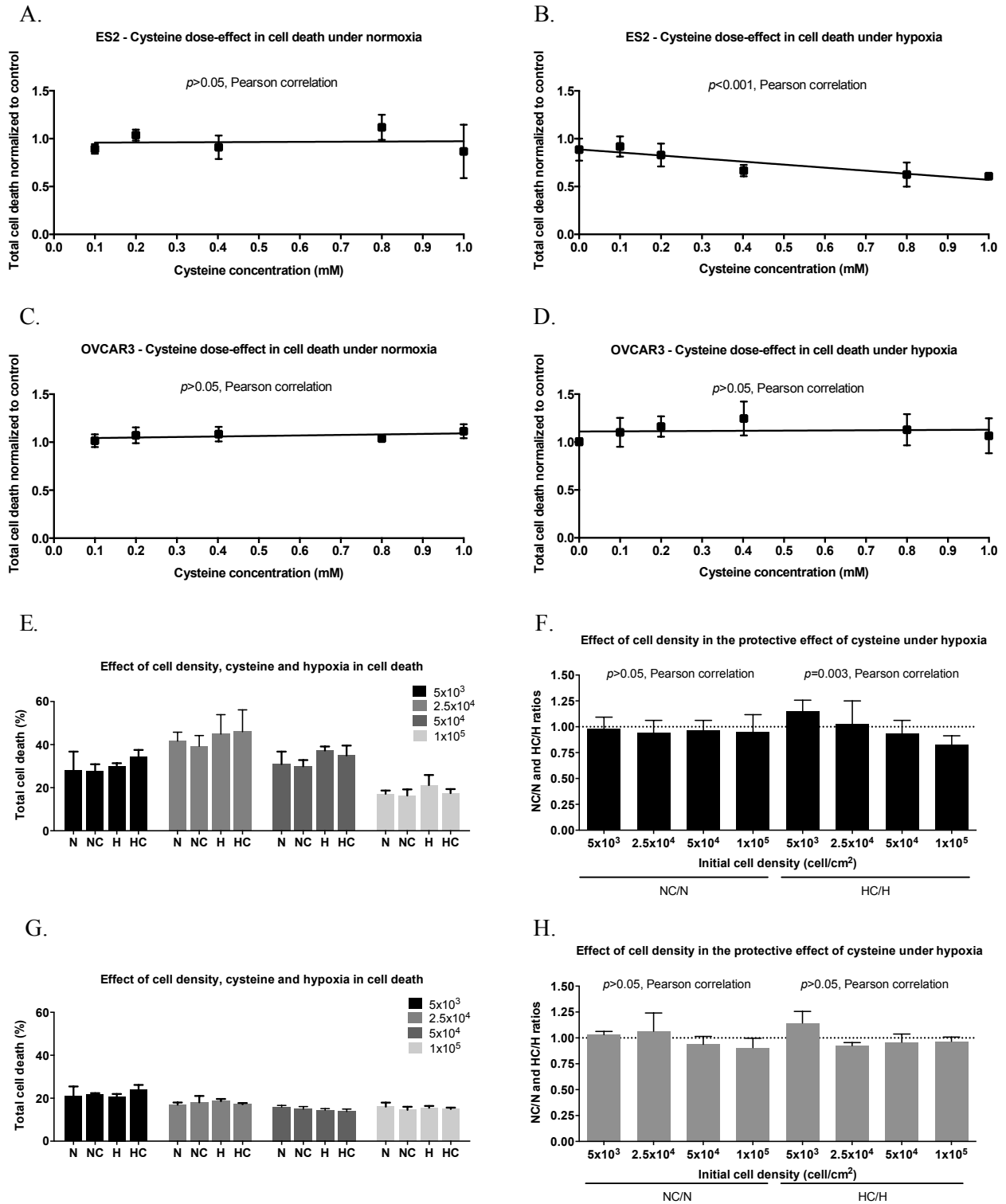


Figure 2. The dose dependent and cell density dependent effects of cysteine in hypoxia adaptation in ES2 and OVCAR3 cells.

A. Pearson correlation under normoxia for ES2 cell line, B. Pearson correlation under hypoxia for ES2 cell line, C. Pearson correlation under normoxia for OVCAR3 cell line and D. Pearson correlation under hypoxia for OVCAR3 cell line for 16 h of assay. Treatments were normalised to the control values (normoxia without cysteine supplementation). E. Percentage of total cell death for ES2 cells for 16 h of assay for different initial cell densities, F. Pearson correlation for NC/N and HC/H ratios for ES2 cells, G. Percentage of total cell death for OVCAR3 cells for 16 h of assay for different initial cell densities

and H. Pearson correlation for NC/N and HC/H ratios for OVCAR3 cells. N – Normoxia; NC – Normoxia supplemented with cysteine; H – Hypoxia; HC – Hypoxia supplemented with cysteine. 5×10^3 , 2.5×10^4 , 5×10^4 and 1×10^5 refers to initial cell densities expressed as cells/cm². Results are shown as mean \pm SD.

Cysteine increases mitochondrial membrane potential in ES2 under normoxia and in OVCAR3 under normoxia and hypoxia

Mitochondrial membrane potential ($\Delta\psi_m$) is associated with ATP production by oxidative phosphorylation, being a good indicator of cells health and functional status[38]. $\Delta\psi_m$ changes can be measured by red/green fluorescence intensity ratio using JC-1 probe, in which $\Delta\psi_m$ loss can be detected by a decrease in this ratio.

For ES2 cells, the $\Delta\psi_m$ loss was lower under N plus cysteine (NC) compared to the other conditions ($p=0.005$ compared to N, $p<0.001$ compared to H and $p=0.001$ compared to HC) (figure 3). However, there were no differences among hypoxia with and without cysteine.

Regarding OVCAR3 cells, the $\Delta\psi_m$ loss was always lower in the presence of cysteine (NC vs N $p=0.002$, NC vs H $p=0.024$, HC vs N $p<0.001$ and HC vs H $p=0.002$) (figure 3).

Together, results suggest that cysteine allows mitochondrial function and cell health, especially under normoxia for ES2 cells and both under normoxia and hypoxia for OVCAR3 cells.

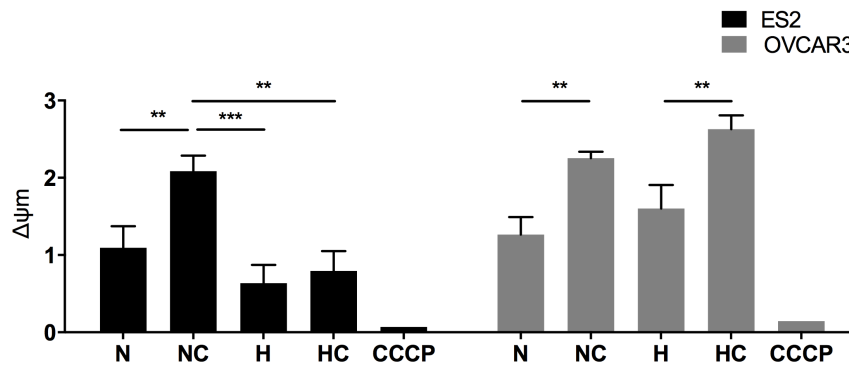


Figure 3. Mitochondrial membrane potential under normoxia and hypoxia with and without cysteine in ES2 and OVCAR3 cells.

Quantification of $\Delta\psi_m$ expressed as a ratio of red/green fluorescence intensity ratio in the different treatments (ratio of geometrical means) for ES2 and OVCAR3 cell lines for 16 h of assay. CCCP is a positive control for depolarization. N – Normoxia; NC – Normoxia supplemented with cysteine; H – Hypoxia; HC – Hypoxia supplemented with cysteine. Results are shown as mean \pm SD. * $p<0.05$, ** $p<0.01$, *** $p<0.001$ (One-way ANOVA with post hoc Tukey tests).

ES2 cells adaptation to hypoxia relies on free intracellular cysteine availability

We then asked if ES2 and OVCAR3 cells presented different capacities to uptake cysteine and whether the dynamics of GSH synthesis and degradation could explain the protective effect of cysteine under hypoxia. For this, the free fraction and the protein-bound fraction of several thiols were measured.

Results have shown that ES2 cells present higher free intracellular levels of cysteine in all treatments than OVCAR3 cells ($p=0.001$ in N, $p<0.001$ in NC, $p=0.003$ in H, $p<0.001$ in HC) (figure 4 A). Also, cysteine supplementation induced higher free intracellular levels of cysteine both under normoxia ($p=0.001$) and hypoxia ($p=0.008$) in ES2 cells. This result supports that hypoxia did not impair ES2 cells capacity to uptake this amino acid or that in these cells cysteine is not channelled for protein-S-cysteinylated pool or to *de novo* GSH synthesis.

Thus, we asked how S-cysteinylated proteins (CysSSP) were comparable between the two cell lines. We observed that hypoxia reduced CysSSP in ES2 cells ($p=0.02$, for N vs H, $p=0.037$ for N vs HC, $p=0.009$ for NC vs H and $p=0.016$ for NC vs HC) (figure 4 B). This might suggest that this intracellular pool of cysteine is reduced to supply free cysteine for cells adaptation to hypoxia. In fact, CysSSP was not increased by cysteine under hypoxia, indicating the need of free cysteine availability and that the supplemented cysteine is not targeting proteins by S-cysteinylated.

We then tried to clarify if the protection provided by cysteine under hypoxia was associated with GSH synthesis or degradation. In ES2 cells, no changes were observed neither for GSH intracellular levels among the experimental conditions (figure 4 C), nor for GluCys, the first product of GSH synthesis, even with supplementation of cysteine (figure 4D), indicating that ES2 cells maintain high levels of available cysteine that are not being canalized to GSH synthesis. Moreover, in hypoxia conditions, the supplementation of cysteine increased GSH catabolism and cysteine recycling, as seen by the increased ratio CysGly/GSH, being CysGly the first product of GSH degradation. Thus, hypoxia decreased CysSSP levels supplying free Cys levels (figure 4 B). Cysteine supplementation under hypoxia led to increased intracellular pool of free Cys (figure 4 A) and the recycling of cysteine through GSH catabolism (figure 4 F). In accordance, the protective effect of cysteine under hypoxia was dependent on its concentration, indicating that intracellular pool of free cysteine in ES2 plays an important role in adaptation to hypoxia.

A different scenario was observed in OVCAR3. This cell line presented lower intracellular levels of cysteine than ES2 and the supplementation of cysteine did not have any effect on its free intracellular levels (figure 4 A). This might suggest an alteration in cysteine import or that imported cysteine is being channelled for CySSP pool or GSH synthesis. In fact, in this cell line, hypoxia did not change CysSSP but cells exposed to cysteine supplementation under hypoxia presented increased CysSSP levels ($p=0.032$ compared to N and $p=0.038$ compared to H) (figure 4 B). Also, under hypoxia with cysteine, ES2 cells presented lower levels of S-cysteinylated proteins (CysSSP) than OVCAR3 cells ($p=0.030$) (figure 4 B). Moreover, the recycling of cysteine through GSH catabolism is much lower in OVCAR3 cells compared to ES2, as evaluated by the ratio CysGly/GSH ($p<0.001$) (figure 4 F). Together, results suggest that OVCAR3 are not so dependent on free cysteine levels as ES2 cells on coping with hypoxia.

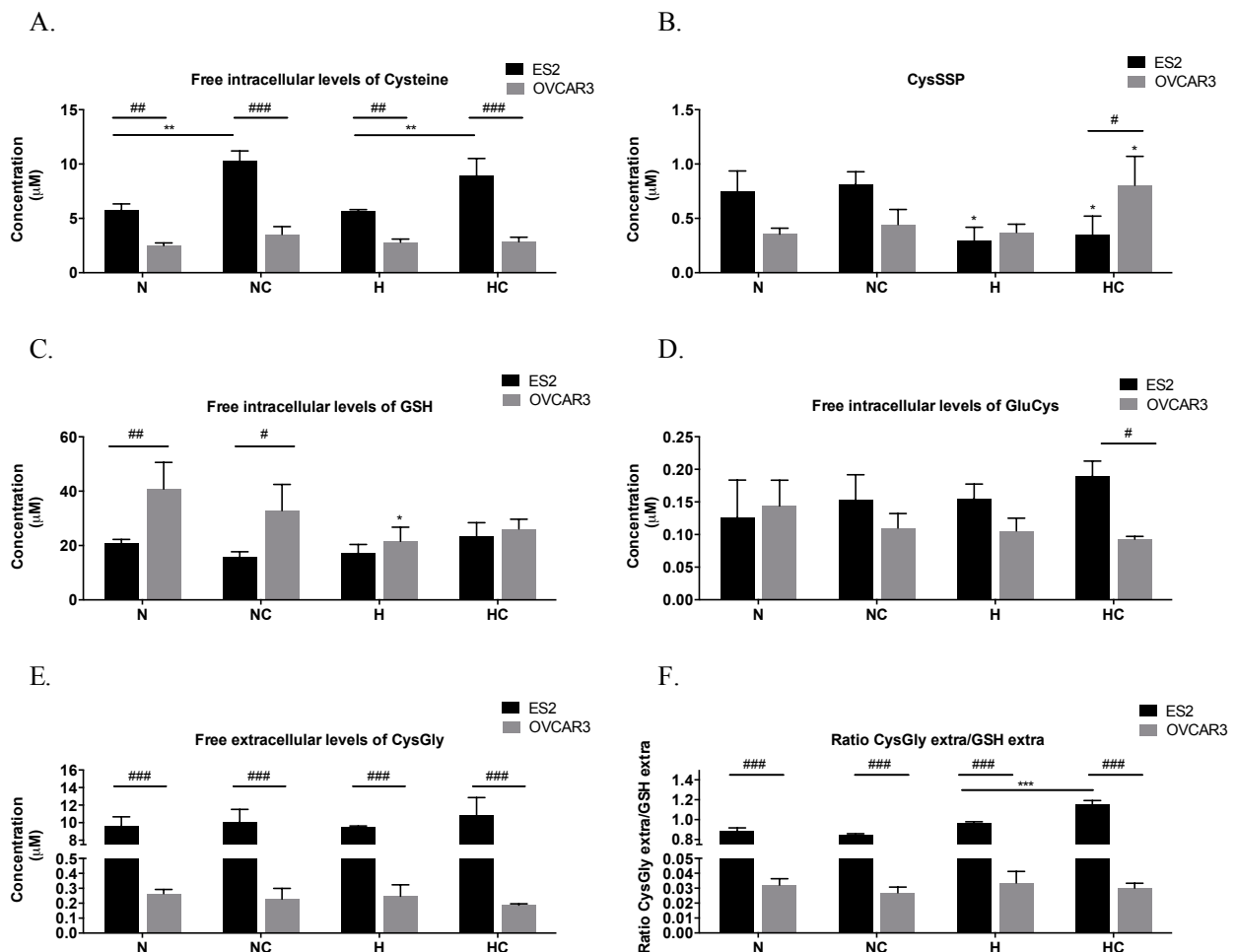


Figure 4. ES2 cells adaptation to hypoxia relies on free intracellular cysteine availability.

Quantification of $\Delta\psi_m$ expressed as a ratio of red/green fluorescence intensity ratio in the different treatments (ratio of geometrical means) for ES2 and OVCAR3 cell lines for 16 h of assay. CCCP is a positive control for depolarization. N – Normoxia; NC – Normoxia supplemented with cysteine; H –

Hypoxia; HC – Hypoxia supplemented with cysteine. Results are shown as mean \pm SD. * p <0.05, ** p <0.01, *** p <0.001 (One-way ANOVA with post hoc Tukey tests).

Cysteine and hypoxia have a role on the response of ovarian cancer cells to carboplatin

Usually, ovarian cancer therapy protocols include platinum salts and taxanes [8]. However, we tested paclitaxel with and without carboplatin and no relevant alterations were found related to hypoxia (figure 5). Under normoxia, it was only observed an increased cell death due to paclitaxel in the presence of cysteine in the first cycle of ES2 cells exposure to drugs (figure 5). So, the experimental course was developed using only carboplatin, as chemically thiols react directly with platinum salts (oxidative compounds) and under hypoxia a protective effect was noticed mainly in ES2 cells.

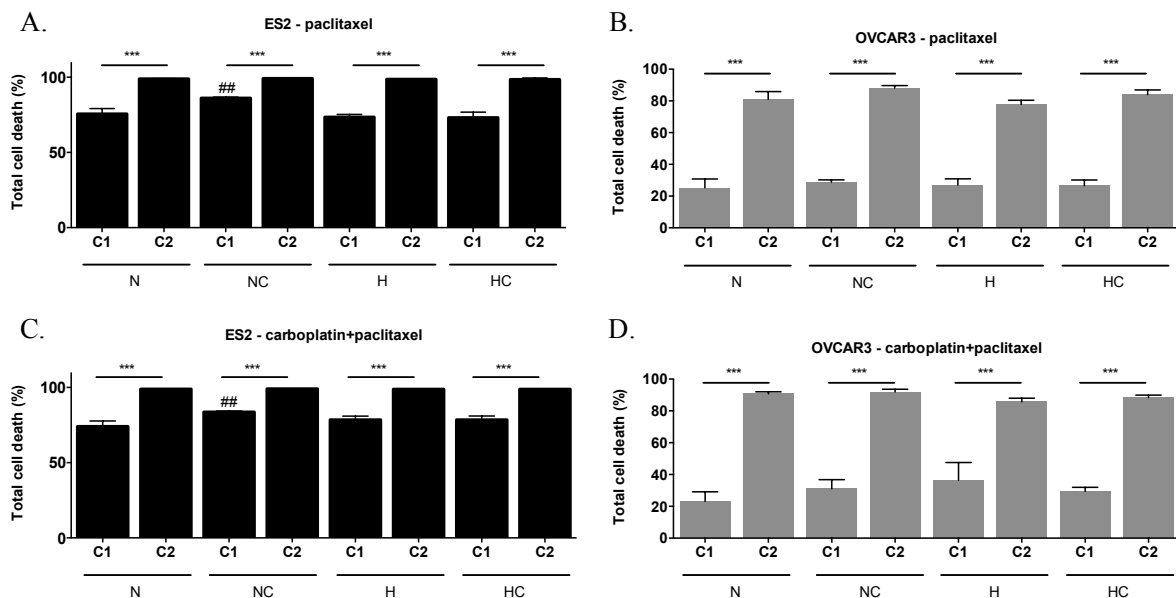


Figure 5. Effect of cysteine and hypoxia in ES2 and OVCAR3 cells response to paclitaxel alone or in combination with carboplatin.

Percentage of cell death levels in the presence of paclitaxel for A. ES2 cells and B. OVCAR3 cells, and in the presence of paclitaxel in combination with carboplatin for C. ES2 cells and D. OVCAR3 cells. N – Normoxia; NC – Normoxia supplemented with cysteine; H – Hypoxia; HC – Hypoxia supplemented with cysteine. Results are shown as mean \pm SD. The asterisks (*) represent statistical significance among cycles of treatments and cardinals (#) represent statistical significance compared to the control (normoxia) within the same cycle of treatments..* p <0.05, ** p <0.01, *** p <0.001 (One-way ANOVA with post hoc Tukey tests).

Herein, we addressed the role of hypoxia and cysteine in ovarian cancer cells response and adaptation to carboplatin, by exposing cells to two cycles of carboplatin and assessing the effects on cell death from the first to the second cycle of drug exposure.

With one cycle of carboplatin, no differences were found among treatments in ES2 cells (figure 6 A). Regarding the effect of two cycles of carboplatin, it was possible to observe differences among treatments ($p=0.002$). Results showed that cysteine protected cells from carboplatin-induced death both under hypoxia and normoxia ($p=0.008$ in H and $p=0.015$ in N) (figure 6 A). When analysing the alterations in ES2 total cell death in consecutive cycles, results showed that carboplatin induced higher cell death at the second cycle only in the absence of cysteine treatment ($p<0.001$ for N and H) (figure 6 A). This result suggests that for ES2 cells, cysteine is not advantageous under hypoxia but also allows faster adaptation to carboplatin both under normoxia and hypoxia.

In OVCAR3 cells (figure 6 B), with one cycle of carboplatin there were no differences among treatments in cell death levels. However, with two cycles, there were differences among conditions ($p=0.001$), in which cell death levels were lower under H supplemented with cysteine compared to the other treatments ($p=0.007$ compared to N; $p=0.003$ compared to NC and $p=0.001$ compared to H). Regarding changes from the first to the second cycle of carboplatin in OVCAR3 cells, there was an increase in total cell death in all treatments in the second cycle ($p<0.001$) (figures 6 B). In this cell line, under hypoxia, cysteine protected cells from death in the second cycle of carboplatin ($p=0.001$). Nevertheless, total cell death was higher in this cycle compared to the first one ($p<0.001$). Under normoxia, cysteine did not confer any advantage for cells in the presence of carboplatin in the second cycle.

We also asked the effect of hypoxia and cysteine in other ovarian cancer cell lines response to carboplatin. For OVCAR8 cells, no differences were observed with one cycle of carboplatin exposure among experimental conditions (figure 6 C). However, with two cycles, hypoxia was especially disadvantageous without cysteine for OVCAR8 cells (N vs H $p<0.001$, NC vs H $p<0.001$, N vs HC $p=0.041$, H vs HC $p<0.001$). When analysing the alterations in total cell death levels from the first to the second cycle in OVCAR8 cells, increased levels were observed under hypoxia with and without cysteine (under H and HC $p<0.001$), without significant differences under normoxia (figure 6 C). Nevertheless, cysteine was advantageous under hypoxia in the second cycle (H vs HC $p<0.001$).

For A2780 parental cells, in the first cycle, no differences were observed among treatments in the presence of carboplatin. In the second cycle of experimental conditions, increased cell death levels were observed under hypoxia with cysteine ($p=0.02$) compared to normoxia with cysteine. When analysing the alterations in total cell death levels from the first to the second cycle, results showed an increased cell death between cycles in all the treatments (figure 6 D).

Regarding A2780 cisR cells, in the first cycle it was observed increased cell death levels under hypoxia with and without cysteine supplementation compared to the control and to normoxia with cysteine (N vs H $p=0.001$, N vs HC $p=0.005$, NC vs H $p=0.007$ and NC vs HC $p=0.026$), with no differences in the other conditions (figure 6 E). In the second cycle, hypoxia was disadvantageous for these cells, especially without cysteine (N/NC vs H/HC, $p<0.001$). When analysing the alterations in total cell death levels from the first to the second cycle, results showed increased cell death levels only under hypoxia, both with ($p<0.001$) and without ($p<0.001$) cysteine (figure 6 F). Nevertheless, cysteine was advantageous in the second cycle of experimental conditions for A2780 cisR under hypoxia also in the presence of carboplatin (H vs HC, $p<0.001$), in contrast to A2780, the parental cell line.

Altogether, results revealed a protective effect of cysteine under hypoxia and in the presence of carboplatin in ovarian cancer cells from different histological types, thus suggesting a widespread role for cysteine in the selection of more aggressive phenotypes in ovarian cancer cells.

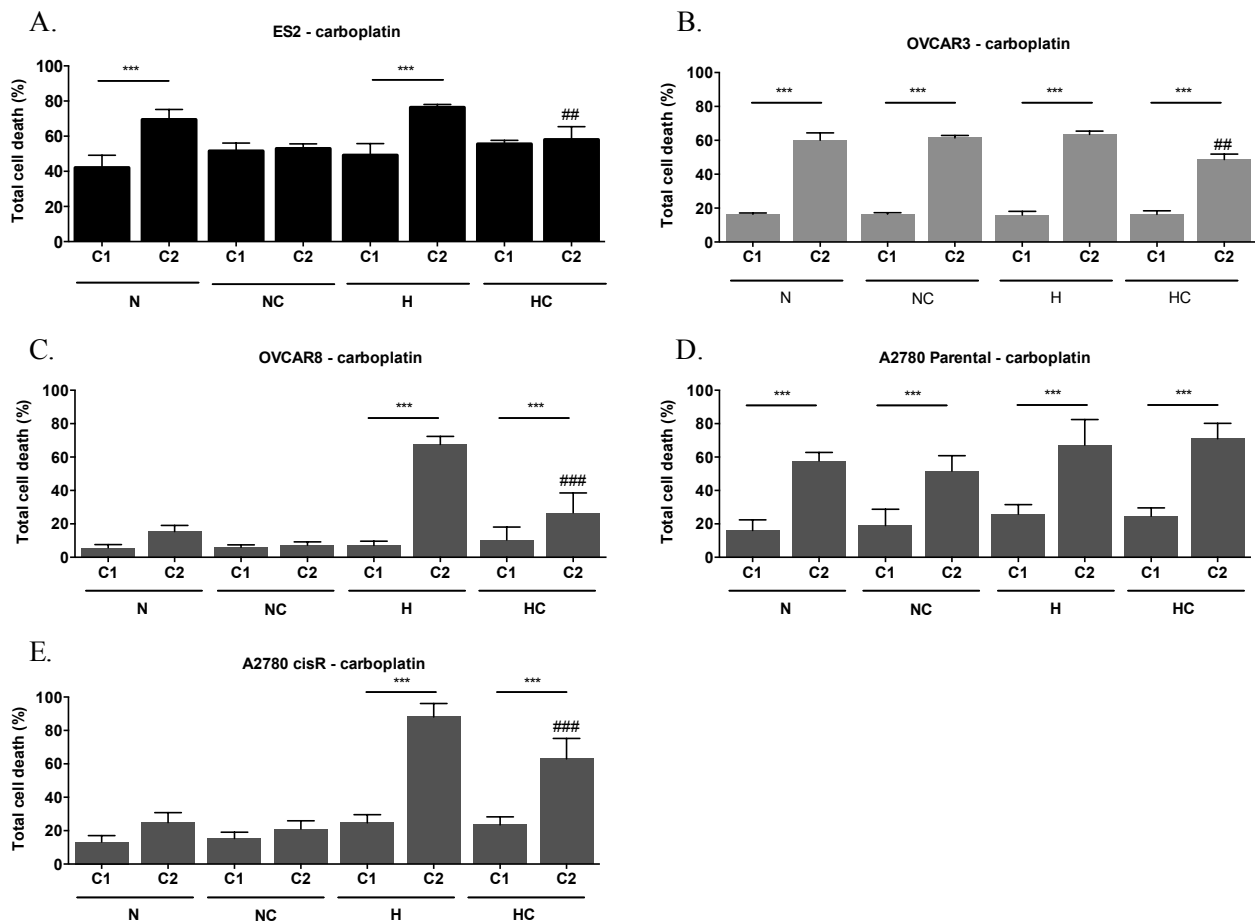


Figure 6. Cysteine and hypoxia have a role on ovarian cancer cells response to carboplatin.

Total cell death in the first (C1) and in the second (C2) cycles of treatments in the presence of Carboplatin for A. ES2, B. OVCAR3, C. OVCAR8, D. A2780 parental cells and E. A2780 cisR cells. N

– Normoxia; NC – Normoxia supplemented with cysteine; H – Hypoxia; HC – Hypoxia supplemented with cysteine. Results are shown as mean \pm SD. Cardinals (#) represent statistical significance among hypoxia with and without cysteine supplementation within the same cycle of treatments. * p <0.05, ** p <0.01, *** p <0.001 (One-way ANOVA with post hoc Tukey tests).

CD133 levels are induced upon hypoxia and carboplatin exposure in ES2, OVCAR8 and A2780

We next asked if cells resistant to hypoxia and carboplatin presented a cancer stem cell-like phenotype.

For that, we compared the changes in the levels of CD133 from the first cycle to the second cycle of treatments.

In ES2 in a drug-free environment, the levels of CD133 were increased under hypoxia (figure 7) (p =0.013). Upon carboplatin exposure, from the first cycle to the second cycle, there was an increase in the levels of CD133 in all treatments (under N, NC, H and HC p <0.001) (figure 7 A).

Interestingly, for OVCAR3 cells and in a drug-free environment, the CD133 levels decreased in treatments with cysteine (NC p =0.001; HC p =0.02). Upon carboplatin exposure, there was a decrease in CD133 levels in treatments under hypoxia (under H p =0.001; under HC p <0.001), with no differences among cycles in treatments under normoxic conditions (figure 7 B).

Regarding OVCAR8 cells, in a drug-free environment, results showed that hypoxia without cysteine increased the levels of CD133 (p =0.001). Moreover, this effect was also observed under normoxia with cysteine supplementation (p <0.001) (figure 7 C). Upon carboplatin exposure, from the first cycle to the second cycle, there was an increase in CD133 levels in all treatments (under N, NC, H and HC p <0.001) (figure 7 C).

A2780 parental cells, in a drug-free environment, showed higher CD133 levels under hypoxia without cysteine (p <0.000), with no significant differences among cycles in the other conditions (figure 7 D). Upon carboplatin exposure, from the first cycle to the second cycle, an increase in CD133 levels was observed in all conditions (under N, NC, H and HC p <0.001) (figure 7 D). A different scenario was observed for A2780 cisR cells. In a drug-free environment, there was a decrease of CD133 levels from the first to the second cycle in all conditions (under N, NC and HC p <0.001) (figure 7 E) with the exception of hypoxia, in which there were no significant differences among cycles (figure 7 E). Upon carboplatin exposure, hypoxia without cysteine increased CD133 levels (p <0.001) from the first to the

second cycle. Under hypoxia with cysteine, there was a trend to increase CD133 levels among cycles ($p=0.053$) (figure 7 E).

Together, results indicate that the levels of CD133 are not related to OVCAR3 cells resistance to neither hypoxia nor carboplatin, contrarily to what was observed in ES2, OVCAR8 and A2780 parental cells. Regarding the cisplatin resistant A2780 cisR cells, results point out that overall carboplatin resistance is not related to CD133 levels, only when combined with hypoxic stress.

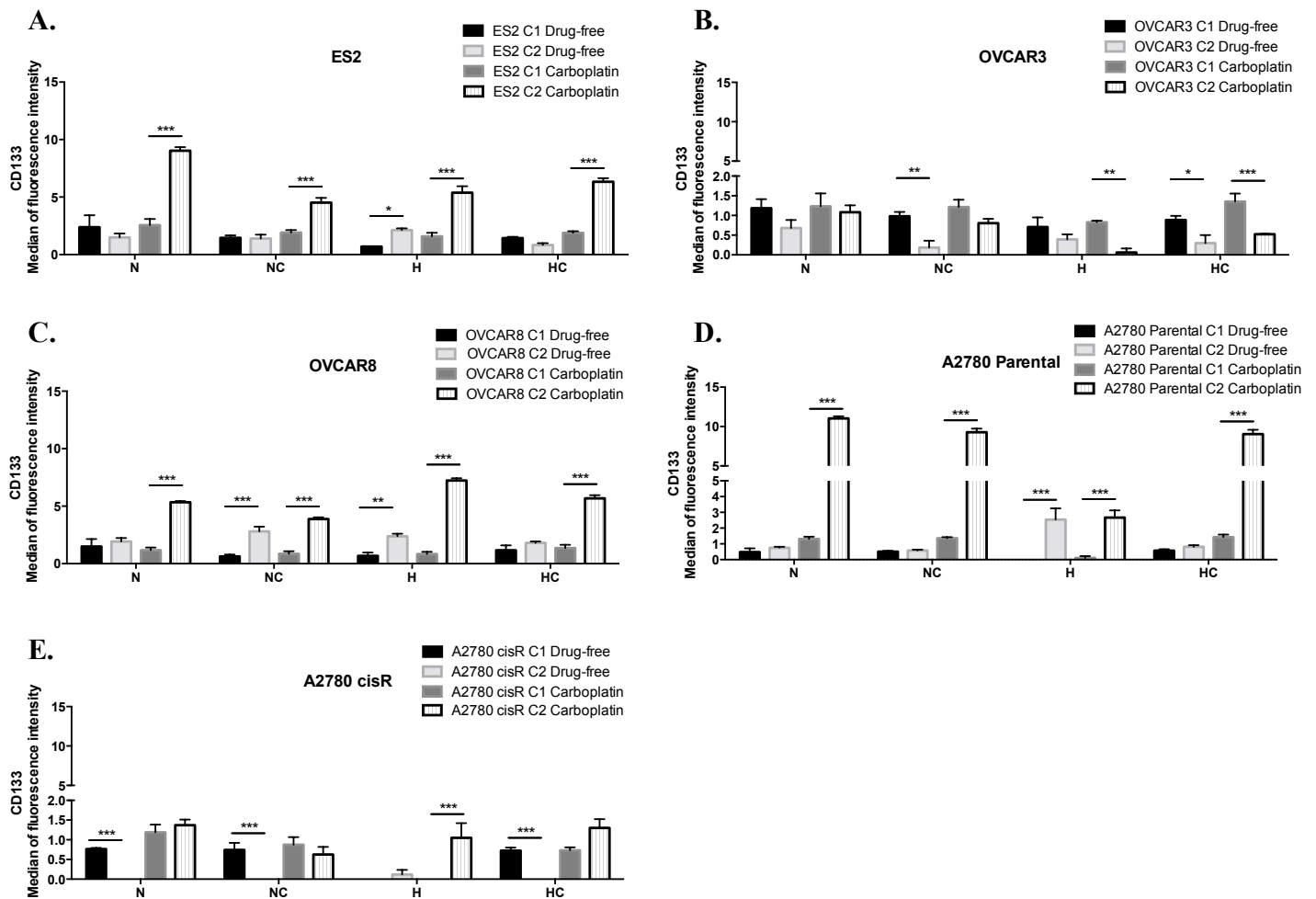


Figure 7. CD133 levels are induced upon hypoxia and carboplatin exposure in ES2, OVCAR8 and A2780.

CD133 levels in a drug-free environment and upon carboplatin exposure for A. ES2 cells, B. OVCAR3 cells, C. OVCAR8 cells, D. A2780 parental cells and E. A2780 cisR cells in the first and in the second cycles of treatments. N – Normoxia; NC – Normoxia supplemented with cysteine; H – Hypoxia; HC – Hypoxia supplemented with cysteine. Results are shown as mean \pm SD. Asterisks (*) represent statistical significance among the first and the second cycle within the same treatment. * $p<0.05$, ** $p<0.01$, *** $p<0.001$ (One-way ANOVA with post hoc Tukey tests).

All thiols but GSH are increased in patients with ovarian tumours- high GSH turnover

Given the role of cysteine in the adaptation of ovarian cancer cell lines to hypoxic conditions and carboplatin exposure, we next assessed if higher serum levels of cysteine or other thiols were associated with ovarian tumours malignancy. Strikingly, total HCys levels were effective in distinguishing patients with malignant tumours from benign tumours and both of them from healthy individuals (figure 8 A). Results showed that increased total levels of Cys and GluCys (GSH precursor) were associated with ovarian tumours regardless malignancy (figure 8 B and C). Total GSH levels did not differ among groups ($p>0.05$) and CysGly (GSH degradation product) was increased in patients with malignant tumours compared only to healthy individuals ($p=0.028$) (figure 8 D and E).

Regarding free thiol content in plasma, free HCys levels were able to distinguish patients with malignant tumours from benign tumours ($p<0.001$) and patients with benign tumours from healthy individuals ($p=0.02$) without significant differences between malignant tumours and healthy individuals (figure 9 A). Cys levels were increased in patients with malignant tumours compared to patients with benign tumours ($p=0.005$) but without significant differences compared to healthy individuals (figure 9 B). In addition, lower free GSH levels were associated with ovarian neoplasms regardless malignancy ($p=0.006$ donors vs benign tumours and $p=0.005$ donors vs malignant tumours) (figure 9 D). Free GluCys and free CysGly levels did not differ among groups ($p>0.05$) (figure 9 C and E).

Regarding the thiol protein-bound fraction, higher levels of S-homocysteinylation proteins (HCysSSP) were associated with malignant ovarian tumours ($p=0.019$ benign vs malignant, $p<0.001$ donors vs malignant) (figure 10 A). Higher levels of S-cysteinylation, S-glutamylcysteinylation, and S-cysteinylglycinylation proteins (CysSSP, GluCysSSP and CysGlySSP) were associated with ovarian neoplasms regardless malignancy (CysSSP: donors vs benign $p<0.001$, donors vs malignant $p<0.001$; GluCysSSP: donors vs benign $p=0.001$, donors vs malignant $p<0.001$; CysGlySSP: donors vs benign $p=0.001$, donors vs malignant $p=0.001$) (figure 10 B, C and E). No significant differences were found in the levels of S-glutathionylation proteins (GSSP) among groups (figure 10 D).

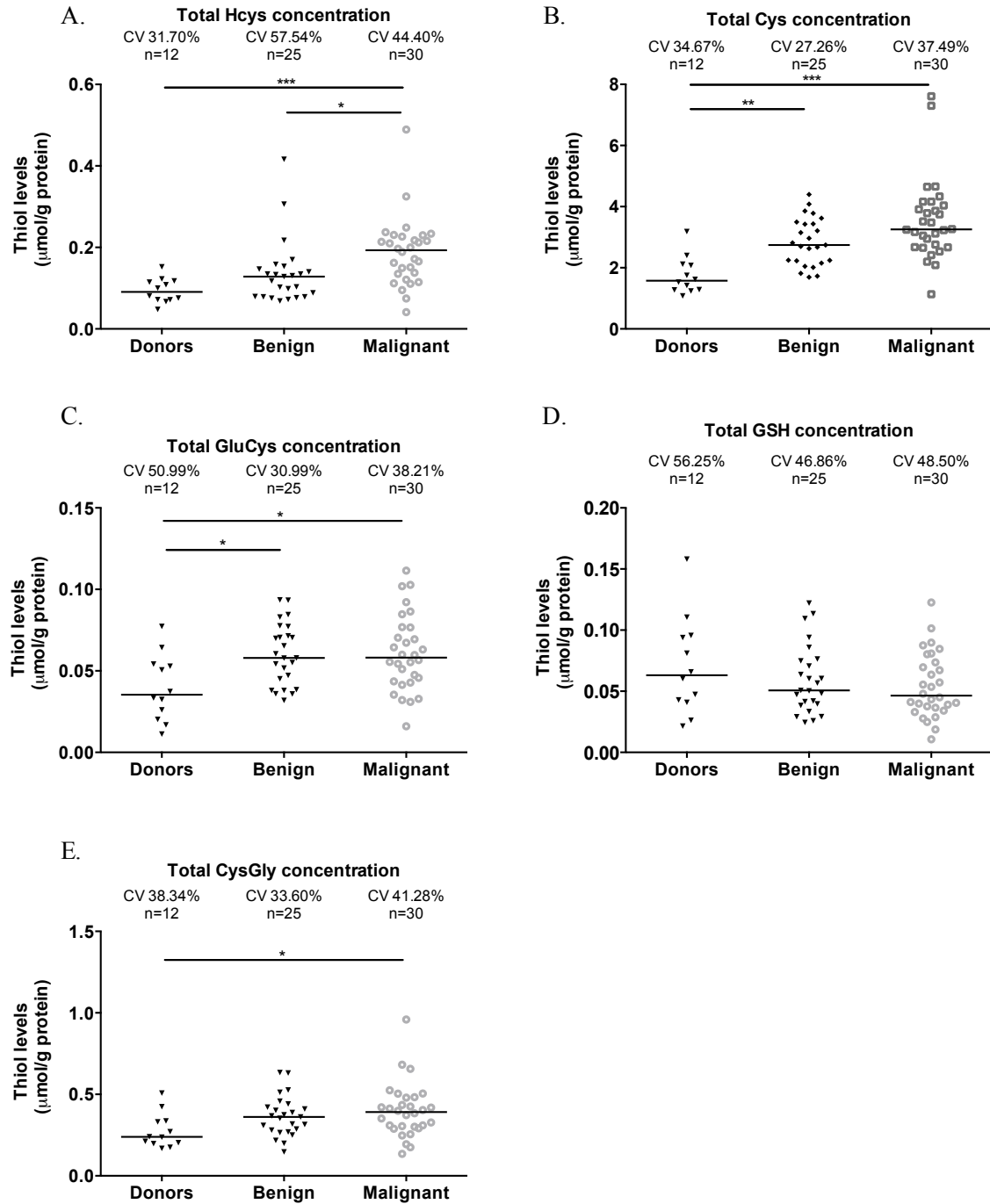


Figure 8. Total thiols in patients with ovarian tumours.

Total thiols quantification in serum from healthy individuals (donors) and in serum from patients with benign and malignant ovarian tumours for A. HCys- Homocysteine, B. Cys – cysteine, C. GluCys – Glutamylcysteine, D. GSH – Glutathione, E. CysGly – Cysteinylglycine. Thiol concentration was normalised to protein concentration. Results are shown as median. The asterisks (*) represent the statistical significance among groups. * $p < 0.05$, ** $p < 0.01$, *** $p < 0.001$ (independent samples Kruskal Wallis One-way ANOVA with multiple comparisons).

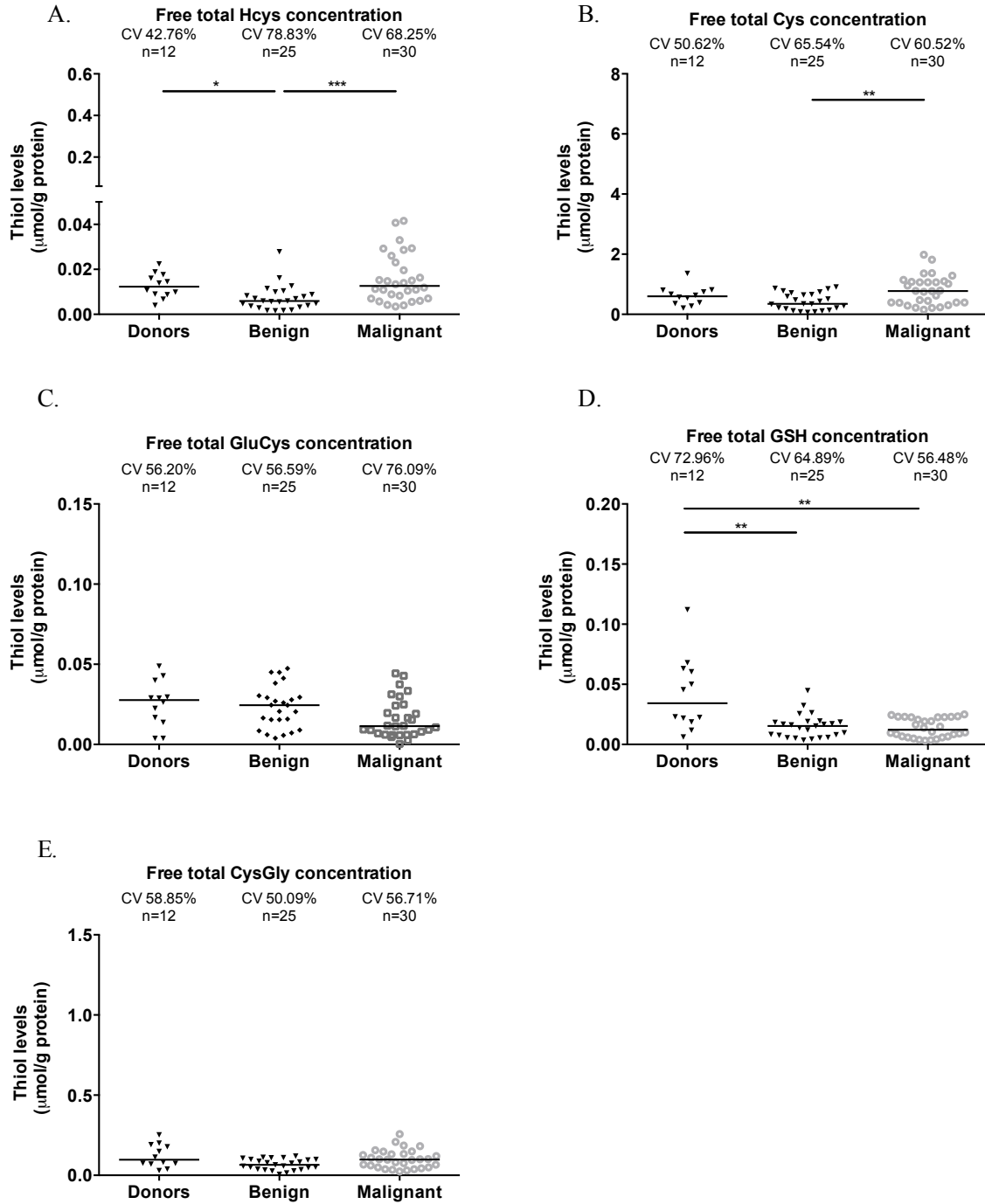


Figure 9. Free total thiols in patients with ovarian tumours.

Free total thiols quantification in serum from healthy individuals (donors) and in serum from patients with benign and malignant ovarian tumours for A. Hcys- Homocysteine, B. Cys – cysteine, C. GluCys – Glutamylcysteine, D. GSH – Glutathione, E. CysGly – Cysteinylglycine. Thiol concentration was normalised to protein concentration. Results are shown as median. The asterisks (*) represent the statistical significance among groups. * $p < 0.05$, ** $p < 0.01$, *** $p < 0.001$ (independent samples Kruskal Wallis One-way ANOVA with multiple comparisons).

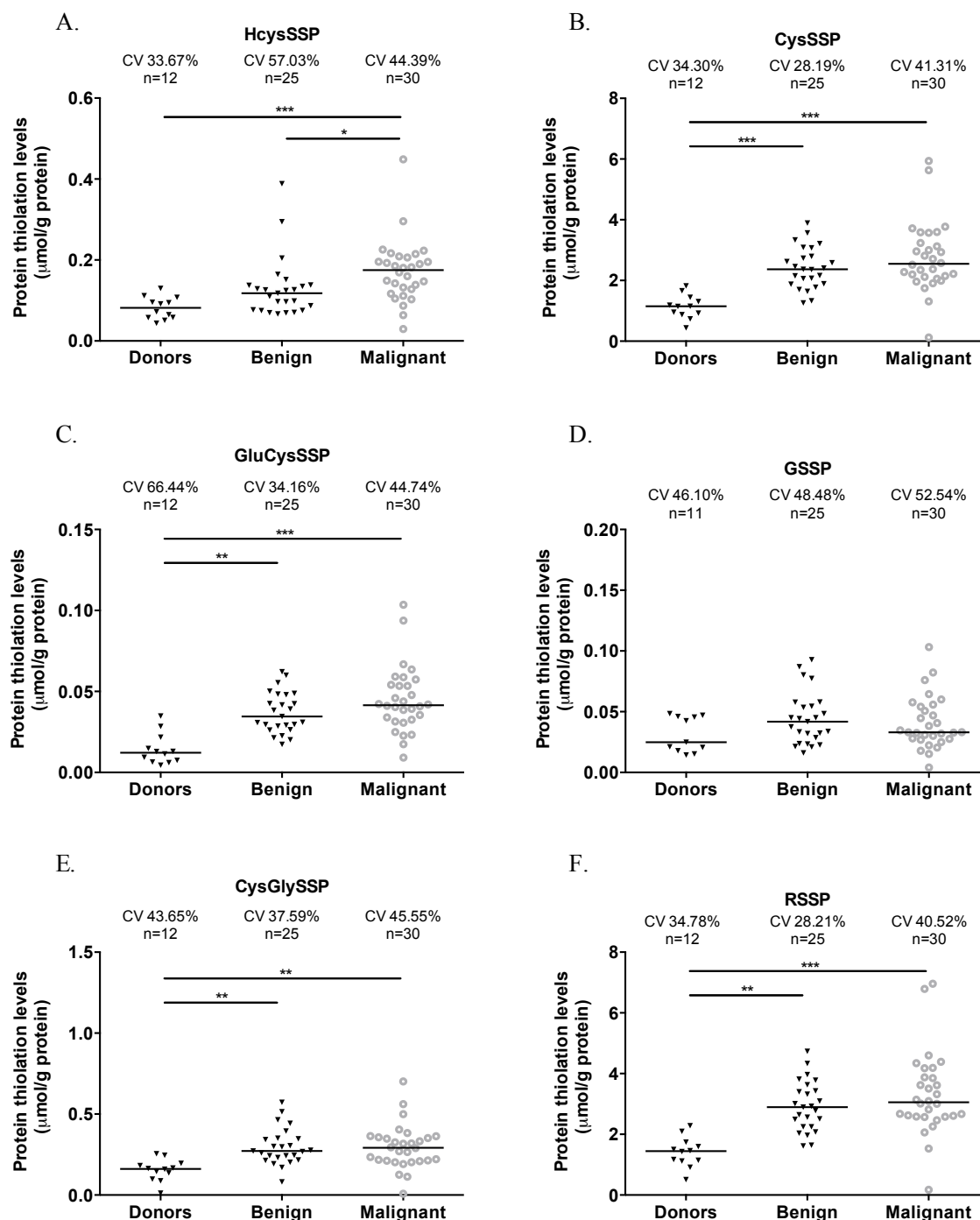


Figure 10. Thiol protein-bound fraction in patients with ovarian tumours.

Thiols concentration bound to proteins (protein thiolation) quantification in serum from healthy individuals (donors) and in serum from patients with benign and malignant ovarian tumours for A. HcysSSP – S-homocysteinylated proteins, B. CysSSP – S-cysteinyllated proteins, C. GluCysSSP – S-Glutamylcysteinyllated proteins, D. GSSP – S-glutathionylated proteins, E. CysGlySSP – S-cysteinylglycinyllated proteins. F. RSSP – total S-thiolated proteins. Thiol concentration was normalised to protein concentration. Results are shown as median. The asterisks (*) represent the statistical significance among groups. * $p < 0.05$, ** $p < 0.01$, *** $p < 0.001$ (independent samples Kruskal Wallis One-way ANOVA with multiple comparisons).

In a general way, with the exception of GSH, higher total levels of thiols were associated

with ovarian neoplasms, showing that patients with ovarian neoplasms present different thiol dynamics. Moreover, with the exception of GSH, thiols were mainly in the protein bound form and not free in serum from patients with ovarian tumours compared to healthy individuals.

Noticeably, total CysSSP was capable of distinguishing serum of healthy blood donors from patients with ovarian tumours (benign and malignant) and total free Cys levels distinguished serum of patients with malignant tumours from patients with benign tumours. Together, data supports that cysteine, free levels together with the protein- bound fraction, are suitable markers for ovarian cancer allowing the development of a screening method to contribute for the screening and early diagnosis of this disease.

Cysteine levels tend to be increased in clear cell carcinomas (OCCC) and endometrioid carcinomas (OEC) and after chemotherapy in high grade serous carcinomas (HG-OSC)

We have also measured thiols levels in tumour samples from different ovarian cancer types. No significant differences were observed among the different histological types of carcinomas in total thiols concentration (figure 11), nor in free total thiols (figure 12) nor in thiols concentration bound to proteins (figure 13). However, in HG-OSC, total and free total homocysteine and cysteine levels tended to increase after chemotherapy. Moreover, HCysSSP levels also tended to increase following chemotherapy, whereas CysSSP tended to decrease. Importantly, the total and free total levels of cysteine and CysGly tended to be higher OCCC and OEC compared to HG-OSC.

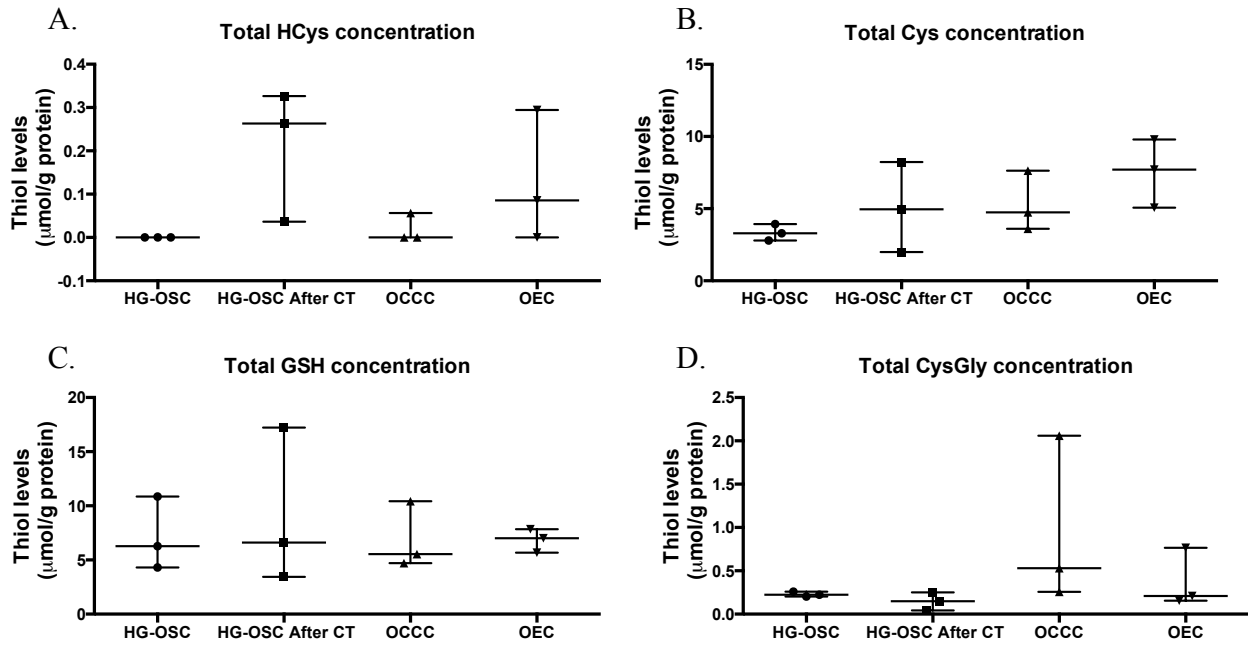


Figure 11. Total thiols in different ovarian carcinomas.

Total thiols quantification in high grade serous carcinoma before chemotherapy (HG-OSC, n=3) and after chemotherapy (HG-OSC After CT, n=3), clear cell carcinoma (CCC, n=3) and endometrioid carcinoma (OEC, n=3) for A. HCys- Homocysteine, B. Cys – cysteine, C. GSH – Glutathione, and D. CysGly – Cysteinylglycine. Thiol concentration was normalised to protein concentration. Results are shown as median. Independent samples Kruskal Wallis One-way ANOVA with multiple comparisons were performed.

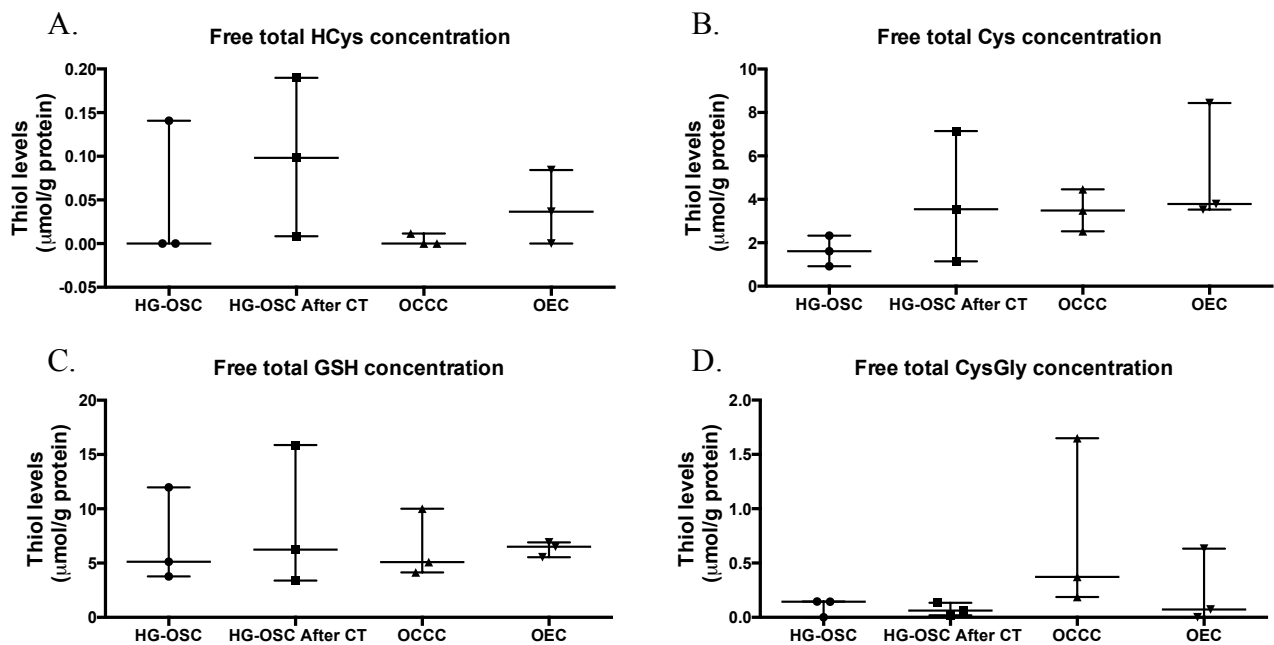


Figure 12. Free total thiols in different ovarian carcinomas.

Free total thiols quantification in high grade serous carcinoma before chemotherapy (HG-OSC, n=3) and after chemotherapy (HG-OSC After CT, n=3), clear cell carcinoma (CCC, n=3) and endometrioid carcinoma (OEC, n=3) for A. HCys- Homocysteine, B. Cys – cysteine, C. GSH – Glutathione and D.

CysGly – Cysteinylglycine. Thiol concentration was normalised to protein concentration. Results are shown as median. Independent samples Kruskal Wallis One-way ANOVA with multiple comparisons were performed.

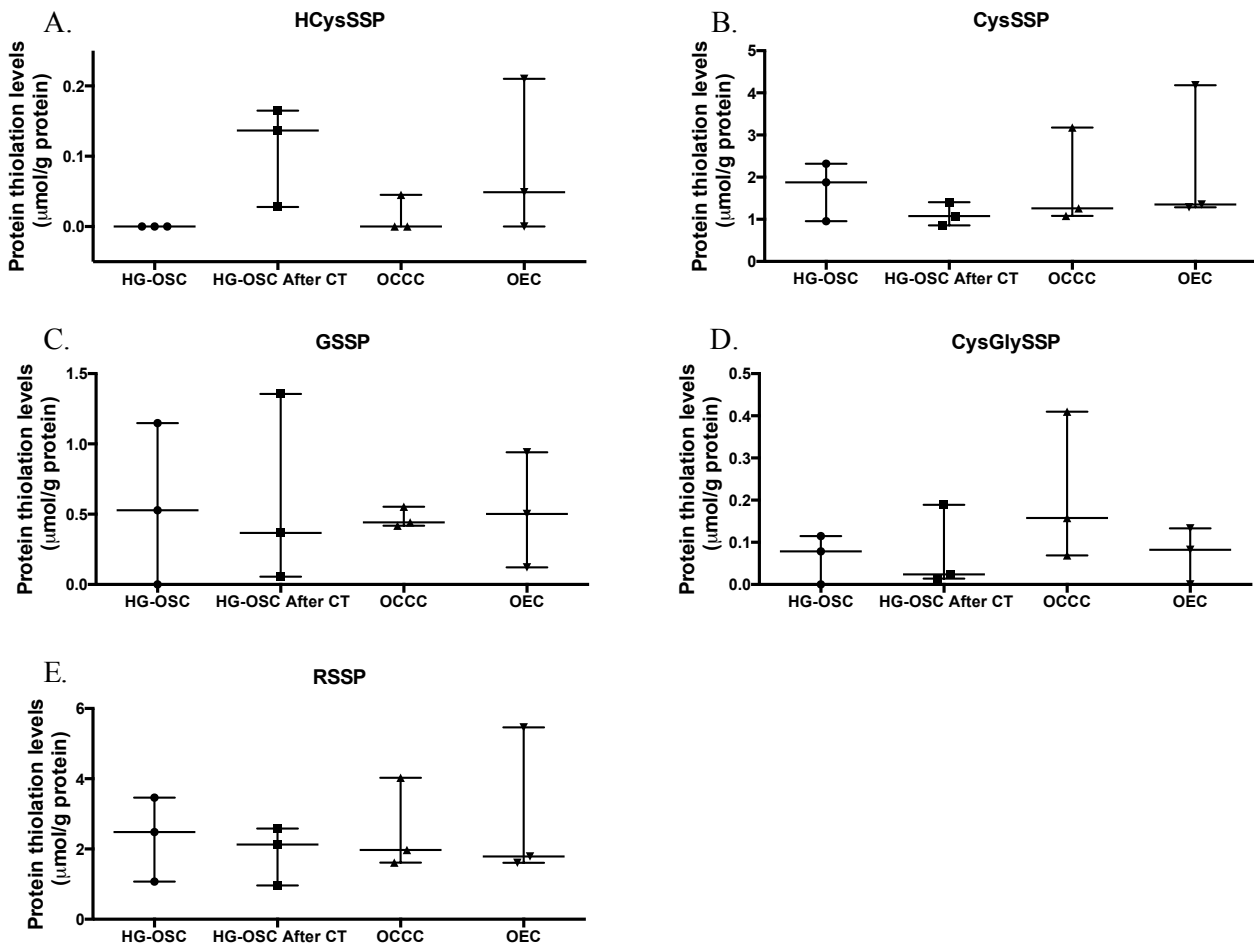


Figure 13. Thiol protein-bound fraction in different ovarian carcinomas.

Thiols concentration bound to proteins (protein thiolation) quantification in high grade serous carcinoma before chemotherapy (HG-OSC, n=3) and after chemotherapy (HG-OSC After CT, n=3), clear cell carcinoma (CCC, n=3) and endometrioid carcinoma (OEC, n=3) for A. HcySSP – S-homocysteinylylated proteins, B. CysSSP – S-cysteinylylated proteins, C. GSSP – S-glutathionylated proteins, D. CysGlySSP – S-cysteinylglycinylylated proteins and E. RSSP – total S-thiolated proteins. Thiol concentration was normalised to protein concentration. Results are shown as median. Independent samples Kruskal Wallis One-way ANOVA with multiple comparisons were performed.

Cysteine is the prevalent thiol found in ascitic fluid from patients with advanced ovarian cancer

As the ascitic fluid is an important component of ovarian tumour cells microenvironment, we wanted to disclose if cysteine and other thiols were present in this biofluid derived from

patients with ovarian cancer. Results have shown that cysteine was the most prevalent thiol in the three pools, total (figure 14 A), free (figure 14 B) and S-cysteinylated proteins (figure 14 C). HCys was mainly present bound to proteins, sequentially followed by Cys and CysGly, and then by GluCys and GSH (figure 14 D).

As the prevalent thiol in the ascitic fluid, cysteine might promote an ideal tumour microenvironment for cancer cells, possibly acting both as a redox buffer and as a modifier of proteins, mediating the adaptation or abrogating the effect of platinum salts, such as carboplatin.

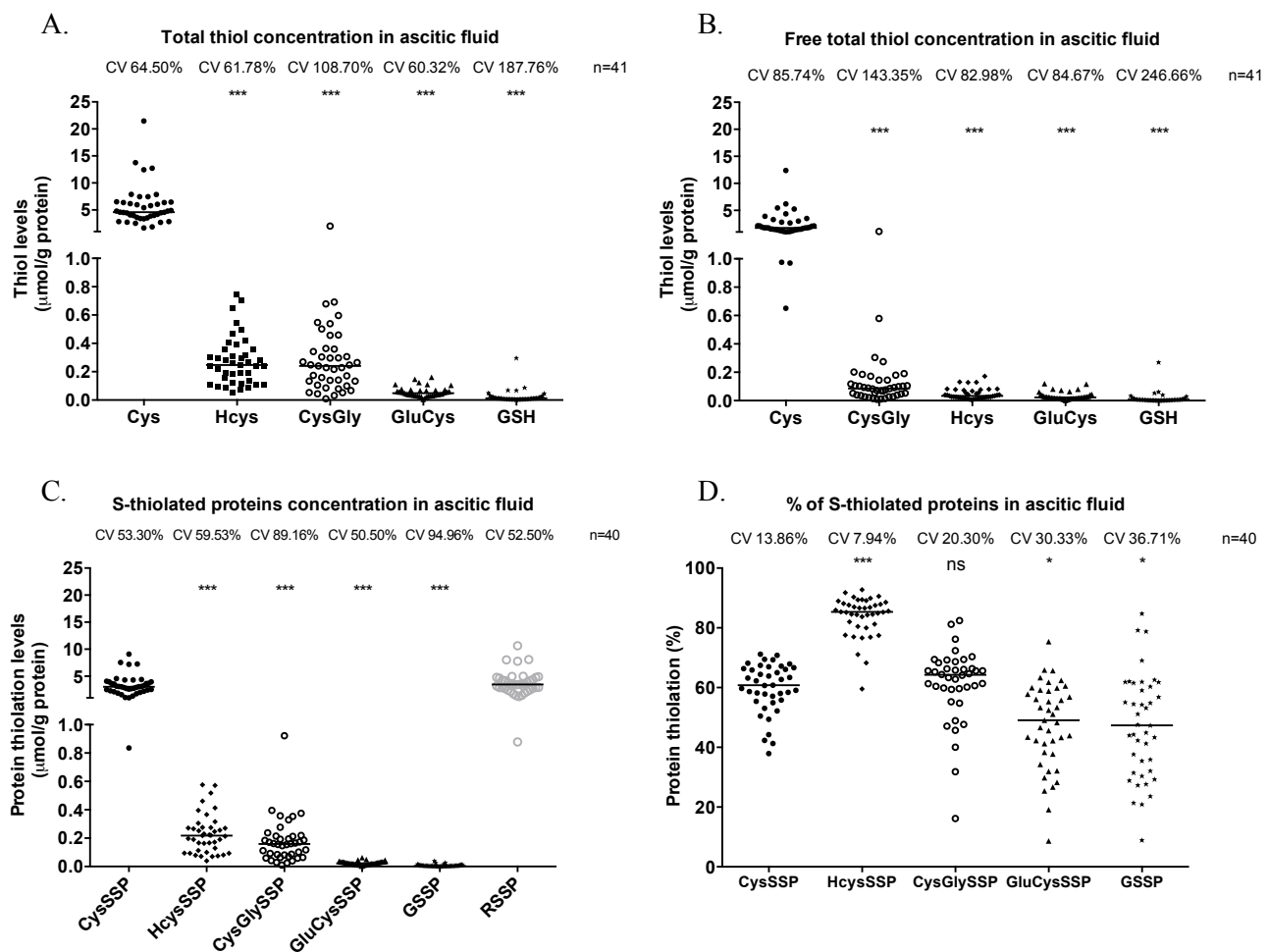


Figure 14. Cysteine is the prevalent thiol in ascitic fluid from patients with ovarian cancer.

Thiols quantification in ascitic fluid from patients with ovarian cancer. A. Total thiols concentration. B. Free total thiols concentration. C. Thiols concentration bound to proteins. D. Percentage of thiols concentration bound to proteins. Cys – cysteine, HCys- Homocysteine, CysGly – Cysteinylglycine, GluCys – Glutamylcysteinyl, GSH – Glutathione, CysSSP – S-cysteinylated proteins, HcysSSP – S-homocysteinylated proteins, CysGlySSP – S-cysteinylglycinylated proteins, GluCysSSP – S-glutamylcysteinylated proteins, GSSP – S-glutathionylated proteins, RSSP – total S-thiolated proteins. Thiol concentration was normalised to protein concentration. Results are shown as median. The asterisks (*) represent the statistical significance in relation to Cysteine concentration. * $p < 0.05$, ** $p < 0.01$, *** $p < 0.001$ (independent samples Kruskal Wallis One-way ANOVA with multiple comparisons).

DISCUSSION

Although the outcome and prognosis of different histological types of ovarian cancer had been a matter of debate, it was shown that patients with OCCC present a significantly worse prognosis than patients with serous carcinoma when matched for age, stage, and level of primary cytoreduction [39]. In 2011, Lee *et al.* also shown that OCCC patients presented a poorer prognosis than those with other histological subtypes of carcinoma, especially in advanced stages [40]. Moreover, while OCCC show intrinsic resistance to conventional platinum-based chemotherapy, HG-OSC usually exhibit first sensitiveness to platinum-based chemotherapy, though the majority of cases develop chemoresistance during the course of treatment [41,42].

The present work supports a widespread protective effect of cysteine both under carboplatin and hypoxia exposure, indicating that cysteine has a role in ovarian cancer cells survival in adverse environments. However, differences were found among cell lines on cysteine dependence on coping with hypoxia and carboplatin. Importantly, ES2 cells and OVCAR8 seemed to present a stronger dependence on cysteine metabolism in handling with hypoxic stress and carboplatin than OVCAR3. We must underline that OVCAR3 cells did not present increased levels of cell death under hypoxia than ES2 cells. Instead, our results supported that these cells manage hypoxic stress by different mechanisms, where ES2 cells present a metabolism that is more dependent on cysteine than OVCAR3 cells. This evidence, on the other hand, points that cysteine metabolism can be strongly related to a worse prognosis of ovarian cancer. It is plausible that the worse prognosis associated to the OCCC histological type is related to cysteine metabolism and or cysteine-dependent redox signalling process. However, we must test other OCCC cell lines in order to clarify the hypothesis that OCCC and HG-OSC tumours are *a priori* metabolically different. Interestingly, cysteine was advantageous for the cisplatin resistant A2780 cells but not for A2780 parental, sensitive cells, reinforcing that cysteine accounts for the selective process of platinum resistant ovarian cancer cells. Moreover, Beaufort and colleagues have explored the associations between the cellular and molecular features of 39 ovarian cancer cell lines and their clinical features [43]. They reported an association of the spindle-like tumours with metastasis, advanced stage, suboptimal debulking and poor prognosis [43]. Importantly, ES2 cells were included in this group whereas OVCAR3 cells were not [43], hence supporting that ES2 cells present a more aggressive phenotype.

Our data have shown increased levels of CD133, a cancer stem cell marker [44], in ES2, OVCAR8 and A2780 parental cells but not in OVCAR3 cells, upon cyclic exposure to hypoxia. Moreover, in these cells, carboplatin also increased the levels of CD133. This fact indicates that the activation of a pool of cancer stem cells underlies the adaptive capacity of these cells to hypoxia and drug resistance, where cysteine acts as a facilitator. Interestingly, upon carboplatin exposure, the CD133 levels did not increase in the already resistant A2780 cisR cells in the majority of treatments, whereas in A2780 parental cells it happened. Those results support that CD133⁺ cells are involved in the process of adaptation to carboplatin but it is lost when cells become chemoresistant, thus suggesting a role for CD133⁺ cells in the adaptation to adverse environments.

Lopes-Coelho *et al.* have shown that, under normoxia, ES2 cells are more resistant to carboplatin than OVCAR3 and that the inhibition of GSH production by buthionine sulphoximine (BSO), sensitizes ES2 cells to carboplatin [23]. Our results suggest that the protective effect against carboplatin under hypoxia is mediated by cysteine. However, it is still unclear if GSH is involved in this protection under hypoxia. Moreover, our team has described recently that under normoxia and in glucose free media ES2 present higher levels of thiols than OVCAR3 [23]. In the present study we cannot see that difference since we used different culture conditions, namely high glucose culture media. It is known that glucose can form adducts with GSH, which can in part explain the observed differences [45]. Despite we have detected lower or equal levels of GSH in ES2 than in OVCAR3 cells, we also detected higher degradation of GSH in ES2, pointing a faster thiols' turnover in this cell line indicated by the levels of cysteinylglycine (Cys-Gly) [46].

In a general way, our results pointed to a tendency to decreased cell death levels with increased cell density. Recently, it was shown that cytosolic lipid droplets, which are known to protect cancer cells from starvation-induced death, increased in content with increased cell density in HeLa cells [47]. This observation could, in part, explain the protective effect of high initial cell densities observed in our cell models. However, in the initial cell density 5×10^3 cells, we observed lower cell death levels than 2.5×10^4 . This can be due to cells dormancy that ensure cells survival in a quiescent metabolic state, due to stressful conditions [48] that are imposed by such a decreased cell density. Moreover, the effect of cell density in the response to carboplatin is an issue that must be addressed in future studies using 3D models. One may expect that increased cell density will have an impact on cells capacity of adapting to carboplatin, since a larger cell population often present more heterogeneity, thus more adaptive potential. In fact, our preliminary results of spheroids models point out a

protective effect of cysteine in ES2 but not in OVCAR3 upon carboplatin exposure (Suppl. figure 1). Interestingly, Lavi and colleagues [49], through mathematical modelling, showed how cancer cell density and cells alteration rate impact the heterogeneity over time, and its consequences on multidrug resistance. Moreover, in the context of ovarian cancer, Greene *et al.* [50] have shown that local cell density and initial global cell density, are able to lead to significant differences in spatial growth, proliferation, and paclitaxel-induced apoptosis rates in OVCAR8 cells, thus having a role not only in cancer cells growth but also in drug response.

Mitochondrial membrane potential ($\Delta\psi_m$) has been considered a good indicator of cells' health [38], as it is critical for maintaining the physiological function of the respiratory chain to generate ATP in mitochondria. A significant loss of $\Delta\psi_m$ will lead to energy depletion with subsequent cell death. Thus, in the present work, a lower loss of $\Delta\psi_m$ under hypoxia plus cysteine compared to cysteine absence was expected. The obtained results are apparently contradictory to the data obtained with annexin V/PI staining for cell death, in which, under hypoxia, cysteine was able to protect cells from death. However, annexin V labels apoptotic cells independently of the apoptotic pathways they underwent and as extrinsic apoptosis does not involve mitochondrial disruption it can be a plausible explanation for these results. On the other hand, to assess $\Delta\psi_m$ only adherent (putatively alive) cells were used. Hence, cells that were dying faster and detaching under hypoxia without cysteine were not used to assess $\Delta\psi_m$. Additionally, Tang *et al.* found that cancer cells were able to survive even after the cells had undergone critical apoptotic events such as mitochondrial fragmentation and dysfunction, nuclear condensation, cell shrinkage and activation of caspases [51]. They observed this apoptosis reversibility in various cancer cell lines and after different apoptotic stimuli [51]. Therefore, another interesting possibility is that, under hypoxia, cysteine is able to reverse apoptosis in ES2 cells.

With the exception of GSH, our results showed an overall increase of thiols concentration in serum from peripheral blood of patients with ovarian neoplasms, regardless malignancy, compared to healthy donors. Strikingly, total and free levels of HCys distinguished all the three groups of individuals and free levels of Cys showed to be effective in distinguishing malignant from benign neoplasms. In disease, the literature has already shown that increased levels of HCys, Cys and CysGly in peripheral blood serum were associated with ischemic heart disease [52] and increased levels of CysGly [53] and Cys [54] were associated with increased risk of breast cancer [53]. Moreover, higher HCys levels were associated with greater risk of breast cancer only when combined with higher levels of Cys

and with low levels of folate [54]. Differently, high plasma HCys levels were also associated with increased risk of colorectal cancer, whereas high Cys levels were associated with decreased risk for this disease [55]. Chiang and colleagues have confirmed the association between increased HCys levels and the risk of colorectal cancer adding that this increased risk was independent of oxidative stress indicators and antioxidant capacities [56]. In contrast, higher serum concentrations of Cys were associated with a significantly reduced risk of oesophageal squamous cell carcinomas and gastric/cardia adenocarcinomas [57]. The assessment of different thiol pools total, free and protein linked confers an innovative approach in our work. We observed that the contribution of protein-S-thiolation was augmented in patients with ovarian neoplasms compared to healthy individuals. The reversible thiolation of proteins was already associated with the regulation of several metabolic processes such as enzyme activity, transport activity, signal transduction and gene expression [58]. Several proteins - such as Ras, JNK- 2, AP-1, NF-kappaB, PKC, caspases, thioredoxin and p53 [58,59] - which are known to have important roles in cancer, are regulated by thiol oxidation [59]. Visscher *et al.* reported that many oncogenic mutations consist in an insertion of a novel cysteine in the protein sequence, as it happens in 12% of KRAS and 88% of FGFR mutations [60]. These facts suggest that newly introduced cysteines should play a role in tumourigenesis by contributing for tumour suppressor genes inactivation and oncogenes activation. Moreover, thiols can also interfere with epigenetic modulation of genes expression, which is pivotal in carcinogenesis [61].

Importantly, our results have shown that cysteine levels are putative biomarkers for ovarian cancer early diagnosis. As seen, the total levels in peripheral blood of protein-S-cysteinylation distinguished healthy blood donors from patients with ovarian neoplasms (benign and malignant) and free cysteine distinguishes patients with ovarian benign tumours from patients with malignant tumours. This is undoubtedly a step forward for ovarian cancer research, as the late diagnosis is one of the most important barriers accounting for the poor outcome and high mortality.

We also observed that cysteine was the prevalent thiol in ascitic fluid from patients with ovarian cancer and that S-cysteinylation was the most abundant form of S-thiolated proteins showing, again, that cysteine is a relevant organic compound in ovarian cancer cells microenvironment.

We must emphasize that most samples analysed from patients with ovarian cancer were from serous carcinoma histotype. It would be interesting to assess thiols levels also in patients with OCCC. Albeit the limitation of the *in vitro* studies with a single OCCC cell line,

we believe that the levels of cysteine and other thiols would be even higher in patients with this histological type compared to serous carcinomas, allowing faster disease progression and recurrence. Despite OCCC is frequently diagnosed at an initial stage [7], in an extraovarian advanced stage the disease has poor prognosis given intrinsic chemoresistance to conventional platinum drugs [7]. Our data supports that ovarian cancer cells that are more dependent on cysteine metabolism are more resistant to carboplatin effects mainly under hypoxia. The ability to take advantage from cysteine accounting for chemoresistance can be intrinsic, as OCCC, or acquired upon cyclic exposure to chemotherapy as happens with recurrent HG-OSC.

Albeit we did not find any statistically significant difference concerning thiols content in the different histological types of ovarian tumours, it is important to highlight that a tendency for higher cysteine levels was observed in the OCCC histotype compared to HG-OSC histotype, hence supporting a more important role of cysteine metabolism also in primary OCCC tumours. Interestingly, we also observed a tendency for increased cysteine levels in HG-OSC after chemotherapy, hence supporting a role of cysteine in the process of acquired resistance, where the chemotherapy may select cancer cells with an increased cysteine metabolism that may further allows their adaptation in the presence of drugs. It is of extreme importance to increase the number of samples analysed in order to confirm these tendencies.

Taken together, results strongly support that cysteine protects cells from the adverse hypoxic microenvironment and from platinum-based chemotherapy, thus having a role in cancer progression. Because of the high cysteine concentrations found in ascitic fluid and in serum from patients with ovarian malignant tumours, we propose that cysteine acts as a first protection barrier for neoplastic cells against hypoxia, having a role as a redox buffer, and against chemotherapy, as sulphur rapidly binds to platinum-based drugs, thus preventing their efficacy (figure 15). In metastatic peritoneal disease, cysteine rich ascites may contribute for the perpetual maintenance of resistance to therapy, as cancer cells proliferate directly embedded in ascitic fluid (figure 15).

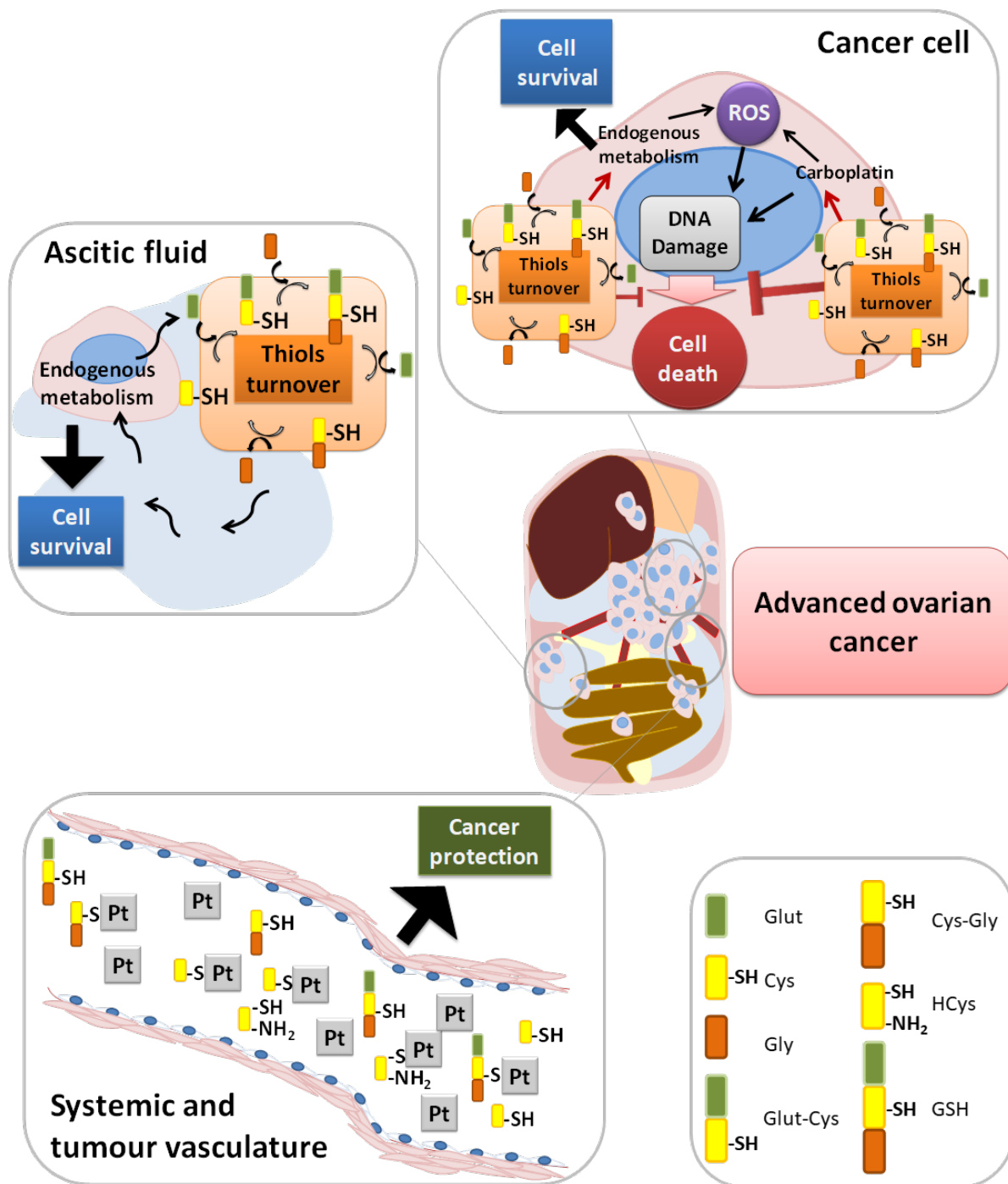


Figure 15. Role of cysteine in cells response to carboplatin and hypoxia adaptation.

In cancer cells, cysteine allows adaptation to adverse hypoxic microenvironments acting as a redox buffer, and to platinum-based chemotherapy as sulphur rapidly binds to carboplatin, avoiding DNA damage and evading apoptosis. Because of the presence of high cysteine concentrations in ascitic fluid from patients with ovarian cancer and also in serum from patients with ovarian malignant neoplasms, we propose that cysteine acts as a first protection barrier for malignant cells against hypoxia and against chemotherapy, thus contributing for disease progression and recurrence.

REFERENCES

1. Vaughan S, Coward JI, Jr RCB, Berchuck A, Berek JS, Brenton JD, *et al.* Rethinking ovarian cancer: recommendations for improving outcomes. *Nat. Rev.* 2011;11:719–25.
2. Bray F, Ferlay J, Soerjomataram I, Siegel RL, Torre LA, Jemal A. Global Cancer Statistics 2018: GLOBOCAN Estimates of Incidence and Mortality Worldwide for 36 Cancers in 185 Countries. *CA Cancer J Clin.* 2018;68:394–424.
3. Bowtell DD. The genesis and evolution of high-grade serous ovarian cancer. *Nat Rev Cancer.* 2010;10:803–8.
4. Chan JK, Cheung MK, Husain A, Teng NN, West D, Whittemore AS, *et al.* Patterns and progress in ovarian cancer over 14 years. *Obstet. Gynecol.* 2006;108:521–8.
5. Prat J. Ovarian carcinomas: Five distinct diseases with different origins, genetic alterations, and clinicopathological features. *Virchows Arch.* 2012;460:237–49.
6. Reid BM, Permuth JB, Sellers TA. Epidemiology of ovarian cancer: a review. *Cancer Biol. Med.* 2017;14:9–32.
7. Itamochi H, Kigawa J, Terakawa N. Mechanisms of chemoresistance and poor prognosis in ovarian clear cell carcinoma. *Cancer Sci.* 2008;99:653–8.
8. Agarwal R, Kaye SB. Ovarian cancer: strategies for overcoming resistance to chemotherapy. *Nat. Rev. Cancer.* 2003;3:502–16.
9. Ip CKM, Li S, Tang MH, Sy SKH, Ren Y. Stemness and chemoresistance in epithelial ovarian carcinoma cells under shear stress. *Sci. Rep.* 2016;6:26788–98.
10. Moradi MM, Carson LF, Weinberg B, Haney AF, Twiggs LB, Ramakrishnan S. Serum and Ascitic Fluid Levels of Necrosis Factor-Alpha in Patients with Ovarian Epithelial Cancer. *Cancer.* 1993;15:2433–40.
11. Mills B, Roifman M, Mellors A. A Putative New Growth Factor in Ascitic Fluid from Ovarian Cancer Patients: Identification, Characterization, and Mechanism of Action. *Cancer Res.* 1988;48:1066–71.
12. Mills GB, May C, Hill M, Campbell S, Shaw P, Marks A. Ascitic Fluid from Human Ovarian Cancer Patients Contains Growth Factors Necessary for Intraperitoneal Growth of Human Ovarian Adenocarcinoma Cells. *J.Clin.Invest.* 1990;86:851–5.
13. Hanahan D, Weinberg RA. Hallmarks of cancer: The next generation. *Cell.* 2011;144:646–74.
14. Pavlova NN, Thompson CB. The Emerging Hallmarks of Cancer Metabolism. *Cell Metab.* 2016;23:27–47.
15. Bhattacharyya S, Saha S, Giri K, Lanza IR, Nair KS, Jennings NB, *et al.* Cystathionine Beta-Synthase (CBS) Contributes to Advanced Ovarian Cancer Progression and Drug Resistance. *PLoS One.* 2013;8:e79167.1–12.
16. Szabo C, Coletta C, Chao C, Módis K, Szczesny B, Papapetropoulos A. Tumor-derived hydrogen sulfide, produced by cystathionine- β -synthase, stimulates bioenergetics, cell proliferation, and angiogenesis in colon cancer. *PNAS Pharmacol.* 2013;110:12474–9.

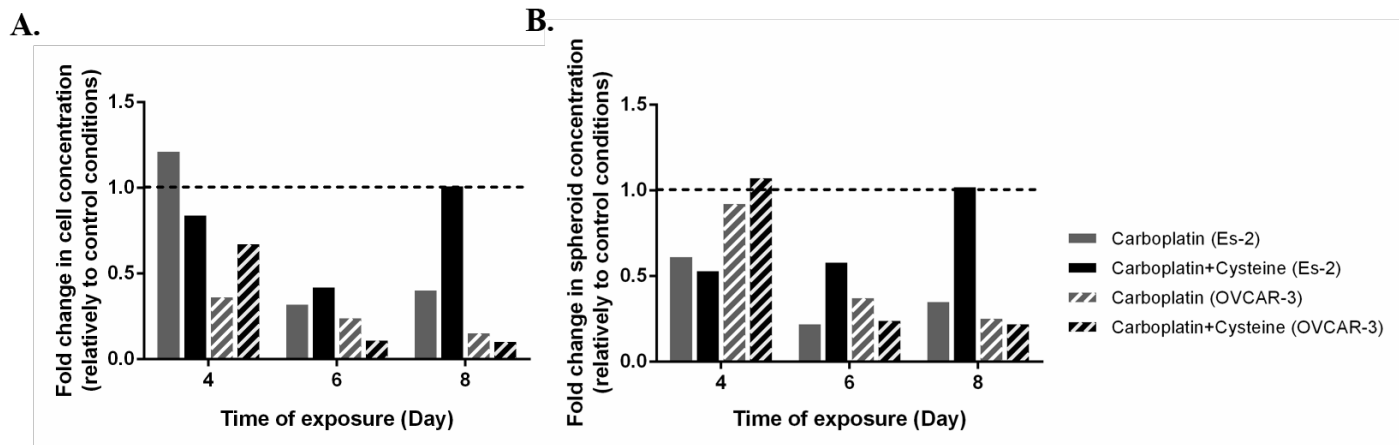
17. Sen S, Kawahara B, Gupta D, Tsai R, Khachatryan M, Farias-eisner R, *et al.* Role of cystathionine β -synthase in human breast Cancer. *Free Radic. Biol. Med.* 2015;86:228–38.
18. Panza E, De Cicco P, Armogida C, Scognamiglio G, Gigantino V, Botti G, *et al.* Role of the cystathionine γ lyase/hydrogen sulfide pathway in human melanoma progression. *Pigment Cell Melanoma Res.* 2015;28:61–72.
19. Gai JW, Qin W, Liu M, Wang HF, Zhang M, Li M, *et al.* Expression profile of hydrogen sulfide and its synthases correlates with tumor stage and grade in urothelial cell carcinoma of bladder. *Urol. Oncol. Semin. Orig. Investig.* 2016;34:166.e15–20.
20. Pan Y, Zhou C, Yuan D, Zhang J, Shao C. Radiation Exposure Promotes Hepatocarcinoma Cell Invasion through Epithelial Mesenchymal Transition Mediated by H₂S/CSE Pathway. *Radiat. Res.* 2015;185:96–105.
21. Schnelldorfer T, Gansauge S, Gansauge F, Schlosser S, Beger HG, Nussler AK. Glutathione depletion causes cell growth inhibition and enhanced apoptosis in pancreatic cancer cells. *Cancer.* 2000;89:1440–7.
22. Balendiran GK, Dabur R, Fraser D. The role of glutathione in cancer. *cell Biochem. Funct.* 2004;22:343–52.
23. Lopes-Coelho F, Gouveia-Fernandes S, Gonçalves LG, Nunes C, Faustino I, Silva F, *et al.* HNF1B drives glutathione (GSH) synthesis underlying intrinsic carboplatin resistance of ovarian clear cell carcinoma (OCCC). *Tumor Biol.* 2016;37:4813–29.
24. Mikalsen SG, Jeppesen Edin N, Sandvik JA, Pettersen EO. Separation of two sub-groups with different DNA content after treatment of T-47D breast cancer cells with low dose-rate irradiation and intermittent hypoxia. *Acta radiol.* 2017;59:26–33.
25. Gutsche K, Randi EB, Blank V, Fink D, Wenger RH, Leo C, *et al.* Intermittent hypoxia confers pro-metastatic gene expression selectively through NF- κ B in inflammatory breast cancer cells. *Free Radic. Biol. Med.* 2016;101:129–42.
26. Semenza GL. Hypoxia-inducible factors: Mediators of cancer progression and targets for cancer therapy. *Trends Pharmacol. Sci.* 2012;33:207–14.
27. Cutter NL, Walther T, Gallagher L, Lucito R, Wrzeszczynski K. Hypoxia signaling pathway plays a role in ovarian cancer chemoresistance. *AACR Annual Meeting 2017; April 1-5, 2017; Washington, DC. Abstract 4525.*
28. Kigawa J, Minagawa Y, Cheng X, Terakawa N. γ -Glutamyl cysteine synthetase up-regulates Multidrug resistance-associated protein in Patients with chemoresistant epithelial ovarian cancer. *Clin. Cancer Res.* 1998;4:1737–41.
29. Kelland L. The resurgence of platinum-based cancer chemotherapy. *Nat. Rev. Cancer.* 2007;7:573–84.
30. Epstein ACR, Gleadle JM, McNeill LA, Hewitson KS, O'Rourke J, Mole DR, *et al.* C. elegans EGL-9 and mammalian homologs define a family of dioxygenases that regulate HIF by prolyl hydroxylation. *Cell.* 2001;107:43–54.
31. Wu D, Yotnda P. Induction and Testing of Hypoxia in Cell Culture. *J. Vis. Exp.* 2011;54:1–4.
32. Goldberg MA, Dunning SP, Bunn HF. Regulation of the erythropoietin gene: evidence that the

- oxygen sensor is a heme protein. *Science*. 1988;242:1412–5.
33. Al Okail MS. Cobalt chloride, a chemical inducer of hypoxia-inducible factor-1 α in U251 human glioblastoma cell line. *J. Saudi Chem. Soc.* 2010;14:197–201.
34. Ghaly AE, Kok R. The effect of sodium sulfite and cobalt chloride on the oxygen transfer coefficient. 1988;19:259–270.
35. Reers M, Smiley ST, Mottola-Hartshorn C, Chen A, Lin M, Chen LB. Mitochondrial Membrane potential monitored by JC-1 Dye. *Methods Enzymol.* 1995;260:406–17.
36. Travedi M V., Laurence JS, Siahann TJ. The role of thiols and disulfides in protein chemical and physical stability. *Curr Protein Pept Sci.* 2009;10:614–25.
37. Grilo NM, João Correia M, Miranda JP, Cipriano M, Serpa J, Matilde Marques M, *et al.* Unmasking efavirenz neurotoxicity: Time matters to the underlying mechanisms. *Eur. J. Pharm. Sci.* 2017;105:47–54.
38. Perry SW, Norman JP, Barbieri J, Brown EB, Harris A. Mitochondrial membrane potential probes and the proton gradient: a practical usage guide. *Biotechniques.* 2011;50:98–115.
39. Tammela J, Geisler J, Eskew PJ, Geisler H. Clear cell carcinoma of the ovary: poor prognosis compared to serous carcinoma. *Eur. J. Gynaecol. Oncol.* 1998;19:438–40.
40. Lee Y, Kim T, Kim M, Kim H, Song T, Kyu M, *et al.* Gynecologic Oncology Prognosis of ovarian clear cell carcinoma compared to other histological subtypes : A meta-analysis. *Gynecol. Oncol.* 2011;122:541–7.
41. Goff BA, de la Cuesta RS, Muntz HG, D. F, Ek M, Rice LW, *et al.* Clear cell carcinoma of the ovary: a distinct histologic type with poor prognosis and resistance to platinum-based chemotherapy in stage III disease. *Gynecol. Oncol.* 1996;417:412–7.
42. Sugiyama T, Kamura T, Kigawa J, Terakawa N, Kikuchi Y, Kita T, *et al.* Clinical characteristics of clear cell carcinoma of the ovary. *Cancer.* 2000;88:2584-9.
43. Beaufort CM, Helmijr JCA, Piskorz AM, Hoogstraat M, Ruigrok-Ritstier K, Besselink N, *et al.* Ovarian cancer cell line panel (OCCP): Clinical importance of in vitro morphological subtypes. *PLoS One.* 2014;9: e103988.1–16.
44. Burgos-ojeda D, Rueda BR, Buckanovich RJ. Ovarian cancer stem cell markers : Prognostic and therapeutic implications. 2012;322:1–7.
45. Szwegold BS, Howell SK, Beisswenger PJ. Transglycation-A Potential New Mechanism for Deglycation of Schiff's Bases. *Ann. N. Y. Acad. Sci.* 2006;1043:845–64.
46. Miranti EH, Freedman ND, Weinstein SJ, Abnet CC, Selhub J, Murphy G, *et al.* Prospective study of serum cysteine and cysteinylglycine and cancer of the head and neck, esophagus, and stomach in a cohort of male smokers. *Am. J. Clin. Nutr.* 2016;104:686–93.
47. Guštin E, Jarc E, Kump A, Petan T. Lipid Droplet Formation in HeLa Cervical Cancer Cells Depends on Cell Density and the Concentration of Exogenous Unsaturated Fatty Acids. *Acta Chim. Slov.* 2017;549–54.
48. Aguirre-Ghiso JA. Models, mechanisms and clinical evidence for cancer dormancy. *Nat. Rev. Cancer.* 2007;7:834–46.

49. Lavi O, Greene JM, Levy D, Gottesman MM. The role of cell density and intratumoral heterogeneity in multidrug resistance. *Cancer Res.* 2013;73:7168–75.
50. Greene JM, Levy D, Herrada SP, Gottesman MM, Lavi O. Mathematical modeling reveals that changes to local cell density dynamically modulate baseline variations in cell growth and drug response. *Cancer Res.* 2016;76:2882–90.
51. Tang HL, Yuen KL, Tang HM, Fung MC. Reversibility of apoptosis in cancer cells. *Br. J. Cancer.* 2009;100:118–22.
52. Mendis S, Athauda SBP, Kenji T. Association between hyperhomocysteinaemia and ischaemic heart disease in Sri Lankans. *Int. J. Cardiol.* 1997;62:221–5.
53. Lin J, Manson JE, Selhub J, Buring JE, Zhang SM. Plasma cysteinylglycine levels and breast cancer risk in women. *Cancer Res.* 2007;67:11123–7.
54. Lin J, Lee I-M, Song Y, Cook NR, Selhub J, Manson JE, *et al.* Plasma homocysteine and cysteine and risk of breast cancer in women. *Cancer Res.* 2010;70:2397–405.
55. Miller JW, Beresford SA, Neuhauser ML, Cheng T-YD, Song X, Brown EC, *et al.* Homocysteine, cysteine, and risk of incident colorectal cancer in the Women ' s Health Initiative observational cohort 1 – 3. *Am J Clin Nutr.* 2013;97:827–34.
56. Chiang FF, Wang HM, Lan YC, Yang MH, Huang SC, Huang YC. High homocysteine is associated with increased risk of colorectal cancer independently of oxidative stress and antioxidant capacities. *Clin. Nutr.* 2014;33:1054–60.
57. Murphy G, Fan J-H, D Mark S, M Dawsey S, Selhub J, Wang J, *et al.* Prospective study of serum cysteine levels and oesophageal and gastric cancers in China. *Gut.* 2011;60:1–6.
58. Traverso N, Ricciarelli R, Nitti M, Marengo B, Furfaro AL, Pronzato MA, *et al.* Role of Glutathione in Cancer Progression and Chemoresistance. *Oxid. Med. Cell. Longev.* 2013;2013:1–10.
59. Mieyal JJ, Gallogly MM, Qanungo S, Sabens EA, Shelton MD. Molecular Mechanisms and Clinical Implications of Reversible Protein S -Glutathionylation. *Antioxid. Redox Signal.* 2008;10:1941–88.
60. Visscher M, Arkin MR, Dansen TB. Covalent targeting of acquired cysteines in cancer. *Curr. Opin. Chem. Biol.* 2016;30:61–7.
61. García-Giménez JL, Romá-Mateo C, Pérez-Machado G, Peiró-Chova L, Pallardó F V. Role of glutathione in the regulation of epigenetic mechanisms in disease. *Free Radic. Biol. Med.* 2017;112:36–48.
62. Santo VE, Estrada MF, Rebelo SP, Abreu S, Silva I, Pinto C, *et al.* Adaptable stirred-tank culture strategies for large scale production of multicellular spheroid-based tumor cell models. *J. Biotechnol.* 2016;221:118–29.

SUPPLEMENTS

Supplement figure 1



Supplement figure 1. ES2 and OVCAR3 spheroid exposure to chemotherapeutic treatment: protective effect of cysteine.

Single cell suspension of OVCAR3 and ES2 cells (5×10^6 cell/mL) were inoculated in spinner vessels and maintained under 60-80 rpm agitation to induce aggregation, according to Santo *et al.* [62] Spheroid cultures were challenged with 2 cycles of exposure with 25 $\mu\text{g/mL}$ carboplatin, with or without supplementation with 0.4 mM cysteine (on day 0 and 4), and compared to control cultures without chemotherapy treatment, with or without cysteine supplementation. A. Cell concentration, determined by detection of cellular DNA, and B. spheroid concentration, determined by phase contrast microscopy and automatic evaluation using ImageJ software (as described in [62]) were evaluated along drug exposure time. Data is presented as fold change relative to the respective control condition.

CHAPTER 4

CYSTEINE MECHANISTIC ROLE IN OVARIAN CANCER CELLS ADAPTATION TO HYPOXIA

Manuscript in preparation

*Will you follow and know
Know me more than you do
Track me down
And try to win me?"*

Morrissey

ABSTRACT

Despite the observation of an improvement in the overall survival of ovarian cancer patients in the last 30 years, this improvement has been mainly achieved due to an increased life expectancy of women with recurrent ovarian cancer, instead of an increased cure rate. The late diagnosis together with resistance to treatment represent the major causes of this poor prognosis disease.

As a solid tumour grows, cancer cells are exposed to regions of hypoxia, known to be a stimulus for tumour progression and resistance to therapy. Since our previous results supported that cysteine allows adaptation to hypoxia, in here, we aimed to investigate the mechanisms by which cysteine protects ovarian cancer cells from hypoxia-induced death, by addressing its role in cellular metabolism, namely through energy production.

Our results strongly supported a role of the xc⁻ system via cystine uptake (the oxidised form of cysteine) in energy production that requires cysteine metabolism instead of H₂S *per se*. Interestingly, albeit CBS and CSE inhibition was not sufficient to impair ATP production, the inhibition of both enzymes affected ATP synthesis mainly under hypoxia in ovarian cancer cells, thus supporting a role of their activity in this environment. However, the specific contribution of CBS/CSE/MpST activities on cysteine-derived ATP synthesis under hypoxia remains unclear. Strikingly, NMR analysis strongly supported a role of cysteine in cellular metabolism rescue under hypoxia, especially in ES2 cells, hence strengthening that cysteine supports cells viability and proliferation in hypoxic environments.

KEYWORDS

Cysteine, hypoxia, ovarian cancer, hydrogen sulphide, xCT, CBS, CSE, MpST

INTRODUCTION

Despite all the progresses developed in prevention and new treatment approaches, cancer corresponds to the second leading cause of death worldwide [1]. In accordance with the International Agency for Research on Cancer, in 2012 14.1 million cancer cases [2] and 8.2 million cancer deaths [3] were estimated worldwide. For 2020, 17.1 million incidences and 10.05 million cancer deaths [2] are estimated. In one hand, these values are explained by the

increasing incidence of cancer cases due to aging and growth of the global population, together with exposition to risk factors such as smoking, obesity, and dietary patterns [1]. In another hand, the late diagnosis combined with resistance to the conventional anti-cancer drugs used, explain cancer poor prognosis.

Ovarian cancer is not an exception to this scenario, being estimated, in 2020, 0.28 million new cases and 0.18 million ovarian cancer deaths worldwide [2]. The late diagnosis together with resistance to treatment represent the major causes of this poor prognosis disease [4].

Epithelial ovarian cancer (EOC) includes most ovarian malignancies [5,6] that can be classified based on histopathology and molecular/genetic features, being the ovarian carcinomas mainly classified as high-grade serous (HG-OSC, 70%), low grade serous carcinomas (LG-OSC, <5%) endometrioid (OEC, 10%), clear cell (OCCC, 10%) and mucinous (OMC, 3%) [7,8].

As a solid tumour grows, cancer cells are exposed to regions of hypoxia, strictly linked to oxidative stress [9,10] and known to be responsible for tumour progression and resistance to therapy [11,12]. In ovarian cancer, oxidative stress was already associated with the pathogenesis of the disease [10,13], indicating that ovarian cancer cells present mechanisms that allow them to cope with the harmful oxidative conditions. Recently, it was proposed that cysteine facilitates the adaptation of ovarian cancer cells to hypoxic environments and also contribute to their escape from carboplatin-induced death [14,15]. The relevance of cysteine in ovarian cancer clinical context was also corroborated, since ascitic fluid from ovarian cancer patients - an important compartment of tumour microenvironment -, showed cysteine as the prevalent thiol and because cysteine levels were also altered in serum from patients with ovarian tumours [15]. Cysteine role in cancer cells survival was already associated with its role as a precursor of the antioxidant glutathione (GSH) [16–18] and due to hydrogen sulphide (H₂S) generation [19–25] by cysteine catalybolism through the activity of the enzymes cystathionine β-synthase (CBS), cystathionine γ-lyase (CSE) and/or 3-mercapto-pyruvate sulfurtransferase (MpST) together with cysteine aminotransferase (CAT) [26–28].

In here, we aimed to address the mechanism by which cysteine protects ovarian cancer cells from hypoxia-induced death, hypothesising that besides GSH synthesis, cysteine has a role also in energy production under hypoxic conditions. To test this hypothesis, we used two different cancer cell lines derived from two different histological types of ovarian cancer, ES2 cells, corresponding to an ovarian clear cell carcinoma (OCCC) cell line and OVCAR3 cells, corresponding to a ovarian serous carcinoma (HG-OSC) cell line.

MATERIALS AND METHODS

Cell culture

Cell lines from OCCC (ES2; CRL-1978) and HG-OSC (OVCAR-3; HTB-161) were obtained from American Type Culture Collection (ATCC). Cells were maintained at 37°C in a humidified 5% CO₂ atmosphere. Cells were cultured in DMEM 1× (41965-039, Gibco, Life Technologies) containing 4.5 g/L of D-glucose and 0.58 g/L of L-glutamine supplemented with 1% FBS (S 0615, Merck), 1% antibiotic-antimycotic (P06-07300, PAN Biotech) and 0.1 % gentamicin (15750-060, Gibco, Life Technologies) and exposed either to 0.402 mM L-cysteine (102839, Merck) and/or exposed to hypoxia induced with 0.1 mM cobalt chloride (CoCl₂) (C8661, Sigma-Aldrich).

Prior to any experiment, cells were synchronized under starvation (culture medium without FBS) for 8 h at 37°C and 5% CO₂.

ATP quantification

To test the effect of xCT inhibition on ATP levels, cells (5×10^5 or 2.5×10^5 cells/well) were seeded in 6-well white plates and exposed to hypoxia induced with 0.100 mM CoCl₂ combined with 0.250 mM sulphasalazine (S0883, Sigma), an xCT inhibitor. After 24 h, the medium was changed and fresh experimental conditions were added. Cells were collected at 48 h after stimulation.

To test the effect of the enzymes involved in cysteine metabolism on ATP synthesis, cells (5×10^5 or 2.5×10^5 cells/well) were seeded in 6-well plates and cultured in control condition and exposed to 0.402 mM L-cysteine and/or hypoxia induced with 0.1 mM CoCl₂. The previous conditions were combined with 1 mM O-(Carboxymethyl)hydroxylamine hemihydrochloride (AOAA, C13408, Sigma) and 3 mM DL-propargylglycine (PAG, P7888, Sigma), which are respectively inhibitors of CBS and CSE. After 24 h, the medium was changed and fresh experimental conditions were added. Cells were collected at 16 and 48 h after stimulation. This assay was also performed with cell collection after 2 h of experimental conditions. In this case, 5×10^5 cells were seeded in 6-well white plates for both ES2 and OVCAR3 cells.

To investigate the effect of cysteine and NaHS upon xCT inhibition on ATP synthesis, cells (5×10^5 or 2.5×10^5 cells/well) were seeded in 6-well plates and exposed to hypoxia

induced with 0.100 mM CoCl₂ with and without 0.402 mM L-cysteine combined with 0.250 mM sulphasalazine, 30 μM NaHS (161527 Sigma-Aldrich) or both. After 24 h, the medium was changed and fresh experimental conditions were added. Cells were collected at 48 h after stimulation. This assay was also performed with cell collection after 1 h of experimental conditions. In this case, 5×10⁵ cells were seeded in 6-well white plates for both ES2 and OVCAR3 cells.

To ascertain the effect of the inhibition of fatty acids degradation (β-oxidation) and glucose degradation (glycolysis) on ATP production, cells (5×10⁵ or 2.5×10⁵ cells/well) were seeded in 6-well plates and exposed to hypoxia induced with 0.100 mM CoCl₂ with and without 0.402 mM L-cysteine combined with 10 μM etomoxir (β-oxidation inhibitor), 20 μM bromopyruvic acid (glycolysis inhibitor) or both. After 24 h, the medium was changed and fresh experimental conditions were added. Cells were collected at 48 h after stimulation.

Cells were scrapped with cold PBS 1x- EDTA 2 mM and homogenized in 1% Nonidet P-40 (NP-40) lysis buffer (1% NP40 N-6507 Sigma, and 1x protease inhibitor, SIGMAFASTTM Protease inhibitor cocktail tablets S8830, Sigma) on ice for 30 minutes and centrifuged at 20000 g for 5 min at 4°C. Protein was quantified and the same amount of total protein was used within each assay, in a range between 2.5 and 10 μg. ATP determination kit (A22066, Molecular probes) was used in accordance with the manufacturer. The measurements were performed using Luciferase protocol from VIKTOR3 instrument from PerkinElmer, using Wallac 1420 Software version 3.0 (Luminometry, Luciferase FIR protocol). The ATP concentration was determined against an ATP calibration curve, within the range of 0 μM and 30 μM.

Immunofluorescence analysis

Cells (1×10⁵ cells/well) were seeded in 24-well plates and cultured in control condition. Cells were collected after 16 h of experimental conditions and fixed with 4% paraformaldehyde for 15 min at 4°C and permeabilised with PBS(1X)-BSA 0.5%-saponin 0.1% for 15 min at room temperature. Cells were then incubated with Anti-xCT (ab175186, abcam) for 30 min (diluted in PBS(1X)-BSA 0.5%-saponin 0.1%; 1:100) and incubated with secondary antibody for 2 h at room temperature (Alexa Fluor® 488 anti-rabbit, A-11034, Invitrogen) (1:1000 in PBS(1X)-BSA 0.5%-saponin 0.1%). The slides were mounted in VECTASHIELD media with DAPI (4'-6-diamidino-2-phenylindole) (Vector Labs) and

examined by standard fluorescence microscopy using a Zeiss Imager.Z1 AX10 microscope. Images were acquired and processed with CytoVision software.

Western blotting analysis with isolated mitochondria

Cells (7×10^6 cells/flask) were cultured in 150 cm² culture flasks and exposed to control condition and exposed to 0.402 mM L-cysteine and/or hypoxia induced with 0.100 mM CoCl₂. Cells were collected after 16 h of experimental conditions, and mitochondria were isolated with Mitochondria Isolation Kit for profiling cultured cells (MITOISO2, Sigma). Briefly, cells were scraped, centrifuged for 5 min at 600 g and washed in ice cold PBS 1x. The cell pellet was resuspended in 650 µL of Lysis Buffer. A 5 min period of incubation was performed on ice and samples were suspended at 1 min intervals by pipetting up and down once. Two volumes of extraction buffer were added and the homogenate was centrifuged at 600 g for 10 min at 4°C. The supernatant was transferred to a fresh tube and centrifuged at 11000 g for 10 min at 4°C, this new supernatant was removed and the pellet suspended in 75 µL of CellLytic M Cell Lysis Reagent.

The lysates were centrifuged at 20817 g for 5 min at 4°C and protein concentration was determined based on Bradford method (500-0006, Bio Rad). For western blotting for xCT and TOMM20 with isolated mitochondria, 15 µg of total protein from each sample was used. For MpST, 20 µg of total protein from each sample was used.

Membranes were incubated with Anti-xCT (1:1000 in PBS 1x-Milk 5%; ab175186 from abcam) or Anti-MpST (1:250 in PBS 1x-Milk 5%; HPA001240 from sigma) at 4°C with agitation, overnight. The membranes were then washed 3 times, for 5 min, with PBS 1x 0.1% (v/v) Tween 20. Posteriorly, the membranes were incubated with the secondary antibody (1:5000 in PBS 1x-Milk 5%; anti-rabbit, 31460 from Thermo Scientific) for 2 h at room temperature. For the membrane that was previously incubated with xCT, the protocol was repeated in the same membrane for anti-TOMM20 antibody (1:1000 in PBS 1x-Milk 5%; ab186734 from abcam).

Measurement of basal H₂S in cell homogenates

Cells (5×10^5 cells/well) were seeded in 6-well black plates and cultured in control condition and exposed to 0.402 mM L-cysteine and/or hypoxia induced with 0.1 mM CoCl₂. After 24 h, the medium was changed and fresh experimental conditions were added. Cells

were collected at 48 h after stimulation. Cells were scrapped with PBS 1x and homogenized in NP40 lysis buffer (1% NP40, 150 mM NaCl, 50 mM Tris-Cl, pH 8.0) on ice for 30 min and centrifuged at 20000 g for 5 min at 4°C. Cell homogenates (20 µl) were incubated in black 96-well plates with 80 µl of 10 µM 7-Azido-4- Methylcoumarin (AzMC, L511455, Sigma) with and without 1 mM AOAA, 3 mM PAG or the combination of both the inhibitors.

The protein concentration was determined with Bradford method using protein assay dye reagent concentrate (500-0006, Bio Rad) and a BSA calibration curve. The H₂S measurements were posteriorly normalised to total protein concentration and to a blank sample (cellular lysates with and without AOO, PAG or both without probe).

H₂S production was monitored following fluorescent signal of AzMC using Umbelliferone protocol from VIKTOR3 instrument from PerkinElmer and Wallac 1420 Software version 3.0 every 30 min for 2 h (Prompt fluorometry, Umbelliferone – 355 nm/460 nm, 0.1 s - protocol).

Cell death analysis

To test whether the protective effect of cysteine under hypoxia was dependent on H₂S production, cells (1×10^5 cells/well) were seeded in 24-well plates. Cells were cultured in control condition and exposed to 0.402 mM L-cysteine and/or hypoxia induced with 0.1 mM CoCl₂, combined to 1 mM O-(Carboxymethyl)hydroxylamine hemihydrochloride (AOAA, C13408, Sigma), to 3 mM of DL-Propargylglycine (PAG, P7888, Sigma), or the combination of both. Cells were collected 16 h after stimulation.

Cells were harvested by centrifugation at 153 g for 3 min, cells were incubated with 0.5 µL FITC Annexin V (640906, BioLegend) in 100 µL annexin V binding buffer 1x (10 mM HEPES (pH 7.4), 0.14 M sodium chloride (NaCl), 2.5 mM calcium chloride (CaCl₂) and incubated at room temperature and in the dark for 15 min. After incubation, samples were rinsed with 0.2% (w/v) BSA (A9647, Sigma) in PBS 1x and centrifuged at 153 g for 3 min. Cells were suspended in 200 µL of annexin V binding buffer 1x and 2.5 µL Propidium Iodide (50 µg/mL). Acquisition was performed in a FACScalibur (Becton Dickinson). Data were analysed with FlowJo software.

Nuclear magnetic resonance (NMR) analysis

Cells (6.5×10^6 cells) were seeded in 175 cm² culture flasks and cultured in control condition and exposed to 0.402 mM L-cysteine and/or hypoxia induced with 0.1 mM CoCl₂.

Cells and supernatants were collected at 48 h after stimulation and stored at -20°C .

Cell extracts were performed with methanol and chloroform to separate organic and aqueous phases. After cold methanol mixture (4 mL methanol/ 1 g weight pellet), 2 volumes (vol) of water were added, mixed, and incubated for 5 min on ice. Chloroform (1 vol) was then added to the sample and mixed. Finally, 1 vol of water was added and samples were incubated for 10 min on ice, following centrifugation at 1699 g for 15 min at 4°C . Aqueous (upper) and organic (lower) phases were collected. After extraction of solvents by evaporation, using a Speed Vac Plus Scllon, the samples were suspended on KPi buffer (50 mM, pH 7.4) in deuterated water (D_2O) with 4% (v/v) sodium azide (NaN_3) and 0.097 mM of 3-(trimethylsilyl)propionic-2,2,3,3- d_4 (TSP). Culture supernatants were also diluted in this solution at 1:10 ratio. The ^1H -NMR (noesypr1d) was obtained at 25°C in Avance 500 II+ (Bruker) operating at 500.133 MHz, equipped with a 5 mm TCI(F)-z H-C/N Prodigy cryo-probe. The chemical shifts in aqueous sample were referred to the TSP. Topspin 3.2 (Bruker) was used for acquisition and spectra analysis. Compound identification was performed by resorting to the Human Metabolome database (HMDB) (<http://www.hmdb.ca/>) and Chenomx NMR suite software version 8.1 (Chenomx Inc.). Metabolites concentration was determined using Chenomx NMR suite software version 8.1 (Chenomx Inc.).

Statistical analysis

All data are presented as the mean \pm SD with the exception of ^1H -NMR data, which are presented as the median with 25th to 75th percentiles. All the graphics were done using the PRISM software package (PRISM 6.0 for Mac OS X; GraphPad software, USA, 2013). Assays were performed with at least 3 biological replicates per treatment. For comparisons of two groups, two-tailed independent-samples T-test was used. For comparison of more than two groups, One-way analysis of variance (ANOVA) with Tukey's multiple-comparisons post hoc test was used. Statistical significance was established as $p < 0.05$. All statistical analyses were performed using the IBM Corp. Released 2013. IBM SPSS Statistics for Macintosh, Version 22.0. Armonk, NY: IBM Corp. software, with the exception of metabolic pathway analysis that was performed with MetaboAnalyst 4.0 (<https://www.metaboanalyst.ca/faces/home.xhtml>).

RESULTS

Hypoxia is able to induce ATP synthesis

Since our previous results have shown that cysteine was able to protect ovarian cancer cells from hypoxia-induced death, we further explored the ability of these cells to synthesize ATP under hypoxic conditions.

Results have shown that in ES2 cells with 16 h of conditions, ATP levels did not differ among hypoxia with and without cysteine supplementation and were higher under hypoxia without cysteine compared to normoxia with cysteine supplementation ($p=0.017$) (figure 1A). With 48 h of experimental conditions, ATP levels were increased under hypoxia without cysteine compared both to hypoxia ($p=0.018$) and normoxia ($p=0.033$) with cysteine supplementation (figure 1 A).

In OVCAR3 cells, with 16 h of conditions no differences were observed among treatments (figure 1B). However, with 48 h of experimental conditions, the results were identical to ES2 cells, where cells cultured under hypoxia without cysteine presented higher ATP levels compared both to normoxia ($p=0.008$) and hypoxia ($p<0.001$) with cysteine (figure 1 B).

These results support that ovarian cancer cells exhibit alternative ways that allow sustaining energy production under hypoxic environments. Because cells cultured under hypoxia without cysteine supplementation also present cysteine in the medium (yet in lower concentrations), and also because cells cultured under hypoxia with cysteine reach higher cellular confluence levels compared to hypoxia without its supplementation, we cannot, nevertheless, rule out a role of cysteine in ATP production.

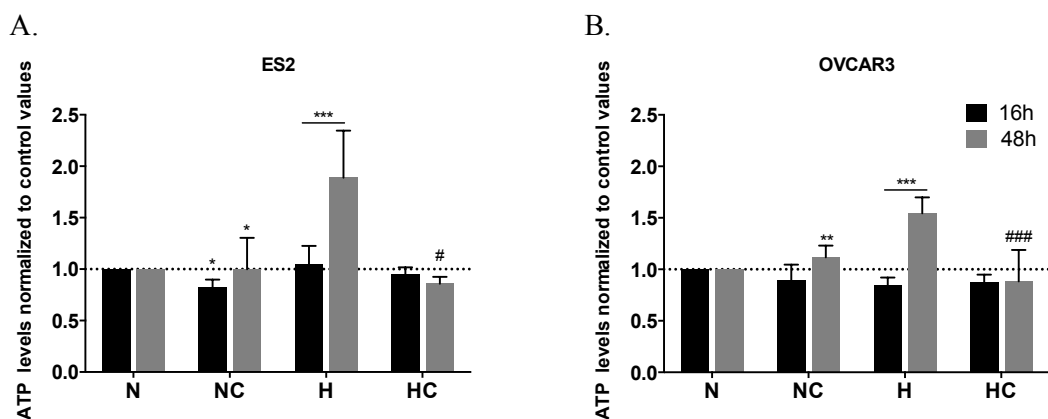


Figure 1. Hypoxia induced ATP synthesis under hypoxia.

ATP levels normalised to control values (normoxia without cysteine) for 16 h and 48 h of experimental

conditions for A. ES2 cells and B. OVCAR3 cells. N – normoxia; NC – normoxia with cysteine, H – hypoxia, HC – hypoxia with cysteine. The asterisks (*) represent the statistical significance compared to normoxia without cysteine and the cardinals (#) represent the statistical significance compared to hypoxia without cysteine within the same time-point. The differences among the different time-points are pointed in the figure. Results are shown as mean \pm SD. * p <0.05, ** p <0.01, *** p <0.001 (One-way ANOVA with post hoc Tukey tests).

xCT transporter localises in ovarian cancer cells' mitochondria and its inhibition impairs ATP synthesis under hypoxia, which cysteine is able to revert

Since no direct associations were found between cysteine and ATP production under hypoxia, we further explored the role of xCT, a member of the cystine-glutamate transporter xc^- system, known to mediate the uptake of cystine [29] (the oxidised form of cysteine), on ATP production. Thus, we started by addressing if this transporter could localise in ovarian cancer cells' mitochondria thus suggesting a role of cysteine metabolism in ATP production via xc^- system. Immunofluorescence analysis suggested a mitochondrial localisation of xCT in both ES2 and OVCAR3 cells (figure 2A) that was further confirmed by western blotting analysis with isolated mitochondria (figure 2 A and B). Interestingly, by western blotting with anti-TOMM20 (a mitochondrial marker) results seem to indicate that ES2 cells present a higher content of mitochondria under hypoxia compared to the other experimental conditions, whereas OVCAR3 cells seem to present the opposite tendency. As a consequence, the ratio xCT/TOMM20 was decreased in ES2 cells and increased in OVCAR3 cells. Nonetheless, these results are preliminary and must be confirmed.

We then explored the effect of xCT inhibition in the ability of ovarian cancer cells to produce ATP under hypoxia. Strikingly, xCT inhibition led to impaired ATP production under hypoxia in both cell lines ($p=0.038$ for ES2 and $p=0.010$ for OVCAR3 cells) (figure 3A), which cysteine was able to revert, since the impact on ATP production was decreased under hypoxia with cysteine supplementation compared to hypoxia alone ($p<0.001$) (figure 3B).

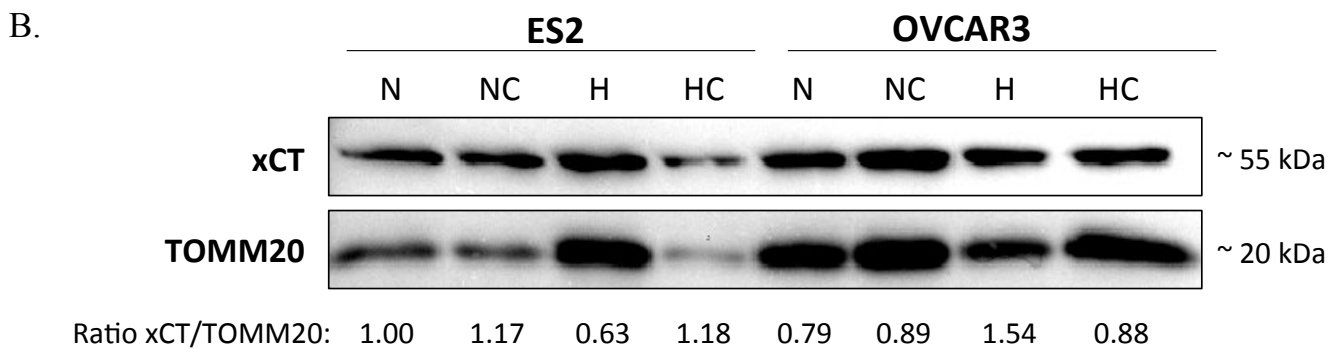
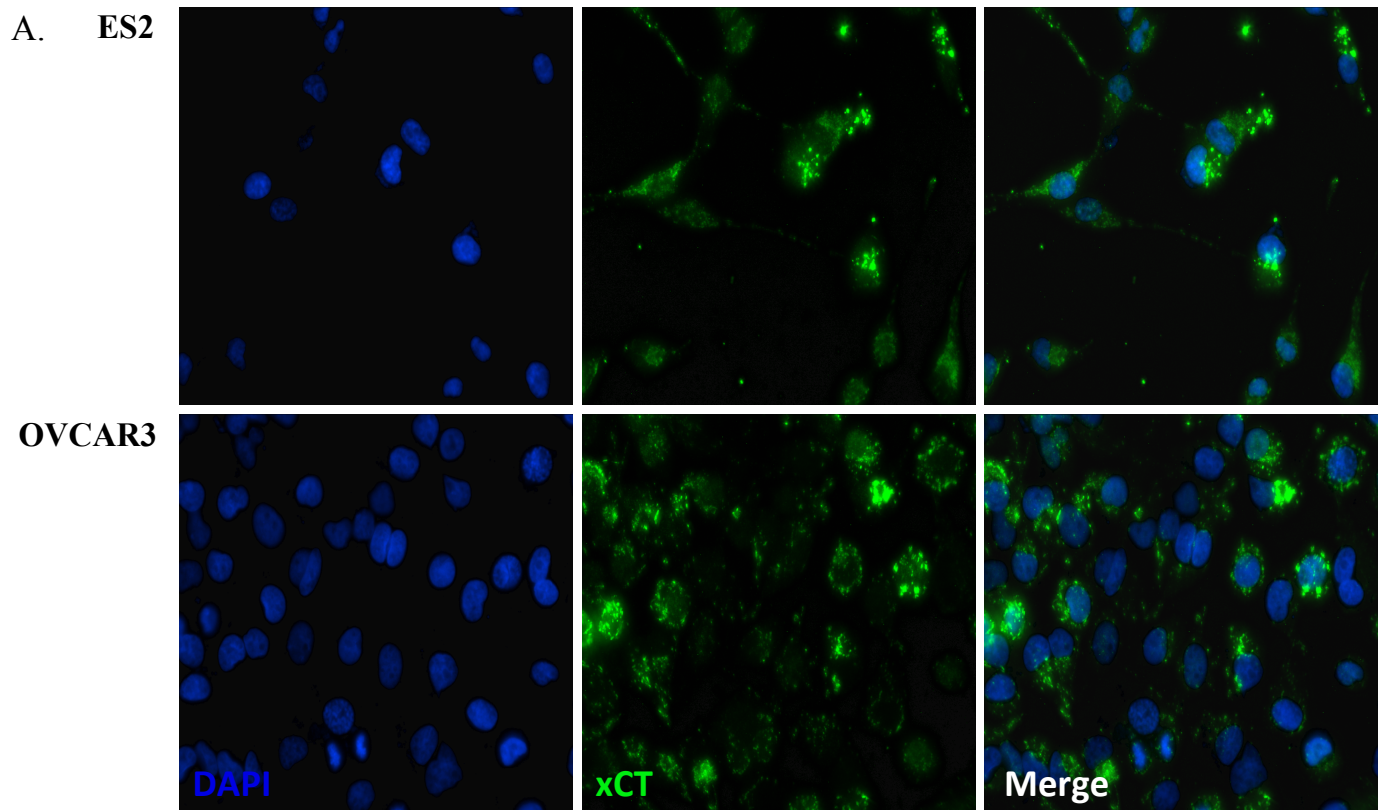


Figure 2. xCT localises in ovarian cancer cells mitochondria.

A. Immunofluorescence analysis for the xCT transporter under control conditions (normoxia) for ES2 and OVCAR3 cells and B. western blot analysis with isolated mitochondria for xCT and TOMM20 in ES2 and OVCAR3 cells. N – normoxia; NC – normoxia with cysteine, H – hypoxia, HC – hypoxia with cysteine.

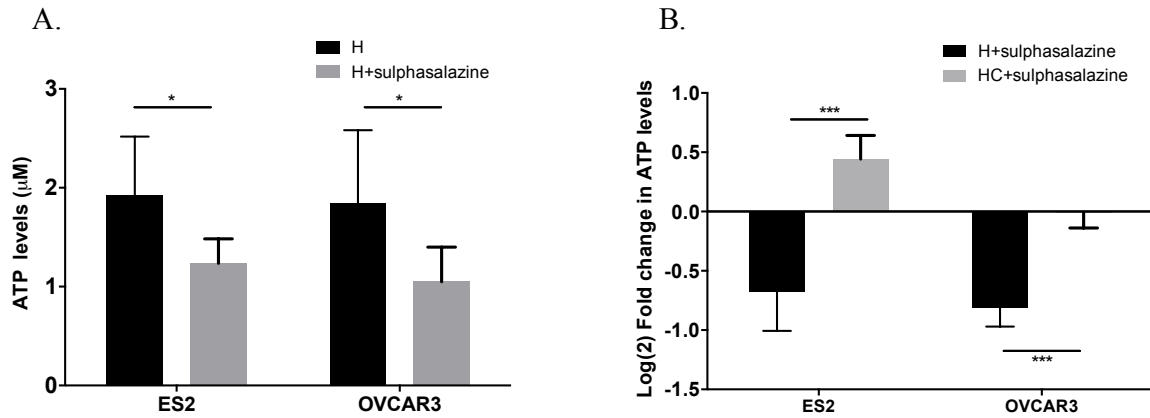


Figure 3. Cysteine is able to rescue the impaired ATP synthesis triggered by xCT inhibition under hypoxia.

ATP levels for 48 h of experimental conditions for ES2 and OVCAR3 cells. A. under hypoxia and in the presence of the xCT inhibitor, sulphasalazine, B. under hypoxia and in the presence of the xCT inhibitor, sulphasalazine and cysteine. In B. the values were normalised to the respective control and $\log(2)$ was calculated. H – hypoxia, HC – hypoxia with cysteine supplementation. Results are shown as mean \pm SD. * $p < 0.05$, ** $p < 0.01$, *** $p < 0.001$ (Independent-samples T test).

H₂S may correlate with ATP synthesis under hypoxia

Since we observed a role of cysteine in ATP synthesis mediated by the xc- system, we next aimed to address if H₂S production would be the source of ATP under hypoxia without cysteine. For that, basal cellular H₂S levels were measured with and without the inhibition of two enzymes involved in cysteine degradation. Thus, AOAA was used to inhibit CBS activity and PAG was used to inhibit CSE activity.

For ES2 cells, results have shown that hypoxia without cysteine (H) induced H₂S production compared to the other treatments ($p < 0.001$ compared both to NC and HC). With AOAA alone, PAG alone or the combination of both, similar results were observed ($p < 0.001$ compared to N, NC and HC) (figure 4 A-E).

Interestingly, in all experimental conditions, PAG alone was not able to decrease H₂S levels (figure 4E). On the contrary, AOAA alone or in combination with PAG was responsible for decreased H₂S levels.

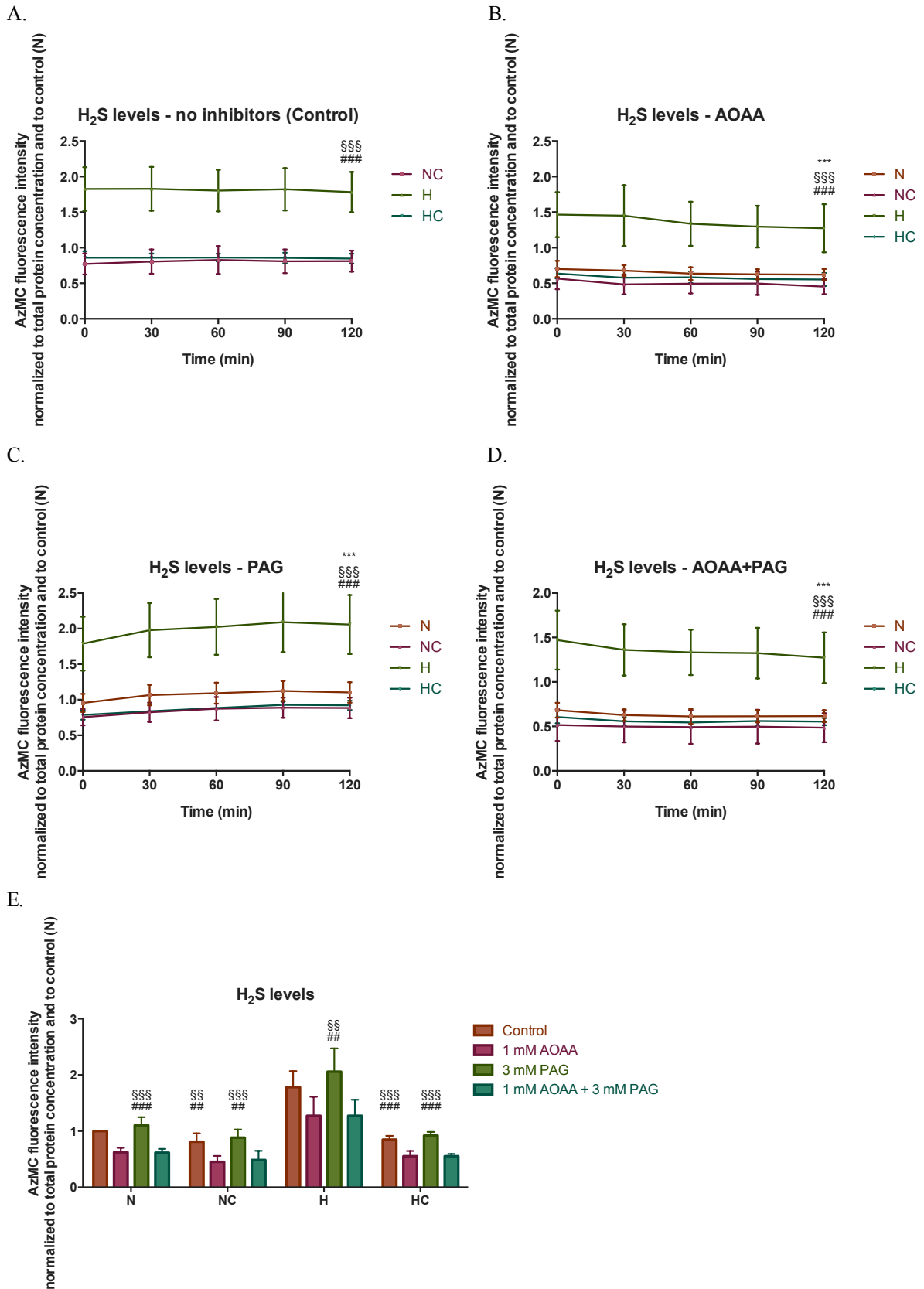


Figure 4. Hypoxia induces H₂S production in ES2 cells.

H₂S levels in ES2 cells for 48 h of experimental conditions in A. Control (no inhibitors), B. With CBS inhibitor (AOAA), C. with CSE inhibitor (PAG), E. with both the inhibitors (AOAA+PAG) and E. in all

experimental conditions. N – normoxia; NC – normoxia with cysteine, H – hypoxia, HC – hypoxia with cysteine. In A-D the asterisks (*) represent the statistical significance compared to N, the section symbols (§) represents the statistical significance compared to NC and the cardinals (#) represent the statistical significance compared to HC. In E, the section symbols (§) represent the statistical significance compared to AOAA and the cardinals (#) represent the statistical significance compared to AOAA+PAG. Results are shown as mean ± SD. * $p < 0.05$, ** $p < 0.01$, *** $p < 0.001$ (One-way ANOVA with post hoc Tukey tests).

Regarding OVCAR3 cells, results also supported that hypoxia without cysteine tends to induce H₂S production compared to the other treatments, although some differences were not significant. Without the inhibitors (control), H₂S levels were increased under hypoxia compared to normoxia with cysteine (NC) ($p=0.006$), without differences compared to hypoxia with cysteine (HC). With AOAA alone, hypoxia induced H₂S levels compared to all conditions ($p=0.008$ compared to N, $p=0.002$ compared to NC and $p=0.031$ compared to HC). With PAG alone, hypoxia (H) induced H₂S levels only when compared to normoxia with cysteine (NC) ($p=0.02$) and with both the inhibitors, hypoxia induced H₂S levels compared to both treatments with cysteine ($p=0.000$ compared to NC and $p=0.022$ compared to HC) (figure 5 A-E).

For this cell line, PAG alone was not able to decrease H₂S levels (figure 5 E). However, AOAA in combination with PAG was responsible for decreased H₂S levels in all experimental conditions. Interestingly, while AOAA alone was also able to decrease H₂S levels under normoxia treatments (N and NC), under hypoxia AOAA failed to significantly decrease H₂S levels (figure 5 E).

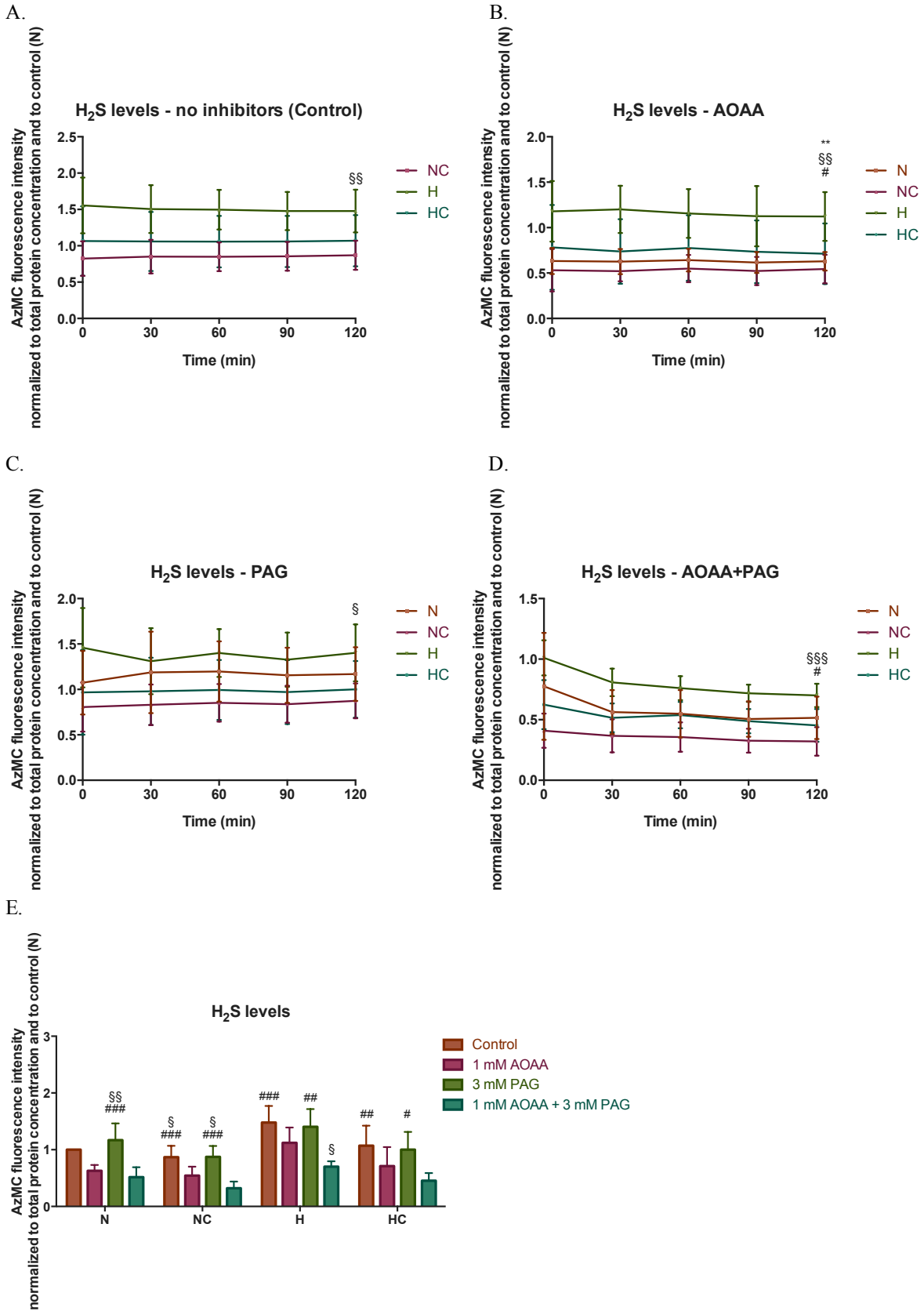


Figure 5. Hypoxia tends to induce H₂S production also in OVCAR3 cells.

H₂S levels in OVCAR3 cells for 48 h of experimental conditions in A. Control (no inhibitors), B. With CBS inhibitor (AOAA), C. with CSE inhibitor (PAG), E. with both the inhibitors (AOAA+PAG) and E.

in all experimental conditions. N – normoxia; NC – normoxia with cysteine, H – hypoxia, HC – hypoxia with cysteine. In A-D the asterisks (*) represent the statistical significance compared to N, the section symbols (§) represents the statistical significance compared to NC and the cardinals (#) represent the statistical significance compared to HC. In E. the section symbols (§) represent the statistical significance compared to AOAA and the cardinals (#) represent the statistical significance compared to AOAA+PAG. Results are shown as mean ± SD. * $p < 0.05$, ** $p < 0.01$, *** $p < 0.001$ (One-way ANOVA with post hoc Tukey tests).

Together, results support an association between H₂S and ATP production under hypoxia, as both were increased in this experimental condition in ovarian cancer cells, especially in ES2 cells.

CBS and CSE inhibition does not impair ATP synthesis but induce cell death in ES2 cells

Since results suggested that cysteine has a role in ATP synthesis mediated by the xCT transporter and that increased ATP levels were concomitant with increased H₂S levels under hypoxia, we next measured ATP levels upon CBS and CSE inhibition.

Results have shown that with 16 h of experimental conditions, no differences were found in ATP levels with or without CSE and CBS inhibitors (PAG and AOAA, respectively) for both ES2 and OVCAR3 cells in any other condition (figure 6 A-D). Moreover, 48 h with the inhibitors resulted in increased ATP levels in all experimental conditions for both ES2 (under N $p = 0.002$, under NC $p = 0.001$, under H $p = 0.004$, under HC $p = 0.001$) and OVCAR3 cells (under N, NC and HC $p < 0.000$ and under H $p = 0.003$) (figure 6 A-D). In what concerns ATP synthesis, interestingly, CBS and CSE inhibitors presented a more pronounced deleterious effect under hypoxia without cysteine (H) and normoxia with cysteine (NC) in ES2 cells and under hypoxia without cysteine (H) in OVCAR3 cells (figure 6 C and D), corroborating the relevance of these enzymes on ATP production under hypoxia.

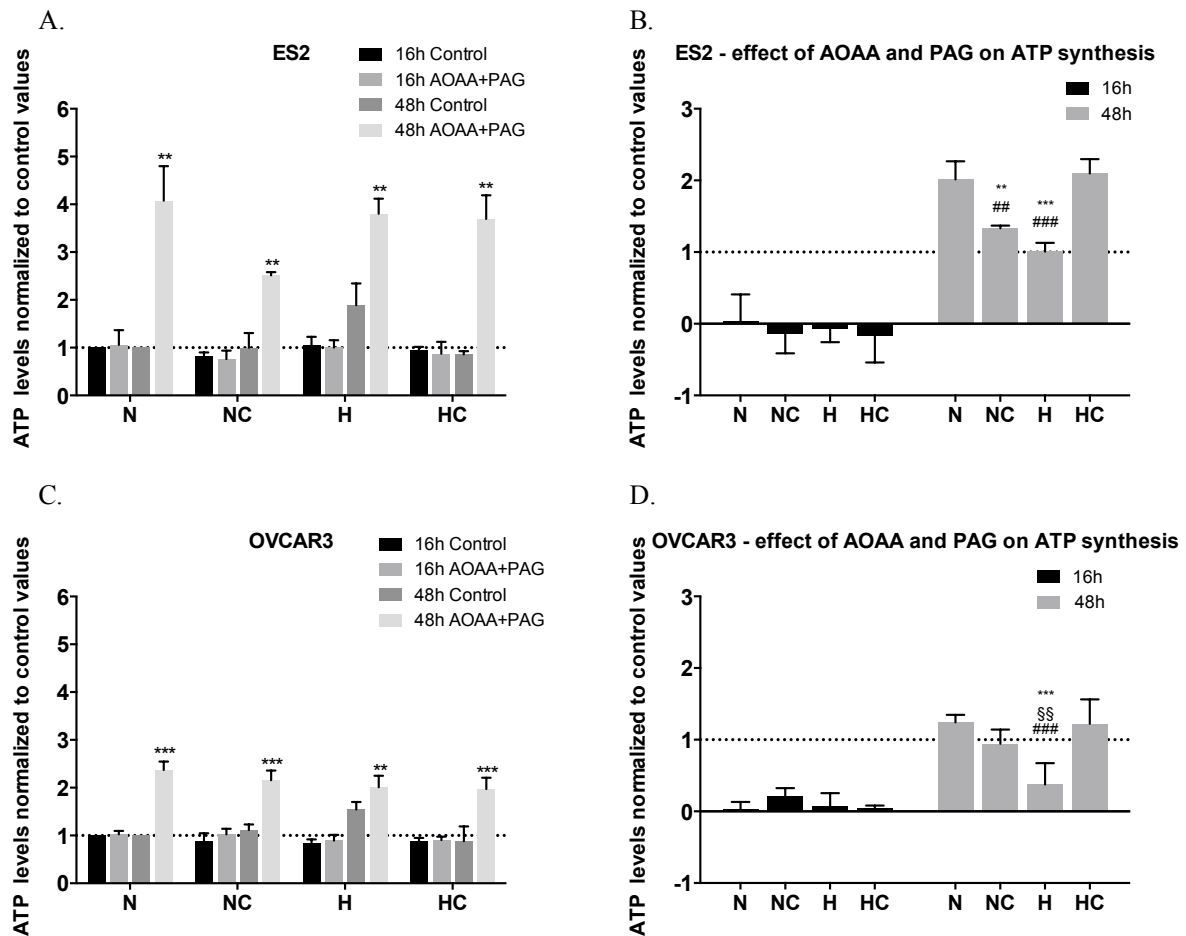


Figure 6. CBS and CSE inhibition does not impair ATP synthesis in ovarian cancer cells.

ATP levels in the presence of 1 mM AOAA and 3 mM PAG for 16 h and 48 h of experimental conditions for A. and B. ES2 cells and C. and D. OVCAR3 cells. In A. and C. the asterisks (*) represent the statistical significance compared to the respective control. Data were normalised to control (normoxia without cysteine and without inhibitors). * $p < 0.05$, ** $p < 0.01$, *** $p < 0.001$ (Independent-samples T test). In B. and D. the asterisks (*) represent the statistical significance compared to N, the section symbols (§) represents the statistical significance compared to NC and the cardinals (#) represent statistical significance compared to HC. Data were normalised to the respective control and Log(2) was calculated. * $p < 0.05$, ** $p < 0.01$, *** $p < 0.001$ (One-way ANOVA with post hoc Tukey tests). N – normoxia; NC – normoxia with cysteine, H – hypoxia, HC – hypoxia with cysteine. Results are shown as mean \pm SD.

Increased ATP levels under stressful conditions were already reported [30]. Thus, we next aimed to explore if increased cell death levels were able to explain the increased ATP levels observed in the presence of AOAA and PAG.

Results have demonstrated that, for ES2 cells, under normoxia both with and without cysteine supplementation (N and NC), PAG alone was more responsible for cell death induction compared to AOAA alone ($p = 0.017$) (figure 7 A and B). Under hypoxia (H), the combination of both inhibitors was more prone to induce cell death compared to the other treatments ($p < 0.001$ compared to all treatments). Interestingly, under hypoxia with cysteine, PAG showed to be disadvantageous also alone ($p = 0.038$ compared to the control) or in

combination with AOAA ($p=0.002$ compared to the control and $p=0.01$ compared to AOAA alone) (figure 7 C and D).

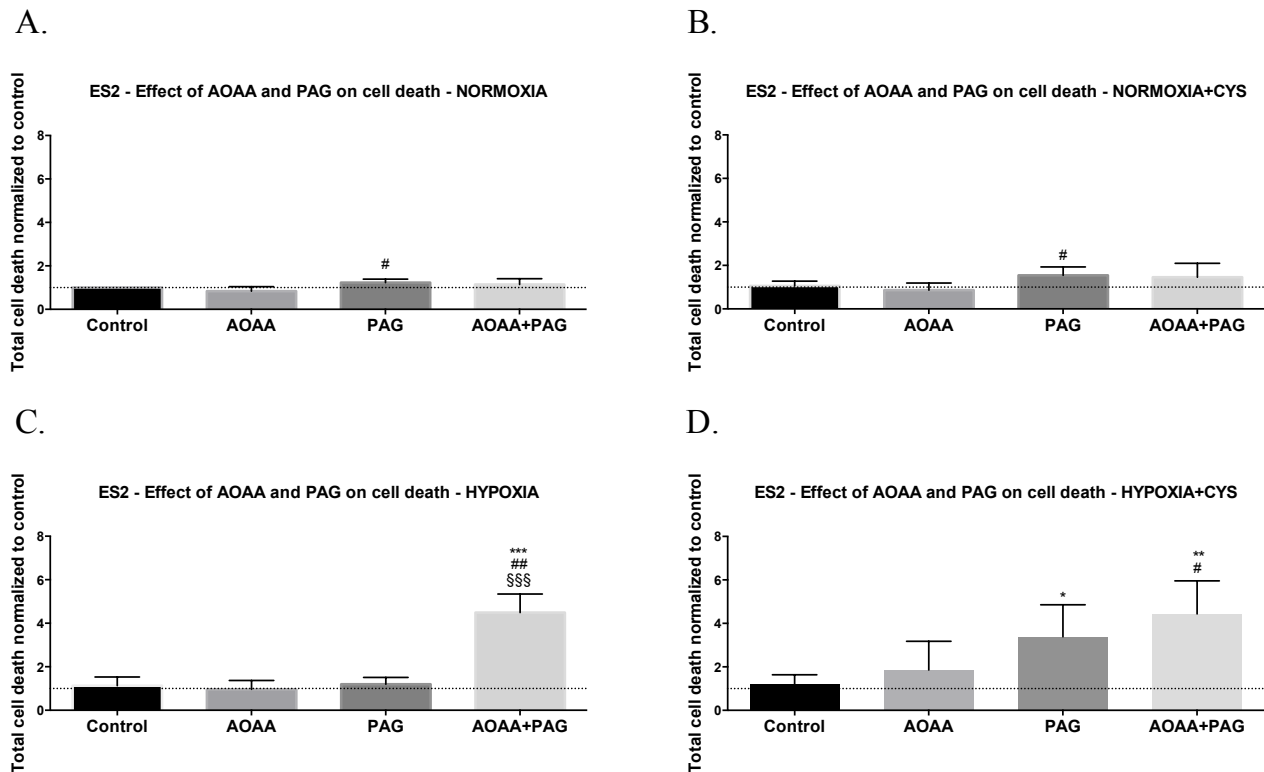


Figure 7. CBS and CSE inhibition affect ES2 cells survival, mainly under hypoxia.

Cell death levels for ES2 cells in the control condition, in the presence of CBS inhibitor (1 mM AOAA), CSE inhibitor (3 mM PAG) or both inhibitors under A. normoxia, B. normoxia with cysteine, C. hypoxia and D. hypoxia with cysteine. Data were normalised to control (normoxia without cysteine and without inhibitors). In A. and B. the cardinals (#) represent statistical significance between AOAA and PAG alone. In C. the asterisks (*) represent statistical significance between AOAA+PAG and its control, the cardinals (#) represent statistical significance between AOAA+PAG and AOAA alone and the section symbols (§) represent statistical significance between AOAA+PAG and PAG alone. In D. the asterisks (*) represent statistical significance between PAG alone/AOAA+PAG and its control and the cardinals (#) represent statistical significance between AOAA+PAG and AOAA alone. Results are shown as mean \pm SD. * $p<0.05$, ** $p<0.01$, *** $p<0.001$ (One-way ANOVA with post hoc Tukey tests).

Regarding OVCAR3 cells, no differences were observed among treatments, with or without the inhibitors (figure 8 A-D).

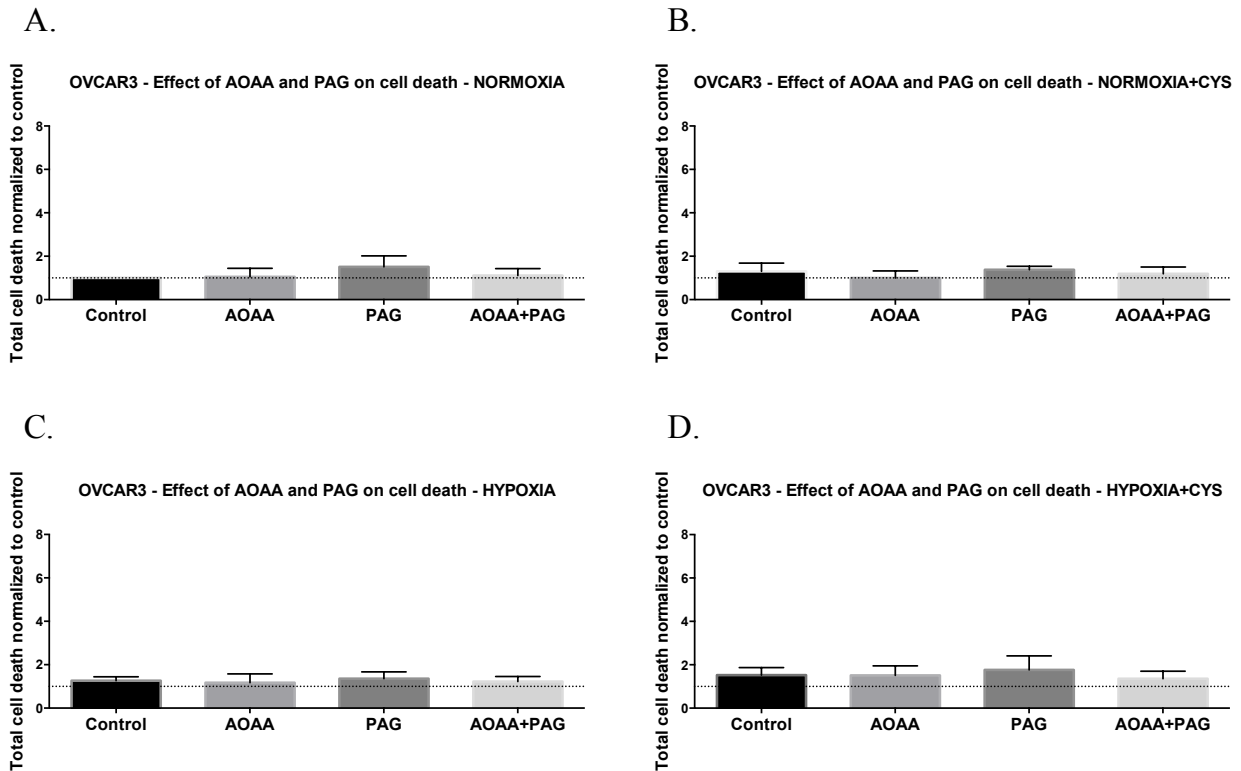


Figure 8. CBS and CSE inhibition does not affect OVCAR3 cells survival.

Cell death levels for OVCAR3 cells in the control condition, in the presence of CBS inhibitor (1 mM AOAA), CSE inhibitor (3 mM PAG) or both inhibitors under A. normoxia, B. normoxia with cysteine, C. hypoxia and D. hypoxia with cysteine. Data were normalised to control (normoxia without cysteine and without inhibitors). Results are shown as mean \pm SD. * p <0.05, ** p <0.01, *** p <0.001 (One-way ANOVA with post hoc Tukey tests).

Together, results indicate that CBS and CSE inhibition is not sufficient to impair ATP production but the inhibition of both enzymes affected ATP synthesis mainly under hypoxia for both cell lines.

Moreover, since ES2 cells viability was reduced upon both CBS and CSE inhibition under hypoxia, this shows that ES2 cells are especially sensitive to the inhibition of these enzymes under hypoxia, hence indicating their role in hypoxia adaptation.

Cysteine degradation is necessary to rescue the impaired ATP production triggered by xCT inhibition

Since results have suggested that cysteine has a role in ATP production under hypoxia that can be in part related to H₂S synthesis, we next aimed to explore if cysteine metabolism

was necessary or if H₂S *per se*, was sufficient to counteract the ATP impairment triggered by xCT inhibition.

Results have shown once again that cysteine was able to revert this ATP impairment upon xCT inhibition in both ES2 and OVCAR3 cells ($p < 0.001$ for both cell lines), however, NaHS alone, an H₂S donor, was not able to counteract this effect, as no differences were found among treatments with NaHS combined with sulphasalazine and sulphasalazine alone ($p > 0.05$ for both cell lines), indicating that H₂S alone might not be able to rescue ATP production and that cysteine degradation is required for both cell lines (figure 9 A and B).

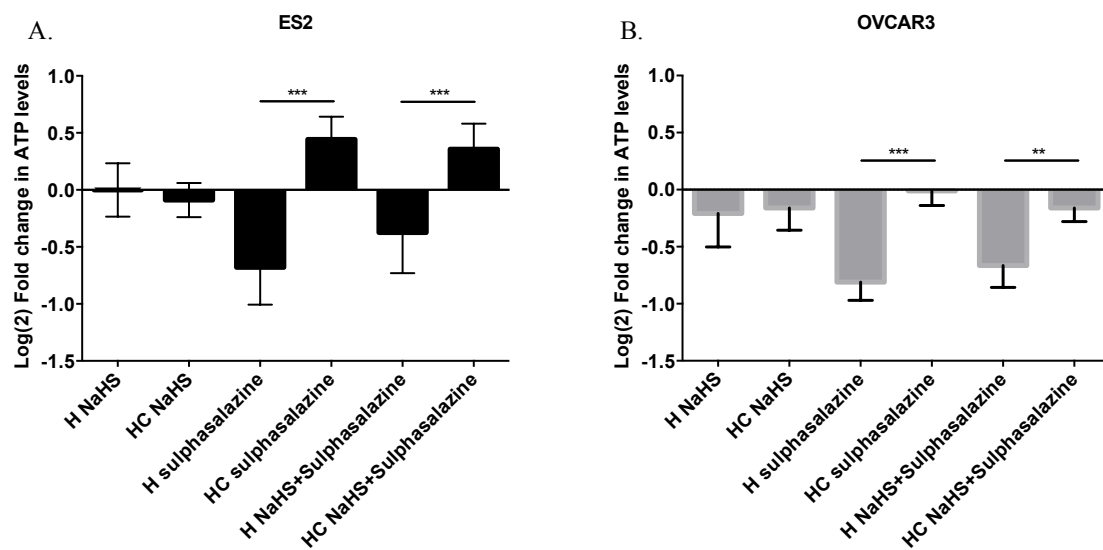


Figure 9. Cysteine, but not NaHS, is able to rescue ATP synthesis under hypoxia triggered by xCT inhibition.

ATP levels for 48 h of experimental conditions for A. ES2 and B. OVCAR3 cells under hypoxia with and without cysteine and in the presence of the xCT inhibitor, sulphasalazine and the H₂S donor, NaHS. Data were normalised to the respective control condition (the same environmental condition H/HC without NaHS or Sulphasalazine). H – hypoxia, HC – hypoxia with cysteine. Results are shown as mean \pm SD. * $p < 0.05$, ** $p < 0.01$, *** $p < 0.001$ (One-way ANOVA with post hoc Tukey tests).

Due to the unstable nature of NaHS that was reported to lead to an instant release of H₂S in culture medium [31] that decays rapidly [32], and because Fu and colleagues have reported that in vascular smooth-muscle cells, 1 h of NaHS exposition was sufficient to increase mitochondrial ATP production under hypoxia [33], we quantified ATP levels upon NaHS exposure for 1 h of the experimental conditions tested before.

Results have shown that, even with 1 h of experimental conditions, H₂S alone was not sufficient to rescue ATP levels under hypoxia upon xCT inhibition. In fact, for ES2 cells under hypoxia without cysteine, NaHS led to decreased ATP levels ($p = 0.047$). However, under hypoxia with cysteine supplementation, NaHS did not affect ATP production. For

OVCAR3 cells, NaHS led to decreased ATP levels both under hypoxia with ($p=0.002$) and without cysteine supplementation ($p=0.003$) (figure 10 A). Moreover, for ES2 cells, both NaHS alone or combined with sulphasalazine lead to decreased ATP levels under hypoxia with and without cysteine supplementation compared to sulphasalazine alone (H NaHS vs H sulphasalazine $p<0.001$; H NaHS+sulphasalazine vs H sulphasalazine $p<0.001$; HC NaHS vs HC sulphasalazine $p=0.002$; HC NaHS+sulphasalazine vs HC sulphasalazine $p<0.001$) (figure 10 B). For OVCAR3, no differences were observed among treatments (figure 10 C).

Finally, while 1 h of sulphasalazine was not sufficient to inhibit ATP levels in ES2 cells, it was in OVCAR3 cells (figure 10 B and C), suggesting that the former could present higher basal levels of the xCT transporter or that these cells activate xCT transcription in a more efficient way compared to OVCAR3 cells. In fact, in basal conditions, ES2 cells express higher xCT levels compared to OVCAR3 cells (Suppl. figure 1), hence supporting that a more prolonged exposure to sulphasalazine is necessary for the effective blocking of xCT in ES2 cells.

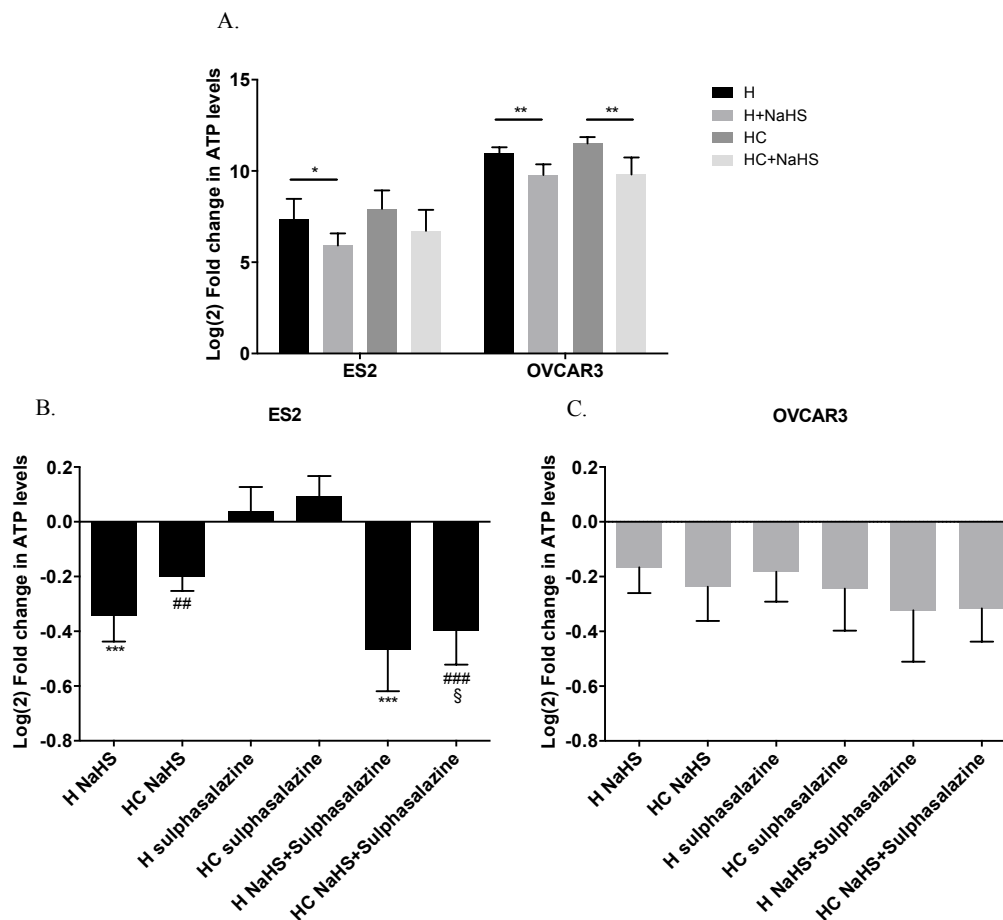


Figure 10. NaHS impairs ATP synthesis under hypoxia in ovarian cancer cells.

ATP levels for 1 h of experimental conditions for A. ES2 and OVCAR3 cells under hypoxia with and without cysteine and in the presence of the H₂S donor, NaHS (un-normalised data), and B ES2 and C.

OVCAR3 cells under hypoxia with and without cysteine supplementation and in the presence of the xCT inhibitor, sulphasalazine and NaHS. In B. and C. data were normalised to the respective control condition (the same environmental condition H/HC without NaHS or Sulphasalazine). H – hypoxia, HC – hypoxia with cysteine. Results are shown as mean \pm SD. In A. the asterisks (*) represent the statistical significance among the indicated conditions. In B, the asterisks (*) represent the statistical significance compared to H+sulphasalazine, the cardinals (#) represent the statistical significance compared to HC+sulphasalazine and the section symbols (§) represent the statistical significance compared to HC+NaHS. * p <0.05, ** p <0.01, *** p <0.001 (Independent-samples T test for A. and One-way ANOVA with post hoc Tukey tests for B. and C.).

Cysteine is not able to rescue ATP production upon β -oxidation and glycolysis inhibition

Since β -oxidation and glycolysis are other important sources of ATP synthesis, we ended by investigating if cysteine was able to rescue ATP production upon the blockage of these pathways under hypoxia.

For ES2 cells, cysteine was not able to rescue ATP synthesis and even presented a negative effect upon β -oxidation inhibition with etomoxir ($p=0.019$).

With bromopyruvic acid, an inhibitor of glycolysis, cysteine also presented a trend to reduce ATP levels, although there was no statistical significance ($p=0.054$) (figure 11 A).

Regarding OVCAR3 cells, cysteine did not affect ATP synthesis neither upon the β -oxidation nor the glycolysis inhibition (figure 11 B).

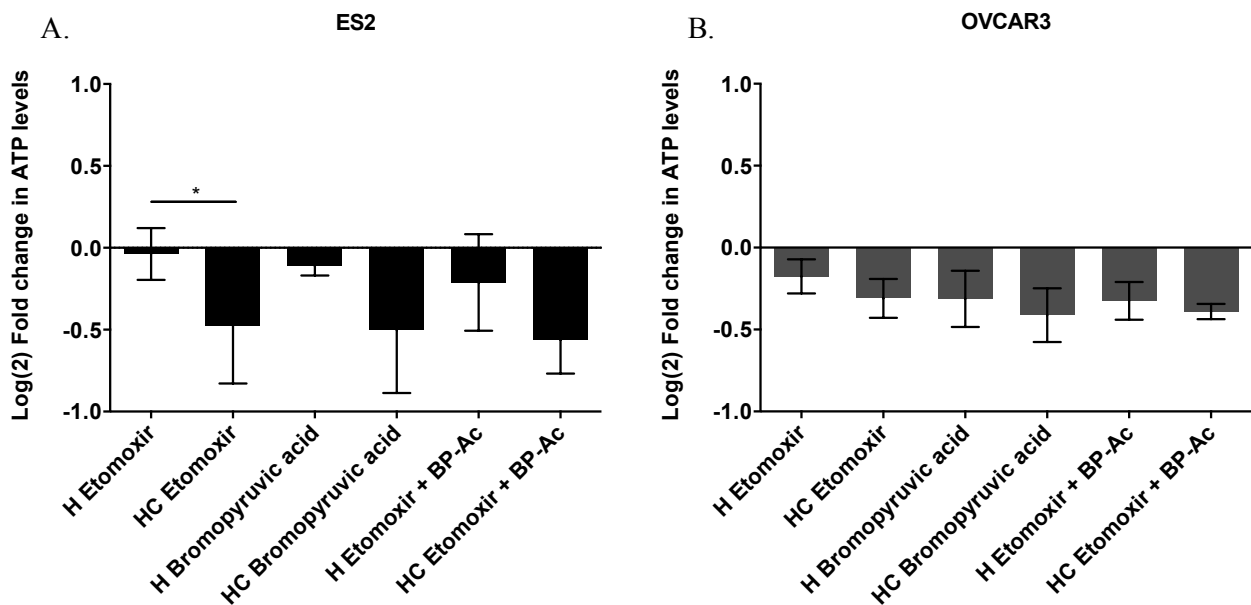


Figure 11. Cysteine is not able to rescue ATP production upon β -oxidation and glycolysis inhibition.

ATP levels for 48 h of experimental conditions for A. ES2 and B. OVCAR3 cells under hypoxia with and without cysteine and in the presence of the β -oxidation inhibitor etomoxir and glycolysis inhibitor,

bromopyruvic acid. Data were normalised to the respective control condition (the same environmental condition H/HC without etomoxir or bromopyruvic acid). H – hypoxia, HC – hypoxia with cysteine. Results are shown as mean \pm SD. * $p < 0.05$, ** $p < 0.01$, *** $p < 0.001$ (Independent-samples T test).

Together, results support a role of cysteine metabolism in ATP synthesis under hypoxia mediated, dependent on xCT transporter for cysteine uptake. However, cysteine was not able to rescue ATP synthesis upon both β -oxidation and glycolysis inhibition, indicating that these metabolic pathways are also sources of ATP production. Furthermore, cysteine can also be canalised to other metabolic pathways that do not contribute directly for ATP production. Nevertheless, these inhibitors can also have off-target effects, affecting other metabolic pathways.

Cysteine rescues cellular metabolism of hypoxic ES2 cells

In order to address the metabolic effects of cysteine under normoxia and hypoxia in ES2 and OVCAR3 cells, we also measured the levels of several metabolites by $^1\text{H-NMR}$ (figures 12 and 13).

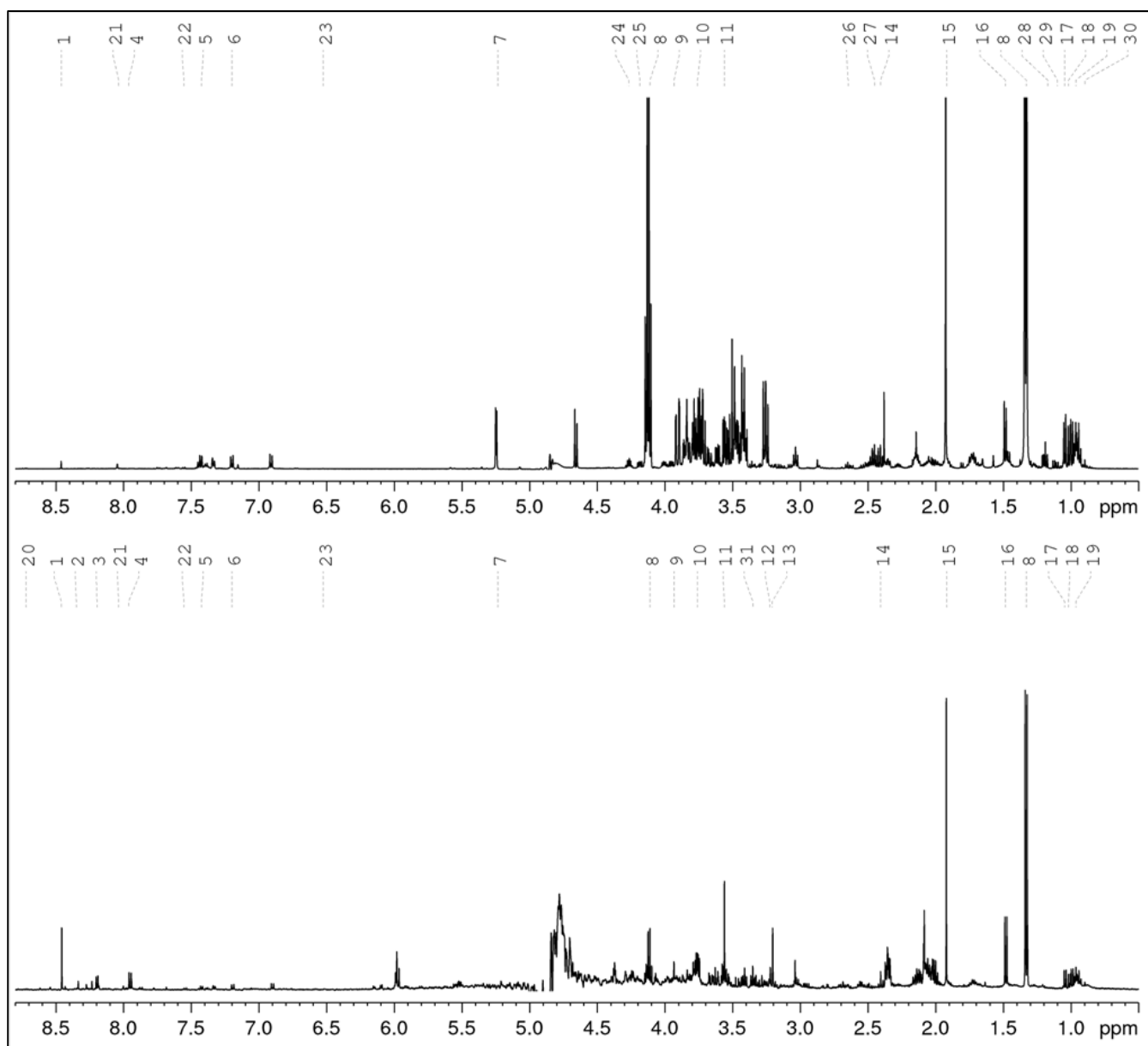


Figure 12. ^1H -NMR spectra of ES2 cells.

Typical ^1H -NMR spectra of the growth media (upper panel) and aqueous phase (bellow panel) of ES2 cells under hypoxia with cysteine.

Metabolites: 1- formate, 2- inosine, 3- hypoxanthine, 4- UDP-N-acetylglucosamine, 5- phenyalanine, 6- tyrosine, 7- glucose, 8- lactate, 9- creatine, 10- glutamate, 11- glycine, 12- O-phosphocholine, 13- choline, 14- succinate, 15- acetate, 16- alanine, 17- valine, 18- isoleucine, 19- leucine, 20- nicotinurate, 21- histidine, 22- tryptophan, 23- fumarate, 24- threonine, 25- pyroglutamate, 26- methionine, 27- glutamine, 28- isopropanol, 29- isobutyrate, 30- 2-hydroxybutyrate, 31- methanol.

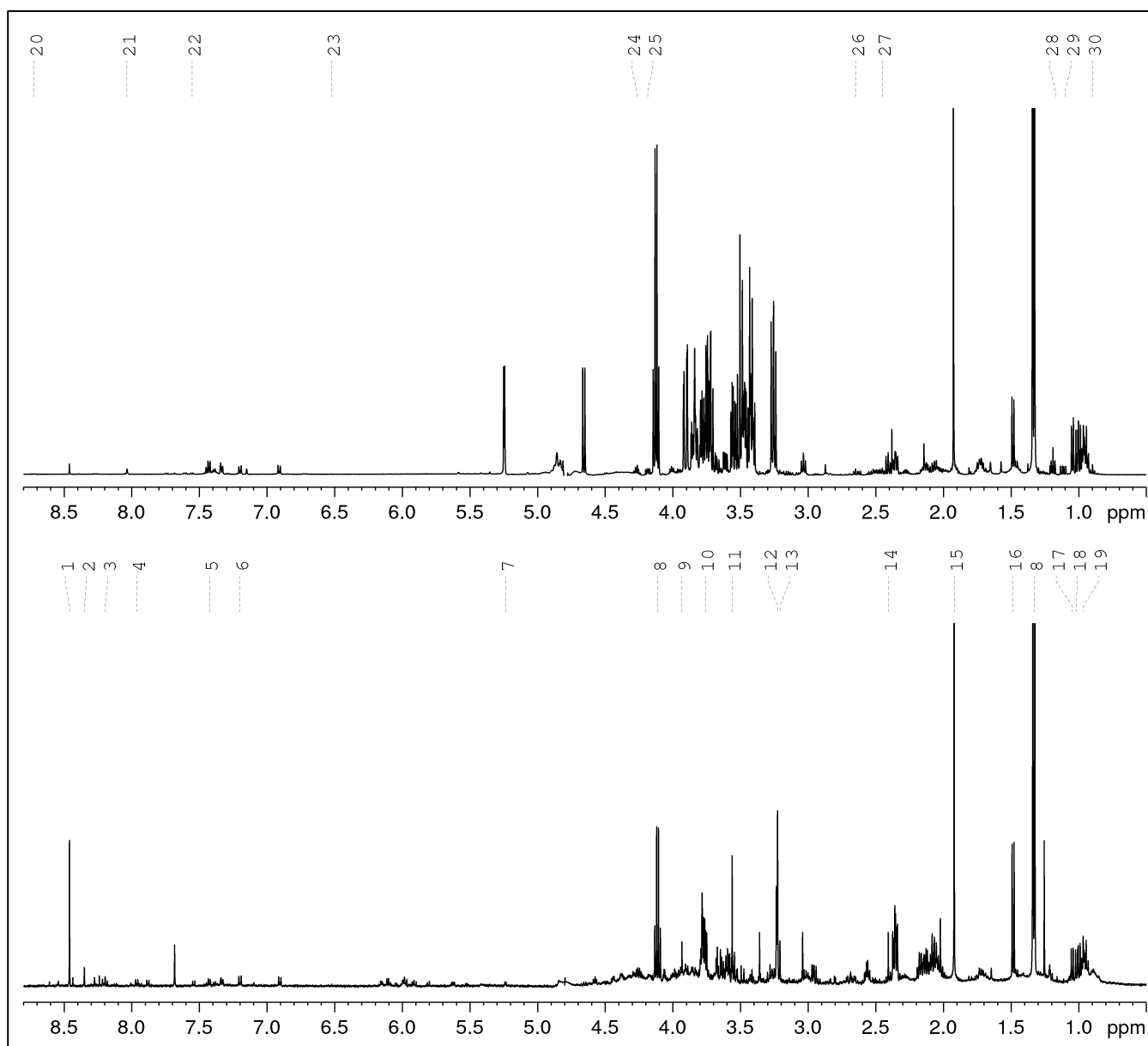


Figure 13. ¹H-NMR spectra of OVCAR3 cells.

Typical ¹H-NMR spectra of the growth media (upper panel) and aqueous phase (bellow panel) of OVCAR3 cells under normoxia with cysteine supplementation.

Metabolites: 1- formate, 2- inosine, 3- hypoxanthine, 4- UDP-N-acetylglucosamine, 5- phenyalanine, 6- tyrosine, 7- glucose, 8- lactate, 9- creatine, 10- glutamate, 11-glycine, 12- O-phosphocholine, 13- choline, 14- succinate, 15- acetate, 16- alanine, 17- valine, 18- isoleucine, 19- leucine, 20- nicotinurate, 21- histidine, 22- tryptophan, 23- fumarate, 24- threonine, 25- pyroglutamate, 26- methionine, 27- glutamine, 28- isopropanol, 29- isobutyrate, 30- 2-hydroxybutyrate, 31- methanol.

The intracellular metabolites were analysed comparing the effect of cysteine in the metabolic profile of cells cultured in hypoxia with cells cultured in normoxia, in order to determine the decrease and increase of organic compounds driven by the presence of cysteine in both environments.

Regarding ES2 intracellular metabolites, cysteine increased the intracellular levels of the amino acids alanine ($p=0.009$), glutamate ($p=0.012$), glycine ($p=0.008$) and threonine ($p=0.016$) under hypoxia (figure 14 A). Cysteine also led to increased intracellular levels of lactate ($p=0.021$) (figure 14 B), choline ($p=0.005$) and creatine ($p=0.005$) (figure 14 C) under hypoxia. In the extracellular media (supernatants), the only significant difference found was in fumarate levels ($p=0.046$), where cysteine under hypoxia decreased the release of this amino acid (figure 14 E). Regarding histidine, when comparing the levels of this amino acid in the control media (without cells) we observed that CoCl_2 reacted with histidine, as seen by its decreased concentrations under hypoxia, especially without cysteine supplementation (figure 15). Therefore, we cannot state that cysteine decreased the uptake of histidine under hypoxia. Instead, results suggest that cysteine increases the release of this amino acid, especially under normoxia ($p<0.001$).

Through metabolic pathway analysis, results predicted that 9 metabolic pathways are significantly and differently altered in ES2 cells by cysteine under hypoxia compared to normoxia. The analysis showed alteration in the pathways of biosynthesis of: 1) glycine, serine and/ threonine; 2) alanine, aspartate and glutamate; 3) glutamine and glutamate; 4) arginine and proline; 5) GSH; 6) primary bile acid; 7) glycerophospholipid; 8) aminoacyl-tRNA; and 9) purine nitrogen bases (figure 16).

Regarding OVCAR3 cells, the only significant difference found on the effect of cysteine under hypoxia and normoxia on intracellular metabolites concentration was on glucose levels, where cysteine decreased the intracellular levels of glucose under hypoxia compared to normoxia ($p=0.021$) (figure 17 B). However, cysteine in hypoxia also provided a general tendency for increased intracellular amino acids such as alanine, glutamate, tyrosine and valine (figure 17 A).

When analysing the amino acids levels present in the cell media, results have shown that cysteine under hypoxia led to a decreased uptake of alanine ($p=0.023$) and proline ($p=0.008$) and to an increased uptake of glycine ($p=0.013$) and phenylalanine ($p=0.049$) (figure 17 D). Cysteine also decreased the release of 2-hydroxybutyrate ($p<0.001$), formate ($p=0.002$) and isobutyrate ($p<0.001$) under hypoxia compared to normoxia in OVCAR3 cells (figures 17 E). Regarding histidine levels, similar to ES2 cells, cysteine seemed to induce a release of this amino acid, especially under normoxia ($p<0.001$) (figure 18).

The metabolite pathway analysis was not performed for OVCAR3 cells because cysteine only altered significantly one metabolite (glucose) under hypoxia, thus making this analysis inaccurate.

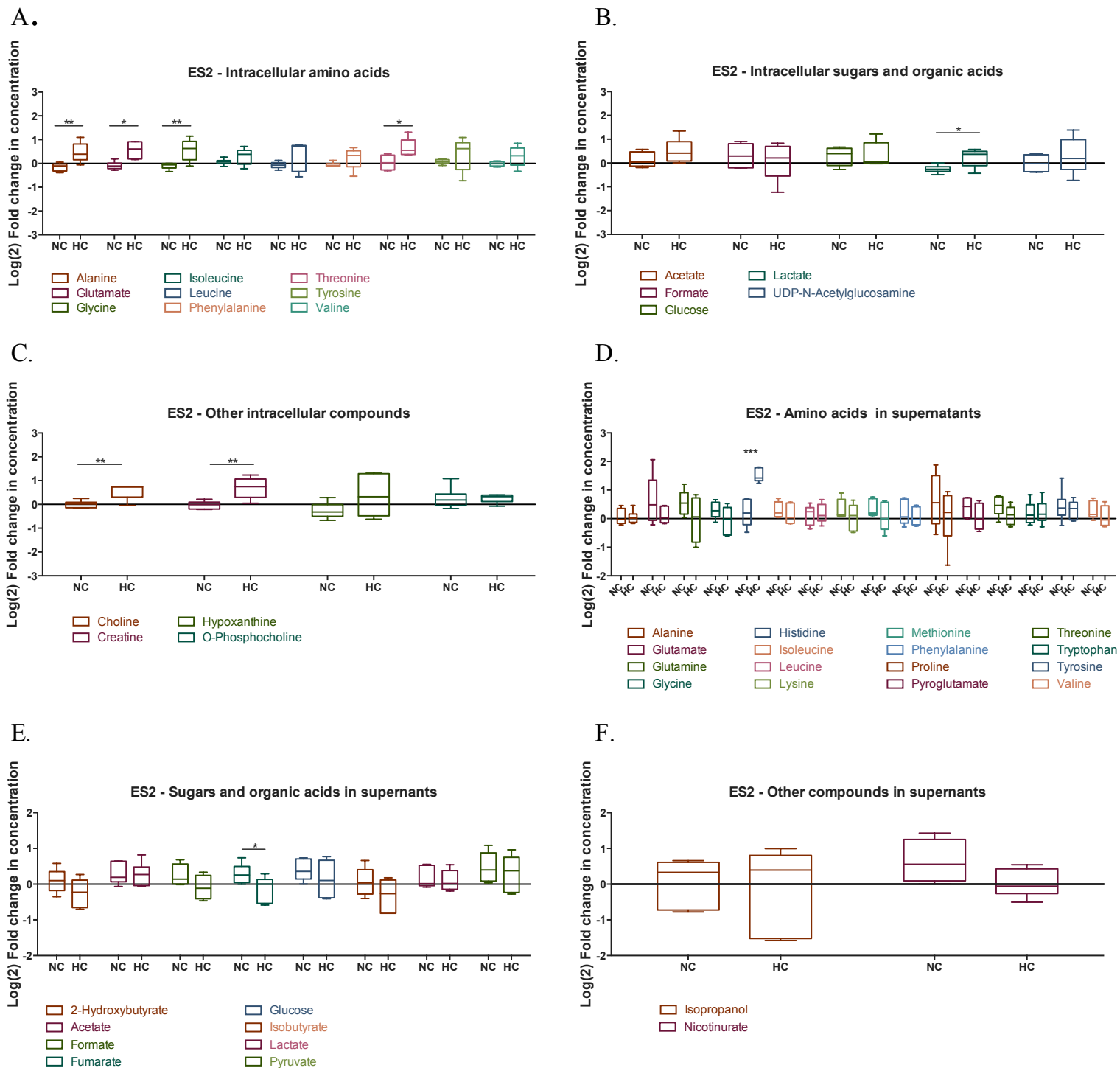


Figure 14. Cysteine rescues ES2 cellular metabolism under hypoxia.

Metabolites levels for 48 h of experimental conditions for ES2 cells A. intracellular amino acids, B. intracellular sugars and organic acids, C. other intracellular compounds, D. amino acids in supernatants, B. sugars and organic acids in supernatants, C. other compounds in supernatants. Data were normalised to the respective control condition (the same environmental condition NC/N and HC/H). NC – Normoxia with cysteine and HC – hypoxia with cysteine. Results are shown as median with 25th to 75th percentiles. * $p < 0.05$, ** $p < 0.01$, *** $p < 0.001$ (Independent-samples T test).

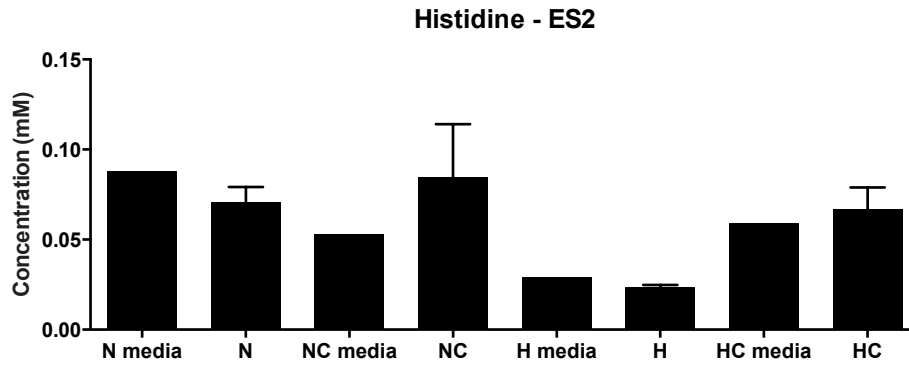


Figure 15. Cobalt chloride (CoCl₂) affects histidine levels.

Histidine levels in control media (without cells) and after 48 h of experimental conditions for ES2 cells. N – Normoxia; NC – Normoxia with cysteine; H – hypoxia and HC – hypoxia with cysteine. Results are shown as mean ± SD.

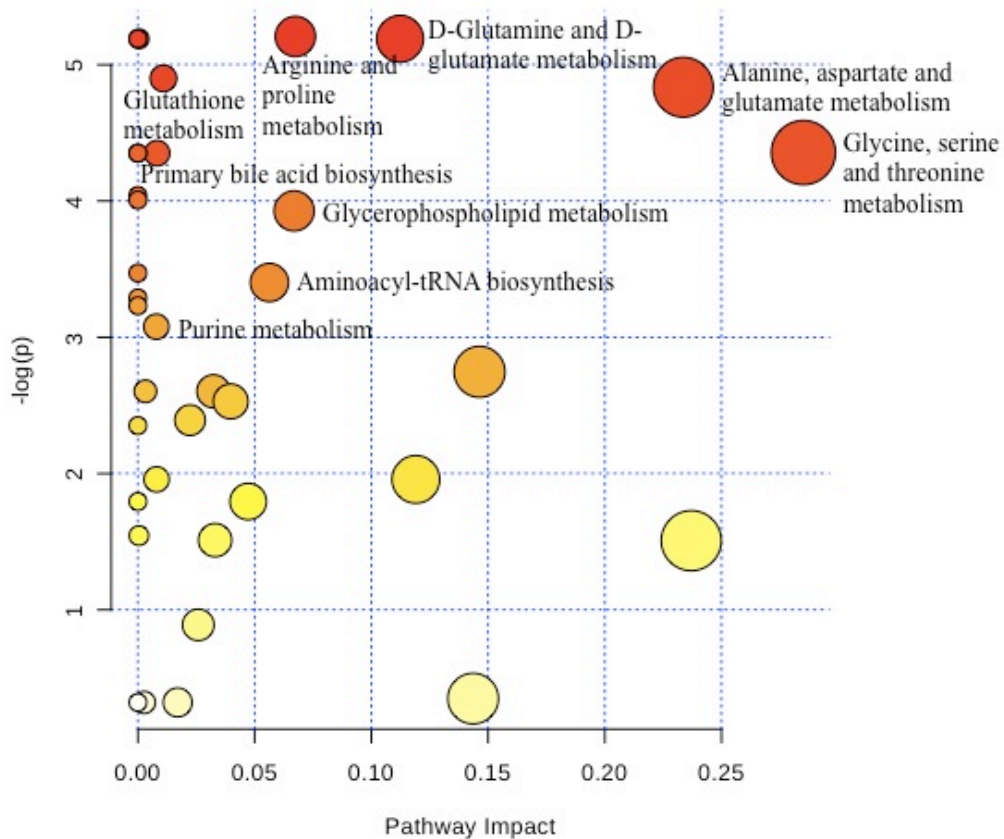


Figure 16. Under hypoxia, cysteine impacts several metabolic pathways in ES2 cells.

Metabolic pathway analysis for the effect of cysteine under normoxia and hypoxia in intracellular ES2 metabolites. All the matched pathways are displayed as circles. The colour and size of each circle are based on *p*-value and pathway impact value, respectively. The most impacted pathways having statistical significance (*p*<0.05) are indicated.

Source: <https://www.metaboanalyst.ca/MetaboAnalyst/faces/home.xhtml>.

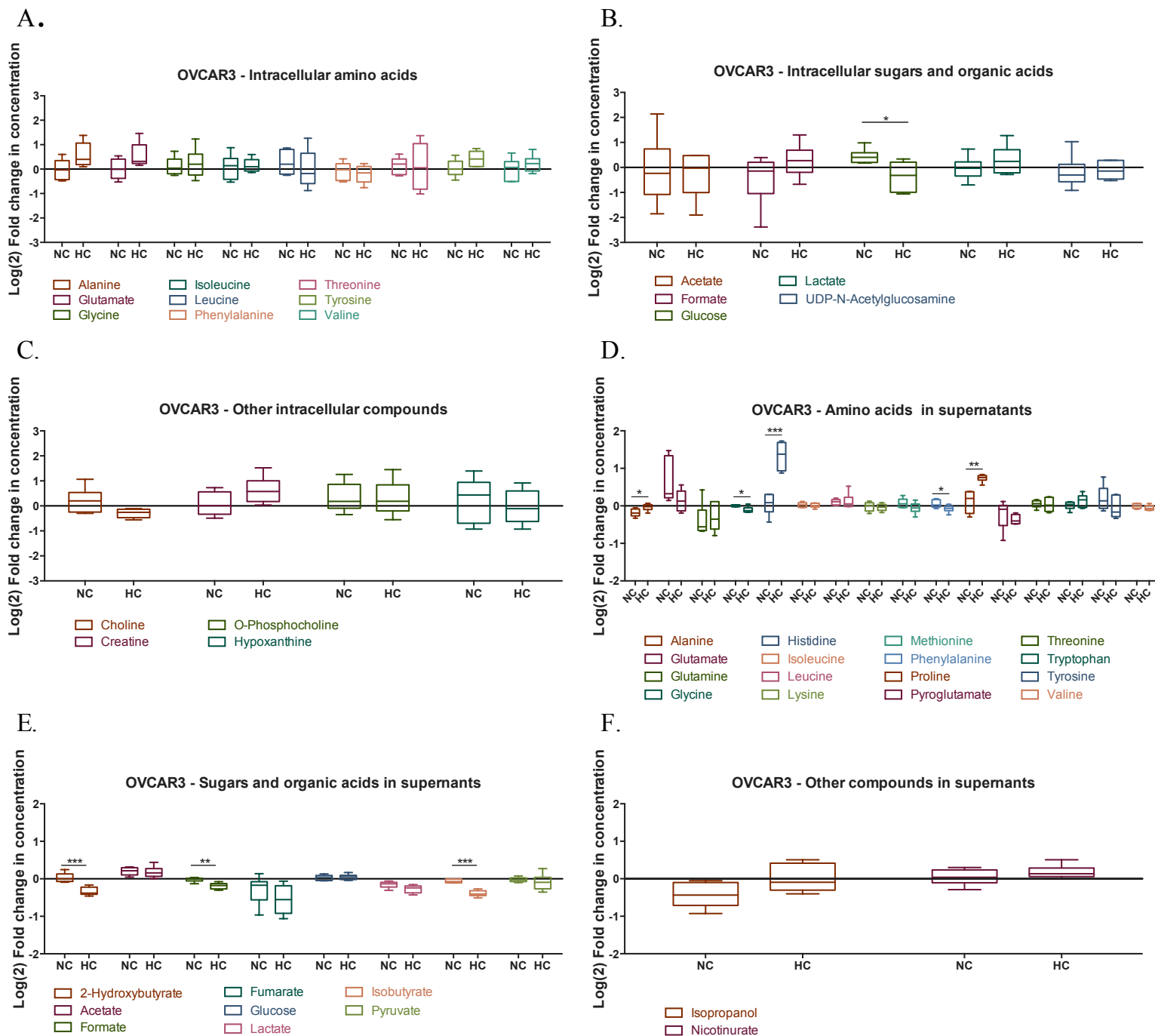


Figure 17. Effect of cysteine in OVCAR3 metabolites under normoxia and hypoxia.

Metabolites levels for 48 h of experimental conditions for OVCAR3 cells A. intracellular amino acids, B. intracellular sugars and organic acids, C. other intracellular compounds, D. amino acids in supernatants, B. sugars and organic acids in supernatants, C. other compounds in supernatants. Data were normalised to the respective control condition (the same environmental condition NC/N and HC/H). NC – Normoxia with cysteine and HC – hypoxia with cysteine. Results are shown as median with 25th to 75th percentiles. * $p < 0.05$, ** $p < 0.01$, *** $p < 0.001$ (Independent-samples T test).

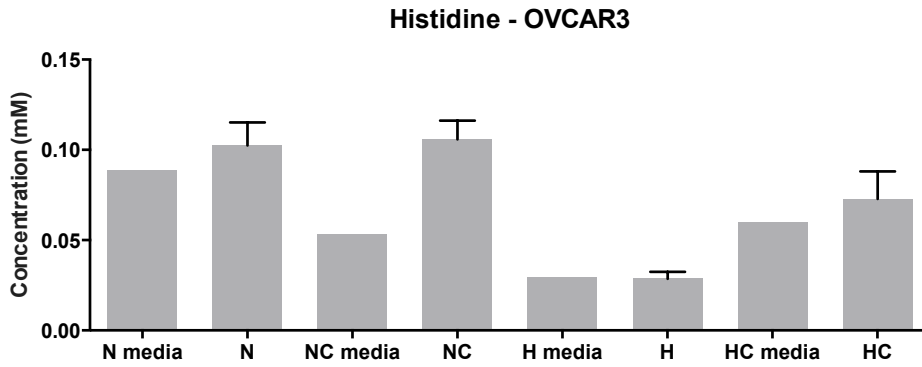


Figure 18. Cobalt chloride (CoCl₂) affects histidine levels.

Histidine levels in control media (without cells) and after 48 h of experimental conditions for OVCAR3 cells. N – Normoxia; NC – Normoxia with cysteine; H – hypoxia and HC – hypoxia with cysteine. Results are shown as mean ± SD.

Importantly, hypoxia did not alter the intracellular and extracellular levels of glucose and lactate in both cell lines. Interestingly, hypoxia led to a decreased uptake of glutamine ($p=0.032$) and to an increased release of fumarate ($p=0.041$) in OVCAR3 cells (figure 19 A and B).

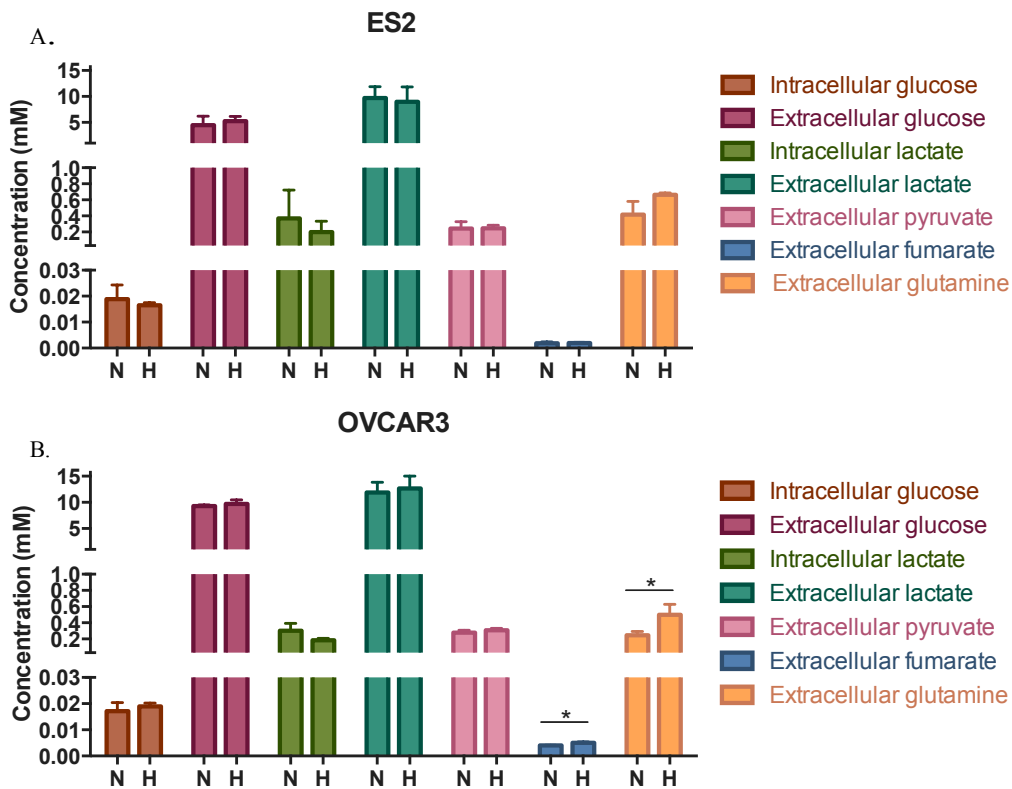


Figure 19. Effect of hypoxia in glucose, lactate, pyruvate, fumarate and glutamine levels in ovarian cancer cells.

Metabolites levels for 48 h of experimental conditions for A. ES2 and B. OVCAR3 cells. N – Normoxia and H – hypoxia. Results are shown as mean ± SD. * $p<0.05$, ** $p<0.01$, *** $p<0.001$ (Independent-samples T test).

Taken together, results suggest that under hypoxia, cysteine allows to increase the rate of some metabolic pathways in ES2 cells, as increased intracellular levels of several amino acids and other compounds were observed. Regarding OVCAR3 cells, results support that cysteine impacts differently the cellular needs of amino acids under normoxia and hypoxia, as cysteine increased the uptake of glycine and phenylalanine under hypoxia, whereas under normoxia, cysteine increased the uptake of alanine and proline. Moreover, under hypoxia, cysteine impacted in a more pronounced way ES2 cells metabolism compared to OVCAR3 cells, as seen by the higher number of metabolic pathways that were significantly altered under hypoxia compared to normoxia in ES2 cells.

DISCUSSION

As a solid tumour grows, cancer cells are exposed to regions of hypoxia, known to be a stimulus for tumour progression and resistance to therapy [11,12]. Recently, we have proposed that cysteine allows adaptation to hypoxic environments and also contribute to escape from carboplatin-induced death in ovarian cancer cells [14,15]. In here, we aimed to explore the mechanisms by which cysteine protects ovarian cancer cells from hypoxia-induced death, by addressing its role in cellular metabolism, namely through energy production.

Cystine uptake, the oxidized form of cysteine, is mediated by xCT (solute carrier family 7 member 11 - SLC7A11), a member of the cystine-glutamate transporter xc^- system [29]. Intracellularly, cystine is reduced to cysteine, which is the rate-limiting substrate for glutathione (GSH) synthesis, making xCT pivotal in the cellular redox balance maintenance (reviewed in [34]). In here, we have shown a mitochondrial localization of the xCT transporter concomitant with an impaired ATP production triggered by its inhibition under hypoxia, thus indicating a role of the xc^- system via cystine uptake also in energy production. These data are in accordance with recent findings supporting a role of Nrf2 in the regulation of mitochondrial ATP synthesis (reviewed in [35]), as Nrf2 was already reported to regulate the expression of xCT and the activity of the xc^- system in response to oxidative stress in human breast cancer cells [36]. Therefore, Nrf2 role in ATP synthesis can be mediated by cysteine via xCT transporter. We have to highlight that albeit sulphasalazine has been reported as a potent inhibitor of xCT function [37–39], it was also reported to inhibit the cystine transporter solute carrier family 3, member 1 (SLC3A1) in breast cancer cells, where increased expression of this transporter was found to enhance cysteine uptake and GSH

accumulation, decreasing ROS levels [40]. It is important to emphasise that SLC7A11 is generally assumed to function at the plasma membrane [41–43], but, in here, a mitochondrial localization was also found in ES2 and OVCAR3 cells. Other cysteine transporter, SLC3A1, was reported to localise on the plasma membrane of breast cancer cells as well [40], however, its localisation in ovarian cancer cells should be investigated in order to exploit its possible role in mitochondrial ATP synthesis. Interestingly, it was reported an up-regulation of SLC3A1 in samples from ovarian clear cell carcinomas compared to non-clear cell samples of epithelial ovarian cancer patients [44], hence suggesting the possible role of cysteine uptake via this transporter especially in ES2 cells.

Cysteine role in mitochondrial ATP synthesis can be due to its degradation into H₂S. H₂S is the only inorganic compound presenting a bioenergetic role in mammalian cells' mitochondria [45], that was already reported to contribute to mitochondrial ATP production through the activity of the enzymes involved in cysteine metabolism: MpST in conjunction with CAT [46,47], CSE [33] and CBS [19,20]. At low concentrations (nM), H₂S is known to stimulate mitochondrial bioenergetics by way of different mechanisms: through donation of electron equivalents to the quinol pool via sulfide:quinone oxidoreductase; by the glycolytic enzyme glyceraldehyde 3-phosphate dehydrogenase activation, and by persulfidation of ATP synthase (reviewed in [28]). In addition, Li and Yang reported a role of CSE/H₂S system in enhancing mtDNA replication and cellular bioenergetics both in smooth muscle cells and mouse aorta tissues [48]. More recently, Chakraborty and colleagues reported a new role of CBS in the regulation of mitochondria morphogenesis, promoting tumour progression in ovarian cancer [49]. Our results pointed to higher ATP levels concomitant with higher H₂S levels, supporting that H₂S can be an important source of mitochondrial ATP under hypoxia. Specifically under hypoxia conditions, H₂S was reported to decrease reactive oxygen species (ROS), mediated by CBS mitochondrial accumulation [50] and induce ATP synthesis, mediated by CSE translocation to the mitochondria [33].

Interestingly, our data have shown that the inhibition of CSE alone was not sufficient to decrease H₂S levels. Miyamoto *et al.*, using peripheral neurons, reported that H₂S synthesis was inhibited by AOAA but not by PAG [51]. Hellmich and colleagues have reported similar results using colon cancer cell lines [52]. These results could explain the high levels of H₂S observed in the presence of PAG in both ES2 and OVCAR3 cells, which, in turn, can be explained by both CBS and MpST activities since they were not inhibited. In the presence of both CBS and CSE inhibitors, the H₂S levels are due to MpST activity in conjunction with CAT. The decreased H₂S levels compared to the control can be related to CAT inhibition,

since AOAA was reported to inhibit also this enzyme in peripheral neurons [51]. We have to highlight that, whereas PAG is a selective CSE inhibitor, AOAA selectivity for CBS activity over CSE or other PLP dependent enzymes is limited, since it leads to an irreversible binding to the prosthetic group PLP [52]. Unfortunately, there are no commercial selective MpST inhibitors available. Just recently, Hanaoka *et al.* reported the discovery of selective MpST inhibitors with promising applications for *in vitro* and *in vivo* studies [53]. Therefore, more selective CBS inhibitors together with MpST inhibitors would allow shedding light on their role in H₂S generation and ATP synthesis. But the simultaneous inhibition of CBS and CSE should undoubtedly show that MpST plays a relevant role in ATP production driven by cysteine degradation.

Since we observed that the inhibition of both CBS and CSE enzymes was sufficient to decrease H₂S levels, an impaired ATP synthesis upon their inhibition was expected. Bhattacharyya *et al.* reported that CBS inhibition with both AOAA and CBS siRNA, led to decreased ATP synthesis in ovarian cancer cells [19]. Strikingly, Chakraborty and colleagues not only reported a role of CBS in the regulation of mitochondria morphogenesis [49] but also in lipid uptake in ovarian cancer cells [54], suggesting a role of CBS in ATP synthesis favouring β -oxidation, which is also a mitochondrial pathway. In our study, we measured ATP levels with both CBS and CSE inhibitors and we did not observe decreased ATP levels, thus indicating that the inhibition of both enzymes leads to compensatory or alternative mechanisms of energy production, namely through MpST activity. We have to highlight that H₂S levels were determined in cellular lysates that were exposed to the inhibitors for only 2 h, while ATP was determined with cells that were exposed for 48 h to the inhibitors. Thus, cells may have adapted to the presence of these inhibitors with a longer exposure period, allowing to compensate the activity of these enzymes, being able to also increase H₂S production. However, we also have analysed ATP levels with 2 h of exposure to CBS and PAG inhibitors and we did not observe significant differences in ATP levels with or without the inhibitors in both cells lines, with the exception of OVCAR3 cells under hypoxia with cysteine supplementation in which the inhibitors led to decreased ATP levels (Suppl. figure 2). Hence, OVCAR3 cells may canalise the extra cysteine available for H₂S synthesis, enhancing ATP synthesis under hypoxia in a short-term exposition but in a long-term, results support the existence of alternative ATP sources besides H₂S under hypoxia.

Interestingly, albeit CBS and CSE inhibition was not sufficient to impair ATP production, the inhibition of both enzymes affected ATP synthesis mainly under hypoxia for

both ES2 and OVCAR3 cells, thus supporting a role of their activity in hypoxic environment. PAG alone was not able to decrease H₂S, but AOAA alone or the combination of both inhibitors generally was, implicating CBS activity inhibition (or MpST/CAT or both) in the decreased ATP synthesis observed upon the exposure to both inhibitors under hypoxia. Teng and colleagues reported that ischemia/hypoxia resulted in the increased accumulation of CBS in liver mitochondria, increased H₂S generation and decreased ROS [50]. These results, therefore, may explain the decreased ATP levels under hypoxia upon the exposure to both inhibitors, where CBS inhibition may lead to increased ROS levels, affecting mitochondria function, hence affecting ATP synthesis. Regarding CSE, in vascular smooth-muscle cells, Fu *et al.*, showed that this enzyme translocate to mitochondria under hypoxia, promoting H₂S generation and resulting in mitochondrial ATP sustainability [33]. The specific contribution of CSE in ATP synthesis in ovarian cancer cells and under hypoxia remains unclear, since PAG alone was not able to decrease H₂S levels, at least with 2 h of exposure. MpST role in H₂S mediated-ATP production under hypoxia remains also unclear. It was reported that oxidative stress suppresses MpST activity, effecting the bioenergetic role of the 3-mercaptopyruvate/MPST/H₂S pathway in murine hepatoma cells [55]. However, we did not observe differences in MpST protein levels in both cell lines (Suppl. figure 3) and H₂S levels were even induced under hypoxia, hence supporting that the activity of this enzyme was not affected under hypoxia in ovarian cancer cells. Moreover, we also observed a mitochondrial MpST enrichment compared to the cytosolic content. These results must be, nonetheless confirmed (Suppl. figure 4). Interestingly, MpST homolog was reported to protect *E. coli* against oxidative stress via L-cysteine utilization [56].

The specific contribution of CBS/CSE/MpST activities on cysteine-derived ATP synthesis under hypoxia remains unclear. Nevertheless, our results pointed to a role of cysteine in energy production mediated by the xc⁻ system that requires its metabolism instead of H₂S *per se*. Remarkably, in vascular smooth-muscle cells, NaHS, an exogenous H₂S source, was reported to be sufficient to increase mitochondrial ATP production under hypoxia [33]. In Fu and colleagues study, the ATP measurements were performed after 1 h of NaHS exposition, and Sun *et al.* reported that NaHS is unstable and leads to an instant release of H₂S in culture medium [31], which decays rapidly [32], we also quantified ATP levels with 1 h of NaHS and sulphasalazine exposure to address if H₂S effect was transient, hence undetectable with 48 h of culture conditions. Our results have shown that H₂S *per se* was not sufficient to counteract the impaired ATP production driven by sulphasalazine, leading even to an impaired ATP production under hypoxia for both ES2 and OVCAR3 cells, suggesting

that cysteine metabolism provides alternative sources for energy production in ovarian cancer cells. In addition to H₂S, cysteine degradation is known to generate pyruvate as well [27], which can further supply substrates to the tricarboxylic acid cycle, sustaining mitochondrial ATP production in ovarian cancer cells. Furthermore, recently, it was shown a role of cysteine hydropersulphide (CysSSH) in the regulation of mitochondrial biogenesis and bioenergetics [57]. Using HEK293T cells, the authors found that CysSSH can be produced not only by CBS and CSE (from cystine) but also by the mitochondrial isoform cysteinyl-tRNA synthetases (CARS2) plays also an important role in CysSSH generation (from cysteine) [57], hence making us hypothesise that this may be other source of ATP production upon the action of both the inhibitors. However, the authors have also shown that the persulphide synthase activity of CARS2 is also dependent on the presence of pyridoxal phosphate (PLP) [57] and AOAA inhibits several PLP-dependent enzymes [52], thus the possible CysSSH contribution in ATP production in hypoxic ovarian cancer cells remains unclear.

Other possibility of cysteine role in ATP production upon xCT inhibition is through an indirect contribution by increasing GSH content. The extra cysteine available can be used in GSH synthesis, thus allowing cells to escape from oxidative stress and enabling increased cell viability and proliferation, therefore leading to increased ATP synthesis. In fact, our previous data have supported a role of a higher thiols turnover in hypoxia adaptation, especially in ES2 cells [15]. Interestingly, H₂S was also reported to increase the production of GSH by inducing the expression of cystine/cysteine transporters and by redistributing GSH to mitochondria in mouse brain neuroblastoma, Neuro2a cells and mouse hippocampal HT22 cells [58]. In here, ¹H-NMR results have also suggested a role of cysteine in cellular metabolism rescue under hypoxia, especially in ES2 cells. Therefore, our data have shown that under hypoxia, cysteine significantly increased the intracellular levels of several amino acids, including alanine, glutamate, glycine and threonine in ES2 cells. Interestingly, Jain and colleagues have reported that increased glycine consumption was associated with increased proliferation rate in 60 cancer cell lines, and that this effect was more evident in ovarian cancer, colon cancer, and melanoma cells [59]. The authors also demonstrated that glycine was used in part for *de novo* purine nucleotide biosynthesis and for GSH in rapidly proliferating cells, as they reported an incorporation of labelled glycine into this thiol [59]. Importantly, the same authors have also shown that this phenotype with increased dependence on glycine metabolism was specific of rapidly proliferating malignant cells [59]. Cysteine was found to increase glycine levels in ES2 cells under hypoxia, hence supporting its role in the putative

rescue of the proliferation of hypoxic ES2 cells. Furthermore, strengthening the proliferation rescue effect of cysteine in hypoxic ES2 cells, Hosios and colleagues have found that the majority of cellular carbon mass is not derived from glucose and glutamine (that contributed only for about 10% of cell mass each one) but from other amino acids that were consumed at lower rates, where glutamine contributed primarily to protein, and glucose contributed as a major source of *de novo* lipogenesis [60]. Valine and serine each contributed only for 2–4% of carbon cell mass but a pooled mixture of amino acids was able to label the majority of cellular carbon in proliferating mammalian cells, including alanine, arginine, asparagine, aspartate, cystine, glutamate, glycine, histidine, isoleucine, leucine, lysine, methionine, phenylalanine, proline, serine, threonine, tryptophan, tyrosine and valine [60], hence supporting a role for these amino acids in biomass building. Importantly, using two different non-small cell lung cancer cell lines, the same authors also reported that hypoxia did not alter glucose and glutamine incorporation in H1299 cells, but the incorporation of both was decreased in A549 cells, while serine and valine incorporation were relatively unaltered in both cell lines [60], hence showing metabolic diversity when coping with hypoxia.

Under hypoxia, cysteine was also able to increase intracellular choline levels in ES2 cells. An activated choline metabolism was already considered as a metabolic hallmark of cancer, where increased levels of phosphocholine and total choline-containing compounds are features of the cholinic phenotype, and are not only important for cancer cells proliferation but also for the malignant transformation [61]. Phosphatidylcholine is the most prevalent phospholipid in eukaryotic cell membranes, contributing to cell growth and programmed cell death [62]. Choline kinase catalyses choline to phosphocholine phosphorylation, which is the first step of phosphatidylcholine biosynthesis [62]. Hypoxia was shown to increase cellular phosphocholine levels and total choline levels by inducing choline kinase protein expression in prostate cancer cells [63]. Interestingly, choline was reported to protect the endothelial function against hypoxia in rats exposed to chronic intermittent hypoxia [64]. In our study, cysteine increased choline levels under hypoxia, supporting again its role in hypoxic ES2 cells metabolic rescue.

Our data supported that cysteine increased histidine release in both ES2 and OVCAR3 cells under hypoxia. Recently, Kanarek and co-workers have reported that the histidine degradation pathway significantly augments the sensitivity of cancer cells to methotrexate, an anti-cancer drug that inhibits the enzyme dihydrofolate reductase, responsible for tetrahydrofolate generation, which is an essential cofactor in nucleotide synthesis, both *in vitro* and *in vivo* in leukaemia context [65]. The authors have reported that histidine

supplementation increased the efficacy of methotrexate in mice leukaemia xenograft models, through tetrahydrofolate depletion within tumour cells [65]. These results may suggest that histidine is disadvantageous in stressful environments, hence leading cells to avoid its consumption. However, in our study, CoCl_2 was found to decrease histidine levels in media without cells. Torii and colleagues have reported that histidine was able to inhibit the cobalt-induced HIF-1 α expression in human breast cancer MCF-7 cells cultured in DMEM, possibly by sequestering the free cobaltous ion in the medium [66]. In fact, cobalt (II) was reported to form tetrahedral complexes with L-histidine [67] and that oxygen interacts with the complex Cobalt(II)-Histidine in basic solutions [68], hence explaining the decreased levels of histidine under hypoxia mimicked with CoCl_2 . Because results suggested that cysteine increased the release of histidine under hypoxia, we hypothesise that histidine release is another way of cellular protection against the oxidative stress imposed by CoCl_2 . However, under normoxia, cysteine also increased the release of this amino acid both in ES2 and OVCAR3 cells, and under hypoxia without cysteine no release of histidine was observed. Thus the role of histidine in the response to hypoxia mimicked with CoCl_2 remains unclear. We have to highlight that albeit histidine might decrease CoCl_2 concentration, our previous results have shown that the CoCl_2 concentration used was able to induce HIF-1 α expression in our experimental setting. Interestingly, the pentose phosphate pathway supplies the biosynthesis of histidine [69], hence an altered glucose metabolism explains the higher levels of histidine release. In fact, our results supported that cysteine increased glucose metabolism under hypoxia for both ES2 (as seen by the increased intracellular lactate levels) and OVCAR3 cells (as seen by the decreased intracellular glucose levels) compared to normoxia, hence supporting that under hypoxia, histidine biosynthesis may be increased due to an increased glycolysis. Remarkably, it was reported that HIF-2 α induces the hepatocyte release of the histidine rich glycoprotein [70]. If this mechanism is spread to other histidine rich proteins and if HIF-2 α is up-regulated under hypoxia in our experimental setting is unknown, but we can speculate that hypoxia induces both HIF-1 α and HIF-2 α , inducing the release of histidine in the presence of cysteine.

Strikingly, the metabolic impact of cysteine under hypoxia was much more pronounced in ES2 cells compared to OVCAR3 cells, as seen by the remarkable number of metabolic pathways that were significantly altered in these cells. Interestingly, hypoxia led to an increased release of fumarate in OVCAR3 cells. Importantly, Schito and colleagues have reported that fumarate accumulation was responsible for an increased antioxidant capacity of hypoxic cancer cells through upregulation of the pentose phosphate pathway. Moreover, the

authors also reported that this fumarate-dependent increase of antioxidants was able to counteract the hypoxic activation of the endoplasmic reticulum kinase (PERK), a possible signalling transducer of the unfolded protein response that inhibits mRNA translation via eIF2 α phosphorylation. This enabled protein synthesis and proliferation, allowing an impaired hypoxia tolerance in cancer cells [71]. Hence, increased fumarate release may play a role in hypoxia tolerance in OVCAR3 cells. Interestingly, cysteine affected differently the uptake of several aminoacids under hypoxia, decreasing the uptake of alanine, histidine and proline and increasing the uptake of glycine and phenylalanine. Nevertheless, these results also support a possible role of cysteine in the rescue of the proliferation of hypoxic OVCAR3 cells, at least in part. In OVCAR3 cells, cysteine decreased the release of 2-hydroxybutyrate, which is a by-product of the conversion of cystathione to cysteine in the methionine-to-glutathione pathway, being its generation directly related to the rate of glutathione synthesis [72]. Therefore, higher extracellular levels of this compound were expected under hypoxia in the presence of extra cysteine. This suggests that OVCAR3 cells show little reliance in GSH synthesis on coping with hypoxia, results supported by our previous observations [15]. Nevertheless, 2-hydroxybutyrate also results from the degradation of long and very long chain fatty acids through β -oxidation [73], and since cysteine decreased the release of this compound under hypoxia, this suggests that this pathway is also decreased. Moreover, isobutyrate, which is a precursor of hydroxybutyrate [74], was also decreased by cysteine in hypoxic OVCAR3 cells.

Cysteine also decreased the release of formate under hypoxia compared to normoxia in OVCAR3 cells. Formate is primarily produced in the mitochondria from serine and functions as a source of one-carbon groups for the synthesis of 10-formyl-tetrahydrofolate and for other one-carbon intermediates, which are mainly used for the synthesis of purine and thymidylate, and for the delivery of methyl groups for synthetic, regulatory, and epigenetic methylation reactions [75]. In cancer, results have strongly supported an enhanced mitochondrial production of formate [75]. Interestingly, Thomas and colleagues suggested formate as a potent reductive force opposing oxidative stress in *Pseudomonas fluorescens*, by contributing both to the synthesis of NADPH and to the reduction of fumarate to succinate [76]. Formate probably has a role also in cancer cells response to oxidative stress, as mitochondrial folate pathway generates excess of formate that cells secrete, suggesting that the folate pathway plays pivotal roles besides the one-carbon delivery, such as the maintenance of mitochondrial NADH and NADPH levels [77]. Importantly, evidence supports an important role of the folate pathway in ovarian cancer, as α -folate receptor (α FR) was found to be expressed in

over 70% of primary ovarian tumours and 80% of recurrent ovarian cancers, whereas the normal ovarian epithelium does not express this receptor [78]. Moreover, the receptor expression was also shown to be associated with the progression of the disease and with chemoresistance [78]. Given the relevance of folate pathway in ovarian cancer, different targeted therapies were already developed with promising results [79]. In OVCAR3 cells cysteine decreased the release of formate levels under hypoxia, hence suggesting that cysteine impairs folate pathway under hypoxia in these cells. However, since formate can also be produced from histidine catabolism and since cysteine significantly reduced histidine uptake or increased histidine release under hypoxia in OVCAR3 cells, this could explain the low levels of formate release in these conditions. Similar trends were found for ES2 cells also, albeit the differences were not statistical significant.

Interestingly, while cysteine was able to rescue the impaired ATP synthesis triggered by xCT inhibition, it was not able to increase ATP synthesis upon β -oxidation and glycolysis inhibition, indicating that cysteine is not enough to replace the contribution of these pathways for ATP production. In fact, for ES2 cells, cysteine tended to decrease ATP synthesis in the presence of these inhibitors. Pike *et al.*, using human glioblastoma cells, demonstrated that etomoxir, an inhibitor of β -oxidation, lead to decreased cellular ATP levels and viability, concomitant with decreased GSH content and increased ROS [80]. These results suggest that the extra cysteine available may be being canalised to GSH synthesis. However, the decreased ATP and GSH content were observed with very high doses of etomoxir (0.75 mM and 1 mM) [80]. Recently, Yao *et al.* reported that 200 μ M lead to etomoxir off-targets effects in BT549 breast cancer cells, inhibiting not only the etomoxir target CPT1 but also the complex I of the electron transport chain, leading to decreased ATP production and cell proliferation independent of β -oxidation [81]. The authors also reported that BT549 cells treated with 10 μ M of etomoxir (the same concentration used in here), while presented a 90% block of β -oxidation without off-target effects on respiration, did not present reduced proliferation, mitochondrial respiration and ATP production. Instead, the authors reported that cells adjusted their nutrients uptake and utilization to compensate for the inhibition of this pathway [81]. Whether this dose was sufficient to increase ROS levels and reduce GSH content in BT549 breast cancer cells is still unclear, since the authors did not address these effects. However, O'Connor and colleagues reported that etomoxir concentrations above 5 μ M presented off-targets effects, inhibiting the oxidative metabolism and inducing severe oxidative stress in T cells [82]. These results therefore support that oxidative stress is a

common off-target effect of etomoxir, even with low doses, indicating that the extra cysteine available is indeed canalised as a ROS scavenger for counteracting the harmful oxidative conditions.

Bromopyruvic acid is an alkylating agent capable of inhibiting not only glycolysis, but also mitochondrial respiration [83], glutaminolysis and TCA cycle functions [84]. This compound, was also shown to induce oxidative stress through antioxidants depletion and inactivation of antioxidant enzymes in human breast cancer cell lines [85]. This decreased GSH content may be explained by the reaction of bromopyruvic acid with GSH, forming a S-conjugate [86]. These results suggest that, in the presence of etomoxir and bromopyruvic acid, ES2 cells preferentially canalised the extra cysteine available for GSH synthesis instead of ATP production, thus allowing the cellular defence against oxidative stress. Nevertheless, cysteine can act by itself as an antioxidant and S-conjugates of bromopyruvic acid can also be established with cysteine instead of GSH. However, we may not have used the right experimental approach to inhibit these pathways without un-specifically interfering with other metabolic reactions.

Together, the results support that ES2 and OVCAR3 cells use cysteine differently in order to cope with hypoxic environments, where cysteine especially impacts hypoxic ES2 cells metabolic features, hence providing a source for metabolism reprogramming under hypoxia conditions. In the figure 20, the possible direct and indirect mechanisms by which cysteine allows ATP production in hypoxic ovarian cancer cells is presented. The profound metabolic impact that cysteine showed under hypoxia, suggesting a strong remodelling of the carbon metabolism is also presented.

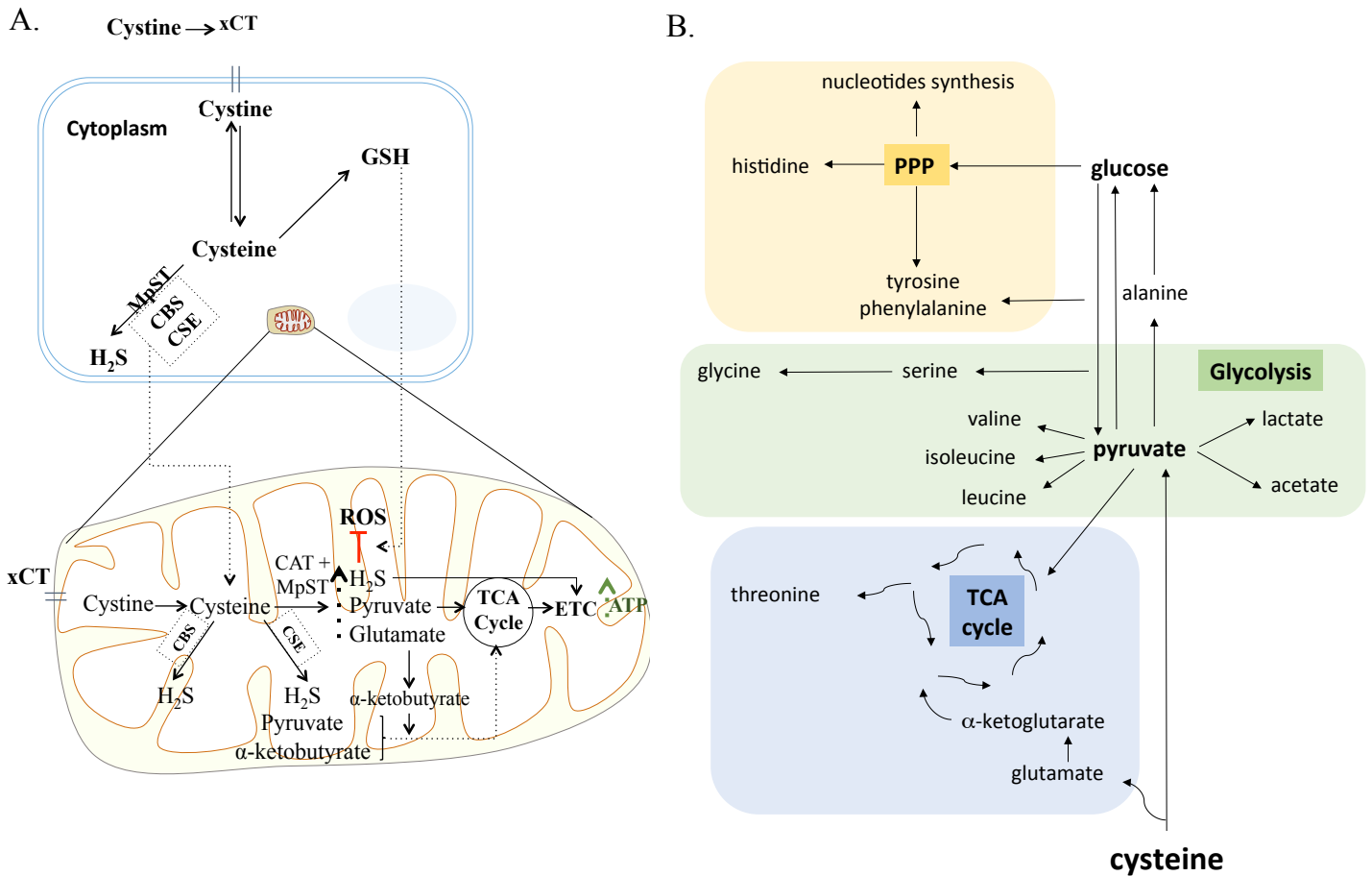


Figure 20. Cysteine possible direct and indirect roles in ATP synthesis and in carbon metabolism reprogramming under hypoxia in ovarian cancer cells.

A. Under hypoxia, cysteine degradation could contribute directly to ATP production via not only H_2S generation, but also via pyruvate and α -ketobutyrate that could further supply the TCA cycle, leading to increased ATP synthesis. Cysteine could also present an indirect role in ATP synthesis mediated by increasing GSH content under hypoxia, hence counteracting oxidative stress and thereby increasing cellular metabolism.

B. The axis cysteine-pyruvate-glucose is central in whole metabolic network of carbon. Cysteine degradation can originate pyruvate and glutamate. Pyruvate besides being a major supplier of tricarboxylic acids (TCA) cycle, it can be converted into valine, isoleucine, leucine, alanine, lactate and acetate. Alanine can be a source of glucose through gluconeogenesis. Glycolysis, produce intermediates to supply the TCA cycle (a hub for many precursors of organic compounds, such as threonine) and the pentose phosphate pathway (PPP). PPP intermediates can be converted into amino acids such as histidine and can be conjugated with glycolysis intermediates, originating tyrosine, phenylalanine and serine, which can be converted into glycine. PPP is also crucial in the nucleotides synthesis. The increased concentration of these compounds under hypoxia, suggests that cysteine is pushing the metabolic flow in order to supply the main carbon metabolic pathways. The direct incorporation of cysteine into this compounds is possible, however further studies are needed to clarify this. Based on information from www.bioinfo.org.cn.

New experiments are needed to ascertain if cysteine is used as substrate to produce some of these organic metabolites. NMR analysis of cells exposed to ^{13}C -cysteine would be very helpful to clearly determine which metabolic pathways are directly dependent on cysteine.

Taken together, our data support that targeting cysteine uptake is a promising tool to fight ovarian cancer, as it allows not only hypoxia adaptation, but also platinum-based drugs resistance. The system xc- was already reported to be up-regulated in several cancer cell

types and it is associated with drug resistance [34] thus, inhibiting its function through sulphasalazine may constitute a valuable tool to fight several types of cancer. Sulphasalazine is already used in the context of other diseases, such as Crohn's disease [87] and rheumatoid arthritis [88,89]. Interestingly, in patients with inflammatory bowel disease, Qiu and colleagues through a systematic review with meta-analysis reported that 5-Aminosalicylic acid (the main metabolite of sulphasalazine and mesalazine) decreased the risk of colorectal cancer but not the risk of dysplasia [90]. However, the authors also reported that whereas mesalazine showed a protective role against colorectal cancer, sulphasalazine did not [90]. Nevertheless, a beneficial use of sulphasalazine in other cancer types was also reported. In the context of pancreatic cancer, Lo *et al.* reported that sulphasalazine was able to enhance gemcitabine efficacy, thus indicating that this combined therapy is more effective in refractory pancreatic cancer [91]. Balza and colleagues, in an experimental model of 3-methylcholantrene induced mouse sarcoma, reported that sulphasalazine combined with the cyclooxygenase 2 inhibitor, ibuprofen, led to decreased sarcoma progression and tumour size as well as an increased survival of treated mice [92]. Later, Balza *et al.* also reported that sulphasalazine combined with esomeprazole (which inhibits membrane v-ATPases) decreased cellular growth and migration in melanoma and sarcoma cells [93]. Remarkably, Nagano *et al.* have already proposed the use of targeted therapy to cancer stem cells that express variant forms of CD44 (CD44v) that stabilize and interact with xCT [94]. This targeted CD44v-xCT system would possibly allow to abrogate cellular ROS defence and redox adaptation, therefore sensitizing cancer stem cells to the available anti-cancer drugs [94].

Collectively, data support the use of cysteine metabolism and transport-targeted therapy, such as sulphasalazine, as a promising strategy in the context of ovarian cancer treatment.

REFERENCES

1. Fitzmaurice C, Dicker D, Pain A, Hamavid H, Moradi-Lakeh M, MacIntyre MF, *et al.* The Global Burden of Cancer 2013. *JAMA Oncol.* 2015;1:505–27.
2. Ferlay J, Soerjomataram I, Ervik M, Dikshit R, Eser S, Mathers C, Rebelo M, Parkin DM, Forman D, Bray F. GLOBOCAN 2012 v1.0, Cancer Incidence and Mortality Worldwide: IARC CancerBase No. 11. Lyon, Fr. Int. Agency Res. Cancer. 2013 [cited 2018 Aug 24]. Available from: <http://globocan.iarc.fr>
3. Ferlay J, Soerjomataram I, Ervik M, Dikshit R, Eser S, Mathers C, Rebelo M, Parkin DM, Forman

D, Bray F. GLOBOCAN 2012 v1.0, Cancer Incidence and Mortality Worldwide: IARC CancerBase No. 11. Lyon, Fr. Int. Agency Res. Cancer. 2013 [cited 2018 Aug 30]. Available from: <http://globocan.iarc.fr>

4. Jayson GC, Kohn EC, Kitchener HC, Ledermann JA. Ovarian cancer. *Lancet*. 2014;384:1376–88.
5. Bast Jr RC, Hennessy B, Mills GB. The biology of ovarian cancer: New opportunities for translation. *Nat. Rev. Cancer*. 2009;9:415–28.
6. Desai A, Xu J, Aysola K, Qin Y, Okoli C, Hariprasad R, *et al.* Epithelial ovarian cancer: An overview. *World J Transl Med*. 2014;3:10–29.
7. Prat J. Ovarian carcinomas: Five distinct diseases with different origins, genetic alterations, and clinicopathological features. *Virchows Arch*. 2012;460:237–49.
8. Reid BM, Permuth JB, Sellers TA. Epidemiology of ovarian cancer: a review. *Cancer Biol. Med*. 2017;14:9–32.
9. Fruehauf JP, Meyskens FL. Reactive oxygen species: A breath of life or death? *Clin. Cancer Res*. 2007;13:789–94.
10. Saed GM, Diamond MP, Fletcher NM. Updates of the role of oxidative stress in the pathogenesis of ovarian cancer. *Gynecol. Oncol*. 2017;145:595–602.
11. Vaupel P, Mayer A. Hypoxia in cancer: Significance and impact on clinical outcome. *Cancer Metastasis Rev*. 2007;26:225–39.
12. Semenza GL. Hypoxia-inducible factors: Mediators of cancer progression and targets for cancer therapy. *Trends Pharmacol. Sci*. 2012;33:207–14.
13. Senthil K, Aranganathan S, Nalini N. Evidence of oxidative stress in the circulation of ovarian cancer patients. *Clin. Chim. Acta*. 2004;339:27–32.
14. Nunes SC, Lopes-Coelho F, Gouveia-Fernandes S, Ramos C, Pereira SA, Serpa J. Cysteine boosts the evolutionary adaptation to CoCl₂ mimicked hypoxia conditions, favouring carboplatin resistance in ovarian cancer. *BMC Evol. Biol*. 2018;18:97–113.
15. Nunes SC, Ramos C, Lopes-Coelho F, Sequeira CO, Silva F, Gouveia-Fernandes S, *et al.* Cysteine allows ovarian cancer cells to adapt to hypoxia and to escape from carboplatin cytotoxicity. *Sci. Rep*. 2018;8:9513–29.
16. Balendiran GK, Dabur R, Fraser D. The role of glutathione in cancer. *cell Biochem. Funct*. 2004;22:343–52.
17. Schnelldorfer T, Gansauge S, Gansauge F, Schlosser S, Beger HG, Nussler AK. Glutathione depletion causes cell growth inhibition and enhanced apoptosis in pancreatic cancer cells. *Cancer*. 2000;89:1440–7.
18. Lopes-Coelho F, Gouveia-Fernandes S, Gonçalves LG, Nunes C, Faustino I, Silva F, *et al.* HNF1B drives glutathione (GSH) synthesis underlying intrinsic carboplatin resistance of ovarian clear cell carcinoma (OCCC). *Tumor Biol*. 2016;37:4813–29.
19. Bhattacharyya S, Saha S, Giri K, Lanza IR, Nair KS, Jennings NB, *et al.* Cystathionine Beta-Synthase (CBS) Contributes to Advanced Ovarian Cancer Progression and Drug Resistance. *PLoS One*. 2013;8: 79167.1-12.

20. Szabo C, Coletta C, Chao C, Módis K, Szczesny B, Papapetropoulos A. Tumor-derived hydrogen sulfide, produced by cystathionine- β -synthase, stimulates bioenergetics, cell proliferation, and angiogenesis in colon cancer. *PNAS Pharmacol.* 2013;110:12474–9.
21. Sen S, Kawahara B, Gupta D, Tsai R, Khachatryan M, Farias-eisner R, *et al.* Role of cystathionine β -synthase in human breast Cancer. *Free Radic. Biol. Med.* 2015;86:228–38.
22. Panza E, De Cicco P, Armogida C, Scognamiglio G, Gigantino V, Botti G, *et al.* Role of the cystathionine γ lyase/hydrogen sulfide pathway in human melanoma progression. *Pigment Cell Melanoma Res.* 2015;28:61–72.
23. Gai JW, Qin W, Liu M, Wang HF, Zhang M, Li M, *et al.* Expression profile of hydrogen sulfide and its synthases correlates with tumor stage and grade in urothelial cell carcinoma of bladder. *Urol. Oncol. Semin. Orig. Investig.* 2016;34:166.e15–20.
24. Pan Y, Zhou C, Yuan D, Zhang J, Shao C. Radiation Exposure Promotes Hepatocarcinoma Cell Invasion through Epithelial Mesenchymal Transition Mediated by H₂S/CSE Pathway. *Radiat. Res.* 2015;185:96–105.
25. Szczesny B, Marcatti M, Zatarain JR, Druzhyna N, Wiktorowicz JE, Nagy P, *et al.* Inhibition of hydrogen sulfide biosynthesis sensitizes lung adenocarcinoma to chemotherapeutic drugs by inhibiting mitochondrial DNA repair and suppressing cellular bioenergetics. *Sci. Rep.* 2016;6:36125-35.
26. Kabil O, Banerjee R. Enzymology of H₂S Biogenesis, Decay and Signaling. *Antioxid. Redox Signal.* 2014;20:770–82.
27. Wang R. Physiological Implications of Hydrogen Sulfide: A Whiff Exploration That Blossomed. *Physiol. Rev.* 2012;92:791–896.
28. Giuffrè A, Vicente JB. Hydrogen Sulfide Biochemistry and Interplay with Other Gaseous. *Oxid. Med. Cell. Longev.* 2018;11:1-31.
29. Sato, H., Tamba, M., Kuriyama-Matsumura, K., Okuno, S., & Bannai S. Molecular cloning and expression of human xCT, the light chain of amino acid transport system xc⁻. *Antioxid Redox Signal.* 2000;2:665–71.
30. Zhou Y, Tozzi F, Chen J, Fan F, Xia L, Wang J, *et al.* Intracellular ATP Levels are a Pivotal Determinant of Chemoresistance in Colon Cancer Cells. *Cancer Res.* 2012;72:304–14.
31. Sun X, Wang W, Dai J, Jin S, Huang J, Guo C, *et al.* A long-term and slow-releasing hydrogen sulfide donor protects against myocardial ischemia/reperfusion injury. *Sci. Rep. Springer US;* 2017;7:1–13.
32. Hu LF, Lu M, Hon Wong PT, Bian J-S. Hydrogen Sulfide: Neurophysiology and Neuropathology. *Antioxid. Redox Signal.* 2011;15:405–19.
33. Fu M, Zhang W, Wu L, Yang G, Li H, Wang R. Hydrogen sulfide (H₂S) metabolism in mitochondria and its regulatory role in energy production. *Proc. Natl. Acad. Sci.* 2012;109:2943–8.
34. Conrad M, Sato H. The oxidative stress-inducible cystine/glutamate antiporter, system xc⁻: cystine supplier and beyond. *Amino Acids.* 2012;42:231–46.
35. Vomund S, Schäfer A, Parnham MJ, Brüne B, Von Knethen A. Nrf2, the master regulator of anti-oxidative responses. *Int. J. Mol. Sci.* 2017;18:1–19.

36. Habib E, Linher-Melville K, Lin HX, Singh G. Expression of xCT and activity of system xc-are regulated by NRF2 in human breast cancer cells in response to oxidative stress. *Redox Biol.* 2015;5:33–42.
37. Gout PW, Buckley AR, Simms CR, Bruchovsky N. Sulfasalazine, a potent suppressor of lymphoma growth by inhibition of the x-cystine transporter: A new action for an old drug. *Leukemia.* 2001;15:1633–40.
38. Nagane M, Kanai E, Shibata Y, Shimizu T, Yoshioka C, Maruo T, *et al.* Sulfasalazine, an inhibitor of the cystine-glutamate antiporter, reduces DNA damage repair and enhances radiosensitivity in murine B16F10 melanoma. *PLoS One.* 2018;13:e0195151.1–19.
39. Cha YJ, Kim ES, Koo JS. Amino acid transporters and glutamine metabolism in breast cancer. *Int. J. Mol. Sci.* 2018;19:907-23.
40. Jiang Y, Cao Y, Wang Y, Li W, Liu X, Lv Y, *et al.* Cysteine transporter slc3a1 promotes breast cancer tumorigenesis. *Theranostics.* 2017;7:1036–46.
41. Lo M, Wang YZ, Gout PW. The xc- cystine/glutamate antiporter: A potential target for therapy of cancer and other diseases. *J. Cell. Physiol.* 2008;215:593–602.
42. Koppula P, Zhang Y, Zhuang L, Gan B. Amino acid transporter SLC7A11/xCT at the crossroads of regulating redox homeostasis and nutrient dependency of cancer. *Cancer Commun.* 2018;38:12-24.
43. Ji X, Qian J, Rahman SMJ, Siska PJ, Zou Y, Harris BK, *et al.* xCT (SLC7A11)-mediated metabolic reprogramming promotes non-small cell lung cancer progression. *Oncogene.* 2018;37:5007–19.
44. Konstantinopoulos PA, Spentzos D, Fountzilas E, Francoeur N, Sanisetty S, Grammatikos AP, *et al.* Keap1 mutations and Nrf2 pathway activation in epithelial ovarian cancer. *Cancer Res.* 2011;71:5081–9.
45. Goubern M, Andriamihaja M, Nubel T, Blachier F, Bouillaud F. Sulfide, the first inorganic substrate for human cells. *FASEB J.* 2007;21:1699–706.
46. Módis K, Coletta C, Erdélyi K, Papapetropoulos A, Szabo C. Intramitochondrial hydrogen sulfide production by 3-mercaptopyruvate sulfurtransferase maintains mitochondrial electron flow and supports cellular bioenergetics. *FASEB J.* 2013;27:601–11.
47. Módis K, Panopoulos P, Coletta C, Papapetropoulos A, Szabo C. Hydrogen sulfide-mediated stimulation of mitochondrial electron transport involves inhibition of the mitochondrial phosphodiesterase 2A, elevation of cAMP and activation of protein kinase A. *Biochem. Pharmacol.* 2013;86:1311–9.
48. Li S, Yang G. Hydrogen Sulfide Maintains Mitochondrial DNA Replication *via* Demethylation of *TFAM*. *Antioxid. Redox Signal.* 2015;23:630–42.
49. Chakraborty PK, Murphy B, Mustafi SB, Dey A, Xiong X, Rao G, *et al.* Cystathionine β -synthase regulates mitochondrial morphogenesis in ovarian cancer. *FASEB J.* 2018;32: 4145-57.
50. Teng H, Wu B, Zhao K, Yang G, Wu L, Wang R. Oxygen-sensitive mitochondrial accumulation of cystathionine-synthase mediated by Lon protease. *Proc. Natl. Acad. Sci.* 2013;110:12679–84.
51. Miyamoto R, Otsuguro KI, Yamaguchi S, Ito S. Contribution of cysteine aminotransferase and mercaptopyruvate sulfurtransferase to hydrogen sulfide production in peripheral neurons. *J.*

Neurochem. 2014;130:29–40.

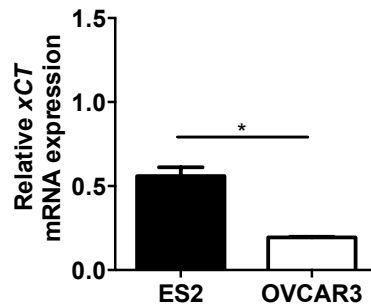
52. Hellmich MR, Coletta C, Chao C, Szabo C. The Therapeutic Potential of Cystathionine β -Synthetase/Hydrogen Sulfide Inhibition in Cancer. *Antioxid. Redox Signal.* 2015;22:424–48.
53. Hanaoka K, Sasakura K, Suwanai Y, Toma-Fukai S, Shimamoto K, Takano Y, *et al.* Discovery and mechanistic characterization of selective inhibitors of H₂S-producing Enzyme: 3-Mercaptopyruvate. *Sci. Rep.* 2017;7:1–7.
54. Chakraborty PK, Xiong X, Mustafi SB, Saha S, Dhanasekaran D, Mandal NA, *et al.* Role of cystathionine beta synthase in lipid metabolism in ovarian cancer. *Oncotarget.* 2015;6:37367-84.
55. Módis K, Asimakopoulou A, Coletta C, Papapetropoulos A, Szabo C. Oxidative stress suppresses the cellular bioenergetic effect of the 3-mercaptopyruvate sulfurtransferase/hydrogen sulfide pathway. *Biochem. Biophys. Res. Commun.* 2013;433:401–7.
56. Mironov A, Seregina T, Nagornyykh M, Luhachack LG, Korolkova N, Lopes LE, *et al.* Mechanism of H₂S-mediated protection against oxidative stress in Escherichia coli. *Proc. Natl. Acad. Sci.* 2017;114:6022–7.
57. Akaike T, Ida T, Wei FY, Nishida M, Kumagai Y, Alam MM, *et al.* Cysteinyl-tRNA synthetase governs cysteine polysulfidation and mitochondrial bioenergetics. *Nat. Commun.* 2017;8:1177-91.
58. Kimura Y, Goto Y-I, Kimura H. Hydrogen Sulfide Increases Glutathione Production and Suppresses Oxidative Stress in Mitochondria. *Antioxid. Redox Signal.* 2010;12:1–13.
59. Jain M, Nilsson R, Sharma S, Madhusudhan N, Kitami T, Souza AL, *et al.* Metabolite Profiling Identifies a Key Role for Glycine in Rapid Cancer Cell Proliferation. *Science.* 2012;336:1040–4.
60. Hosios AM, Hecht VC, Danaei L V, Johnson MO, Jeffrey C, Steinhauer ML, *et al.* Amino acids rather than glucose account for the majority of cell mass in proliferating mammalian cells. *Dev Cell.* 2016;36:540–9.
61. Glunde K, Bhujwalla ZM, Ronen SM. Choline metabolism in malignant transformation. *Nat. Rev. Cancer.* 2011;11:835–48.
62. Mori N, Wildes F, Takagi T, Glunde K, Bhujwalla ZM. The Tumor Microenvironment Modulates Choline and Lipid Metabolism. *Front. Oncol.* 2016;6:1–10.
63. Glunde K, Shah T, Jr. PTW, Raman V, Takagi T, Vesuna F, *et al.* Hypoxia Regulates Choline Kinase Expression through Hypoxia- Inducible Factor-1 α Signaling in a Human Prostate Cancer Model. 2008;68:172–80.
64. Zhang LC, Jin X, Huang Z, Yan ZN, Li PB, Duan RF, *et al.* Protective effects of choline against hypoxia-induced injuries of vessels and endothelial cells. *Exp. Ther. Med.* 2017;13:2316–24.
65. Kanarek N, Keys HR, Cantor JR, Lewis CA, Chan SH, Kunchok T, *et al.* Histidine catabolism is a major determinant of methotrexate sensitivity. *Nature.* 2018;559:632–6.
66. Torii S, Kurihara A, Li XY, Yasumoto KI, Sogawa K. Inhibitory effect of extracellular histidine on cobalt-induced HIF-1 α expression. *J. Biochem.* 2011;149:171–6.
67. Morris PJ, Martin RB. Tetrahedral Complexes of Cobalt (II) with L-Histidine, Histamine, Imidazole, and N-Acetyl-L-histidine. *J. Am. Chem. Soc.* 1970;92:1543–6.

68. Watters KL, Wilkins RG, Cruces L. Interaction of Oxygen with the Cobalt(II)-Histidine Complex in Strongly Basic Solution. *Inorg. Chem.* 1974;13:752–3.
69. Stincone A, Prigione A, Cramer T, Wamelink MMC, Campbell K, Cheung E, *et al.* The return of metabolism: Biochemistry and physiology of the pentose phosphate pathway. *Biol. Rev.* 2015;90:927–63.
70. Morello E, Sutti S, Foglia B, Novo E, Cannito S, Bocca C, *et al.* Hypoxia-inducible factor 2 α drives nonalcoholic fatty liver progression by triggering hepatocyte release of histidine rich glycoprotein. *Hepatology.* 2017;67:2196–214.
71. Schito L, Rey S, Wouters BG, Koritzinsky M. The oncometabolite fumarate prevents hypoxia-induced ER stress by enhancing the pentose phosphate pathway. *Proc. Am. Assoc. Cancer Res. Annu. Meet.* 2017; April 1-5, 2017; Washington, DC. Philadelphia (PA); p. 77(13 Suppl):Abstract 4499.
72. Lord RS, Bralley JA. Clinical applications of urinary organic acids. Part 2. Dysbiosis markers. *Altern. Med. Rev.* 2008;13:292–306.
73. King MW. Lipids: Lipolysis, Fatty Acid Oxidation, and Ketogenesis. In: Medical NYM-HE, editor. *Integr. Med. Biochem. Exam. Board Rev.* 2014.
74. Rinaldi MA, Patel AB, Park J, Lee K, Strader LC, Bartel B. The roles of β -oxidation and cofactor homeostasis in peroxisome distribution and function in *Arabidopsis thaliana*. *Genetics.* 2016;204:1089–115.
75. Brosnan ME, Brosnan JT. Formate: The Neglected Member of One-Carbon Metabolism. *Annu. Rev. Nutr.* 2016;36:369–88.
76. Thomas SC, Alhasawi A, Auger C, Omri A, Appanna VD. The role of formate in combatting oxidative stress. *Antonie van Leeuwenhoek, Int. J. Gen. Mol. Microbiol.* 2016;109:263–71.
77. Yang M, Vousden KH. Serine and one-carbon metabolism in cancer. *Nat. Rev. Cancer.* 2016;16:650–62.
78. Vergote IB, Marth C, Coleman RL. Role of the folate receptor in ovarian cancer treatment: evidence, mechanism, and clinical implications. *Cancer Metastasis Rev.* 2015;34:41–52.
79. Lim HJ, Ledger W. Targeted therapy in ovarian cancer. *Women's Heal.* 2016;12:363–78.
80. Pike LS, Smift AL, Croteau NJ, Ferrick DA, Wu M. Inhibition of fatty acid oxidation by etomoxir impairs NADPH production and increases reactive oxygen species resulting in ATP depletion and cell death in human glioblastoma cells. *Biochim. Biophys. Acta - Bioenerg.* 2011;1807:726–31.
81. Yao C-H, Liu G-Y, Wang R, Moon SH, Gross RW, Patti GJ. Identifying off-target effects of etomoxir reveals that carnitine palmitoyltransferase I is essential for cancer cell proliferation independent of β -oxidation. *PLOS Biol.* 2018;16:e2003782.1–26.
82. O'Connor RS, Guo L, Ghassemi S, Snyder NW, Worth AJ, Weng L, *et al.* The CPT1a inhibitor, etomoxir induces severe oxidative stress at commonly used concentrations. *Sci. Rep.* 2018;8:1–9.
83. Shoshan MC. 3-bromopyruvate: Targets and outcomes. *J. Bioenerg. Biomembr.* 2012;44:7–15.
84. Jardim-Messeder D, Moreira-Pacheco F. 3-Bromopyruvic Acid Inhibits Tricarboxylic Acid Cycle and Glutaminolysis in HepG2 Cells. *Anticancer Res.* 2016;36:2233–41.

85. Kwiatkowska E, Wojtala M, Gajewska A, Soszyński M, Bartosz G, Sadowska-Bartosz I. Effect of 3-bromopyruvate acid on the redox equilibrium in non-invasive MCF-7 and invasive MDA-MB-231 breast cancer cells. *J. Bioenerg. Biomembr.* 2016;48:23–32.
86. Sadowska-Bartosz I, Szewczyk R, Jaremko L, Jaremko M, Bartosz G. Anticancer agent 3-bromopyruvic acid forms a conjugate with glutathione. *Pharmacol. Reports. Institute of Pharmacology, Polish Academy of Sciences;* 2016;68:502–5.
87. Lichtenstein GR, Loftus E V, Isaacs KL, Regueiro MD, Gerson LB, Sands BE. ACG Clinical Guideline: Management of Crohn’s Disease in Adults. *Am. J. Gastroenterol.* 2018;113:481–517.
88. Kwoh CK, Anderson LG, Greene JM, Johnson DA, O’Dell JR, Robbins ML, *et al.* Guidelines for the management of rheumatoid arthritis: 2002 update - American College of Rheumatology Subcommittee on Rheumatoid Arthritis Guidelines. *Arthritis Rheum.* 2002;46:328–46.
89. Smolen JS, Landewé R, Bijlsma J, Burmester G, Chatzidionysiou K, Dougados M, *et al.* EULAR recommendations for the management of rheumatoid arthritis with synthetic and biological disease-modifying antirheumatic drugs: 2016. *Ann. Rheum. Dis.* 2017;76:960–77.
90. Qiu X, Ma J, Wang K, Zhang H. Chemopreventive effects of 5-aminosalicylic acid on inflammatory bowel disease-associated colorectal cancer and dysplasia: a systematic review with meta-analysis. *Oncotarget.* 2017;8:1031–45.
91. Lo M, Ling V, Low C, Wang YZ, Gout PW. Potential use of the anti-inflammatory drug, sulfasalazine, for targeted therapy of pancreatic cancer. *Curr. Oncol.* 2010;17:9–16.
92. Balza E, Castellani P, Delfino L, Truini M, Rubartelli A. The pharmacologic inhibition of the xc-antioxidant system improves the antitumor efficacy of COX inhibitors in the in vivo model of 3-MCA tumorigenesis. *Carcinogenesis.* 2013;34:620–6.
93. Balza E, Castellani P, Moreno PS, Piccioli P, Medraño-Fernandez I, Semino C, *et al.* Restoring microenvironmental redox and pH homeostasis inhibits neoplastic cell growth and migration: therapeutic efficacy of esomeprazole plus sulfasalazine on 3-MCA-induced sarcoma. *Oncotarget.* 2017;8:67482–96.
94. Nagano O, Okazaki S, Saya H. Redox regulation in stem-like cancer cells by CD44 variant isoforms. *Oncogene.* 2013;32:5191–8.

SUPPLEMENTS

Supplement figure 1

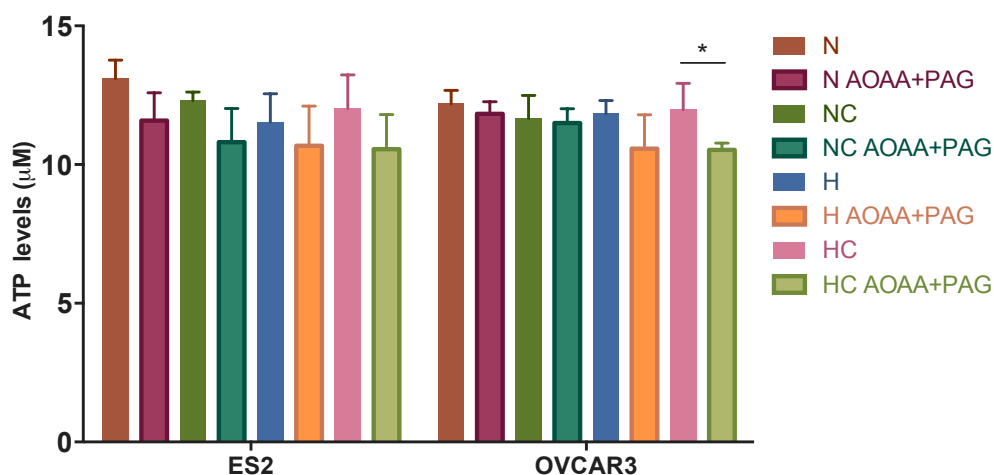


Supplement figure 1. ES2 cells express higher basal mRNA levels of xCT than OVCAR3 cells.

Basal relative xCT mRNA expression for ES2 and OVCAR3 cells.

Briefly, ES2 and OVCAR3 cells were cultured in 6-well plates (5×10^5 cells/well) and cultured under basal conditions (normoxia without cysteine supplementation with 1% of FBS). Cells were collected and RNA was extracted with RNeasy Mini Extraction kit (74104, Qiagen), according to the manufacturer's protocol. cDNA was synthesized from 1 μ g RNA and reversely transcribed by SuperScript II Reverse Transcriptase (18064-22, Invitrogen), according to the manufacturer's protocol. Quantitative Real-Time PCR was performed using LightCycler 480 SYBR Green I master (04707516001, Roche), according to manufacturer's protocol. Primers for xCT (For: 5' GGTCCTGTCACCTATTGGAGC 3'; Rev: 5' GAGGAGTTCCACCCAGACTC 3') were used. Real-time PCR was carried out in LightCycler 480 instrument (Roche). Results are shown as mean \pm SD. * $p < 0.05$, ** $p < 0.01$, *** $p < 0.001$ (Independent-samples T test).

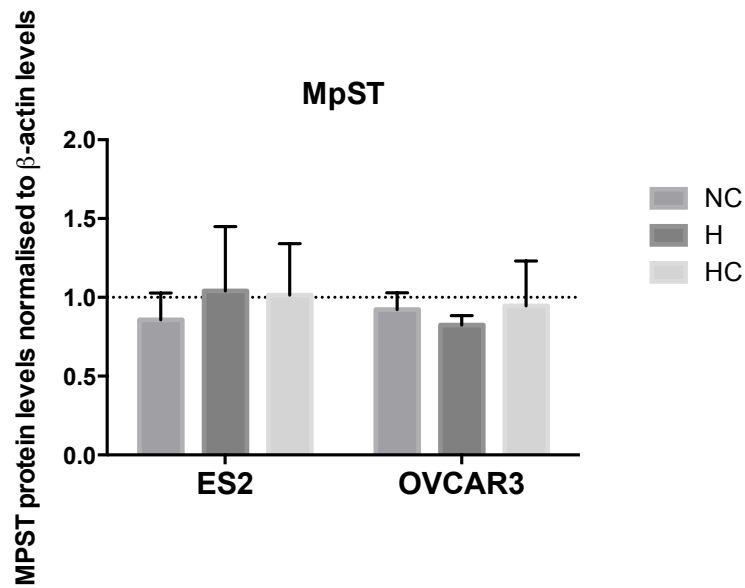
Supplement figure 2



Supplement figure 2. Effect of CBS and CSE inhibition in ATP synthesis in ovarian cancer cells.

ATP levels in control conditions and in the presence of 1 mM AOOA and 3 mM PAG for 2 h of experimental conditions for ES2 and OVCAR3 cells. The asterisks (*) represent the statistical significance compared to the respective control. * $p < 0.05$, ** $p < 0.01$, *** $p < 0.001$ (One-way ANOVA with post hoc Tukey tests). N – normoxia; NC – normoxia with cysteine, H – hypoxia, HC – hypoxia with cysteine. Results are shown as mean \pm SD.

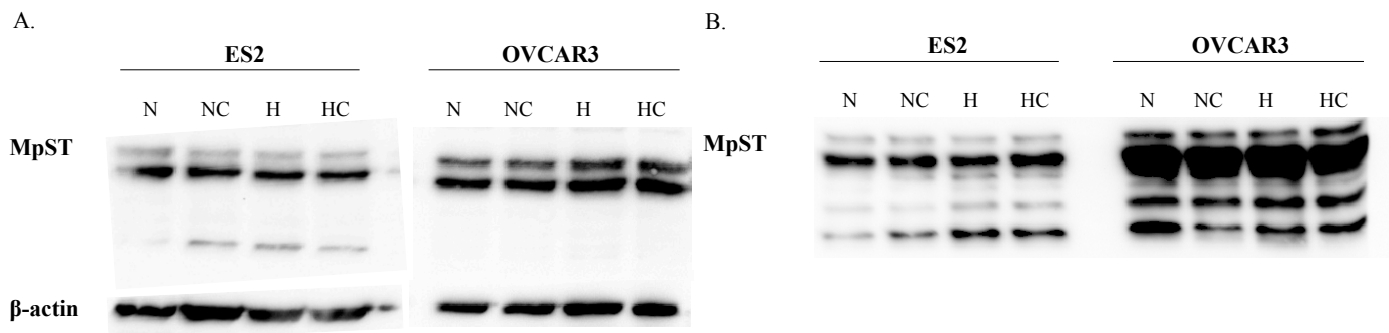
Supplement figure 3



Supplement figure 3. MpST protein levels in ES2 and OVCAR3 cells.

Quantification of anti-MpST western blotting for ES2 and OVCAR3 cells. Data were normalised to control (normoxia). NC – normoxia with cysteine, H – hypoxia, HC – hypoxia with cysteine.

Supplement figure 4



Supplement figure 4. Cytosolic and mitochondrial MpST protein levels in ES2 and OVCAR3 cells.

Western blotting for A. cytosolic MpST and B. mitochondrial MpST in ES2 and OVCAR3 cells. For western blotting for cytosolic MpST, briefly, cells (2.5×10^6) were cultured in 25-cm² tissue culture flasks in control conditions and exposed either to 0.402 mM L-cysteine and/or 0.100mM cobalt chloride for 16 h. Cells were collected with trypsin and western blot analysis was performed. Anti-MpST (1:250; HPA001240 from sigma) and anti- β -actin (1:5000; A5441 from Sigma Aldrich) antibodies were used. Secondary antibodies (1:5000; anti-rabbit, 31460, from Thermo Scientific or anti-mouse 31430 from Thermo Scientific) were used. For the western blotting presented, 100 μ g of total protein was used. For western blotting with isolated mitochondria, the methods are described previously in the materials and methods section.

CHAPTER 5

GENERAL DISCUSSION

*“Though I'm past one hundred thousand miles,
I'm feeling very still
And I think my spaceship knows which way to go”*
David Bowie

GENERAL DISCUSSION

The present thesis aimed to clarify the relevance of cysteine metabolism in ovarian cancer cells capacity of adapting to both hypoxia and carboplatin, both of which responsible for imposing strong evolutionary selection pressures on cancer cells.

In the next sections, we will discuss the most relevant results obtained during this thesis.

5.1 HYPOXIA ADAPTATION FAVOURS A GENERALIST PHENOTYPE IN OVARIAN CANCER CELLS AND DRIVES CARBOPLATIN RESISTANCE

The adaptation to a specific environment is widely associated to deterioration in other non-selective environments, being accompanied by an evolutionary trade-off [1–4]. In fact, in the second chapter, our results supported an evolutionary trade-off in ovarian cancer cells selection under normoxic conditions, where these cells presented decreased survival in novel environments. However, in hypoxia-selected cells, no evolutionary trade-offs in non-selective environments were found, as cells did not present increased mortality, hence showing a generalist phenotype. Albeit no trade-offs were found in other non-selective environments, cells selected under hypoxia exhibited a trade-off among survival and cell growth, as the increased survival was accompanied by lower proliferation rates. This observation, together with the evidence that each patient's tumours exhibit large variation in proliferation rates [5] may have clinical implications for cancer patients, as therapy protocols effectiveness may depend on the evolutionary strategy of cancer cells. For instance, the rationale that cytotoxic drugs kills preferentially cells with increased proliferation rates, such as paclitaxel, might not be effective for quiescent or low proliferating cancer cells such as hypoxic or chemoresistant ones. Therefore, the maintenance of quiescent cells, as the cancer stem cells, will allow its proliferation once the chemotherapy drugs are removed, leading to disease relapse and metastasis [6]. Interestingly, we observed induced CD133 levels, a cancer stem cell marker, both upon hypoxia and carboplatin exposure in several ovarian cancer cell lines. CD133 is a membrane glycoprotein already reported as an ovarian cancer stem cell marker and associated with increased tumour initiating capacity and chemoresistance [7]. Interestingly, upon carboplatin exposure, the already resistant A2780 cisR cells did not increase CD133 levels in the majority of treatments, whereas A2780 parental, the chemosensitive cells, did. These results support that CD133 positive phenotype is part of the process of carboplatin acquiring resistance that is lost when cells become chemoresistant. It would be interesting, therefore, to

assess the dynamics of other ovarian cancer stem cell markers such as CD44 and CD117 [7,8] in chemosensitive and chemoresistant cells.

Strikingly, our data supported that 48h of hypoxia exposure were sufficient to drive carboplatin adaptation in ES2 cells, independent of the regime of selection. This observation shows that this simple exposure of cancer cells to a hypoxic environment, without considering all the complex microenvironmental interactions that also favours chemoresistance [9], is sufficient to alter the ovarian cancer cells outcome. It is well known the importance of hypoxia during the normal mammalian development, which is accompanied by a moderate-to-severe hypoxic environment, being HIF expression and activity tightly regulated in space and time by oxygen availability in several developmental processes, making oxygen a crucial morphogen regulating cell fate [10]. As Nobre and colleagues argued, cancer cells recapitulate this process in an abnormal way, where hypoxia strongly regulates cancer cells fate [10]. Hence, it is obvious to reason that hypoxia severity and duration and intermittent hypoxia dynamics (cycles of re-oxygenation) impact differently the outcome of cancer cells. However, no clear definitions for the duration of acute and chronic hypoxia exist in experimental oncology; *in vitro* and *in vivo* exposure times for both hypoxia regimes reported in the literature vary greatly and even overlap [11]. There are controversies also when trying to associate one or the other hypoxia regime to a poorer disease outcome, but generally an acute cellular exposure to hypoxia is linked to a more aggressive phenotype compared to a chronic exposure, as the former was associated with the induction of spontaneous metastasis [11–13]. However, the opposite was also reported in a recent review [10].

Hence, we argue that the fluctuation of oxygen rate might be more important in cancer cells outcome, as a moderate rate of hypoxia-reoxygenation. Thus, such a moderate rate of microenvironmental change might contribute for the maintenance of metabolic diversity and for a faster metabolic response/higher adaptive capacity in novel environments. An extreme lower rate of environmental change can contribute for a reduced cellular diversity due to the selection of an exclusive phenotype that is better adapted to that specific environment. We argue that, albeit *in vitro* 2D culture assays do not recapitulate the *in vivo* complexity, our model of selection under hypoxia represents a chronic hypoxia exposure with a high rate of oxygen fluctuations, as oxygen is continuously entering and reacting with CoCl_2 . Hence, this environment allowed the selection of an aggressive phenotype with a high degree of metabolic adaptability in novel environments. Therefore, it would be interesting to further

address the effects of different hypoxia regimes in the outcome of ovarian cancer cells not only in 2D but also in 3D cell culture models.

5.2 CYSTEINE FACILITATES THE ADAPTATION OF OVARIAN CANCER CELLS TO BOTH HYPOXIA AND CARBOPLATIN

The second chapter of this thesis provided evidence that cysteine metabolism has a biological role in ovarian cancer cells, as it allows a fast response and adaptation to hypoxic conditions that, in turn, are capable of driving chemoresistance. Noticeably, data supported that cysteine was even able to suppress the evolutionary trade-off of normoxia adaptation under hypoxia conditions, hence showing that normoxia selected cells still present metabolic diversity, allowing them to use cysteine and survive in a novel hypoxic environment.

In the third chapter, cysteine role upon hypoxia and carboplatin exposure was strengthened, where cysteine showed to present a widespread protective effect against both hypoxia and carboplatin-induced death among ovarian cancer cell lines. Interestingly, cysteine was advantageous for the cisplatin resistant A2780 cells but not for A2780 parental, sensitive cells, reinforcing that cysteine accounts for the selective process of platinum resistance in ovarian cancer cells.

Therefore, these results support that targeting cysteine can be an effective strategy to fight several histological types of ovarian carcinomas, as it allows a metabolic response to microenvironmental conditions associated to a poorer disease prognosis.

5.3 CYSTEINE MECHANISTIC ROLE IN HYPOXIC OVARIAN CANCER CELLS

Given the protective role of cysteine under hypoxic conditions, we aimed to clearer the mechanism by which cysteine protects ovarian cancer cells from hypoxia-induced death.

In the third chapter, results supported that thiols dynamics of synthesis and degradation underlie mainly ES2 cells hypoxia adaptation, as a higher rate of GSH degradation was found under hypoxia with cysteine supplementation. These results have also proposed that ovarian cancer cells from different origins may manage hypoxic stress by different mechanisms, where ES2 cells present a metabolism that is more dependent on cysteine than OVCAR3 cells. This evidence, on the other hand, points that cysteine metabolism can be related to a worse outcome of the disease, as OCCC is generally associated with a worse disease

prognosis compared to serous carcinomas and other histological types [14,15]. This hypothesis should be further explored, as this confirmation brings a valuable tool to manage the different ovarian carcinomas that have been, so far, treated mainly with identical clinical approaches. Nevertheless, what we disclosed in this thesis was the fact that ovarian carcinoma cells, whose metabolism relies more on cysteine bioavailability, exhibit a higher capacity to adapt to metabolic and toxic stressful conditions.

In the fourth chapter, we additionally aimed to explore other possible mechanisms by which cysteine can benefit hypoxic ovarian cancer cells. Our results have pointed to a role of cysteine also in energy production mediated by the xc^- system, emphasizing the importance of cysteine metabolism beyond the production of H_2S *per se*. These data are in accordance with recent findings supporting a role of Nrf2 in the regulation of mitochondrial ATP synthesis (reviewed in [16]). Nrf2 is a transcription factor that was already reported as pivotal in the regulation of xCT expression and consequently in the activation of the xc^- system in response to oxidative stress [17]. Therefore, our results support that ATP synthesis can be also mediated by cystine/cysteine uptake via the xCT transporter. The mitochondrial localization of xCT together with the absence of *de novo* synthesis of GSH in the mitochondrial matrix [18], strongly supports a role of this transporter in energy production mediated by cysteine uptake, besides its pivotal role in redox maintenance. Whether cysteine has a direct or indirect role in energy production, the relative importance of CBS, CSE and MpST activities are still unclear.

The direct role of cysteine in ATP production is still uncertain as this amino acid can have an indirect contribution to ATP synthesis driven by increased GSH content, allowing the redox equilibrium crucial for the overall metabolic flow. In fact, as already mentioned, in the chapter three our results have supported a role of a higher thiols turnover in hypoxia adaptation, especially in ES2 cells [19]. Moreover, in the fourth chapter, $^1\text{H-NMR}$ results have suggested that under hypoxia, the presence of cysteine augments glycine and glutamate content in ES2 cells, the other components of GSH besides cysteine. Besides that, these amino acids also contribute to *de novo* purine synthesis [20], proposing other indirect role of cysteine in energy production mediated by the increased bioavailability of these amino acids that can also account for ATP synthesis. Nonetheless, a role of cysteine in cellular metabolism reprogramming under hypoxia, especially in ES2 cells was observed. Strikingly, data supports an extremely pronounced metabolic impact of cysteine under hypoxia in ES2 cells, as seen by the remarkable number of metabolic pathways that were significantly altered in these cells. In the figure 1, we present a summarized model with all the possible

contributions of cysteine in ovarian cancer cells metabolism and adaptation to hypoxic environments.

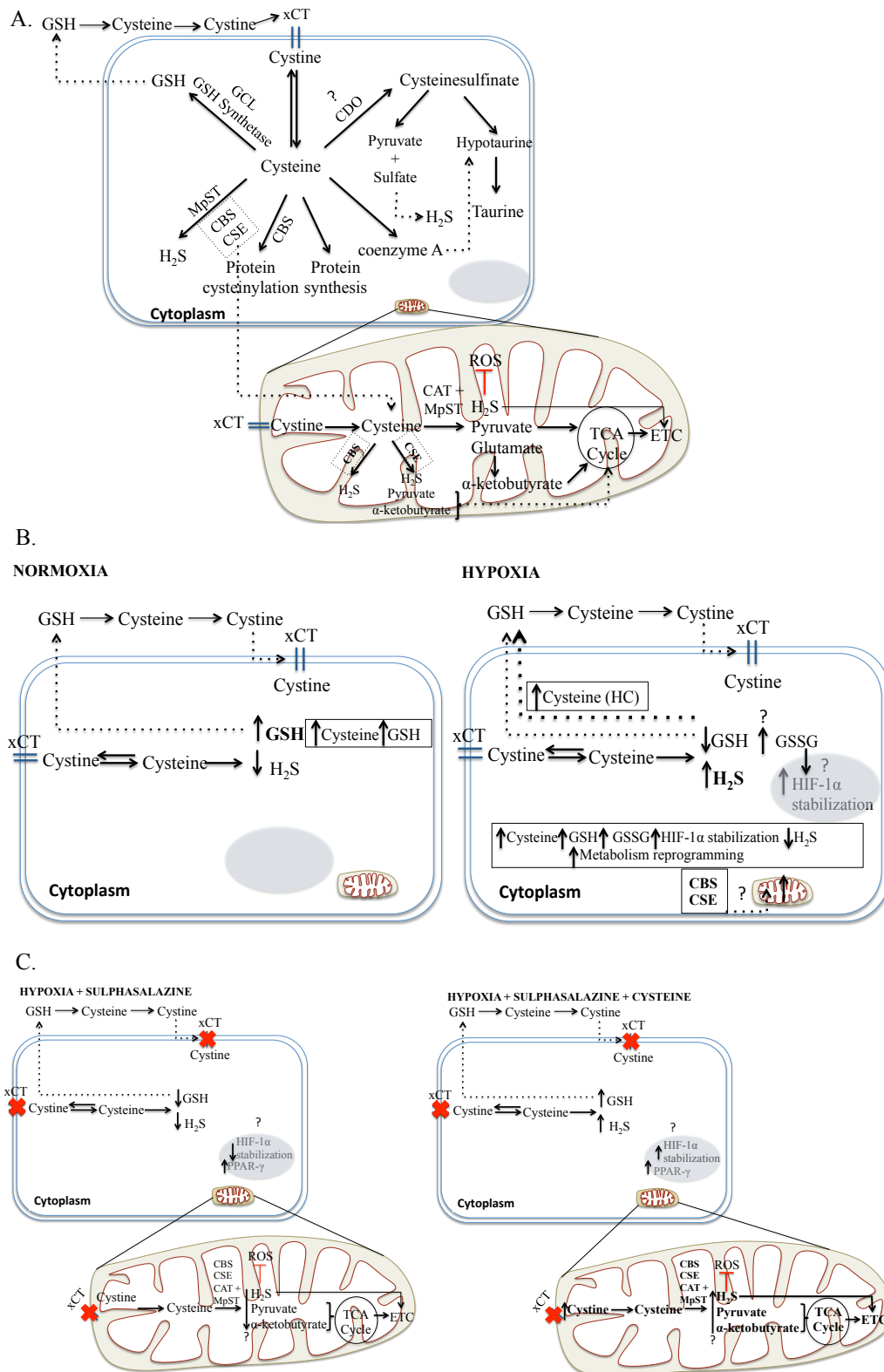


Figure 1. Proposed model for cysteine protective effect under hypoxia in ovarian cancer cells.

A. In a basal condition, cysteine can be imported by the xCT transporter [21]. In the intracellular compartment, cysteine is reduced into cysteine [22], which can be further canalized to GSH synthesis, to

protein synthesis and cysteinylolation, to coenzyme A, to H₂S, to pyruvate and to taurine. In basal conditions, CBS, CSE and MpST are the main enzymes involved in H₂S generation in the cytosol. CBS and CSE were already reported to re-localize to the mitochondria in conditions of oxidative stress [23,24]. In basal conditions, in the mitochondria, MpST in conjunction with CAT are the main enzymes responsible for H₂S generation [24]. CBS was also reported to be involved in the regulation of protein cysteinylolation [25]. Cysteine can also be catabolized by cysteine dioxygenase (CDO), into cysteine sulfinate, that subsequently can originate pyruvate, sulfite and hypotaurine, which then can originate taurine and H₂S [26]. In cancer, CDO was reported to be downregulated in several cancer types, including ovarian cancer [27,28]. However, when both CBS and CSE were inhibited with AOAA in combination with PAG, one possible route to increase H₂S levels would be an increased CDO activity. Importantly, CDO activity was reported to be modulated dependently on cysteine concentration in human hepatic cell lines [29], suggesting that with cysteine, this enzyme can be increased in ovarian cancer cells, increasing H₂S production. With CBS and CSE inhibitors, other possible mechanism to increase H₂S levels would be an enhanced MpST activity. Adapted from [26].

B. Under normoxia, cells canalize cysteine especially to GSH synthesis that is oxidized to GSSG and also to H₂S, which is increased under hypoxia (possibly both cytosolic and mitochondrial). With cysteine supplementation, a higher GSH turnover under hypoxia was found. This mechanism is particularly relevant for ES2 cells. With increased ROS, GSH oxidation (GSSG) can also increase and it is not only a source of cystine through its extracellular catabolism, but was also reported to increase HIF-1 α stabilization [30]. This high thiols turnover, together with increased H₂S levels under hypoxia, explains cysteine role in ATP synthesis and in cellular metabolism reprogramming, as seen by the high number of metabolic pathways that cysteine altered under hypoxia compared to normoxia. HC - hypoxia with cysteine.

C. Sulphasalazine inhibits the xCT transporter, and 5-Aminosalicylic acid (the main metabolite of sulphasalazine) [31] was also reported to induce both the mRNA and protein expression of the nuclear receptor peroxisome proliferator-activated receptor-gamma (PPAR- γ) [32]. Hypoxia was also reported to induce this nuclear receptor [33]. PPAR- γ has important roles in lipid and carbohydrate metabolism [34], hence possibly inducing β -oxidation of fatty acids upon sulphasalazine and hypoxia exposure. Under hypoxia, upon sulphasalazine exposure, it is expected an impaired cystine uptake, leading to decreased cysteine concentrations available for cells, which consequently, would lead to GSH depletion, decreased H₂S synthesis and impaired ATP synthesis. With cysteine supplementation, the cells possibly canalize this extra cysteine to GSH synthesis, hence allowing to counteract oxidative stress, allowing an increased ATP generation resulting in an increased cellular metabolism.

Remarkably, Shin and colleagues have reported a new function of the xCT transporter in the regulation of nutrient requirements in cancer cells [35]. They have shown that the Nrf2 and xc- system upregulation was responsible for a glucose addicted phenotype [35]. Therefore, they have reported that the downregulation of xc- system led to an enhanced cell viability under glucose-deficient conditions due to an improved ability of cells to use intracellular glutamate [35]. Glutamate is converted into α -ketoglutarate, replenishing intermediates for the mitochondrial tricarboxylic acid cycle (TCA), thus maintaining the respiratory chain activity [36]. The authors argued that, since tumours are often subject to high oxidative stress, the upregulation of Nrf2 and *xCT/SLC7A11* allows the redox homeostasis maintenance at the cost of a reduced efficacy of glutamine metabolism, affecting also mitochondrial respiration [35]. Nonetheless, albeit the glucose addiction phenotype, the upregulation of system xc- should be beneficial when glucose is abundant [35]. Other study develop by Koppula and colleagues have also proposed a role of glutamate export driven by xCT in increased sensitivity to glucose or glutamine starvation [37].

Furthermore, recently, Khamari and colleagues have reported a role of the Nrf2 pathway, together with an increased xCT expression, on melanoma with acquired resistance to BRAF inhibitors, where its strong activation was found to be responsible for an increased pentose phosphate pathway (PPP) [38]. PPP is crucial for several molecular processes as the regeneration of reduced GSH [38] to maintain the redox balance, the synthesis of nucleotides [39] supporting cell proliferation and gene expression, and also the histidine synthesis, which has a role in the protection against metals toxicity [40,41]. Importantly, the acquisition of BRAF inhibitors resistance was linked with both an increased mitochondrial OXPHOS and with glutamine metabolism [38]. Thus, they have linked chemoresistance with mitochondrial metabolism adaptations that favours glucose-derived-glutamate synthesis, cysteine uptake and GSH synthesis [38].

In our study, we did not address the role of cysteine uptake through xCT in ATP generation simultaneously under hypoxia and glucose withdrawal. Nevertheless, we can predict that cysteine benefits would remain or be even higher in ATP synthesis, as cysteine not only contributes for GSH and H₂S synthesis, allowing redox homeostasis but also for TCA intermediates such as pyruvate and glutamate (the latter in the mitochondria via CAT activity) [42,43], hence replenishing glutamine functions. However, another study reported that cystine was responsible for glutamine dependence via xCT [44]. They found that cystine administration to tumour bearing mice increased glutamine use by tumour cells *in vivo* [44]. If glutamate derived from cysteine catabolism is sufficient to balance glutamate export via xCT action under glucose deprivation is an interesting issue that should be further addressed in ovarian cancer cells.

Shin and colleagues also analysed 59 breast cancer cell lines and found a strong negative correlation between *xCT/SLC7A11* expression and mitochondrial OXPHOS genes expression [35]. These results are contradictory with a role of xCT in mitochondrial ATP generation via OXPHOS, because: 1) xCT is a direct transcriptional target of Nrf2 (reviewed in [16]); 2) a role of Nrf2 on respiration was reported, since Nrf2 deficiency resulted in a decreased efficacy of OXPHOS, whereas Nrf2 activation led to the opposite effect in both brain and liver mitochondria (reviewed in [16]); 3) data also supports a role of Nrf2 in β -oxidation enhancement (reviewed in [16]) and 4) this also opposes a role of H₂S in mitochondrial ATP production by stimulating electron transport chain. Hence, the assessment of OXPHOS related genes expression in ovarian cancer cells with overexpression and down-regulation of xCT should allow gaining further insights on the effects of xCT in OXPHOS. Nonetheless,

the study of gene expression by Shin and co-workers was based on mRNA expression [35], and mRNA profiles may not be reliable to predict the protein profile which in fact represents the metabolic functioning [45].

Recently, cysteine import via xc- system and its metabolism were reported to be pivotal in pancreatic cancer. This disease is characterized by its remarkably poor prognosis, where after initial diagnosis, only 8.2% of patients survive over 5 years [46]. In this study, a critical role of cysteine in the proliferation of several pancreatic cancer cell lines, by avoiding ROS accumulation, especially lipid ROS was reported [46]. In a mouse model of pancreatic cancer, the authors also found that the deletion of *SLC7A11/xCT* was able to delay and decrease tumour growth, leading to an increase in the overall median survival of mice [46]. Confirming the importance of cystine (the oxidized form of cysteine) and cysteine in the context of pancreatic cancer, Kshatry and colleagues have reported that their extracellular depletion by using the human enzyme Cyst(e)inase genetically engineered, led to cell growth inhibition and that Cyst(e)inase sensitivity was related to ROS accumulation [47]. The beneficial effects of this altered enzyme were also supported using an *in vivo* model of pancreatic cancer cell xenografts in nude mice [47]. The authors suggested the possible use of this compound in a clinical context of pancreatic cancer as a monotherapy or in combination with other drugs [47]. In the context of breast cancer, Tang and colleagues have reported that the epithelial-mesenchymal transition, process with a pivotal role in tumour progression of this disease, was accompanied by a cystine-addiction phenotype of the breast cancer cells [48]. Importantly, whereas the authors found this cystine addictive phenotype in the basal-type breast cancer cells that are characteristic of triple negative breast cancer, they did not find this phenotype in luminal-type breast cancer cells [48], hence supporting a role of cystine/cysteine in more aggressive histotypes also in breast cancer context.

In here, we did not address the role of cysteine hydropersulphide (CysSSH) in hypoxia adaptation. Since it simultaneously functions as a strong nucleophile and an antioxidant that may also be important in cellular oxidative stress and redox signalling regulation [49,50], we can speculate a critical role of CysSSH in ovarian cancer cells adaptation to hypoxia and also to platinum drugs. Fujii and colleagues have reported that besides CBS and CSE contribution to CysSSH using cystine as a substrate, cysteinyl-tRNA synthetase is crucial in CysSSH generation using L-cysteine. They reported that cysteinyl-tRNA synthetase is involved in the direct incorporation of CysSSH into proteins during translation, resulting in the formation of protein persulphides and polysulphides [50,51]. Moreover, they noticeably reported a novel

role for CysSSH in the regulation of mitochondrial biogenesis and bioenergetics and they firstly demonstrated sulphur respiration, a bacterial feature, in mammalian cells [50,51]. Together, these observations can pave the path to demonstrate that cysteine, directly or through CysSSH, can play an important role in cancer cells adaptation to hypoxia, functioning as a donor of sulphur to sustain sulphur respiration. This adaptive mechanism will undoubtedly change the paradigm of cells respiration as using exclusively oxygen as the electron acceptor and will open several different cues of research in order to change the way cancer metabolic remodelling is seen.

In addition to the role of cysteine in interfering with the function of proteins through a cysteinylolation process, the introduction of cysteines in the protein sequence driven by gene mutation seems to be also pivotal in cancer. Strikingly, Visscher and colleagues have reported that many oncogenic mutations cause the switch of the natural amino acid in the protein sequence by a cysteine [52]. They also reported that these cysteines account for at least 12% of all activating mutations found in Kirsten ras oncogene (KRAS) in cancer, and 88% of mutations in fibroblast growth factor receptor (FGFR). They suggested that when acquired cysteines are found that often, they should play a role in tumourigenesis [52]. Tsuber and co-workers have confirmed this cysteine gain by analysing two thousand proteins in over 18000 cancer samples [53]. Moreover, the authors have also found a gain in histidine, and tryptophan at the expense of an arginine loss [53]. They hypothesised that the gain of cysteine, histidine, and tryptophan can be related to an increased antioxidant and metal-binding capacity of the proteome of the cancer cells, hence compensating oxidative stress and re-establishing the redox balance required for cell survival. They explained the loss of arginine due to the remarkably high mutation rate in four of the six codons that code for this amino acid or due to a targeted loss of arginine in essential tumour suppressor proteins that are frequently mutated in cancer [53]. Remarkably, Sojourner and colleagues have reported that mutations disturbing the histidine-proline-aspartic acid motif and cysteine-rich region of yeast DNAJ, a J-domain heat-shock protein 40 lead to the sensitization of *S. cerevisiae* cells both to doxorubicin and cisplatin, and that this sensitivity was specifically due to oxidative stress and not to DNA double-strand breaks [54]. This observation strengthens a functional role of cysteine gain in cancer, interfering structurally with the cellular machinery supported by proteins.

Together, evidence reinforces a profound impact of cysteine in tumourigenesis, allowing metabolism reprogramming and consequently, an enhanced ability of ovarian cancer cells to adapt to novel and changing environments. In one hand, the environmental cysteine provides

the opportunity to sulphur and carbon metabolism reprogramming and protein cysteinylolation. In the other hand, mutation-derived cysteine incorporation can also contribute to the modulation of the function of proteins that are crucial for the carcinogenic phenotype. Cysteine-mutated proteins with roles in cell signalling (Kras) and cell cycle control (p53) [52] were reported and these mutations may also be involved in an increased redox homeostasis capacity [53]. In certain conditions, the incorporation of a new-inserted cysteine in a protein sequence might turn proteins more susceptible to abnormal structural conformational changes or other protein thiolation modifications, enabling these mutated variants to form disulphide bonds that can switch their natural structure and function; and allows the interaction with other compounds as a thiol, interfering in the redox intracellular balance and building new molecular partnerships. Hence, cysteine can have wide effects on cancer cells, favouring their survival and disease progression within their microenvironment.

5.4 CYSTEINE AS A SUITABLE BIOMARKER FOR OVARIAN CANCER SCREENING, DIAGNOSIS, PROGNOSIS AND TARGETED-THERAPY

Given the established role of cysteine in ovarian cancer cell lines, we also aimed to address if this thiolic amino acid has a clinical significance. For that, we quantified thiols in serum from peripheral blood of patients with ovarian benign and malignant tumours and from healthy individuals (women). In the third chapter, our data have shown, with the exception of GSH, an overall increase of thiols concentration in serum from patients with ovarian neoplasms, regardless malignancy. Strikingly, total and free serum levels of homocysteine (HCys) distinguished serum from the three groups of individuals and the free levels of cysteine (Cys) and protein-S-cysteinylolation (CysSSP) were also able to distinguish all the three groups, hence suggesting that cysteine and homocysteine levels can be putative biomarkers for ovarian cancer screening and early diagnosis. This is undoubtedly a major outcome of this thesis, constituting a step forward for ovarian cancer research, as the late diagnosis represents one of the most important barriers responsible for ovarian cancer poor prognosis.

We also aimed to address cysteine role in disease progression. Therefore, we have quantified thiols in the ascitic fluid derived from patients with advanced disease, an important compartment of the ovarian cancer cells microenvironment. Strikingly, our data showed that cysteine was the prevalent thiol and that S-cysteinylolation was the most abundant form of S-thiolated proteins showing, once again, a clinical relevance of cysteine in disease progression.

We have thus hypothesised that cysteine acts as a first protection barrier for ovarian malignant cells against hypoxia and chemotherapy, therefore contributing for disease progression and recurrence.

It would be interesting to additionally explore which proteins are being thiolated, not only in serum from patients with ovarian neoplasms, but also in the ascitic fluid, in order to gain further insights on the role of this post-translational modification of proteins in ovarian cancer. The knowledge of how far this alteration interferes with the function of proteins would give us more insights on ovarian cancer and cancer biology in general.

Together, our data endorses cysteine targeting as a promising tool to fight not only ovarian cancer, but several cancer types. Inhibitors of cystine transporters like sulphasalazine are already used in the context of other diseases, such as Crohn's disease and rheumatoid arthritis, suggesting that its use may be also a valuable strategy in cancer. However, albeit several pre-clinical models have shown promising results, indicating the use of sulphasalazine as an efficient and advantageous drug in the management of several cancer types [55–60], two clinical trials have reported the opposite [61]. Thus, Robe and co-workers have reported a phase 1/2 clinical study of sulphasalazine for the treatment of recurrent grade 3 and 4 astrocytic gliomas in adults [61]. The authors concluded that sulphasalazine should not be generally used for the treatment of glioblastoma patients, as no clinical response was found and adverse side effects were common [61]. Shitara and colleagues have reported similar findings in a phase 1 study of sulphasalazine combined with cisplatin in patients with advanced gastric cancer with CD44v-positive cells that did not respond to cisplatin-based chemotherapy and exhibited gastrointestinal toxicity [62]. Only one patient was able to complete six cycles of treatment with stable disease for more than 4 months and with decreased intratumoral GSH levels [62]. In ovarian cancer, as far as we know, no clinical trials with sulphasalazine were reported. These two clinical trials show the complexity and the difficulties of the bench to the bedside applications, where, for example, the drug concentration used, the schedule of administration and the side and adverse effects impose extreme difficulties and may vary the outcome of the therapy. The development of sulphasalazine analogous with decreased side and adverse effects would be of extreme importance. In fact, several sulphasalazine analogous were already developed and, in the context of inflammatory bowel diseases, these analogous allow a differently distribution of drug delivery in the gastrointestinal tract, via pH-sensitive coating or delayed-release formulations [63], hence avoiding the adverse systemic effects of 5-ASA, the main metabolite of sulphasalazine [31]. Regarding ovarian cancer context, the development of such strategies

using for instance a formulation conjugated to a specific biomarker of ovarian cancer cells would allow targeted therapies, possibly allowing a more effective drug action, decreasing the damage of normal cell and increasing the drug delivery to cancer cells. Recently, Bolli and colleagues have developed a virus-like-particle immunotherapy that targeted the xCT protein and have shown that this system inhibited xCT activity, impaired breast cancer stem cells biology and decreased metastatic progression in preclinical models [64], hence opening new therapeutic approaches that target cysteine metabolism via the xCT transporter.

The follow up of cancer cells metabolic features and adaptations should be considered in cancer management, as they can present a valuable mean to predict and overcome cancer chemoresistance. Together, our results support that cysteine metabolism can offer a good panel of biomarkers for ovarian cancer screening, diagnosis and prognosis and for targeted-therapy.

5.5 FINAL REMARKS

With this thesis we aimed to disclose the role of cysteine in ovarian cancer progression and chemoresistance. Taken together, our data supports a protective effect of cysteine in ovarian cancer cells, allowing their adaptation and survival upon hypoxia and carboplatin exposure. Cysteine role in the mediation of GSH synthesis and ATP production via xCT-mediated cysteine transport and also by its degradation in the mitochondria are presented in the figure 2. Specifically under hypoxia, cysteine is responsible for a cellular metabolism rescue mainly in ES2 cells, hence supporting its role in cells viability and proliferation. Our findings were also supported in a clinical context, hence strengthening the use of cysteine not only as a biomarker for early diagnosis and disease progression but also in a targeted-therapy.

Taken together, we have disclosed a pivotal role of cysteine metabolism in ovarian cancer cells adaptation to hypoxia and resistance to carboplatin. These two features are highly linked with poor disease prognosis, hence, this thesis allowed gaining new insights not only on a novel possible therapeutic strategy, but also on a new powerful tool in screening, early diagnosis and outcome of this disease. Since the late diagnosis is profoundly associated with the poor prognosis of ovarian cancer, cysteine contribution as novel biomarker for an early diagnosis should be of extreme importance. Also, since cysteine metabolism was found to alter both hypoxia and anti-cancer drugs resistance, its' targeting can constitute a potential strategy to overcome resistance. Moreover, since xCT was found overexpressed in several

types of cancer, this suggests that cysteine metabolism dependence is a common feature of cancer cells biology, opening the opportunity for a general therapeutic use in cancer. Thus, this thesis has opened new diagnostic, prognostic and therapeutic paths in cancer research, where cysteine metabolic profile allows the design of new and useful approaches to fight these diseases.

This thesis raises the veil of new exciting aspects of the biological processes, supporting carcinogenesis and disease progression, with cancer metabolism and cysteine as core players.

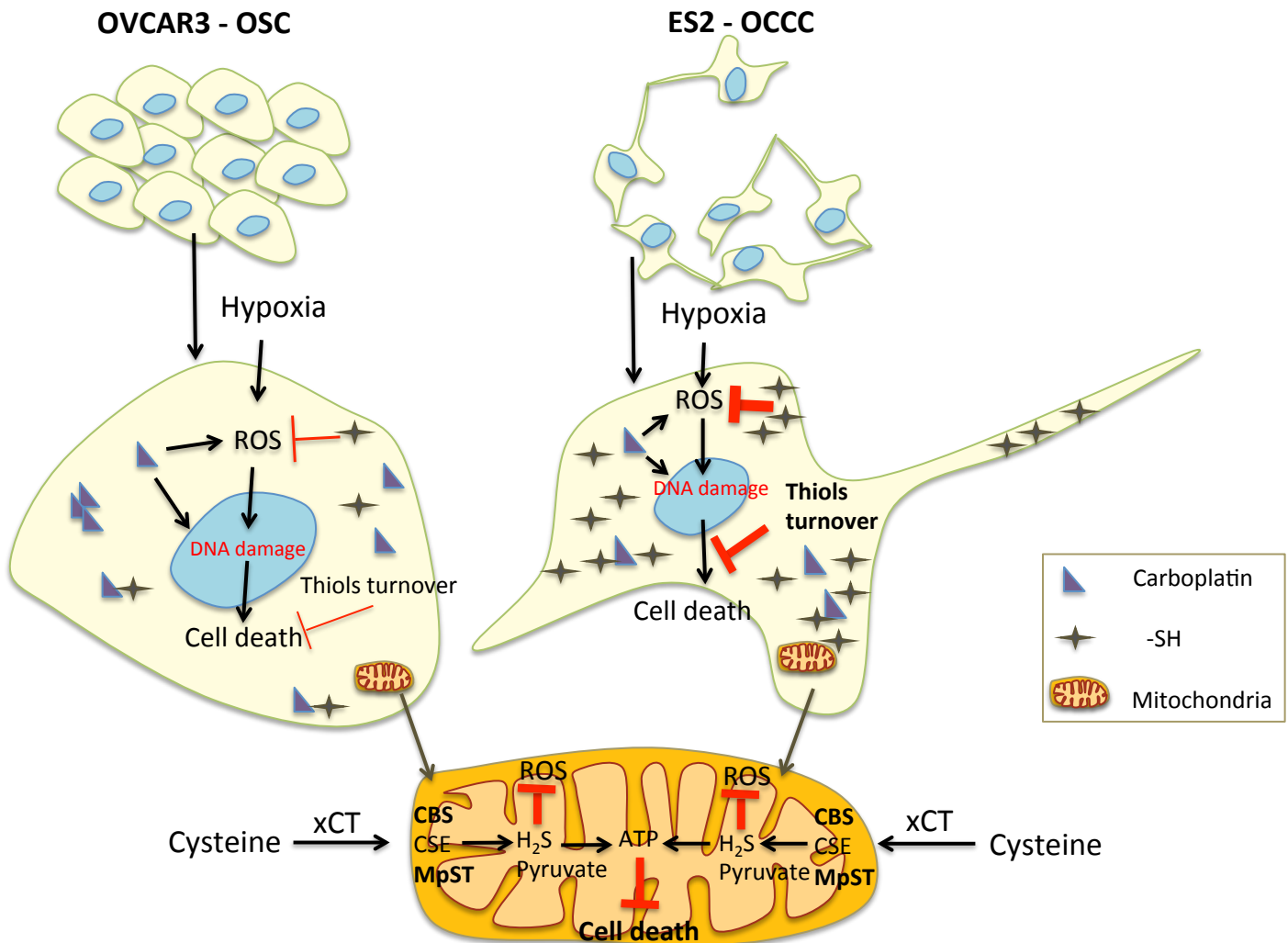


Figure 2. Proposed model for the protective effect of cysteine in ovarian cancer cells upon hypoxia and carboplatin exposure.

Cysteine role in ovarian cancer cells adaptation to hypoxia can be mediated by GSH synthesis and also by its catabolism. Under hypoxia, the dynamics of thiol synthesis and degradation contribute to hypoxia adaptation mainly in ES2 cells. Cysteine catabolism can also have a role in ATP production via its degradation in the mitochondria. Thus, xCT transporter can mediate cysteine mitochondrial uptake and the enzymes CBS, CSE and MpST can lead to H₂S synthesis. Pyruvate and glutamate also results from cysteine catabolism, hence allowing the replenishing of the TCA cycle. Under hypoxia, cysteine allowed a cellular metabolism rescue mainly in ES2 cells, having effects in several metabolic pathways. Since carboplatin also involves ROS generation, a similar protective effect of cysteine upon carboplatin exposure would drive ovarian cancer cells resistance.

5.6 FUTURE PERSPECTIVES

This thesis left several open questions that merit additional attention. Some of them were already mentioned but others are also relevant, such as the clarification of the role of cysteine as a carbon source. This would allow gaining additional insight into the protective role of cysteine in hypoxic ovarian cancer cells, as it would enable following all the metabolites directly derived from cysteine.

It would be also interesting to analyse the relative importance of each H₂S-generating enzymes in ATP production in hypoxic ovarian cancer cells. Interestingly, the biological consequences of the modulation of MpST, together with its partner CAT, in cancer cells were not addressed yet, thus the knock-down and re-expression of this enzyme in ovarian cancer cells would bring new insights into its role in cancer biology. The validation of the activity of enzymes involved in cysteine metabolism (CBS, CSE and MpST) as a tool to follow and predict chemoresistance would be of a capital relevance in clinics. The design of new and fully specific inhibitors for these enzymes would for certain contribute for a more reliable evaluation of cancer reliance on these cysteine-dependent metabolic pathways. It would be also interesting to address the role of other cystine transporters such as SLC3A1 and cystinosin in ovarian cancer cells adaptation to hypoxia. Cystinosin is a lysosomal transmembrane protein involved in the transport of cystine from the lysosomes to the cytosol [65]. In the kidney proximal tubular cells, which highly express cystinosin, lysosomal cystine is a major source of cytosolic cysteine, by the degradation of cystine-containing proteins catalyzed by chatepsins [65]. Therefore, it would be interesting to investigate the role of this protein in the redox homeostasis of hypoxic ovarian cancer cells.

The effect of sulphasalazine in ovarian cancer cells chemoresistance should be also investigated, not only in the presence of carboplatin but also in the presence of paclitaxel, in order to address its role on chemoresistance reversion.

The role of Nrf2 in the orchestration of the dynamics, involving the role of cysteine uptake and metabolism, is undoubtedly an interesting cue to follow in order to understand the molecular mechanisms underlying the whole metabolic remodelling network.

The biochemical process and alterations supporting the role of cysteine and CysSSH in sulphur respiration and the evidence that this adaptation can be the key to cancer cells survival in hypoxia is an open repertoire of experimental and biological questions.

The proteomic profiling of S-cysteinylylated proteins with the objective of identifying which proteins are preferentially targeted by this process, will be a good tool to identify

mechanistic alterations interfering with the various phases of the oncologic disease. This definition may serve as a starting point for the design of new therapeutic approaches and follow-up methods. In order to validate the use of cysteine as a biomarker for ovarian cancer screening, early diagnosis and progression of the disease, we also propose a pilot clinical observational study including women in different stages of the disease and healthy controls, matched for age. Women with endometriosis should be also included, since endometriosis was already associated with an increased risk for both endometrioid and clear cell carcinomas [66]. Free levels and protein bound levels of cysteine and homocysteine should be quantified in serum from patients within these groups in order to evaluate if the levels of these thiols vary among groups and within ovarian cancer patients, in order to address if their levels increase along with the progression of the disease. A follow-up should also be considered, performing the quantification of these thiols at diagnosis and over time, before and after chemotherapy (figure 3). This proof-of-concept would possibly allow the use of cysteine/cysteinylated proteins and homocysteine/homocysteinylated proteins as indicators of ovarian cancer cells chemoresistance, guiding therapeutic interventions in the view of precision medicine.

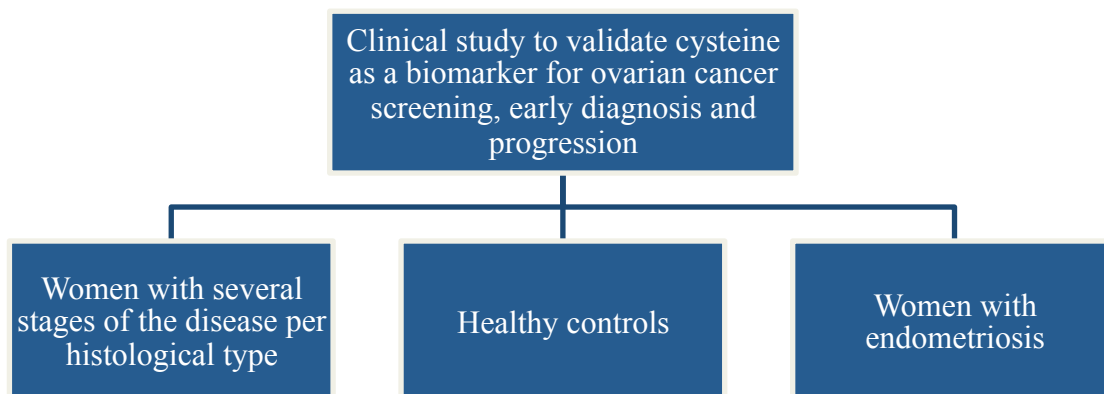


Figure 3. Proposed groups for a pilot clinical study to validate cysteine (and homocysteine) as biomarkers for ovarian cancer screening, early diagnosis and progression.

In this strategy, we propose to include groups of women in different stages of the disease per histological type, healthy controls and also women with endometriosis, matched for age. Cysteine and homocysteine levels (free and bound to proteins) should be measured over time in order to address if the levels of these thiols increase along with the progression of the disease.

Furthermore, the effect of cysteine metabolism in the adaptability to hypoxia and chemoresistance in other cancer types should be analysed in order to assess if the protective effect of cysteine is a widespread metabolic feature of cancer cells. This would ultimately impact cancer management, as a general cancer cells targeted-therapy may be developed.

5.7 REFERENCES

1. Futuyma DJ, Moreno G. The evolution of ecological specialization. *Annu. Rev. Ecol. Evol. Syst.* 1988;19:207–33.
2. Novak M, Pfeiffer T, Lenski RE, Sauer U, Bonhoeffer S. Experimental tests for an evolutionary trade-off between growth rate and yield in *E. coli*. *Am. Nat.* 2006;168:242–51.
3. Bennett AF, Lenski RE. An experimental test of evolutionary trade-offs during temperature adaptation. *Proc. Natl. Acad. Sci. U. S. A.* 2007;104 Supp 1:8649–54.
4. Stearns S. Trade-offs in life-history evolution. *Funct. Ecol.* 1989;3:259–68.
5. Mitchison TJ. The proliferation rate paradox in antimetabolic chemotherapy. *Mol. Biol. Cell.* 2012;23:1–6.
6. Liu H, Lv L, Yang K. Chemotherapy targeting cancer stem cells. *Am. J. Cancer Res.* 2015;5:880–93.
7. Burgos-ovejeda D, Rueda BR, Buckanovich RJ. Ovarian cancer stem cell markers : Prognostic and therapeutic implications. 2012;322:1–7.
8. Chung H, Kim Y-H, Kwon M, Shin S-J, Kwon S-H, Cha S-D, *et al.* The effect of salinomycin on ovarian cancer stem-like cells. *Obstet. Gynecol. Sci.* 2016;59: 261-8.
9. Son B, Lee S, Youn H, Kim E, Kim W, Youn B. The role of tumor microenvironment in therapeutic resistance. *Oncotarget.* 2017;8:3933–45.
10. Nobre AR, Entenberg D, Wang Y, Condeelis J, Aguirre-Ghiso JA. The Different Routes to Metastasis via Hypoxia-Regulated Programs. *Trends Cell Biol.* 2018;28:941–56.
11. Bayer C, Vaupel P. Acute versus chronic hypoxia in tumors : Controversial data concerning time frames and biological consequences. *Strahlentherapie und Onkol.* 2012;188:616–27.
12. Bristow RG, Hill RP. Hypoxia and metabolism: hypoxia, DNA repair and genetic instability. *Nat. Rev. Cancer.* 2008;8:180–92.
13. Muz B, de la Puente P, Azab F, Azab AK. The role of hypoxia in cancer progression, angiogenesis, metastasis, and resistance to therapy. *Hypoxia.* 2015;3:83–92.
14. Tammela J, Geisler J, Eskew PJ, Geisler H. Clear cell carcinoma of the ovary: poor prognosis compared to serous carcinoma. *Eur. J. Gynaecol. Oncol.* 1998;19:438–40.
15. Lee Y, Kim T, Kim M, Kim H, Song T, Kyu M, *et al.* Gynecologic Oncology Prognosis of ovarian clear cell carcinoma compared to other histological subtypes : A meta-analysis. *Gynecol. Oncol.* 2011;122:541–7.
16. Dinkova-Kostova AT, Abramov AY. The emerging role of Nrf2 in mitochondrial function. *Free Radic. Biol. Med.* 2015;88:179–88.
17. Habib E, Linher-Melville K, Lin HX, Singh G. Expression of xCT and activity of system xc-are regulated by NRF2 in human breast cancer cells in response to oxidative stress. *Redox Biol.* 2015;5:33–42.
18. Ribas V, Carmen G-R, Fernández-Checa JC. Glutathione and mitochondria. *Front. Pharmacol.*

2014;5:1–19.

19. Nunes SC, Ramos C, Lopes-Coelho F, Sequeira CO, Silva F, Gouveia-Fernandes S, *et al.* Cysteine allows ovarian cancer cells to adapt to hypoxia and to escape from carboplatin cytotoxicity. *Sci. Rep.* 2018;8:9513–29.

20. Newman AC, Maddocks ODK. Serine and Functional Metabolites in Cancer. *Trends Cell Biol.* 2017;27:645–57.

21. Sato, H., Tamba, M., Kuriyama-Matsumura, K., Okuno, S., & Bannai S. Molecular cloning and expression of human xCT, the light chain of amino acid transport system xc-. *Antioxid Redox Signal.* 2000;2:665–71.

22. Conrad M, Sato H. The oxidative stress-inducible cystine/glutamate antiporter, system xc-: cystine supplier and beyond. *Amino Acids.* 2012;42:231–46.

23. Teng H, Wu B, Zhao K, Yang G, Wu L, Wang R. Oxygen-sensitive mitochondrial accumulation of cystathionine β -synthase mediated by Lon protease. *Proc. Natl. Acad. Sci.* 2013;110:12679–84.

24. Fu M, Zhang W, Wu L, Yang G, Li H, Wang R. Hydrogen sulfide (H₂S) metabolism in mitochondria and its regulatory role in energy production. *Proc. Natl. Acad. Sci.* 2012;109:2943–8.

25. Bar-Or D, Curtis CG, Sullivan A, Rael LT, Thomas GW, Craun M, *et al.* Plasma albumin cysteinylolation is regulated by cystathionine β -synthase. *Biochem. Biophys. Res. Commun.* 2004;325:1449–53.

26. Stipanuk MH, Dominy JE, Lee J, Coloso RM. Mammalian Cysteine Metabolism: New Insights into Regulation of Cysteine Metabolism. *Am. Soc. Nutr.* 2006;136:S1652–9.

27. Brait M, Ling S, Nagpal JK, Chang X, Park HL, Lee J, *et al.* Cysteine dioxygenase 1 is a tumor suppressor gene silenced by promoter methylation in multiple human cancers. *PLoS One.* 2012;7:e44951.1-19.

28. Niu S, Cui B, Huang J, Guo Y. PPAR γ is correlated with prognosis of epithelial ovarian cancer patients and affects tumor cell progression in vitro. *Int J Clin Exp Pathol.* 2017;10:3235–42.

29. Wilkinson LJ, Waring RH. Cysteine dioxygenase: Modulation of expression in human cell lines by cytokines and control of sulphate production. *Toxicol. Vitro.* 2002;16:481–3.

30. Jeon D, Park HJ, Kim HS. Protein S-glutathionylation induced by hypoxia increases hypoxia-inducible factor-1 α in human colon cancer cells. *Biochem. Biophys. Res. Commun.* 2018;495:212–6.

31. Lo M, Ling V, Low C, Wang YZ, Gout PW. Potential use of the anti-inflammatory drug, sulfasalazine, for targeted therapy of pancreatic cancer. *Curr. Oncol.* 2010;17:9–16.

32. Rousseaux C, Lefebvre B, Dubuquoy L, Lefebvre P, Romano O, Auwerx J, *et al.* Intestinal antiinflammatory effect of 5-aminosalicylic acid is dependent on peroxisome proliferator-activated receptor- γ . *J. Exp. Med.* 2005;201:1205–15.

33. Zhao YZ, Liu XL, Shen GM, Ma YN, Zhang FL, Chen MT, *et al.* Hypoxia induces peroxisome proliferator-activated receptor γ expression via HIF-1-dependent mechanisms in HepG2 cell line. *Arch. Biochem. Biophys.* 2014;543:40–7.

34. Itoh T, Fairall L, Amin K, Inaba Y, Szanto A, Balint BL, *et al.* Structural basis for the activation of PPAR γ by oxidized fatty acids. *Nat Struct Mol Biol.* 2008;15:924–31.

35. Shin CS, Mishra P, Watrous JD, Carelli V, D'Aurelio M, Jain M, *et al.* The glutamate/cystine xCT antiporter antagonizes glutamine metabolism and reduces nutrient flexibility. *Nat. Commun.* 2017;8:15074-84.
36. Hensley CT, Wasti AT, DeBerardinis RJ. Glutamine and cancer: cell biology, physiology, and clinical opportunities. *J. Clin. Invest.* 2013;123:3678-84.
37. Koppula P, Zhang Y, Shi J, Li W, Gan B. The glutamate/cystine antiporter SLC7A11/xCT enhances cancer cell dependency on glucose by exporting glutamate. *J. Biol. Chem.* 2017;292:14240-9.
38. Khamari R, Trinh A, Gabert PE, Corazao-Rozas P, Riveros-Cruz S, Balayssac S, *et al.* Glucose metabolism and NRF2 coordinate the antioxidant response in melanoma resistant to MAPK inhibitors. *Cell Death Dis.* 2018;9:325-38.
39. Stincone A, Prigione A, Cramer T, Wamelink MMC, Campbell K, Cheung E, *et al.* The return of metabolism: Biochemistry and physiology of the pentose phosphate pathway. *Biol. Rev.* 2015;90:927-63.
40. Valko M, Morris H, Cronin MTD. Metals, Toxicity and Oxidative Stress. *Curr. Med. Chem.* 2005;12:1161-208.
41. Murphy JT, Bruinsma JJ, Schneider DL, Collier S, Guthrie J, Chinwalla A, *et al.* Histidine protects against zinc and nickel toxicity in *Caenorhabditis elegans*. *PLoS Genet.* 2011;7:e1002013.1-12.
42. Olson KR, DeLeon ER, Gao Y, Hurley K, Sadauskas V, Batz C, *et al.* Thiosulfate: a readily accessible source of hydrogen sulfide in oxygen sensing. *AJP Regul. Integr. Comp. Physiol.* 2013;305:R592-603.
43. Wang R. Physiological Implications of Hydrogen Sulfide: A Whiff Exploration That Blossomed. *Physiol. Rev.* 2012;92:791-896.
44. Muir A, Danai L V., Gui DY, Waingarten CY, Lewis CA, Vander Heiden MG. Environmental cystine drives glutamine anaplerosis and sensitizes cancer cells to glutaminase inhibition. *Elife.* 2017;6:1-27.
45. Chen G, Gharib TG, Huang C-C, Taylor JMG, Misek DE, Kardia SLR, *et al.* Discordant Protein and mRNA Expression in Lung Adenocarcinomas. *Mol. Cell. Proteomics.* 2002;1:304-13.
46. Badgley MA. The critical role of cysteine import and metabolism in pancreatic cancer. 2018. PhD Thesis. Columbia University.
47. Kshattray S, Saha A, Cramer S, DiGiovanni J, Tiziani S, Munoz N, *et al.* Depletion of extracellular cystine and cysteine by a mutagenized human enzyme causes ROS mediated cytotoxicity in pancreatic cancer cells. *Proc. Am. Assoc. Cancer Res. Annu. Meet.* 2017; Apr 1-5, 2017; Washington, DC. Philadelphia (PA):77(13 Suppl):Abstract 105.
48. Tang X, Ding C-K, Wu J, Sjol J, Wardell S, George D, *et al.* Cystine addiction of triple negative breast cancer associated with EMT augmented death signaling. *Oncogene.* 2017;36:4235-42.
49. Ida T, Sawa T, Ihara H, Tsuchiya Y, Watanabe Y, Kumagai Y, *et al.* Reactive cysteine persulfides and S-polythiolation regulate oxidative stress and redox signaling. *Proc. Natl. Acad. Sci.* 2014;111:7606-11.

50. Fujii S, Sawa T, Motohashi H, Akaike T. Persulfide synthases that are functionally coupled with translation mediate sulfur respiration in mammalian cells. *Br. J. Pharmacol.* 2018.
51. Akaike T, Ida T, Wei FY, Nishida M, Kumagai Y, Alam MM, *et al.* Cysteinyl-tRNA synthetase governs cysteine polysulfidation and mitochondrial bioenergetics. *Nat. Commun.* 2017;8:1177-91.
52. Visscher M, Arkin MR, Dansen TB. Covalent targeting of acquired cysteines in cancer. *Curr. Opin. Chem. Biol.* 2016;30:61-7.
53. Tsuber V, Kadamov Y, Brautigam L, Berglund UW, Helleday T. Mutations in cancer cause gain of cysteine, histidine, and tryptophan at the expense of a net loss of arginine on the proteome level. *Biomolecules.* 2017;7:1-17.
54. Sojourner SJ, Graham WM, Whitmore AM, Miles JS, Freeny D, Flores-Rozas H. The Role of HSP40 Conserved Motifs in the Response to Cytotoxic Stress. *J Nat Sci.* 2018;4:1-19.
55. Lo M, Wang Y, W Gout P. The xc⁻ cystine/glutamate antiporter: A potential target for therapy of cancer and other diseases. *J. Cell. Physiol.* 2008.
56. Balza E, Castellani P, Delfino L, Truini M, Rubartelli A. The pharmacologic inhibition of the xc⁻ antioxidant system improves the antitumor efficacy of COX inhibitors in the in vivo model of 3-MCA tumorigenesis. *Carcinogenesis.* 2013;34:620-6.
57. Sleire L, Skeie BS, Netland IA, Førde HE, Dodoo E, Selheim F, *et al.* Drug repurposing: Sulfasalazine sensitizes gliomas to gamma knife radiosurgery by blocking cystine uptake through system Xc⁻, leading to glutathione depletion. *Oncogene.* 2015;34:5951-9.
58. Balza E, Castellani P, Moreno PS, Piccioli P, Medraño-Fernandez I, Semino C, *et al.* Restoring microenvironmental redox and pH homeostasis inhibits neoplastic cell growth and migration: therapeutic efficacy of esomeprazole plus sulfasalazine on 3-MCA-induced sarcoma. *Oncotarget.* 2017;8:67482-96.
59. Subhashini GV, Swarna B, Jayadev M. Sulfasalazine Inhibits IL-2 Expression in Ovarian Cancer Cells. *Imp. J. Interdiscip. Res.* 2017;3:486-9.
60. Nagane M, Kanai E, Shibata Y, Shimizu T, Yoshioka C, Maruo T, *et al.* Sulfasalazine, an inhibitor of the cystine-glutamate antiporter, reduces DNA damage repair and enhances radiosensitivity in murine B16F10 melanoma. *PLoS One.* 2018;13:1-19.
61. Robe PA, Martin DH, Nguyen-Khac MT, Artesi M, Deprez M, Albert A, *et al.* Early termination of ISRCTN45828668, a phase 1/2 prospective, randomized study of sulfasalazine for the treatment of progressing malignant gliomas in adults. *BMC Cancer.* 2009;9: 372-9.
62. Shitara K, Doi T, Nagano O, Fukutani M, Hasegawa H, Nomura S, *et al.* Phase 1 study of sulfasalazine and cisplatin for patients with CD44v-positive gastric cancer refractory to cisplatin (EPOC1407). *Gastric Cancer.* 2017;20:1004-9.
63. Goodman L, Gilman A. Goodman and Gilman's the pharmacological basis of therapeutics. 13th ed. Laurence L. Brunton, Randa Hilal-Dandan BCK, editor. New York: McGraw-Hill; 2018.
64. Bolli E, O'Rourke JP, Conti L, Lanzardo S, Rolih V, Christen JM, *et al.* A Virus-Like-Particle immunotherapy targeting Epitope-Specific anti-xCT expressed on cancer stem cell inhibits the progression of metastatic cancer in vivo. *Oncoimmunology.* 2018;7:e1408746.1-14.
65. Sumayao R, Newsholme P, McMorrow T. The Role of Cystinosin in the Intermediary Thiol

Metabolism and Redox Homeostasis in Kidney Proximal Tubular Cells. *Antioxidants*. 2018;7:179–95.

66. Wentzensen N, Poole EM, Trabert B, White E, Arslan AA, Patel A V., *et al*. Ovarian cancer risk factors by histologic subtype: An analysis from the Ovarian Cancer Cohort Consortium. *J. Clin. Oncol.* 2016;34:2888–98.